Order Number 8821075

Modelling and performance of an integrated six-port reflectometer operated with pulsed signals

Colef, Gabriel-Dumitru, Ph.D.

City University of New York, 1988

U·M·I
300 N. Zeeb Rd.
Ann Arbor, MI 48106

PLEASE NOTE:

In all cases this material has been filmed in the best possible way from the available copy. Problems encountered with this document have been identified here with a check mark __✓__.

1. Glossy photographs or pages __✓__
2. Colored illustrations, paper or print _____
3. Photographs with dark background __✓__
4. Illustrations are poor copy _____
5. Pages with black marks, not original copy _____
6. Print shows through as there is text on both sides of page _____
7. Indistinct, broken or small print on several pages __✓__
8. Print exceeds margin requirements _____
9. Tightly bound copy with print lost in spine _____
10. Computer printout pages with indistinct print _____
11. Page(s) _____ lacking when material received, and not available from school or author.
12. Page(s) _____ seem to be missing in numbering only as text follows.
13. Two pages numbered _____. Text follows.
14. Curling and wrinkled pages _____
15. Dissertation contains pages with print at a slant, filmed as received __✓__
16. Other _____

_____

_____

MODELING AND PERFORMANCE OF AN INTEGRATED SIX-PORT REFLECTOMETER OPERATED WITH PULSED SIGNALS

by

Gabriel-Dumitru Colef

A dissertation submitted to the Graduate Faculty in Engineering in partial fulfillment of the degree of Doctor of Philosophy, The City University of New York.

1988

This manuscript has been read and accepted for the Graduate Faculty in Engineering in satisfaction of the dissertation requirement for the degree of Doctor of Philosophy.

April 22, 1988
Date

Morris Ettenberg
Chair of Examining Committee

4/22/88
Date

Jacques E. Benveniste
Executive Officer

Prof. Paul R. Karmel

Prof. Samir Ahmed

Prof. Ping Ho

Prof. Morris Ettenberg, Chair
Supervisory Committee

The City University of New York

ABSTRACT

MODELING AND PERFORMANCE OF AN INTEGRATED SIX-PORT REFLECTOMETER OPERATED WITH PULSED SIGNALS

by

Gabriel-Dumitru Colef

Adviser: Professor M. Ettenberg

The research presented here introduces the modeling of an integrated six-port reflectometer and the operation of a microstrip integrated six-port reflectometer using pulsed signals.

The research presents the modeling of an integrated six-port reflectometer using a powerful CAD program, called MIDAS, developed at the SRI David Sarnoff Research Center. The program is capable of simulating networks with any number of ports, and further integrate them into larger networks. A six-port configuration, that consists of quadrature hybrids and an in-phase power divider, is simulated on MIDAS. The six-port reflectometer operation is modeled using two approaches.

One approach uses power ratios obtained from MIDAS directly, and the other one uses the S-parameters obtained from MIDAS to calculate the power ratios, which are needed to calibrate the six-port and to perform measurements of different loads. The six-port reflectometer is modeled for frequencies from 7 GHz to 9 GHz and measurements of reflection coefficients for various loads are reported.

The pulsed operation of a microstrip six-port reflectometer using diode detectors is investigated. The circuit configuration, the calibration and measurement procedures are presented. The operation of the six-port reflectometer is investigated under CW and pulsed signals operation conditions. The CW performance is investigated over the band of frequencies from 2 GHz to 14 GHz, and measurements of reflection coefficients for different loads are reported. The diode calibration procedure is also addressed, and two new techniques are introduced. The operation of the six-port reflectometer with pulsed signals is investigated and results with pulse widths as low as 3 microseconds are presented. Different peak detectors are presented and the problems associated with their use in six-port reflectometers operated with pulsed signals are discussed. All the measurement results are compared to the ones given by an HP-8409 Automatic Network Analyzer.

ACKNOWLEDGEMENTS

I wish to express my sincere gratitude to my mentor, Professor Morris Ettenberg for his expert counsel and constant encouragement throughout this research.

In addition, I wish to especially thank Professor Paul R. Karmel for his continuous support, expert advice and encouragement.

I wish to express my gratitude to Mr. Bernard Schwartz, Chief Executive Officer, LORAL Corporation, for supporting me as the first LORAL Fellow, and also for his generous donation of the LORAL Microwave Laboratory at The City College of New York, where all the research took place. I also appreciate the help of Mr. Joseph Browdy, Vice-President, LORAL Electronic Systems.

I wish to express my gratitude to the SRI David Sarnoff Research Center for allowing me to use their simulation program MIDAS and to Dr. Raymond L. Camisa who assisted me in using their facilities.

I especially wish to thank my brother Michael for his counseling and support.

Finally, I wish to thank my parents, Ivan and Jana-Ioana, for their love, encouragement, patience and support.

To my family

TABLE OF CONTENTS

LIST OF TABLES

LIST OF ILLUSTRATIONS

1. THE SIX-PORT MEASUREMENT CONCEPT

1.1. THEORETICAL BACKGROUND

The concept of power measurements for determining the phase as well as the magnitude of the reflection coefficient or any other complex parameter of a network, came from the need for a measurement technique which did not require components approaching the ideal, and was also less time consuming [1,4]. The advantage of the six-port measurement technique over the existing technique is the fact that power measurements are easier to perform than amplitude and phase measurements.

1.1.1. INTRODUCTION

Consider a known vector a_1 and an unknown vector a_2. These vectors may be voltages on a transmission line [2,3,6] or any phasor. A graphical representation of the two vectors is given in Fig.1.1-1. We are interested in using only magnitudes of vectors in order to find the phase angle of the unknown vector a_2 with

respect to the reference one a_1. Looking at the magnitudes of the sum and the difference of the two vectors, we get:

$$|a_1 + a_2|^2 = |a_1|^2 + |a_2|^2 + 2 \cdot |a_1 \cdot a_2| \cdot \cos\Phi \qquad (1.1-1)$$

$$|a_1 - a_2|^2 = |a_1|^2 + |a_2|^2 - 2 \cdot |a_1 \cdot a_2| \cdot \cos\Phi \qquad (1.1-2)$$

We also need information about $\sin\Phi$ in order to be able to completely specify Φ without any ambiguity in sign or quadrant. A convenient way of getting $\sin\Phi$ is to rotate a_2 by 90 degrees and add or subtract the rotated vector to or from the reference one, respectively. This operation is depicted in Fig.1.1-2. Thus, we have:

$$|a_1 - ja_2|^2 = |a_1|^2 + |a_2|^2 + 2 \cdot |a_1 \cdot a_2| \sin\Phi \qquad (1.1-3)$$

$$|a_1 + ja_2|^2 = |a_1|^2 + |a_2|^2 - 2 \cdot |a_1 \cdot a_2| \sin\Phi \qquad (1.1-4)$$

We see from the onset that the equations (1.1-1) to (1.1-4) are not independent, since the sum of equations (1.1-1) and (1.1-2) is equal to the sum of equations (1.1-3) and (1.1-4). Therefore, we need only three of the above equations to determine the value of Φ. Let:

$$P_1 = |a_1 - a_2|^2 = |a_1|^2 + |a_2|^2 - 2|a_1 a_2| \cos\Phi \qquad (1.1-5)$$

$$P_2 = |a_1 + a_2|^2 = |a_1|^2 + |a_2|^2 + 2|a_1 a_2| \cos\Phi \qquad (1.1-6)$$

$$P_3 = |a_1 - ja_2|^2 = |a_1|^2 + |a_2|^2 + 2|a_1 a_2| \sin\Phi \qquad (1.1-7)$$

$$P_4 = |a_1 + ja_2|^2 = |a_1|^2 + |a_2|^2 - 2|a_1 a_2| \sin\Phi \qquad (1.1-8)$$

The phase angle Φ may be found by obtaining both $\cos\Phi$ and $\sin\Phi$ from the above equations as follows:

$$\cos\Phi = \frac{P_2 - P_1}{4 \cdot |a_1 \cdot a_2|} \qquad (1.1-9)$$

$$\sin\Phi = \frac{P_3 - P_4}{4 \cdot |a_1 \cdot a_2|} \qquad (1.1-10)$$

Since we have :

$$P_1 + P_2 = P_3 + P_4 \qquad (1.1-11)$$

we solve for P_4 :

$$P_4 = P_1 + P_2 - P_3 \qquad (1.1-11a)$$

Therefore, equation (1.1-10) becomes:

$$\sin\Phi = \frac{2P_3 - P_1 - P_2}{4 \cdot |a_1 \cdot a_2|} \qquad (1.1-12)$$

Thus, knowing the magnitude of the two vectors and a proper combination of magnitude measurements, the phase angle of the unknown vector may be determined. We could also use equations (1.1-1) and (1.1-2) to find the magnitude of the unknown vector a_2, if we know the a_1 vector. Adding equations (1.1-1) and (1.1-2), we get:

$$P_1 + P_2 = 2 \cdot |a_1|^2 + 2 \cdot |a_2|^2 \qquad (1.1-13a)$$

Therefore:

$$|a_2| = \sqrt{\frac{P_1 + P_2}{2} - |a_1|^2} \qquad (1.1-13b)$$

In this case the proper combination of magnitude measurements was obtained by taking the magnitudes of the sum of the vectors, the difference of the vectors, and then the sum and the difference of the unknown vector, rotated by 90 degrees, to and from the known vector, respectively. A similar set of combinations of power measurements may be obtained by rotating the unknown vector by two arbitrary number of degrees θ_1, θ_2. The equations obtained in this case are:

$$P'_1 = \left| a_1 - a_2 e^{j\theta_1} \right|^2 = |a_1|^2 + |a_2|^2 - 2|a_1 a_2| \cos(\theta_1 + \Phi) \qquad (1.1-14a)$$

$$P'_2 = \left| a_1 + a_2 e^{j\theta_1} \right|^2 = |a_1|^2 + |a_2|^2 + 2|a_1 a_2| \cos(\theta_1 + \Phi) \qquad (1.1-14b)$$

$$P'_3 = \left| a_1 - a_2 e^{j\theta_2} \right|^2 = |a_1|^2 + |a_2|^2 - 2|a_1 a_2| \cos(\theta_2 + \Phi) \qquad (1.1-14c)$$

$$P'_4 = \left| a_1 + a_2 e^{j\theta_2} \right|^2 = |a_1|^2 + |a_2|^2 + 2|a_1 a_2| \cos(\theta_2 + \Phi) \qquad (1.1-14d)$$

Solving for $\cos(\theta_1 - \Phi)$ and $\cos(\theta_2 - \Phi)$:

$$\cos(\theta_1 + \Phi) = \frac{P'_2 - P'_1}{4|a_1 a_2|} \qquad (1.1-14e)$$

$$\cos(\theta_2 + \Phi) = \frac{P'_4 - P'_3}{4|a_1 a_2|} \qquad (1.1-14f)$$

Also:

$$\cos(\theta_1 + \Phi) = \cos\theta_1 \cos\Phi - \sin\theta_1 \sin\Phi$$

$$\cos(\theta_2 + \Phi) = \cos\theta_2 \cos\Phi - \sin\theta_2 \sin\Phi$$

The above system of linear equations in the unknowns $\cos\Phi$ and $\sin\Phi$ can be solved by Kramer's rule. The choice of angles by which the unknown vector is rotated is limited only by the condition that the determinant of the system's matrix be different than zero. This condition is satisfied when:

$$\theta_1 \neq \theta_2 + k\,180^0$$

The four magnitude measurements are not independent,

and can be reduced to only three by noticing that:

$$P'_1 + P'_2 = P'_3 + P'_4$$

When the vectors represent complex magnitudes of propagating waves, the magnitude measurements become power measurements, and a proper set of power measurements suffices to determine the relative phase angle of one propagating wave to the other. In the next section it is shown that an arbitrary network may be used to derive enough power measurements to achieve the desired phase angle determination at an unknown port.

1.1.2. S-PARAMETER APPROACH

Suppose that we are dealing with a microwave junction with six ports out of which one is considered to be the input port, one is the output port, and the remaining four ports are power measurement ports with the object of determining the reflection coefficient at the output port. The six-port junction is shown in Fig.1.1-3 in which the four power meters are not matched. On the input side consider only the normalizing input wave a_1, which is dependent on the input wave a_i and the source reflection coefficient Γ_s:

$$a_1 = a_i + \Gamma_s b_1$$

In doing so, there is no loss of generality of the conclusions we draw. Let the reflection coefficient at the power meter i be Γ_i, i=3,4,5,6. Using the S-parameter representation of the sixport network, we have:

$$\underline{b} = [S]\underline{a} \qquad (1.1-15)$$

where $\underline{b} = [b_1 b_2 \ldots b_6]^t$

and $\underline{a} = [a_1 a_2 \ldots a_6]^t$

where t means transpose, i.e. $\underline{a}$ and $\underline{b}$ are column vectors. We also have:

$$a_j = \Gamma_j b_j, \qquad j = 3,4,5,6$$

We also define Γ by: $a_2 = \Gamma b_2$, where Γ is the reflection coefficient looking into the device under test (DUT).

The system of equations in (1.1-15) becomes;

$$b_j = a_1 S_{j1} + S_{j2}\Gamma b_2 + \sum_{k=3}^{6} S_{jk}\Gamma_k b_k \qquad (1.1-16)$$

The derivation of the expressions of the waves b_j, $j = 3,4,5,6$ in terms of Γ and the normalizing input wave is given in Appendix A. Appendix A also contains the derivation of the power equations at ports 3,4,5, and 6.

Therefore, we have:

$$P_3 = A'_3 \frac{|1 - q_3\Gamma|^2}{|1 - q\Gamma|^2} P_{in} \qquad (1.1-17)$$

$$P_4 = A'_4 \frac{|\Gamma - q_4|^2}{|1 - q\Gamma|^2} P_{in} \qquad (1.1-18)$$

$$P_5 = A'_5 \frac{|\Gamma - q_5|^2}{|1 - q\Gamma|^2} P_{in} \qquad (1.1-19)$$

$$P_6 = A'_6 \frac{|\Gamma - q_6|^2}{|1 - q\Gamma|^2} P_{in} \qquad (1.1-20)$$

In order to eliminate P_{in}, we take the ratio of equations (1.1-18) through (1.1-20) to equation (1.1-17) and we get:

$$\frac{P_4}{P_3} = A_4 \frac{|\Gamma - q_4|^2}{|1 - q_3\Gamma|^2} \qquad (1.1-21)$$

$$\frac{P_5}{P_3} = A_5 \frac{|\Gamma - q_5|^2}{|1 - q_3\Gamma|^2} \qquad (1.1-22)$$

$$\frac{P_6}{P_3} = A_6 \frac{|\Gamma - q_6|^2}{|1 - q_3\Gamma|^2} \qquad (1.1-23)$$

where $A_j = A'_j/A'_3$, $j = 4,5,6$.

Thus, any six-port reflectometer may be characterized by a set of power equations of the form of those in (1.1-21) through (1.1-23).

In general, all the parameters A_i, $i = 4,5,6$ and q_j, $j = 3,4,5,6$ are frequency dependent. They are not known to the user, and therefore, have to be calculated by the use of an appropriate technique. This technique is called the calibration of the six-port and will be discussed in section 1.2.2.

The three equations (1.1-21) through (1.1-23) represent circles in the Γ-plane. A proof that these equations are circles and the derivation of the expressions for their centers and radii is given in Appendix B. Since $\Gamma_1 = x - jy$ satisfies all three equations, then the three circles representing the above mentioned equations intersect in only one point. Knowing the eleven real parameters involved in the above equations A_i, $i = 4,5,6$, and $Re\{q_n\}$ and $Im\{q_n\}$, $n = 3,4,5,6$, allows us to solve for the unknown reflection coefficient $\Gamma_1 = x - jy$. Through

calibration, the eleven real parameters are determined and the only varying quantities in the circle equations are the power ratios P_j/P_3, $j=4,5,6$ and the reflection coefficient corresponding to those power ratios, $\Gamma_l = x + jy$. Consider the following procedure. We take the power ratios obtained after measuring the powers corresponding to some unknown load (DUT), and substitute them into the expressions for the centers and radii of the three circles. The circles will intersect at a single point, which gives the unknown load reflection coefficient Γ_l. This is proven from the fact that the expressions for the power ratios are given by equations (1.1-21) to (1.1-23). Thus, for any load reflection coefficient Γ_l, the power ratios are related to Γ_l through the parameters A_i, $i=4,5,6$ and q_j, $j=3,4,5,6$ via equations (1.1-21) through (1.1-23). Γ is a point on each of the three circles, and, therefore, represents the unique point of intersection.

In other words, for any load reflection coefficient Γ_l, we measure powers and calculate power ratios, which satisfy:

$$p_i = \frac{P_i}{P_3} = A_i \frac{|\Gamma_l - q_i|^2}{|1 - q_3 \Gamma_l|^2} \quad , \quad i = 4,5,6$$

Since r_i satisfies all three equations, it is the unique solution. The uniqueness of the solution is given by the fact that three circles may have at most one common point, provided they are not identical, or their centers do not lie on a straight line.

In practical situations when measurements are corrupted by noise, the measured power may differ from the actual power, that should have been obtained if noise had not been present. This error in powers influences the position of the centers and radii of the three circles. Therefore, the circles may not have any common point. A geometrical condition that two circles intersect is that the distance between their centers be smaller than the sum of the radii of the two circles. If the three circles satisfy the above condition taken two at a time, then they will intersect. If measurements are corrupted by noise, then the condition for intersection may be violated and we have no intersection. That represents the worst case condition and some averaging methods must be employed in order to estimate the solution.

1.1.3. S-PARAMETER APPROACH WITH MATCHED POWER METERS

Consider the six-port network in Fig.1.1-3, in which ports 3,4,5, and 6 are matched. Therefore:

$$a_3 = a_4 = a_5 = a_6 = 0$$

The representation of the six-port network using S-parameters is the following:

$$\underline{b} = [S]\underline{a} \qquad (1.1-24)$$

where: $\underline{b} = [b_1 b_2 b_3 b_4 b_5 b_6]^t$

$\underline{a} = [a_1 a_2 a_3 a_4 a_5 a_6]^t$

Thus:

$$b_j = S_{j1} a_1 + S_{j2} a_2 \quad , \quad j = 1,2,\ldots 6 \qquad (1.1-25)$$

We define $\Gamma = a_2/b_2$, where Γ is the reflection coefficient looking into the device under test.

Equation (1.1-25) for j=2 becomes:

$$b_2 = S_{21} a_1 + S_{22} \Gamma b_2 \qquad (1.1-26)$$

Solving for b_2, we get:

$$b_2 - S_{22} \Gamma b_2 = S_{21} a_1$$

$$b_2 (1 - S_{22} \Gamma) = S_{21} a_1$$

$$b_2 = \frac{S_{21} a_1}{1 - \Gamma S_{22}} \qquad (1.1-27)$$

Therefore:

$$a_2 = \frac{\Gamma S_{21}}{1 - \Gamma S_{22}} a_1 \qquad (1.1-28)$$

By substituting (1.1-28) into (1.1-25) for j=3,4,5,6 we get:

$$b_j = S_{j1} a_1 + \frac{S_{j2} S_{21} \Gamma}{1 - \Gamma S_{22}} a_1 \qquad (1.1-29)$$

Knowing that $a_j = 0,\ j = 3,4,5,6$, the powers at ports 3, 4, 5, and 6 are given by:

$$P_j = \frac{1}{2}|b_j|^2 - \frac{1}{2}|a_j|^2 = \frac{1}{2}|b_j|^2 \qquad (1.1-30)$$

and letting $P_{in} = |a_1|^2/2$, we get:

$$P_3 = \frac{1}{2}|b_3|^2 = \left|\frac{S_{31} - (S_{31}S_{22} - S_{32}S_{21})\Gamma}{1 - S_{22}\Gamma}\right|^2 P_{in} \qquad (1.1-31)$$

$$P_4 = \frac{1}{2}|b_4|^2 = \left|\frac{S_{41} - (S_{41}S_{22} - S_{42}S_{21})\Gamma}{1 - S_{22}\Gamma}\right|^2 P_{in} \qquad (1.1-32)$$

$$P_5 = \frac{1}{2}|b_5|^2 = \left|\frac{S_{51} - (S_{51}S_{22} - S_{52}S_{21})\Gamma}{1 - S_{22}\Gamma}\right|^2 P_{in} \qquad (1.1-33)$$

$$P_6 = \frac{1}{2}|b_6|^2 = \left|\frac{S_{61} - (S_{61}S_{22} - S_{62}S_{21})\Gamma}{1 - S_{22}\Gamma}\right|^2 P_{in} \qquad (1.1-34)$$

In order to make the results in equations (1.1-31) through (1.1-34) independent of P_{in}, we take the ratio of P_4, P_5, and P_6 to P_3.

$$\frac{P_4}{P_3} = \frac{|S_{41}S_{22} - S_{42}S_{21}|^2}{|S_{31}S_{22} - S_{32}S_{21}|^2} \cdot \frac{\left|\Gamma - \frac{S_{41}}{S_{41}S_{22} - S_{42}S_{21}}\right|^2}{\left|\Gamma - \frac{S_{31}}{S_{31}S_{22} - S_{32}S_{21}}\right|^2} \qquad (1.1-35)$$

$$\frac{P_5}{P_3} = \frac{|S_{51}S_{22} - S_{52}S_{21}|^2}{|S_{31}S_{22} - S_{32}S_{21}|^2} \cdot \frac{\left|\Gamma - \frac{S_{51}}{S_{51}S_{22} - S_{52}S_{21}}\right|^2}{\left|\Gamma - \frac{S_{31}}{S_{31}S_{22} - S_{32}S_{21}}\right|^2} \qquad (1.1-36)$$

$$\frac{P_6}{P_3} = \frac{|S_{61}S_{22} - S_{62}S_{21}|^2}{|S_{31}S_{22} - S_{32}S_{21}|^2} \cdot \frac{\left|\Gamma - \frac{S_{61}}{S_{61}S_{22} - S_{62}S_{21}}\right|^2}{\left|\Gamma - \frac{S_{31}}{S_{31}S_{22} - S_{32}S_{21}}\right|^2} \qquad (1.1-37)$$

Equations (1.1-35) through (1.1-37) may be written in a general form as:

$$\frac{P_4}{P_3} = A'_4 \frac{|\Gamma - q'_4|^2}{|\Gamma - q'_3|^2} \qquad (1.1-38)$$

$$\frac{P_5}{P_3} = A'_5 \frac{|\Gamma - q'_5|^2}{|\Gamma - q'_3|^2} \qquad (1.1-39)$$

$$\frac{P_6}{P_3} = A'_6 \frac{|\Gamma - q'_6|^2}{|\Gamma - q'_3|^2} \qquad (1.1-40)$$

where:

$$A'_j = \frac{|S_{j1}S_{22} - S_{j2}S_{21}|^2}{|S_{31}S_{22} - S_{32}S_{21}|^2} \quad , \quad j = 4,5,6$$

$$q'_n = \frac{S_{n1}}{S_{n1}S_{22} - S_{n2}S_{21}} \quad , \quad n = 3,4,5,6$$

The constants A'_j, $j = 4,5,6$ take positive real values, and q_n, $n = 3,4,5,6$ are complex numbers.

In some six-port networks the q_3 parameter may go to infinity at some frequencies. This occurs when:

$$S_{31}S_{22} - S_{32}S_{21} = 0 \qquad (1.1-41)$$

This condition is satisfied by networks with either

$$S_{32} = S_{22} = 0$$

or

$$\frac{S_{31}}{S_{32}} = \frac{S_{21}}{S_{22}}$$

The first condition of $S_{32}=0$ means that the transmission coefficient from port 2 to port 3 is zero, or port 3 is isolated from port 2. $S_{22}=0$ means that the reflection coeficient looking into port 2 is zero, i.e. port 2 is matched. These conditions may be satisfied by a variety of six-port networks. Examples of such networks are given in sections 1.2.1. and 2.2.1.

The parameters S_{31} and S_{21} are not zero in a useful six-port network, because we need nonzero transmission paths between the input and all the other five ports 2,3,4,5, and 6, in general.

If the q_3 parameter goes to infinity, the above set of power equations is not useful. Another way of representing the six-port network is using the following set of power equations, obtained from equations (1.1-35) through (1.1-37):

$$\frac{P_4}{P_3} = A_4 \frac{|\Gamma - q_4|^2}{|1 - q_3\Gamma|^2} \qquad (1.1-42)$$

$$\frac{P_5}{P_3} = A_5 \frac{|\Gamma - q_5|^2}{|1 - q_3\Gamma|^2} \qquad (1.1-43)$$

$$\frac{P_6}{P_3} = A_6 \frac{|\Gamma - q_6|^2}{|1 - q_3\Gamma|^2} \qquad (1.1-44)$$

where:

$$A_j = \frac{|S_{j1}S_{22} - S_{j2}S_{21}|^2}{|S_{31}|^2} \quad , \quad j = 4,5,6$$

$$q_n = \frac{S_{n1}}{S_{n1}S_{22} - S_{n2}S_{21}} \quad , \quad n = 4,5,6$$

$$q_3 = \frac{S_{31}S_{22} - S_{32}S_{21}}{S_{31}}$$

The new q_3 does not go to infinity because S_{31} is not zero in any six-port network to be used as a reflectometer.

The parameters q_n do not go to infinity because S_{n1}, S_{21}, S_{n2} are not zero. Ports 4, 5, and 6 are used to compare the input wave with the reflected wave, therefore, we need nonzero transmission paths between these ports, the input port, and the output port. In the case in which at least one of the ports 4, 5, or 6

does not satisfy these conditions, see q_3 case, the same procedure used for q_3 will be employed for that particular q-point.

The equations that we obtained (1.1-42) to (1.1-44) are identical with equations (1.1-21) to (1.1-23), as expected because the second set was obtained in a more general case. Equations (1.1-42) to (1.1-44) are a particular case of (1.1-21) to (1.1-23). The importance of (1.1-42) to (1.1-44) is that they give the dependence of the A_j, $j=4,5,6$ and q_n, $n=3,4,5,6$ parameters on the S-parameters of the six-port network in the case of matched power detectors ($\Gamma_i=0$, $i=3,4,5,6$). Therefore, it is possible to simulate or calculate the performance of various networks to be evaluated as six-ports.

1.1.4. DISCUSSION OF FOUR-PORT AND FIVE-PORT VERSUS SIX-PORT NETWORKS

A four-port microwave network is shown in Fig.1.1-4. Using the S-parameter approach we have:

$$\begin{pmatrix} b_1 \\ b_2 \\ b_3 \\ b_4 \end{pmatrix} = \begin{pmatrix} S_{11} & S_{12} & S_{13} & S_{14} \\ S_{21} & S_{22} & S_{23} & S_{24} \\ S_{31} & S_{32} & S_{33} & S_{34} \\ S_{41} & S_{42} & S_{43} & S_{44} \end{pmatrix} \cdot \begin{pmatrix} a_1 \\ a_2 \\ a_3 \\ a_4 \end{pmatrix} \qquad (1.1-45)$$

We define $\Gamma_j = a_j/b_j,\ j=3,4$ as the reflection coefficient looking into the power meters connected at ports 3 and 4. The system of equations (1.1-45) becomes:

$$\begin{pmatrix} b_1 \\ b_2 \\ b_3 \\ b_4 \end{pmatrix} = \begin{pmatrix} S_{11} & S_{12} & S_{13} & S_{14} \\ S_{21} & S_{22} & S_{23} & S_{24} \\ S_{31} & S_{32} & S_{33} & S_{34} \\ S_{41} & S_{42} & S_{43} & S_{44} \end{pmatrix} \begin{pmatrix} a_1 & \\ a_2 & \\ \Gamma_3 & b_3 \\ \Gamma_4 & b_4 \end{pmatrix} \qquad (1.1-46)$$

The expression of b_3 and b_4 are the following:

$$b_3 = S_{31}a_1 + S_{32}a_2 + S_{33}\Gamma_3 b_3 + S_{34}\Gamma_4 b_4 \qquad (1.1-47)$$

$$b_4 = S_{41}a_1 + S_{42}a_2 + S_{43}\Gamma_3 b_3 + S_{44}\Gamma_4 b_4 \qquad (1.1-48)$$

b_3 and b_4 waves may be expressed in terms of the a_2 and b_2 waves, since their ratio defines the reflection coefficient at port 2 looking into the load:

$$\Gamma = \frac{a_2}{b_2}$$

Looking at the expression for b_2:

$$b_2 = S_{21}a_1 + S_{22}a_2 + S_{23}\Gamma_3 b_3 + S_{24}\Gamma_4 b_4 \qquad (1.1-49)$$

Solving for a_1 in equation (1.1-49), we find:

$$a_1 = \frac{1}{S_{21}} \cdot \left(b_2 - S_{22}a_2 - S_{23}\Gamma_3 b_3 - S_{24}\Gamma_4 b_4\right) \qquad (1.1-50)$$

Substituting (1.1-50) into (1.1-47) and (1.1-48), we get:

$$b_3 = A' a_2 + B' b_2 \qquad (1.1-51)$$

$$b_4 = C' a_2 + D' b_2 \qquad (1.1-52)$$

where A', B', C', D' are complex constants which are functions of the S-parameters of the junction and the reflection coefficients looking into the power meters connected at ports 3 and 4. Therefore, the b waves at ports 3 and 4 of a four-port microwave junction may be expressed in terms of the waves at port 2 as shown in equations (1.1-51) and (1.1-52).

The powers at ports 3 and 4 are given by:

$$P_3 = \frac{1}{2}|b_3|^2 - \frac{1}{2}|a_3|^2 = \frac{1}{2}\left(1 - |\Gamma_3|^2\right)|b_3|^2 \qquad (1.1-53)$$

$$P_4 = \frac{1}{2}|b_4|^2 - \frac{1}{2}|a_4|^2 = \frac{1}{2}\left(1 - |\Gamma_4|^2\right)|b_4|^2 \qquad (1.1-54)$$

Substituting (1.1-51) and (1.1-52) into (1.1-53) and (1.1-54) respectively, we get:

$$P_3 = |Aa_2 + Bb_2|^2 \qquad (1.1-55)$$

$$P_4 = |Ca_2 + Db_2|^2 \qquad (1.1-56)$$

where:

$$A = A' \sqrt{\frac{1 - |\Gamma_3|^2}{2}} \qquad (1.1-57a)$$

$$B = B' \sqrt{\frac{1 - |\Gamma_3|^2}{2}} \qquad (1.1-57b)$$

$$C = C' \sqrt{\frac{1 - |\Gamma_4|^2}{2}} \qquad (1.1-57c)$$

$$D = D' \sqrt{\frac{1 - |\Gamma_4|^2}{2}} \qquad (1.1-57d)$$

Substituting (1.1-48) into (1.1-55) and (1.1-56), we get:

$$P_3 = |A\Gamma + B|^2 |b_2|^2 \qquad (1.1-58)$$

$$P_4 = |C\Gamma + D|^2 |b_2|^2 \qquad (1.1-59)$$

Taking the ratio of equations (1.1-58) and (1.1-59) in order to eliminate $|b_2|^2$ which is not known to us, we obtain:

$$\frac{P_4}{P_3} = \frac{|C\Gamma + D|^2}{|A\Gamma + B|^2} \qquad (1.1-60)$$

Since Γ is a complex parameter, it cannot be completely determined from a single equation which involves absolute values, like (1.1-60). For some specific cases in which either A = D = 0 or C = B = 0, it is possible to determine only the magnitude of the reflection coefficient. Due to equations (1.1-57), A and D are zero if A' and D' are zero. Similarly, C and B are zero if C' and B' are zero. The conditions that A' and D' be zero, or C' and B' be zero require the junction to have S-parameters that satisfy certain conditions. These conditions are derived in Appendix C. These conditions, for Γ_3 and Γ_4 equal to zero, are:

$$S_{32}S_{21} - S_{31}S_{22} = 0 \qquad (1.1-61)$$

and

$$S_{41} = 0 \qquad (1.1-62)$$

The first condition (1.1-61) will be satisfied if $S_{22} = 0$ and $S_{32} = 0$, which means that port 3 is isolated from port 2 and that port 2 is matched (the reflection coefficient looking into port 2 is equal to zero). The other possible solutions are ruled out because S_{21} must not be zero and S_{31} must not be zero if S_{32} is zero. These conditions have to be satisfied because we need a nonzero transmission path between the input port (port 1) and the output port (port 2), and also a nonzero transmission path between ports 1 and 3 when ports 2 and 3 are isolated. We need these nonzero paths because the powers at the measuring ports are supposed to be linear combinations of the incident and reflected waves at the load. The condition (1.1-62) means that port 4 is isolated from port 1. Summing up all of the above conditions, we have characteristics similar to a directional coupler.

The conditions regarding C' and B' reduce to a similar set of conditions, thus, requiring that the junction be similar to a directional coupler with S-matrix:

$$S = \begin{pmatrix} 0 & S_{12} & S_{13} & 0 \\ S_{21} & 0 & 0 & S_{24} \\ S_{31} & 0 & 0 & S_{34} \\ 0 & S_{42} & S_{43} & 0 \end{pmatrix} \qquad (1.1-63)$$

We see that equation (1.1-60) and , therefore, the junction in Fig.1.1-4 are not enough, in general, to completely specify the reflection coefficient $\Gamma = a_2/b_2$. Therefore, a four-port network cannot be used for measurements of Γ.

Introducing one more port as shown in Fig.1.1-5, and following a derivation similar to the one at the beginning of this section, we conclude that:

$$P_3 = |Aa_2 + Bb_2|^2 \qquad (1.1-64)$$

$$P_4 = |Ca_2 + Db_2|^2 \qquad (1.1-65)$$

$$P_5 = |Ea_2 + Fb_2|^2 \qquad (1.1-66)$$

where A, B, C, D, E, and F are complex constants which are functions of the S-parameters of the five-port junction and the reflection coefficients looking into the power meters connected at ports 3, 4, and 5. Substituting $\Gamma = a_2/b_2$ in equations (1.1-64) to (1.1-66), we get:

$$P_3 = |A''\Gamma + B''|^2 |b_2|^2 \qquad (1.1-67)$$

$$P_4 = |C''\Gamma + D''|^2 |b_2|^2 \qquad (1.1-68)$$

$$P_5 = |E''\Gamma + F''|^2 |b_2|^2 \qquad (1.1-69)$$

Taking the ratio of equations (1.1-68) and (1.1-69) to equation (1.1-67), in order to get rid of the $|b_2|^2$, we get:

$$\frac{P_4}{P_3} = A'_4 \frac{|\Gamma - q'_4|^2}{|1 - q'_3\Gamma|^2} \qquad (1.1-70)$$

$$\frac{P_5}{P_3} = A'_5 \frac{|\Gamma - q'_5|^2}{|1 - q'_3\Gamma|^2} \qquad (1.1-71)$$

where:

$$A'_4 = \frac{C''}{B''} \quad , \qquad A'_5 = \frac{E''}{B''}$$

$$q'_3 = -\frac{A''}{B''} \quad , \qquad q'_4 = -\frac{D''}{C''} \quad , \qquad q'_5 = -\frac{F''}{E''} \quad .$$

In Appendix B, it is shown that equations (1.1-70) and (1.1-71) represent circles in the Γ-plane. A graphical interpretation is shown in Fig.1.1-6. Since Γ satisfies both equations, it represents the intersection of the two circles. Two circles intersect in one or two points. In general, the two intersecting circles represented by the above equations have two points in common, as shown in Fig.1.1-6. Therefore, the set of equations given by (1.1-70) and (1.1-71) has two solutions. Because of this ambiguity in the solution for the reflection coefficient, the five-port junction is not a very attractive network. The use of the five-port junction as a reflectometer may be limited by the need to know if the device under test is passive or active. Once we know that, we may choose the solution that lies either inside or outside the unit circle,

respectively. Both intersections of the circles may fall either inside or outside the unit circle, in which case the five-port cannot be used as a reflectometer at all. In order to eliminate any ambiguity, an additional power detector is needed.

Following a similar procedure as before, we conclude that the powers at the ports of the junction shown in Fig.1.1-7 are given by:

$$P_3 = |A^\circ a_2 + B^\circ b_2|^2 \qquad (1.1-72)$$

$$P_4 = |C^\circ a_2 + D^\circ b_2|^2 \qquad (1.1-73)$$

$$P_5 = |E^\circ a_2 + F^\circ b_2|^2 \qquad (1.1-74)$$

$$P_6 = |G^\circ a_2 + H^\circ b_2|^2 \qquad (1.1-75)$$

where A°, B°, C°, D°, E°, F°, G°, and H° are complex constants which depend on the S-parameters of the six-port junction and the reflection coefficients looking into the power meters connected to ports 3, 4, 5 and 6. Substituting $\Gamma = a_2/b_2$ and taking the ratio of equations (1.1-73) through (1.1-75) to equation (1.1-72), in order to get rid of the $|b_2|^2$ term, we get:

$$\frac{P_4}{P_3} = A_4 \frac{|\Gamma - q_4|^2}{1 - q_3\Gamma|^2} \qquad (1.1-76)$$

$$\frac{P_5}{P_3} = A_5 \frac{|\Gamma - q_5|^2}{1 - q_3\Gamma|^2} \qquad (1.1-77)$$

$$\frac{P_6}{P_3} = A_6 \frac{|\Gamma - q_6|^2}{1 - q_3\Gamma|^2} \qquad (1.1-78)$$

These equations represent three circles in the Γ -plane. A discussion of their intersection and the uniqueness of the solution for Γ is given in section 1.1.2. Fig.1.1-8 gives a graphical interpretation of equations (1.1-76) to (1.1-78).

The six-port reflectometer is superior to the five-port reflectometer in the fact that it eliminates any ambiguity in the solution for Γ.

To summarize this section, we may say that as we introduce more ports for measurement of power, more information is gained towards the complete specification of the reflection coefficient:

1. A four-port microwave junction, which was determined to be a directional coupler, geved enough information for determining the magnitude of Γ.

2. A five-port microwave junction may be used to determine the magnitude and phase of Γ for passive devices.

3. A six-port microwave junction may be used to determine the magnitude and phase of Γ for any device under test, may that be passive or active.

1.2. THE SIX-PORT MEASUREMENT CONCEPT AND ITS DEVELOPMENT

The concept of six-port measurements stems from the idea of Engen and Hoer [1] to use power measurements to determine the phase of the reflection coefficient or any parameter of a network. This idea was born from the need for a measurement technique which required very few "ideal" components, was less time consuming, and was simpler than the existing techniques.

The real advantage of the six-port reflectometers over the existing automatic network analyzers (ANA's) is that it is easier to measure amplitude, which is the square root of the power, than to measure both amplitude and phase. This advantage becomes more important at high frequencies where the measurement of the phase is very difficult. To measure phase, the existing ANA techniques employ down conversion of frequency to a range where the phase can be measured accurately. These techniques are more complicated than the simple power measurements taken at four ports of a linear six-port junction. These power measurements are then manipulated numerically to determine the phase information.

Since 1972, when the six-port concept was introduced by G.F. Engen and C.A. Hoer [2,3,7], microwave metrologists have given more and more attention to this new technique, which proved to be just as accurate as the existing ANA's.

From the accuracy point of view, the emphasis was switched from improvement of the hardware to improvement of the software to account for the imperfections of the hardware [8].

The following review of the past and present work in this field will be divided in three parts in which circuit configurations, calibration procedures, and methods of realization of the six-port reflectometers are introduced.

1.2.1. CIRCUIT CONFIGURATIONS

Many circuit configurations were used throughout the development of the six-port measurement technique.

Engen and Hoer at the National Bureau of Standards (NBS) started their design from equations (1.1-1) through (1.1-4), and tried to implement them using standard circuit elements [6]. Therefore, they decided to use a correlator, or phase discriminator, which is a circuit which compares two incoming signals, one being known and taken as a reference, and the other one being unknown. The correlator determines the relative magnitude and phase of the unknown signal with respect to the known one. Different configurations of correlators were studied even as early as 1964 by Cohn and Weinhouse [6]. Equations illustrating the operation of a typical correlator are given in section 1.1.1. as equations (1.1-9) through (1.1-12). A correlator that implemented the equations (1.1-1) to (1.1-4) is shown in Fig.1.2-1. Using the representation of each block that is given in Fig.1.2-2, the power terms shown in Fig.1.2-1 are calculated in Appendix D. The correlator in Fig.1.2-1 is favored over other ones because of the cost problems

[6]. Using this kind of circuit as a central element, Engen and Hoer [6] developed a series of six-port network analyzers. Most of the other circuit configurations follow their design, trying to improve them [44].

In 1977, Cronson and Susman [11] used the correlator as their central element. All the references mentioned in this research paper with the exception of [17,24,25,27,29,32], use designs that follow the NBS concepts, or are variations of these configurations.

Hoer and Engen investigated the designs of six-port ANA's in 1977 [8,9,10], and, interpreting the power equations geometrically, drew important conclusions for good designs. They first discussed the sensitivity of the solution obtained by intersecting only two circles (five-port problem), and they discovered that positions of Γ_t in a direction perpendicular to the line connecting the centers of the two circles, as shown in Fig.1.1-6, have a high sensitivity to errors in $\Gamma_t - q_4$ or $\Gamma_t - q_5$. In the parallel direction (parallel to the line connecting q_4 and q_5), the sensitivity is appreciably less [9]. The addition of an extra detector (thus obtaining a six-port network) enhances the accuracy with which Γ_t may be determined. The problem of sensitivity to errors of certain positions of Γ_t is now somewhat relieved. The

positions of Γ_i in the direction perpendicular to the line connecting q_4 and q_5 in Fig.1.1-7, which were quite sensitive to errors in P_4 and P_5, will now be inferred primarily from $\Gamma_i - q_6$ which is not so sensitive to errors [9]. Thus, the best choice for positions of the centers q_4, q_5, q_6 is 120 degrees apart. This feature assures that no position of Γ_i in any direction is more sensitive to errors than others, and this sensitivity is reduced because any direction, that is perpendicular to the line connecting any two centers, is 30 degrees away from lines connecting these centers to the remaining third center. This fact ensures that no direction is more sensitive to errors than others.

The distances from the centers to the origin for each circle are important because the accuracy is decreased if the value of Γ_i is in the neighborhood of any of the centers of the circles [9]. Therefore, the magnitudes of q_4, q_5, and q_6 are best situated in the range from 0.5 to 1.5. These limits come from the fact that ill-conditioned situations will result if the distances from Γ_i to q_i, $i=4,5,6$ become too large compared to the relative distances among q_i, $i=4,5,6$ [9].

Substantial interest is shown in values of Γ_i with a nominal magnitude of unity, thus eliminating the choice of $q_i \geq 1$, $i = 4,5,6$. Too large values of q_i, $i = 4,5,6$ are not desirable from the accuracy point of view [9].

Another region of special interest is for $\Gamma_i \leq 0.3$. Therefore, the choice of $q_i \cong 1.5$ or $q_i \cong 0.5$ seem to be optimal [9].

The conclusions of Engen and Hoer [9] were that the centers of the circles representing the power equations should lie in the neighborhood of 0.5 or 1.5, and they should be 120 degrees apart in the Γ-plane, for better performance. A circuit which follows these design criteria was built by Engen [10] using only quadrature hybrids and 180 degrees hybrids, plus a 6 dB directional coupler. The circuit is shown in Fig.1.2-3. This circuit exhibited the following differences in arguments of the q-points: 135 degrees, 90 degrees, and 135 degrees, compared to the 120 degrees wanted for better performance. The 120 degrees phase difference between any two centers of the circles was not obtained because only 90 degree and 180 degree hybrids were employed, the existance of a broad band circuit which yielded 120 degrees phase shift being unknown to the author at that time [10]. In the same paper [10], the authors tried to

have a real time oscilloscope display of the results, with a very reduced accuracy. Looking at the power outputs of the six-port circuit in Fig.1.2.-3, we get:

$$P_6 = \frac{1}{2}\left| -\frac{\sqrt{3}}{4} b\left(\Gamma_l - (1-j)\sqrt{2}\right)\right|^2 \qquad (1.2-1)$$

$$P_5 = \frac{1}{2}\left| -j\frac{\sqrt{3}}{4} b\left(\Gamma_l + (1+j)\sqrt{2}\right)\right|^2 \qquad (1.2-2)$$

$$P_4 = \frac{1}{2}\left| -j\frac{b}{2}\sqrt{3}\right|^2 \qquad (1.2-3)$$

$$P_3 = \frac{1}{2}\left| \frac{\sqrt{6}}{4} b\left(\Gamma_l - j\sqrt{2}\right)\right|^2 \qquad (1.2-4)$$

Subtracting (1.2-1) from (1.2-2), we get:

$$P_5 - P_6 = \frac{3}{32}|b|^2\left\{\left|-j\left(\Gamma_l + (1+j)\sqrt{2}\right)\right|^2 - \left|\Gamma_l - (1-j)\sqrt{2}\right|^2\right\} \qquad (1.2-5)$$

Thus:

$$P_5 - P_6 = \frac{3}{32}|b|^2\sqrt{2}+Re(\Gamma_l) \qquad (1.2\text{-}6)$$

Taking the ratio of (1.2-6) to (1.2-3), we get:

$$\frac{P_5 - P_6}{P_4} = \frac{\frac{3}{8}|b|^2\sqrt{2}Re(\Gamma_l)}{\frac{3}{8}|b|^2} = \sqrt{2}Re(\Gamma_l) \qquad (1.2\text{-}7)$$

Thus:

$$Re(\Gamma_l) = \frac{P_5 - P_6}{\sqrt{2}P_4} \qquad (1.2\text{-}8)$$

Similarly:

$$Im(\Gamma_l) = \frac{P_5 + P_6 - P_3 - P_4}{2\sqrt{2}P_4} \qquad (1.2\text{-}9)$$

Since the powers P_i, $i = 3,4,5,6$ are available in analog form, one could obtain signals proportional to the real and imaginary parts of Γ_l following equation (1.2-8) and

(1.2-9), thus being able to display Γ_l visually on an oscilloscope where the x input is the result in (1.2-8), and the y input is the result in (1.2-9).

M.P. Wiedman [13] designed a semiautomated six-port for measuring millimeter-wave power and complex reflection coefficient in the 50-75 GHz range. Semiautomated meant that the frequency and switching control for the signal source were not automated. The six-port circuit that was used is shown in Fig.1.2-4. The only difference betweeen this circuit and the one suggested by Engen is that instead of the two-way, equal-phase power splitter, the author used a three-way directional coupler, since the former was not available in WR-15 waveguide size.

Another approach in the six-port circuit configuration was introduced by R.J. Collier and N.A. El-Deeb [17]. They used a microstrip three-line system, and investigated the properties of such a system. The three-line system can be used as one class of six-port reflectometer which allows an unknown impedance to be measured by using a standard impedance. The conditions for the ideal performance of such a reflectometer are that all ports be matched, and nonadjacent ports, ports 1-3 and 4-6 in Fig.1.2-5, be isolated. These two

conditions cannot be met, at the same time, by the three-line system proposed by the authors. They came up with three possible configurations out of which only one proved to be suitable for reflectometer applications. This configuration requires matching at side ports 1, 3, 4, and 6 and no transmission between ports 1-5, 2-4, 2-6, and 3-5, i.e. $S_{15} = S_{51} = S_{24} = S_{42} = S_{26} = S_{62} = S_{35} = S_{53} = 0$. Out of the many possible connections, only one proved to be suitable for six-port reflectometry. This circuit is shown in Fig.1.2-6. We notice that there are only three power measuring ports instead of four as indicated in the general six-port reflectometer theory. This circuit will have to have an input source which is very stable, in order to be able to eliminate the need to take ratios of powers (the ratios of powers are taken to eliminate the dependence of the power equations on the input power). Thus, this circuit will give three circles that represent the power equations at the three ports 3, 4, and 5, which intersect at one point with a good degree of accuracy, only if the signal source is very stable. On the other hand, the circuit could be used as a five-port reflectometer, and one has to deal with the problems shown in section 1.1.4.

Another problem with this circuit is that the positions of the three centers of the circles are far from ideal and make the performance of the circuit sensitive to errors.

A similar microstrip six-port reflectometer was made in Cairo, Egypt by N.A. El-Deeb [25]. The circuit shows a useful bandwidth from 0.5 GHz to 5.5 GHz and it is shown in Fig.1.2-7. Z_u is the unknown impedance, Z_s is the standard short, and $\lambda/8$ is considered at the center frequency of 3 GHz. The accuracy of the six-port was good in the range of 2 GHz to 4 GHz. The circuit exhibits the same shortcomings as the one presented in [17]. The accuracy of the circuit is not illustrated in terms of listings of results, but it is not expected to be very good, due to the position of the three centers of the circles representing the power equations. As the author mentions, the accuracy decreases as the ends of the frequency band are approached.

In 1983, E.R.B. Hansson and G.P. Riblet [24] investigated the behavior of an ideal six-port network consisting of a matched reciprocal lossless five-port and a perfect directional coupler. D.I. Kim, K. Araki, and Y. Naito [27] also investigated the properties of the five-port circuit and its broadband design. This is

a new circuit configuration that can be used as a reflectometer. The design was presented in strip-line and exhibited the characteristics of the desired six-port predicted by Engen and Hoer. The q-points were 120 degrees apart, and had a magnitude in the neighborhood of 1.5. The circuit they used is shown in Fig.1.2-8. If only the five-port were used, one had to deal with some ambiguity in the solution for the reflection coefficient. The intersections of the two circles in the Γ -plane have to be compared with the unit circle in order to determine which one is inside and which one is outside.

The "ideal" six-port network consisting of a matched reciprocal lossless five-port and a perfect directional coupler, when properly calibrated, gave good results at least at the low frequency end of the bandwidth. The results were good even when the five-port network was not matched (even when $|S_{11}| \cong 0.5$). Good results were given from 5 GHz to 5.6 GHz and good results are also predicted over a bandwidth greater than an octave.

Since the symmetrical, reciprocal five-port together with a directional coupler proved to be a good choice for a six-port reflectometer, G.P. Riblet and E.R.B.

Hansson [29] looked into the properties of a matched symmetrical six-port junction. The results were not so encouraging.

Let the six-port junction be the one in Fig.1.2-9. If the detectors are matched, we get: $a_3 = a_4 = a_5 = a_6 = 0$. From the S-parameter representation of the six-port, we get:

$$b_2 = S_{12} a_1 + S_{12} a_3 \qquad (1.2-10)$$

$$b_3 = S_{13} a_1 \qquad (1.2-11)$$

$$b_4 = S_{14} a_1 + S_{12} a_3 \qquad (1.2-12)$$

$$b_5 = S_{13} a_1 + S_{13} a_3 \qquad (1.2-13)$$

$$b_6 = S_{12} a_1 + S_{14} a_3 \qquad (1.2-14)$$

where

$$S_{23} = S_{12}$$

$$S_{43} = S_{12}$$

$$S_{53} = S_{13}$$

$$S_{63} = S_{14}$$

If $S_{12} = 0$, in order to make one detector measure the incident power on the test device, we get the q-points located at $-1/S_{13}$, and 0, and the power emerging to detector 1 being zero. Another possible situation is that $S_{14} = 0$. In this case P_6 measures the incident power to the test device and the other q-points are located at $-1/S_{13}$, 0, and $-1/S_{13}$, thus, making the six-port unsuitable for six-port measurements.

There was still a chance of using the six-port junction in conjunction with a directional coupler to get a seven-port, but the powers obtained were such that two power detectors gave information redundant with that obtained from the other two.

Even though the cases treated above [29] did not cover all possible connections as six-port reflectometer, they gave a good indication of the of the matched symmetrical, reciprocal six-port junction for six-port measurements.

A further development of the six-port ANA was the introduction of the dual six-port ANA, capable of measuring all the S-parameters of a two-port network [12,15,16,18,28,30,35,39]. A typical dual six-port ANA is shown in Fig.1.2-10.

As we have been discussing, there were many circuit configurations that were developed. All these designs attempted to come as close as possible to an ideal six-port reflectometer which would give the best performance. The hardware part of the reflectometer is a very important part, but an important role in the operation of the six-port reflectometer is played by the calibration technique.

1.2.2. CALIBRATION TECHNIQUES

The six-port network is characterized by the power equations (1.1-21) to (1.1-23) from section 1.1.2. The determining of the constants A_i, $i=4,5,6$ and q_n, $n=3,4,5,6$ at all the frequencies of interest, is called the calibration of the six-port ANA.

The spirit of six-port measurements is that the calibration technique is able to account for the imperfections and unknowns in the hardware [24].

The calibration is performed by loading the six-port with different known standards and observing the powers at the measurement ports. Then, the calibration constants are found by solving the system of equations obtained from the above process.

The calibration procedure has been worked on ever since the concept has been introduced [5]. Normally, a minimum of four standards are needed to calculate the eleven calibration constants, A_i, $i=4,5,6$ and q_n, $n=3,4,5,6$, since each standard will yield three equations like the ones in (1.1-21) through (1.1-23). Four standards will yield twelve equations, thus, giving enough information

to solve for the eleven real calibration constants. Due to measurement errors, the number of standards is increased and complex averaging processes are performed to minimize errors due to noise as well as measurement errors.

In 1975, C.A. Hoer and K.C. Roe [7] improved the analysis of the concept by accounting for ill-conditioned data from the point of view of the more general theory.

In 1977, at the Microwave Symposium, a group of papers by members of the NBS and other groups introduced new ideas that led to the improvement and expansion of the six-port measurement concept [9,10,11,12].

M.P. Weidman [13] calculated the calibration constants for his millimeter-wave six-port at one frequency only [13]. The standards that he used were: five sliding short positions, three sliding load positions, one reflection standard and one terminating power standard. The accuracy in power measurements was ±1.5%. The standard deviation for reflection coefficient magnitude measurements was ±0.002 and ±0.5° to ±3.0° in phase. The systematic uncertainties of ±0.005 were not unreasonable for that system.

H.M. Cronson and L. Susman [11,18] from Sperry Research Center in Sudbury designed and tested a six-port ANA using a new calibration method. The calibration constants appeared as the solution of an eigenvalue problem, resulting in new insights and faster numerical computation. The new approach gives a matrix description of the six-port network based on a circuit like the one in Fig.1.1-7. Each of the power detectors i, i=3,4,5,6, has a reflection coefficient Γ_i such that:

$$a_i = \Gamma_i b_i, \quad i = 3,4,5,6$$

The b waves become:

$$b_i = A_i a_1 + B_i a_2 = C_i a_2 + D_i b_2$$

where the scalars A_i, B_i, C_i, D_i depend on the topology of the six-port, namely the S-parameters and the reflection coefficients looking into the power detectors. The expressions given above are obtained using a similar derivation to the one in section 1.1.4. in which equations like (1.1-51) and (1.1-52) were derived. The power at port i is given by:

$$P_i = \frac{1}{2}|b_i|^2 - \frac{1}{2}|a_i|^2 = \frac{1}{2}\left(1 - |\Gamma_i|^2\right)|b_i|^2$$

Knowing that the square of the absolute value of a complex number equals the product of the number itself and its complex conjugate, we get:

$$P_i = \frac{1}{2}\left(1 - |\Gamma_i|^2\right)\left(A_i a_1 + B_i a_2\right)\left(A_i^* a_1^* + B_i^* a_2^*\right)$$

Thus:

$$P_i = \frac{1}{2}\left(1 - |\Gamma_i|^2\right)\left(|A_i|^2|a_1|^2 + |B_i|^2|a_2|^2 + 2Re\left(A_i B_i^*\right)Re\left(a_1 a_2^*\right)\right.$$

$$\left. - 2Im\left(A_i B_i^*\right)Im\left(a_1 a_2^*\right)\right)$$

The output power at all the measuring ports can be written in matrix form as follows:

$$\vec{P} = \underline{C}_I^{-1}\vec{a}_q \quad or \quad \vec{P} = \underline{C}_R^{-1}\vec{b}_q$$

where $\vec{P}$ is the column matrix of power readings, and $\vec{a}_q$ and $\vec{b}_q$ are column matrices whose entries are quadratic

functions of the input variables. The subscripts I and R refer to insertion loss and reflection loss respectively. The two square matrices $\underline{C}_I$ and $\underline{C}_R$ are different, depending on the configuration of the circuit used for the different tasks. Examples of choices for the $\vec{a}_q$ and $\vec{b}_q$ vectors are given below:

$$\vec{a}_q = \begin{pmatrix} |a_1|^2 \\ Re(a_1 a_2^*) \\ Im(a_1 a_2^*) \\ |a_2|^2 \end{pmatrix}$$

$$\vec{b}_q = \begin{pmatrix} |b_2|^2 \\ Re(b_2 a_2^*) \\ Im(b_2 a_2^*) \\ |a_2|^2 \end{pmatrix}$$

Since $\underline{C}_I$ and $\underline{C}_R$ are square matrices and if they are nonsingular, they have inverses, and we have:

$$\vec{a}_q = \underline{C}_I \vec{P}$$

and

$$\vec{b}_q = \underline{C}_R \vec{P}$$

Thus, the knowledge of the entries of the C matrix, to within a constant multiplier, enables the calculation of complex ratios like:

$$\frac{a_2}{a_1} = \frac{a_2 a_1^*}{|a_1|^2} = \frac{\sum_{i=1}^{4} (C_{2i} - jC_{3i} P_i)}{\sum_{i=1}^{4} C_{1i} P_i}$$

The calibration methods used were the following: standards were used to calibrate the network for S_{11} measurements employing a method which was previously used at a conference in Rome, Italy in 1976 [48]. In order to measure S_{21}, they used a self-calibration technique originally presented by Hoer [7]. The self-calibration technique made use of a repeatable, but otherwise unknown, two-position insertion device, which inserted a complex attenuation L into one of the input channels. Measurements with the device in the "out" position are taken for at least $i \geq 4$ different ratios of the a_2/a_1, and denoted by a matrix P. Measurements are also taken with the device in the "in" position, and the

results are stored in a matrix P'. Since L is a constant, the following nonlinear equations are obtained:

$$L = \frac{a'_2}{a_2} = \frac{a'_2 a'_1 / |a'_1|^2}{a_2 a_1^* / |a_1|^2} = \frac{\sum_{i=1}^{4} (C_{2i} - jC_{3i}) P'_i}{\sum_{i=1}^{4} (C_{2i} - jC_{3i}) P_i}$$

where $a_1 = a'_1$. Up to that time, these equations were solved by an iterative procedure, based on a Taylor expansion of the above equation about the correct values for the unknowns C_{2i}, C_{3i}, and L. The authors contribution was that they recognized the above problem to be an eigenvalue problem. They showed that:

$$(\underline{C}^T)^{-1} W^T \underline{C}^T = (\underline{C}^T)^{-1} (P P^T)^{-1} P (P')^T \underline{C}^T = \Lambda$$

where:

$$\Lambda = \begin{pmatrix} 1 & 0 & 0 & 0 \\ 0 & L^* & 0 & 0 \\ 0 & 0 & L & 0 \\ 0 & 0 & 0 & |L|^2 L \end{pmatrix}$$

The above equation gives the diagonalization of the W^T, which is a function of the matrices P and P', which in turn are functions of the measured powers. The eigenvector corresponding to the eigenvalue $\lambda = L$ contains the calibration constants. The difficulties encountered by the NBS technique, that used the Taylor expansion, lie in the possibility of converging to the wrong eigenvalue, that is 1, L^*, or $|L|^2$, rather than to the right value $\lambda = L$. This calibration method [11,18] was developed for measuring the S_{21} parameter.

The calibration procedures were made to be more accurate and to use easily accessible standards. Eigen [14] improved the sliding termination technique by separating the problem in two parts. The first part consisted of the reduction of the six-port to a four-port, and the second part dealt with the calculation of the constants that characterized the four-port.

In 1982 G.P. Riblet and E.R.B. Hansson [22] studied some aspects of the calibration of a six-port using offset reflection standards. The authors tried to give some insight into what standards were more suitable to optimize the calibration over a frequency range. They also tackled the problem of transferability of the

calibration, i.e. the calibration constants can be normalized in such a way that the recalibration of the six-port can be performed with only a good load on the output. Thus, the need for recalibration is eliminated.

P.I. Somlo and J.D. Hunter [20] described a method of calibration using either 5 and 1/2 or 6 and 1/2 standard terminations. The use of 5 and 1/2 standards means that actually 6 standards were used, but only half of the information provided by the sixth standard was employed in the calibration. The extra standard in 6 and 1/2 provides for correction of imperfections. Following the procedure set by Hoer [6], the authors investigated the performance of their six-port using the above calibration.

Since the number of standards used during the calibration procedure determines the time consumption, two trends became obvious. One of them dealt with the reduction of the number of standards, and the other one dealt with the stability of the calibration constants with time, meaning that once the calibration was performed, it was good for use of the six-port at any time in the future.

J.D. Hunter and P.I. Somlo [36] gave an explicit calibration method that used five standards. The standards that were needed in their calibration procedure were not assumed to be ideal, but only one was suggested to be near a matched load, in order to improve the performance near the center of the Smith chart.

Another fact that needs to be mentioned deals with the calibration of the dual six-port ANA. Calibration methods for dual six-port ANA's are described in [12,15,16,18,28,30,35,39]. The capability of the dual six-port ANA of measuring all the S-parameters of a two-port network made that circuit very attractive and a lot of work has been done in that area.

As we have seen, many calibration methods, using various standards, have been devised. The important difference between these methods are the number of standards needed, restrictions on what types of standards to be used for optimum performance [23], and the amount of computation needed to solve for the calibration constants [5,31,41,43].

1.2.3. METHODS OF REALIZATION OF SIX-PORT CIRCUITS

The methods of realizing the six-port reflectometers vary widely among designers. Some designers try to achieve maximum bandwidth, others try to reduce the size and simplify the design, and others try to bring the frequency of operation higher and higher.

The first circuits proposed by Engen and Hoer were built using separate components like quadrature hybrids, power dividers, and couplers. Since the largest bandwidth was achieved with stripline components, they used stripline quadrature hybrids and other components [6,9,10].

Waveguide components were also used at high frequencies by Griffin and Hill [37] using WG22. The frequency was increased to 75 - 105 GHz by Hill [38] and waveguide components in WG27 were used. H.M. Cronson and R.A. Fong-Tom [21] built a six-port ANA at 94 GHz in WR10 waveguide with good results.

The reduced size and cost, and the simplicity of the design and realization of circuits using microstrip transmission lines, made this kind of ANA very

attractive. Thus, microstrip six-port ANA's have been built using three-line couplers [17,25] with good results.

Stripline six-port circuits have also been built using symmetrical five-ports and directional couplers [24,27].

Dielectric waveguides were used at Hughes [19]. The frequency of operation was also increased, and by inlaying Teflon guides in properly designed contours, cut in a low dielectric constant foam material, passive components, such as quadrature hybrids, power dividers, and others have been designed. Using those components, a six-port ANA was developed. The performance of the 94 GHz six-port ANA showed that the imbalance between outputs of individual devices could be kept within 1 dB at frequencies between 93 GHz and 94.5 GHz.

U. Stumper [40] designed and operated a six-port ANA at submillimeter wavelengths. He also measured the dielectric characteristics of some materials using the six-port.

Another important problem to be discussed in connection with the realization of the six-port circuit is the detection devices. In general, two kinds of

detection devices have been used, one being thermistors, and the other one being diode detectors. Each detection device has its own advantages and disadvantages. The thermistor mounts were shown to be more accurate than diode detectors. Diode detectors require less power than the thermistors, and they are preferred over thermistors at higher frequencies were the level of power is reduced.

Somlo and Hunter [20] developed a six-port ANA which used uncalibrated semiconductor diodes, operating at a constant level. Each diode was followed by auto-zeroing buffer amplifiers, as shown in Fig.1.2-11. The detectors act as leveling sensors as shown in Fig.1.2-12. The multiplexing process eliminated the use of four linear power meters. Operating all diodes at fixed levels, accomodates the changes of sensitivity by the use of scaling factors. That operating mode may offer flexibility in the choice of diodes, but has a disadvantage in that it could not measure nonlinear (level dependent) impedances, since the level at the measuring port was held constant during the measurement.

1.2.4. USES OF SIX-PORT ANA

Six-port ANA's were extensively used as reflectometers and attenuation measuring devices.

L. Kalioby and R. Bosisio [34,36] developed a new swept frequency six-port measurement. They used two charts, an amplitude chart and a phase chart. This new achievement enabled detection of spurious responses and tuning of microwave circuits with sufficient accuracy.

The first use of the six-port in high precision phase shifting techniques was done by J. Forest [26].

The range of applications of the six-port measurements has broadened over the years reaching the medical field as well. J.R. Juroshek and C.A. Hoer [33] developed a high power automatic network analyzer, and measured the RF power absorbtion by biological samples situated in a TEM cell. These results may be used in the study of hyperthermia treatment of cancer. The system proved to be accurate in detecting power absorbed by the cell up to 0.05 % of the incident power. The system needed seven calibration steps and proved to be very stable with time.

Six-port ANA's are now used to set standards on reflection coefficients, attenuation measurements, and other parameters [42].

Even though a lot of research in the area of six-port measurements has been done, there are still problems that need to be analyzed. Some of these topics that deal with the theory and applications of the six-port techniques are the following.

One of the applications of the six-port reflectometers is the measurement of reflection coefficients of devices using pulsed signals. Until the work described in this dissertation, no research has been done in this area, and, because of its applications, it is an area which presents interest to researchers.

The three nonlinear equations that characterize the six-port reflectometer (equations (1.1-21) through (1.1-23) have as unknowns only two real parameters, the real and imaginary parts of the reflection coefficient. These nonlinear equations contain redundant information, and further research is needed in making optimum use of this redundancy to improve accuracy, predict random errors, and possibly determine detector nonlinearities.

Another research area that has not been investigated is the use of six-ports with multimode operation (more than one mode is present at the measurement port). This could lead to applications in optics.

The reduction in size of the six-port circuits points towards the use of the six-port in microcircuits, in order to measure the reflection coefficient at different places in a circuit for diagnostic or other purposes. In these cases, the main problem is the calibration of the six-port. An immediate solution, which remains to be tested, is the calibration of a prototype six-port of the same dimensions and the same characteristics, outside the microcircuit, and the use of the calibration constants obtained from the prototype circuit on the six-port circuits inside the micro circuit. The accuracy of this method depends on the repeatability with which the six-ports may be built. A problem associated with this topic is the real estate occupied by the six-ports themselves. This may make the microcircuit too large.

Another area of research is the increase in the dynamic range of attenuation measurements. The present range is 60 dB. The NBS aim is about 120 dB.

The largest source of errors in the six-port measurements of the reflection coefficient are the imperfections of the connectors used. There is a need to model these connectors and to be able to predict the limits of error by treating the imperfections statistically.

These are some of the problems that have not yet been solved and require further research.

1.3. GENERAL THEORY OF CALIBRATION

1.3.1. INTRODUCTION

As discussed in section 1.1.2., the equations that represent the six-port reflectometer are given by:

$$p_4 = \frac{P_4}{P_3} = A_4 \frac{|\Gamma - q_4|^2}{|1 - q_3\Gamma|^2} \qquad (1.3-1)$$

$$p_5 = \frac{P_5}{P_3} = A_5 \frac{|\Gamma - q_5|^2}{|1 - q_3\Gamma|^2} \qquad (1.3-2)$$

$$p_6 = \frac{P_6}{P_3} = A_6 \frac{|\Gamma - q_6|^2}{|1 - q_3\Gamma|^2} \qquad (1.3-3)$$

The notation p_i, $i = 4,5,6$ represents the power ratios:

$$p_i = \frac{P_i}{P_3} \qquad (1.3-4)$$

The constants A_i, $i = 4,5,6$ and q_j, $j = 3,4,5,6$ are unknown to the user at all the frequencies over which the

six-port will be used. At the center frequency, or the design frequency, it is possible to calculate these constants, but these calculated values may be used only as a means of comparison to determine accuracy. Therefore, these constants need to be determined in order to be able to use the six-port for accurate measurements. The process through which these constants are found is called the calibration of the six-port reflectometer.

The calibration is performed by loading the six-port with known loads (reflection standards), and looking at the powers that we obtain at the measurement ports. From the above system of equations, we see that each standard load will yield three equations (corresponding to p_4, p_5, and p_6). Since there are eleven real unknowns, there will be a need for at least four standards, which will provide twelve equations. The system that will be obtained is a nonlinear system:

$$p_{ni} = A_i \frac{|\Gamma_n - q_i|^2}{|1 - q_3 \Gamma_n|^2} \qquad (1.3\text{-}5)$$

where i=4,5,6 represents the port at which we observe the power, and n=1,2,3,4 represents which standard was used.

Eleven of the above equations will be selected and solved for the unknowns, using some method for solving a nonlinear system, one of which is Newton's method. The twelfth equation will be used to improve the accuracy of the solution, which is obtained by iterative methods.

Since the method for solving the nonlinear system of equations that will be used in this paper is Newton's method, we present it in the next section.

Manipulating the equations (1.3-5) to bring them in a more suitable form for Newton's method [47], we get:

$$p_{ni}\left|1-q_3\Gamma_n\right|^2-A_i\left|\Gamma_n-q_i\right|^2=0 \qquad (1.3-6)$$

where i=4,5,6, and n=1,2,3,4.

Replacing the complex constants by their rectangular form (real and imaginary parts), and expanding the absolute values, we get:

$$p_{ni}\left|1-(r_3+js_3)(x_n+jy_n)\right|^2-A_i\left|(x_n+jy_n)-(r_i+js_i)\right|^2=0$$

(1.3-7)

where

$$q_3 = r_3 + js_3 \quad , \qquad q_i = r_i + js_i \quad , \quad i = 4,5,6$$

$$\Gamma_n = x_n + jy_n \quad , \quad n = 1,2,3,4$$

Thus, we get:

$$p_{ni}\left[1 + \left(r_3^2 + s_3^2\right)\left(x_n^2 + y_n^2\right) - 2x_n r_3 + 2y_n s_3\right] -$$
$$A_i\left(x_n^2 + y_n^2 - 2x_n r_i - 2y_n s_i + r_i^2 + s_i^2\right) = 0 \qquad (1.3-8)$$

The above nonlinear system of equations can be solved by Newton's method.

1.3.2. NEWTON'S METHOD

Before introducing Newton's method for m unknowns, we consider the iterative solution of a nonlinear equation in only one unknown:

$$f(z)=0 \tag{1.3-9}$$

where the function f(z) is a nonlinear function of the variable z. A graphical representation of such a function is given in Fig.1.3-1. We are interested in finding z_1 such that $f(z_1)=0$. A method of finding the solution is to choose an initial guess z_0 in a carefully chosen interval about the exact solution. We start from this initial point and, according to Newton's method, we draw the line which is tangent to f(z) at z_0. The value of z at the intersection of this line with the abscissa is taken to be the next choice. The slope of this line is given by the derivative of f(z) evaluated at z_0. The equation of this tangent line is given by:

$$(z-z_0)f'(z_0)+f(z_0)=0 \tag{1.3-10}$$

Rearranging terms, we get:

$$f'(z_0)(z - z_0) = -f(z_0) \qquad (1.3-11)$$

The above procedure is then repeated until the approximate solutions are within the accuracy limits set by the problem, i.e. $z_0 - z_1 < tol$, where "tol" is the maximum error that can be tolerated in that particular problem.

If we are now dealing with a nonlinear system of equations in which we have n functions of n variables, equation (1.3-11) requires the introduction of the Jacobian of the system, which contains all the partial derivatives of all the functions with respect to all the variables. In order to be more specific, consider the following system of equations:

$$f_1(z_1, z_2, \ldots, z_n) = 0$$

$$f_2(z_1, z_2, \ldots, z_n) = 0 \qquad (1.3-12)$$

...

$$f_n(z_1, z_2, \ldots, z_n) = 0$$

or: $\underline{F}(\underline{z}) = 0$, where:

$$\underline{F} = (f_1, f_2, \ldots, f_n)^t$$

$$\underline{z} = (z_1, z_2, \ldots, z_n)^t$$

Then, the Jacobian matrix of the system is defined as follows:

$$J(\underline{z}) = \begin{pmatrix} \frac{df_1(\underline{z})}{dz_1} & \cdots & \frac{df_1(\underline{z})}{dz_n} \\ \cdot & & \cdot \\ \frac{df_n(\underline{z})}{dz_1} & \cdots & \frac{df_n(\underline{z})}{dz_n} \end{pmatrix}$$

There is a general theory which includes Newton's method. This theory is based on the definition of a function g(x), such that:

$$g(x) = x - \phi(x) f(x)$$

which gives quadratic convergence to the fixed point p of g. The equation to be solved is:

$$f(x) = 0$$

Newton's method results from choosing:

$$\phi(x) = \frac{1}{f'(x)}$$

Generalizing this one dimensional case to an n-dimensional case, we get:

$$\underline{G}(\underline{x}) = \underline{x} - \underline{A}^{-1}(\underline{x})\underline{F}(\underline{x})$$

which gives quadratic convergence to the solution of F(x)=0. A condition for this to be true is that $\underline{A}(\underline{x})$ be nonsingular at the fixed point of G.

We also need to define the fixed point of a function:

A function G from $D \subset R^n$ into R^n is said to have a fixed point at $p \in D$ if G(p)=p.

Developing the theory for the n-dimensional case [47], it turns out that A(p) = J(p), where J(p) is the Jacobian matrix.

Generalizing Newton's method from a nonlinear equation with one unknown to a system of n nonlinear equations with n unknowns, we have the following steps to follow:

Step 1: Choose an initial solution

$$\underline{z} = \underline{z}_0 = (z_{10}, z_{20}, \ldots, z_{n0})'$$

Step 2: Solve the following linear system with unknown y:

$$J(\underline{z})\underline{y} = -\underline{F}(\underline{z})$$

This system of linear equations may be solved by various methods. The method used in this paper is Gauss' method.

Step 3: Update the solution z by the error vector y, i.e.:

$$\underline{z} \leftarrow \underline{z} + \underline{y}$$

Step 4: If the error vector y satisfies the accuracy criterion, then stop. If not, go to Step 2 and continue the procedure.

We now particularize this problem to our problem, and denote as our functions f_i, the following expressions:

$$f_{(i-4)4+j} = A_i\left[x_j^2 + y_j^2 - 2x_j r_i - 2y_j s_i + r_i^2 + s_i^2\right] -$$
$$p_{ij}\left[1 + \left(x_j^2 + y_j^2\right)\left(r_3^2 + s_3^2\right) - 2x_j r_3 + 2y_j s_3\right]$$

where i = 4, 5, 6 represents the port number, j = 1, 2, 3, 4 represents the standard load number, and where the unknowns of the system are r_3, s_3, and r_i, s_i, A_i, $i = 4,5,6$. When we evaluate the entries of the Jacobian matrix, we take the partial derivatives of the above functions with respect to each unknown. The procedure presented above is followed step by step until the solution is found. There are techniques which speed up the calculation by not updating the Jacobian for each iteration.

Since the unknown constants A_i, $i = 4,5,6$, and q_j, $j = 3,4,5,6$ are frequency dependent, the above procedure is repeated for each frequency in the frequency band.

1.4. GENERAL MEASUREMENT PROCEDURE

After calibrating the six-port, the measurement of unknown loads follows. The six-port circuit is loaded with an unknown impedance, and the powers at the four power measuring ports are observed. Let these powers be denoted by P_i, $i=3,4,5,6$. The equations that represent the six-port reflectometer are (1.1-21) through (1.1-23) which are repeated here for convenience:

$$p_4 = \frac{P_4}{P_3} = A_4 \frac{|\Gamma - q_4|^2}{|1 - q_3\Gamma|^2} \qquad (1.4-1)$$

$$p_5 = \frac{P_5}{P_3} = A_5 \frac{|\Gamma - q_5|^2}{|1 - q_3\Gamma|^2} \qquad (1.4-2)$$

$$p_6 = \frac{P_6}{P_3} = A_6 \frac{|\Gamma - q_6|^2}{|1 - q_3\Gamma|^2} \qquad (1.4-3)$$

Let the unknown Γ be given by $\Gamma = x + jy$. Using the notation: $q_i = r_i + js_i$, $i=3,4,5,6$, the above equations become:

$$p_4\left[1 + (r_3^2 + s_3^2)(x^2 + y^2) - 2xr_3 + 2ys_3\right] =$$

$$A_4\left(x^2+y^2-2xr_4-2ys_4+r_4^2+s_4^2\right) \qquad (1.4-4)$$

$$p_5\left[1+\left(r_3^2+s_3^2\right)\left(x^2+y^2\right)-2xr_3+2ys_3\right]=$$
$$A_5\left(x^2+y^2-2xr_5-2ys_5+r_5^2+s_5^2\right) \qquad (1.4-5)$$

$$p_6\left[1+\left(r_3^2+s_3^2\right)\left(x^2+y^2\right)-2xr_3+2ys_3\right]=$$
$$A_6\left(x^2+y^2-2xr_6-2ys_6+r_6^2+s_6^2\right) \qquad (1.4-6)$$

Grouping factors that contain $x^2 + y^2$, x, and y together, we get:

$$p_4\left(r_3^2+s_3^2\right)-A_4\left(x^2+y^2\right)+2\left(r_4A_4-r_3p_4\right)x+2\left(s_4A_4+s_3p_4\right)y=$$
$$A_4\left(r_4^2+s_4^2\right)-p_4 \qquad (1.4-7)$$

$$p_5\left(r_3^2+s_3^2\right)-A_5\left(x^2+y^2\right)+2\left(r_5A_5-r_3p_5\right)x+2\left(s_5A_5+s_3p_5\right)y=$$
$$A_5\left(r_5^2+s_5^2\right)-p_5 \qquad (1.4-8)$$

$$p_6\left(r_3^2+s_3^2\right)-A_6\left(x^2+y^2\right)+2\left(r_6A_6-r_3p_6\right)x+2\left(s_6A_6+s_3p_6\right)y=$$
$$A_6\left(r_6^2+s_6^2\right)-p_6 \qquad (1.4-9)$$

Making the following simplifying substitutions:

$$\delta_i=p_i\left(r_3^2+s_3^2\right)-A_i \quad , \quad i=4,5,6 \qquad (1.4-10)$$

$$\rho_i = 2(r_i A_i - r_3 p_i) \quad , \quad i = 4,5,6 \qquad (1.4-11)$$

$$\sigma_i = 2(s_i A_i + s_3 p_i) \quad , \quad i = 4,5,6 \qquad (1.4-12)$$

$$\tau_i = A_i(r_i^2 + s_i^2) - p_i \quad , \quad i = 4,5,6 \qquad (1.4-13)$$

Our system becomes:

$$\delta_4(x^2 + y^2) + \rho_4 x + \sigma_4 y = \tau_4 \qquad (1.4-14)$$

$$\delta_5(x^2 + y^2) + \rho_5 x + \sigma_5 y = \tau_5 \qquad (1.4-15)$$

$$\delta_6(x^2 + y^2) + \rho_6 x + \sigma_6 y = \tau_6 \qquad (1.4-16)$$

Eliminating the quadratic term $x^2 + y^2$, we get:

$$(\rho_4\delta_5 - \rho_5\delta_4)x + (\sigma_4\delta_5 - \sigma_5\delta_4)y = \tau_4\delta_5 - \tau_5\delta_4 \qquad (1.4-17)$$

$$(\rho_4\delta_6 - \rho_6\delta_4)x + (\sigma_4\delta_6 - \sigma_6\delta_4)y = \tau_4\delta_6 - \tau_6\delta_4 \qquad (1.4-18)$$

Making another simplifying substitution, we get:

$$\alpha_{11} = \rho_4\delta_5 - \rho_5\delta_4 \qquad (1.4-19)$$

$$\alpha_{12} = \sigma_4 \delta_5 - \sigma_5 \delta_4 \qquad (1.4-20)$$

$$\alpha_{21} = \rho_4 \delta_6 - \rho_6 \delta_4 \qquad (1.4-21)$$

$$\alpha_{22} = \sigma_4 \delta_6 - \sigma_6 \delta_4 \qquad (1.4-22)$$

$$\beta_1 = \tau_4 \delta_5 - \tau_5 \delta_4 \qquad (1.4-23)$$

$$\beta_2 = \tau_4 \delta_6 - \tau_6 \delta_4 \qquad (1.4-24)$$

The system becomes:

$$\alpha_{11} x + \alpha_{12} y = \beta_1 \qquad (1.4-25)$$

$$\alpha_{21} x + \alpha_{22} y = \beta_2 \qquad (1.4-26)$$

The solution of this system is given by:

$$x = \frac{\beta_1 \alpha_{22} - \alpha_{12} \beta_2}{\alpha_{11} \alpha_{22} - \alpha_{12} \alpha_{21}} \qquad (1.4-27)$$

$$y = \frac{\beta_2 \alpha_{11} - \beta_1 \alpha_{21}}{\alpha_{11} \alpha_{22} - \alpha_{12} \alpha_{21}} \qquad (1.4-28)$$

Thus, the unknown Γ is given by $\Gamma = x + jy$.

2. COMPUTER AIDED MODELING

2.1. INTRODUCTION

The integration of microwave circuits and the incorporation of more circuits in one micro circuit requires a good understanding of the operation of each component in this environment. Tests have to be perfomed and parameters measured without disconnecting the device under test. Thus, there is a need for integration of the test equipment. The modeling of an integrated six-port reflectometer becomes a useful tool in understanding and later incorporating these instruments in microcircuits.

Another important aspect of the microwave measurements is the measurement of parameters of circuits when operated with pulsed signals. Therefore, a six-port reflectometer will be operated with pulsed signals, and its performance investigated.

The following chapters describe:

1. The modeling of an integrated six-port reflectometer using a powerful CAD program called MIDAS, developed at the David Sarnoff Research Center and used with their kind permission.

2. The fabrication of microstrip integrated six-port reflectometers, and the investigation of their performance.

3. The investigation of the performance of an integrated six-port reflectometer operated with pulsed signals.

4. New calibration techniques to account for non-square law behavior of the diode detectors.

2.2. MODELING OF AN INTEGRATED SIX-PORT REFLECTOMETER

2.2.1. CONFIGURATION OF THE SIX-PORT CIRCUIT

To date there have been many configurations of the six-port network used in reflectometry. Some of the designs center around the use of a correlator, which compares two incoming signals, one is a reference signal, and the other is an unknown signal, giving information about the unknown signal in terms of the reference. In other words, it gives information about the phase and magnitude of the unknown signal [6]. An example of such a correlator is given in Fig.2.2-1.

Correlators may be implemented using quadrature hybrids and a power divider. An example of a circuit that implements the correlator in Fig.2.2-1 is given in Fig.2.2-2. Q stands for quadrature hybrid, and D stands for power divider.

Other designs are based on the use of symmetrical five-ports and an additional power divider or coupler [24,27]. Other designs use three coupled lines to obtain a six-port network [17,25].

All of the above are suitable for integration and realization in microstrip circuits.

A design of six-port reflectometer using the correlator is shown in Fig.2.2-3. The characteristics of this design that made it more attractive than others of the same kind are that it has easier access to the input port, which makes it easier to incorporate in another integrated circuit. The q-points, at the center frequency, lie outside the unit circle, in the neighborhood of 1.5. This ensures better accuracy [9]. The q-points are spaced apart by 90, 90, and 180 degrees. A derivation of the power outputs is given in Appendix E.

Another characteristic of this design is that it contains, with the exception of the Wilkinson power divider, only identical quadrature hybrids, which makes the fabrication process easier and repeatable.

The six-port refelctometer was modeled using the CAD program called MIDAS, which was developed at the David Sarnoff Research Center, in Princeton, New Jersey. The choice of this program was based on the capability of simulating networks with any number of ports, which can then be incorporated in other networks.

Since the circuit in Fig.2.2-3 makes use of five identical quadrature hybrids, a subnetwork, which simulated a single quadrature hybrid, was first created, i.e. a four-port network was simulated, which would later be used in the larger six-port network. The quadrature hybrid was modeled using transmission lines, and it is shown in Fig.2.2-4.

The six-port was then simulated using the above hybrid as a construction unit. A listing of the MIDAS program that simulates the quadrature hybrid is given in Table 2.1-1. Table 2.2-2 contains a listing of the MIDAS program that simulates the entire six-port circuit.

2.2.2. MODELING PROCEDURE

The modeling of the six-port reflectometer consists of the following steps.

First the six-port reflectometer has to be calibrated. In order to do that, the six-port network is "loaded" with "standard" or reflection loads with reflection coefficients Γ_1, Γ_2, Γ_3, Γ_4. The "loading" of the six-port network is accomplished by changing the value of the impedance of the device under test in the MIDAS program. Then, the power ratios are obtained by running the program MIDAS. Having obtained the power ratios, the calibration constants are calculated using the procedure outlined in the following subsection, which follows the procedure in section 1.3. Thus, the constants A_i, $i=4,5,6$, and q_j, $j=3,4,5,6$ are now known to us.

The six-port reflectometer is calibrated and ready for measurements.

The measurement simulation consists of applying an "unknown" load Γ_l to the output of the reflectometer. The "unknown" load may be different from the loads used for calibration. The MIDAS program will then give the

power ratios for the unknown load. Using the calibration constants found during calibration, and the power ratios obtained from MIDAS, the value of Γ_l is calculated following the procedure illustrated in section 1.4. The value that we calculate for Γ_l should be the same as the "unknown" value specified in the MIDAS simulation measurements.

2.2.2.1. CALIBRATION PROCEDURE USED WITH SIMULATION RESULTS

In the simulation of the six-port reflectometer, using the MIDAS program, the power gains from port 1 to ports 3,4,5, and 6 were obtained. Since there is no need to eliminate the input power term, the ratios of powers at ports 4,5, and 6 to the power at port 3 (actually power gains from ports 3,4,5,6 to port 1) were not calculated anymore. This decission was also based on the fact that only three power ratios suffice to determine the unknown reflection coefficient. The ratios of powers at ports 4, 5, and 6 to the power at port 3 could have been considered, but no more information could be gained by doing so. The power gain P_3/P_1 was not considered any longer, and the port 3 has been terminated with a matched load. The power equations, therefore, become:

$$\frac{P_4}{P_1} = A'_4 \frac{|\Gamma - q_4|^2}{|1 - q\Gamma|^2} \qquad (2.2\text{-}1)$$

$$\frac{P_5}{P_1} = A'_5 \frac{|\Gamma - q_5|^2}{|1 - q\Gamma|^2} \qquad (2.2\text{-}2)$$

$$\frac{P_6}{P_1} = A'_6 \frac{|\Gamma - q_6|^2}{|1 - q\Gamma|^2} \qquad (2.2\text{-}3)$$

The above equations are the same as equations (A-23) through (A-25) from appendix A, in which $P_{in} = P_1$, and both sides of the equations were divided by P_{in}.

The equations (2.2-1) to (2.2-3) are of the same form as the general equations (1.1-21) to (1.1-23). The number of calibration constants is not different from the ones used in the general theory, so no information is either lost or gained by using these power gains instead of the power ratios defined in the general theory. Since port 3 is needed to sample the input power in the general six-port theory, no information is lost by not using the power gain from port 1 to port 3. The calibration method follows section 1.3 step by step.

The system of nonlinear equations is solved using Newton's method, and the linear system, which is required to be solved during a step of Newton's method, is solved by a Gauss elimination routine, which uses as a pivot the largest element in the matrix.

The convergence of the solution depends on both the solution of the linear system as well as on the initial

guess. The choice of the initial guess will determine mainly the time it takes to converge, and also if the solution will converge to the right zero (or solution of $\underline{F}(\underline{z})=0$).

This method has been implemented using the FORTRAN 77 programming language. The unknowns were denoted:

$$z_1 = A'_4, \quad z_2 = r_4, \quad z_3 = s_4, \quad z_4 = A'_5, \quad z_5 = r_5, \quad z_6 = s_5$$

$$z_7 = A'_6, \quad z_8 = r_6, \quad z_9 = s_6, \quad z_{10} = r_3, \quad z_{11} = s_3$$

where:

$$q_i = r_i + j s_i, \qquad i = 3,4,5,6$$

Since the same program is intended to be used on physical systems, the calibration routine will be equiped with error analysis. More standards will be employed to reduce the errors in the calibration constants due to measurement errors and noise errors. For the purpose of modeling the six-port reflectometer, the minimum number of standards will be used (four standards).

The calibration constants are functions of frequency, and the calibration procedure has to determine these constants at all the frequencies of interest. The variation of the calibration constants with the frequency is smooth. This fact can be used in choosing the initial guess in the solution of the nonlinear system, at each frequency.

At the design frequency (or the center frequency) the A_i, $i=4,5,6$, and q_j, $j=3,4,5,6$ may be computed by hand, given the fact that we know the topology of the six-port and the behavior of each component (at the center frequency). This task becomes prohibitive when the frequency departs from the design frequency. The center frequency result is then used for the Newton's method solution at the next higher and lower frequencies. After Newton's method converges, these solutions are used as initial guesses for the Newton's method solution at the next higher and lower frequencies. The process continues through the frequency range. This process gives fast convergence and has increased reliability, i.e. the chances of converging to the wrong solution are minimized.

There is also another way to choose the initial guess, which is based on the fact that most six-port

reflectometers satisfy the condition that $q \neq 0$, where q appears in the denominator of equations (2.2-1) to (2.2-3). This method starts by setting q equal to zero. The following system of equations is obtained:

$$\frac{P_4}{P_1} = A'_4 \left| \Gamma - q_4 \right|^2 \qquad (2.2-4)$$

$$\frac{P_5}{P_1} = A'_5 \left| \Gamma - q_5 \right|^2 \qquad (2.2-5)$$

$$\frac{P_6}{P_1} = A'_6 \left| \Gamma - q_6 \right|^2 \qquad (2.2-6)$$

These equations are now decoupled, i.e. the equations do not share common unknowns. Each nonlinear equation contains three unknowns A_i and $q_i = r_i + js_i$, $i = 4,5,6$. Since we have the power gains obtained by loading the six-port with four standards, the twelve equations thus obtained are then grouped in three sets of four equations for each set of decoupled unknowns. Each set of equations is then solved by using one of the four equations to eliminate the quadratic term, $r_i^2 + s_i^2$, and the

other three to solve the remaining linear system of three equations with three unknowns. The general form of the equations when standard j was used is:

$$\frac{P_i(j)}{P_1(j)} = A_i\left(x_j^2 + y_j^2 - 2x_j r_i - 2y_j s_i + r_i^2 + s_i^2\right) \qquad (2.2\text{-}7)$$

where i denotes the port at which we calculate the calibration constants and j denotes the standard used. $P_i(j)$ represents the power measured at port i when standard j was connected as a load.

The solution obtained following the above procedure, and the fact that q was set to zero, are then used as initial guess in Newton's method. This procedure is repeated at each frequency of interest. This method does not use the solution from the neighboring frequency as the initial guess.

In general, we want to make the calibration procedure as independent of the six-port network as possible. In this case, a combination of both methods may turn out to be more useful than either of them separately. This combination of the above methods proceeds as follows. First, the second method is used

at the center frequency, where it is expected that $q \cong 0$. Then, the first method is used for the other frequencies. This way, the calibration routine is made independent of the six-port network used to implement the reflectometer.

In the following work, the last method, which is a combination of the first two methods, was used.

2.2.2.2. MEASUREMENT PROCEDURE

The measurement simulation consists of applying the "unknown" load to be measured at the output of the reflectometer. The MIDAS program will then give the power gains corresponding to the "unknown" load under test. These power gains are then used together with the calibration constants, calculated during the calibration procedure discussed in section 2.2.2.1, to calculate the reflection coefficient of the "unknown" load. The mathematical details are presented in section 1.4.

2.2.3. SIMULATION RESULTS

The modeling of the six-port reflectometer has been checked for many loads over a band of frequencies ranging from 7 GHz to 9 GHz, the design frequency for the circuit being 8 GHz. The calibration standards were also included in this measurement part of the modeling, and they were a matched load, a short circuit, and two offset shorts with offsets of 22.5 degrees and 45 degrees.

The first check is conducted at the center frequency. The loads that were measured are loads with reflection coefficients having magnitudes of 0, 0.2, 0.4, 0.6, 0.8, 1.0, and phases such that they are spaced apart by 22.5 degrees covering the whole Smith chart (i.e. 16 evenly spaced points around the Smith chart for each value of the magnitude of the reflection coefficient, summing up to 81 points). A graphical representation of these loads is given in Fig. 2.2-5. These loads are drawn inside the unit circle. The errors associated with these loads are less than 0.19 percent in magnitude and less than 0.17 degrees in phase. The largest error in magnitude occurred for an

offset short with an offset of 90 degrees, and the largest error in phase occurred for an offset short with an offset of 101.25 degrees.

The next check was conducted over a band of frequencies from 7 GHz to 9 GHz. The reflection coefficient of each load is listed in a table together with the errors in both magnitude and phase between the "measured" and the "applied" reflection coefficient.

The loads that were applied to the six-port reflectometer are offset shorts with offsets 0, 22.5, 30, 45, 67.5 degrees, a matched load, an open circuit, and two loads with magnitudes of 0.111, respectively. Tables 2.2-3 through 2.2-11 contain the results for the above loads.

Each table contains in column 1 the frequency, columns 2 and 3 the "measured" reflection coefficient, in column 4 the error in magnitude, and column 5 the error in phase in degrees.

The error in reflection coefficient of the four standards used in the calibration procedure is zero in three of them, and very small in the fourth. The errors in the magnitude of the fourth standard do not exceed ± 0.19 per cent, and the largest error occurs at a

frequency of 7 GHz. The errors in phase are less than ± 0.122 degrees, and the largest error occurs at the same frequency of 7 GHz. The reason for the difference in errors in the fourth standard is that only two of the three equations for that standard are used in the calibration routine. This is so, because out of the 12 equations that are obtained from the four standards, only 11 are needed to solve for the 11 calibration constants. The twelfth equation may be used to improve the accuracy of the six-port.

The results for the offset shorts with offsets of 30 degrees and 67.5 degrees show errors in magnitude of less than ±0.42 per cent and ±0.33 per cent, respectively. The largest errors occur at a frequency of 7 GHz for the 30 degree offset short, and 7.9 GHz for the 67.5 degree offset short. The errors in phase do not exceed ±0.17 degrees for the 30 degree offset short, and ±0.43 degrees for the 67.5 offset short. The largest errors in phase occur at 7 GHz for the 30 degree offset short, and at 8.8 GHz for the 67.5 degree offset short.

The measurement results of the matched load show no error in magnitude and the phase column should be ignored since the phase of a reflection coefficient with zero magnitude does not mean anything.

The results obtained for the load with $\Gamma = -0.111$ show magnitude errors less than ±0.99 per cent, and errors in phase of less than ±1.42 degrees. The largest error in magnitude occurred at 7.7 GHz and the largest error in phase occurred at 8.6 GHz. Smaller errors are recorded for the load with the reflection coefficient magnitude of 0.111 and the phase give by an offset of 45 degrees from the short. They do not exceed ±0.38 per cent in magnitude and ±0.84 degrees in phase. The largest errors occur at 8.8 GHz.

Table 2.2-11 shows the measurement results for an open circuit. The errors in magnitude are less than ± 1.84 per cent, and the errors in phase do not exceed ± 1.166 degrees. The largest errors occur at 7 GHz.

The frequencies at which the largest errors occur vary from load to load. This shows that the errors are not systematic errors, and they are errors due to the simulation program MIDAS. This is proven in the remainder of this section.

The errors that occur in the "measured" reflection coefficient come from the precision with which the results from MIDAS are given. The power gains, in dB, that were calculated by MIDAS, were listed with up to 4 significant figure precision.

Since the data files obtained from MIDAS had only 4 significant figure precision, it is not expected to get better results even if double precision were employed in the FORTRAN program used to calibrate the six-port and measure the reflection coefficient of different loads.

Thus, the main source of errors is the precision and accuracy of the MIDAS simulation program.

In order to check the precision and accuracy of the Fortran program, the following approach was used. A set of S-parameters was obtained from MIDAS for the six-port network. A listing of the program that simulated that network is given in Table 2.2-2. Since all the ports were matched, we could employ the set of equations (1.1-32) to (1.1-34) in section 1.1.3 to calculate the power gains from ports 4, 5, 6 to the input port 1, for any value of the reflection coefficient. The modeling of the six-port reflectometer proceeded as in section 2.2, with the only exception that the power gains are not obtained from MIDAS, but are calculated using the equations (1.1-32) to (1.1-34).

Looking at the results of the modeling for the same set of loads, shown in Tables 2.2-12 to 2.2-20, we see that the second procedure gives more accurate results

than the ones obtained with the first procedure (shown in Tables 2.2-3 trough 2.2-11 respectively). The errors in magnitude are zero and the phase errors are less than ±0.0001 degrees. This analysis shows that the main source of errors is the simulation program MIDAS. The errors may be coming from the simulation procedure itself, or, from the precision with which the results are output.

3. SIX-PORT REFLECTOMETER. PHYSICAL CIRCUIT

3.1 SIX-PORT CONFIGURATION

The six-port configuration that was chosen for the pulsed signal operation was a version of the design proposed by Hansson and Riblet [24].

The six-port consists of a symmetrical five-port junction and a Wilkinson power divider. The reason for this choice was the ideal positions of the q-points at the design frequency (120 degrees apart from one another) and the wide bandwidth reported by the authors. The design shows easy access to the power measuring ports and the input and output ports. The six-port configuration is shown in Fig.3.1-1. The design parameters calculation follows the design given in [24] with the exception of the design frequency, which was chosen to be 8 GHz.

3.2 THE FABRICATION OF THE SIX-PORT

The six-port network was built in microstrip configuration. This choice was dictated by the ease in fabrication and the low cost.

The material used was teflon based copper cladding with a thickness of the teflon of 20 mils, and a copper thickness given by 1 ounce per square foot.

Photographs of the six-port are given in Fig. 3.2-1 and Fig. 3.2-2.

The construction of the six-port followed these steps:

A mask was built for the microstrip circuit. The mask was drawn with the aid of a program developed at the SRI David Sarnoff Research Center. The line width to height ratios and physical widths for various characteristic impedances were calculated using the equations given in [24]. Table 3.2-1 contains all these dimensions. The same program, called MASK, was used to cut the rubylith mask which was needed for Step 2. The program was used to drive an IBM plotter to draw and cut a 10:1 mask of the six-port circuit. In the cutting process, a cutting tool replaced the pen in the plotter. The program was designed to slow down the motion of the

plotter in order to allow for proper cutting of the rubylith mask. After peeling off the unwanted regions on the mask, the rubylith work was ready for the next step. This first step was performed in the LORAL Microwave Laboratory at the City College of New York.

The rubylith mask was used to get a negative film of the six-port reduced from a 10:1 scale to 1:1. This step and the following ones were performed at Narda Corporation, Long Island, New York.

The following steps include photoresist deposition, fixing of the photoresist, ultra-violet light exposure using the negative film on top of the copper cladding, developing of the photoresist, and etching with ferric chloride solution.

In order to obtain the desired widths after etching, the lines were designed 1 mil wider on each side. The reason for that is the fact that during etching, about 1 mil on each side is undercut by the etching solution. This safety margin is a function of the thickness of the copper.

The Wilkinson power divider required a 100 ohm resistor. A chip resistor was used for that purpose.

External diode detectors of the HP-8472B type were connected at the four power measuring ports.

The input and output ports were equipped with SMA to microstrip connectors, which were soldered on the microstrip side.

3.3 SIX-PORT NETWORK ANALYZER. SYSTEM CONFIGURATION

The system configuration in block diagram is given in Fig.3.3-1. The HP-8350A sweep oscillator equiped with the HP-83590A broad band RF plug-in (2 - 18 GHz) was operated both CW and in the pulsed mode. For the pulsed operation, an external commercial pulse generator was used to modulate the RF signal. The signal is transmitted to the six-port via a coaxial cable. The four power measuring ports are equiped with HP-8472B diode detectors. The voltages detected at the four diode detectors are fed into the HP-3497A Data Aquisition and Control Unit.

The operation of all the components of this system is controlled by a Fortran 77 program implemented on the HP-1000 (A-700 series) computer. Only the pulse generator is not controlled by the computer since it was not programmable.

4. PULSED MEASUREMENTS

4.1 INTRODUCTION

When operating the six-port network analyzer with pulsed signals, the RF source is amplitude modulated with a train of pulses.

This mode of operation of the six-port makes it useful in measurements of components that are operated with pulsed signals only, such as antenna arrays or optical systems.

Fig.4.1-1 shows the RF signal before modulation, the train of pulses and the pulsed modulated signal.

The pulsed signals that are applied to the six-port network analyzer have to be detected in order to evaluate the reflection coefficient of the device to be measured. The optimum detector for pulsed signals is the peak detector, which will be presented in section 4.2. The detected power of the train of pulses will have a magnitude which is proportional to the detected magnitude when CW signals are used. Thus, the voltages that are read at the four measuring ports are proportional to the voltages that we read when the six-port is operated in the CW mode.

The pulsed signals that are present at the four

measuring ports are first detected by the diode detectors. The diode detectors will give us the envelope, because they operate as rectifiers with time constants that are suited for microwave frequencies. Thus the signals that we read at the four diode detectors are trains of pulses. The peaks of these pulses can be detected as it will be shown in section 4.2 by the use of peak detectors, or by the use of voltmeters that give RMS values. The second method run into limitations when the duty cycle of the pulse train is very small, because the level of the RMS value may run into the noise level.

4.2 THE PEAK DETECTOR

The peak detector is the optimum detector for pulsed signals. A typical peak detector is shown in Fig.4.2-1. This detector follows negative pulses because the first detectors are negative voltage detectors. The RC circuit provides a slow discharge of the capacitor C such that the output voltage does not rise significantly when the input signal is at the ground level.

The diode D needs a turn on voltage of about 0.3 to 0.6 volts. This fact together with the low levels of voltages that are detected at the four measuring ports (in the order of tens of millivolts or less) render this type of peak detector useless. At low levels of input voltage (negative), the diode is not completely turned on, thus exhibiting a very large forward impedance. This very large resistance makes the charging time constant of the capacitor C too large to reach the peak of the pulse. The value of this large forward resistance also varies with the level of input voltage. Thus, the charging time constant varies as the input voltage varies. As expected from the theoretical point of view, the experimental results with such a peak detector showed that the voltages detected at the output

were a fraction of the peak values and were functions of the input voltage.

A second type of peak detector is shown in Fig.4.2-2, which uses an active device, an operational amplifier, to reduce the turn on voltage of the diode to zero. The problem associated with this peak detector is the DC offset of the operational amplifier, that sometimes amounts to levels comparable to the voltage levels that are obtained at the four diodes which are connected at the power measuring ports. The problem can be corrected by adjusting the DC offset of the op-amp as shown in Fig.4.2-2. The offset adjustment is achieved with the aid of a potentiometer connected as shown if Fig. 4.2-2.

When this circuit was implemented the following observations were made:

1. For pulse trains with periods less than 1 ms and duty cycles of 15 per cent or less, the peak detector did not work, giving an output level much less than the peak.

2. For pulse trains with larger duty cycles, the output followed the peaks but an instability of the voltage level was noticed.

The failure of the peak detector for pulse trains with low periods and low duty cycles comes from the

limitations of the operational amplifier as far as the slew rate and driving capabilities are concerned. The operational amplifier that was used had a very low slew rate, thus making the responce to narrow pulses impossible. The results improved when a higher slew rate amplifier was used.

The instabilities in the voltage level could come from the fact that the op-amp is operated in practically open loop fashion when the diode is reverse biased. A circuit to correct this problem is presented in Fig.4.2-3. The feedback loop consisting of the second op-amp and the diode helps keep the voltage at the output of the operational amplifier from jumping to the extreme values when the noise levels at the differential input of the op-amp cause this effect.

Further increase of the frequency of the train of pulses and decrease of the duty cycle may reach the limitations of the first diode detectors connected at the four measuring ports. A considerable degradation of the pulse shape has been noticed for pulse widths smaller than 10 microseconds.

All these limitations on the detection side of the six-port network analyzer can be extended with the proper choice of components, namely diode detectors

which can follow faster pulses, operational amplifiers with faster slew rates, or a better design of the peak detector.

There are commercially available peak power meters which work with pulse widths as low as a microsecond and input power levels from 0 dBm to 20 dBm (the information was taken from an HP 1988 catalog and is characteristic to the HP-9600 peak power meters). These peak power meters may not have enough input power dynamic range for all possible standards to be measured. This statement is based on the observation that for some standards, some power ratios exceed 20 dB in absolute value. On the other hand, these peak power meters are not programmable, thus making them quite unsuitable for an automatic network analyzer. Their high cost would increase the total cost of the ANA by a few thousand dollars.

4.3 CALIBRATION PROCEDURE

The calibration of the six-port network analyzer, when operated with pulsed signals, follows the same steps that were followed when the six-port was calibrated with CW input.

The calibration that was obtained with CW signals can be used to perform measurements with pulsed signals as well. The reason is that the power ratios remain constant for both CW and pulsed operation, provided the voltages that are detected in the pulse operation mode are made proportional to the powers at the respective ports by a proper calibration of the diode detectors. This fact eliminates the need for the calibration of the six-port network analyzer with pulsed signals. This conclusion will be very useful in the further study of integrating the six-port network analyzer in larger systems such as phased array antennas.

The only change from the theory developed up to now is the form of the equations that was used. The three power ratio equations are:

$$\frac{P_4}{P_3} = A''_4 \frac{|1 - q''_4 \Gamma|^2}{|1 - q_3 \Gamma|^2} \qquad (4.3-1)$$

$$\frac{P_5}{P_3} = A''_5 \frac{|1 - q''_5 \Gamma|^2}{|1 - q_3 \Gamma|^2} \qquad (4.3-2)$$

$$\frac{P_6}{P_3} = A''_6 \frac{|1 - q''_6 \Gamma|^2}{|1 - q_3 \Gamma|^2} \qquad (4.3-3)$$

The only change appears in the numerator of the power ratios, which is put in the same form as the denominator. The change was performed because of the concern that some of the q-points, at some frequencies, may go to infinity. As described in section 1.1.3, there is a possibility that some q-points may go to infinity under certain conditions. These conditions were derived in section 1.1.3. and given in equation (1.1-41) for q_3.

The three power ratio equations given in equations (1.1-42) through (1.1-44) are repeated here for convenience:

$$\frac{P_4}{P_3} = A_4 \frac{|\Gamma - q_4|^2}{|1 - q_3 \Gamma|^2} \qquad (4.3-4)$$

$$\frac{P_5}{P_3} = A_5 \frac{|\Gamma - q_5|^2}{|1 - q_3 \Gamma|^2} \qquad (4.3-5)$$

$$\frac{P_6}{P_3} = A_6 \frac{|\Gamma - q_6|^2}{|1 - q_3\Gamma|^2} \qquad (4.3\text{-}6)$$

where, for matched power detectors:

$$A_j = \frac{|S_{j1}S_{22} - S_{j2}S_{21}|^2}{|S_{31}|^2} \quad , \qquad j = 4,5,6$$

$$q_n = \frac{S_{n1}}{S_{n1}S_{22} - S_{n2}S_{21}} \quad , \qquad n = 4,5,6$$

$$q_3 = \frac{S_{31}S_{22} - S_{32}S_{21}}{S_{31}}$$

If q_4, q_5, and q_6 are taken as common factors in the numerator, equations (4.3-4) through (4.3-6) become:

$$\frac{P_4}{P_3} = A_4 |q_4|^2 \frac{|1 - q''_4\Gamma|^2}{|1 - q_3\Gamma|^2} \qquad (4.3\text{-}7)$$

$$\frac{P_5}{P_3} = A_5 |q_5|^2 \frac{|1 - q''_5\Gamma|^2}{|1 - q_3\Gamma|^2} \qquad (4.3\text{-}8)$$

$$\frac{P_6}{P_3} = A_6 |q_6|^2 \frac{|1 - q''_5 \Gamma|^2}{|1 - q_3 \Gamma|^2} \qquad (4.3-9)$$

where:

$$q''_n = \frac{1}{q_n} \quad , \qquad n = 4,5,6$$

Substituting:

$$A''_j = A_j |q_j|^2 \quad , \qquad j = 4,5,6$$

we get the equations (4.3-1) through (4.3-3). The expressions of the new calibration constants in terms of the S-parameters, in the case of matched power detectors, are:

$$A''_j = \frac{|S_{j1}|^2}{|S_{31}|^2} \quad , \qquad j = 4,5,6$$

$$q_3 = \frac{S_{31} S_{22} - S_{32} S_{21}}{S_{31}}$$

$$q''_n = \frac{S_{n1} S_{22} - S_{n2} S_{21}}{S_{n1}} \quad , \qquad n = 4,5,6$$

This change also makes the calculation of the A constants easier, because when the load is a matched load we have:

$$A''_j = \frac{P_{jm}}{P_{3m}} \quad , \qquad j = 4,5,6 \tag{4.3-10}$$

where P_{jm} represents the power measured at port j when the matched load is connected (j = 4, 5, 6).

The calculation of the q-points and the A constants follow steps consistent with the steepest descent method. The A constants were calculated from the power ratios obtained by loading the six-port with a matched load using equation (4.3-10). The steepest descent method was used to minimize the sum of the squares of the remaining nine equations obtained from loading the six-port with three more standards (the minimum number of standards). The unknowns calculated via the steepest descent method were the real and imaginary parts of the four q-points, q_3, q_4, q_5, and q_6.

4.4 MEASUREMENT PROCEDURE

The measurement procedure consists in connecting the unknown load at the measurement port, and observing the powers at the four power measuring ports. The equations relating the power ratios, the calibration constants, and the unknown reflection coefficient are equations (4.3-1) through (4.3-3), which are repeated here as equation (4.4-1):

$$\frac{P_i}{P_3} = A_i \frac{|1 - q_i \Gamma|^2}{|1 - q_3 \Gamma|^2} \quad , \quad i = 4,5,6 \qquad (4.4-1)$$

These equations differ from the equations used in the simulation because the numerator was changed the same way the denominator was changed, in order to avoid the possibility that some of the q-points go to infinity under certain conditions. This fact in elaborated in the calibration section 4.3.

There are three equations in three unknowns, x, y, and $x^2 + y^2$, where $\Gamma = x + j\ y$. This system of equations may be solved linearly for the real and imaginary parts of Γ following a similar procedure with the one described in section 1.4. In some ill

conditioned cases this method fails to give the right solution. In order to account for those cases, one has to look at the three equations as representing three circles in the Γ-plane. If the three circles are not concentric or if their centers are not situated on a straight line, the linear system solution will give the right solution. In the cases of ill-positioned centers of the above three circles, the solution for Γ requires a different method. The method used in this presentation consists of finding all the intersections of the circles and choosing the right solution from all those intersections. In order to choose the right solution, the intersection points of each pair of circles are compared to some reference value. The closest intersection point to that reference value is chosen. Then, the three thus chosen intersection points (one from each pair of circles) are averaged to get the estimate of the solution for Γ. A graphical interpretation of this is shown in Fig. 4.4-1.

Due to measurement errors some circles may not even intersect. In this case the points on each circle that are closest to the other circle are found. Fig.4.4-2 depicts this situation. Then, the "intersection" of the two circles is taken to be the mean of the two points.

After all possible intersections are found (a

maximum of six points), the choice for the solution at various frequencies is taken as follows. At the design frequency, the three centers of the circles are not ill-positioned (unless the design of the six-port is bad and therefore should not be considered any more) and the solution for Γ is obtained by solving the linear system that results from the set of equations (4.3-1). The solution may be improved by using the "circle intersection" method. This method, described earlier, involves the comparison of the six possible intersection points to some reference value. This reference value, at the design frequency, is chosen to be the solution of the linear system of equations obtained from (4.3-1).

The solution for Γ at the design frequency is used as reference for the immediately following frequencies, until the whole band of frequencies is covered. The reason for this choice is the fact that reflection coefficients do not change by too much when the frequency is varied by a small amount.

The above described method shows very good results in cases in which the centers of the circles representing the power equations are situated on a straight line. In those cases, there are two possible intersections of the three circles as shown in

Fig.4.4-3. This method to find the intersection of the three circles discriminates between the two solutions thus choosing the correct one.

4.5 DIODE CALIBRATION

The six-port network analyzer can be equiped with thermistors or diode detectors at the four power measuring ports.

Diode detectors are preferred over thermistors for their reduced input power level and for their speed in the detection process. Thermistors require a higher level of input power and, since they operate on the principle of thermal detection across a resistor, take longer to indicate the average power. The advantage of the thermistors over the diode detectors is that they give a true measure of the average power at that port. Voltages detected by diode detectors are not in general proportional to the power at that port. It is only in a certain region of their characteristic that the diode voltage is proportional to the power, and that region is called the square law region. In general the diode detector deviates from the square law and for it to be used in the six-port network analyzer it has to be calibrated.

The calibration of the diode detector consists of the measurement of the incident power to the diode and the detected voltage, when the incident power varies

over a wide enough range to cover the operating range of the diode as part of the network analyzer. Then a curve of the form:

$$P = kv^{\left(1+b_1v+b_2v^2+b_3v^3+b_4v^4+b_5v^5\right)} \qquad (4.5-1)$$

is fitted to the measurement data, such that the mean square error is minimized.

The diodes used in the six-port network analyzer can be calibrated individualy, outside the six-port network, or they can be calibrated "in situ" without disconnecting them from the network.

The second type of calibration seems to be more attractive and it requires an additional directional coupler and a power meter as shown in Fig.4.5-1. The directional coupler does not have to be calibrated since it is needed only to get a measure of the input power, the actual relationship between the power read at the power meter and the input power does not have to be known.

A matched load is connected as the device under test. Then the power at the power meter P is measured together with the voltages at the detectors D_1, D_2, D_3, and D_4. Each detector is calibrated according to the law defined in equation (4.5-1) by varying the input

power over a large enough range, usualy 20 dB about a chosen level. This method was implemented and the input power was varied from -11 dBm to 9dBm. Fifteen readings were taken out of which six were chosen. The choice of six readings corresponds to the six unknowns in equation (4.5-1), k, b_1, b_2, b_3, b_4, and b_5, that have to be calculated. The six chosen readings, corresponding to six levels of power equally spaced in the above mentioned interval, were used to calculate the constants in equation (4.5-1). It can be shown that one can obtain a linear system of equations by taking the logarithm of both sides of the equation. Then, the solution is used as initial guess in the steepest descent method in order to minimize the sum of squares of all the equations corresponding to all the readings.

Another method to calibrate the diode detectors uses a calibrated attenuator only as shown in Fig.4.5-2. The load at the measurement port is a matched load. The diode calibration peoceeds as follows. The voltages read at the four detectors are corrected such that they become proportional to the power at that port. This correction procedure uses the ratio of the powers at each port for different levels of input power. The method assumes that the voltages read for a chosen initial setting of the attenuator are proportional to

the powers at corresponding ports, and are therefore taken as references. Fig. 4.5-3 shows the calibration curve of the read voltage versus the corrected voltage.

Using equation 4.5-1, we find that at the initial setting of the attenuator, the voltage v_{co} at any of the measuring ports is related to the power at that port as follows:

$$P_0 = k v_{c0}^{\left(1 + b_1 v_{c0} + b_2 v_{c0}^2 + b_3 v_{c0}^3 + b_4 v_{c0}^4 + b_5 v_{c0}^5\right)} \qquad (4.5-2)$$

For a different setting of the attenuator, the voltage v_r read at the measuring port and the power at the same port are related as follows:

$$P_1 = k v_r^{\left(1 + b_1 v_r + b_2 v_r^2 + b_3 v_r^3 + b_4 v_r^4 + b_5 v_r^5\right)} \qquad (4.5-3)$$

Since the corrected value of the voltage has to be proportional to the power, it is given by:

$$v_c = \frac{P_1}{P_0} v_{c0} \qquad (4.5-4)$$

where the correct value for the initial setting of the attenuator is the read value :v_{c0}

Substituting (4.5-2) and (4.5-3) into (4.5-4) we get:

$$v_c = v_{c0} \frac{k v_r^{\left(1 + b_1 v_r + b_2 v_r^2 + \ldots + b_5 v_r^5\right)}}{k v_{c0}^{\left(1 + b_1 v_{c0} + b_2 v_{c0}^2 + \ldots + b_5 v_{c0}^5\right)}} \qquad (4.5\text{-}5a)$$

$$v_c = k_1 v_r^{\left(1 + b_1 v_r + b_2 v_r^2 + \ldots\right)} \qquad (4.5\text{-}5b)$$

where:

$$k_1 = v_{c0}^{-\left(b_1 v_{c0} + b_2 v_{c0}^2 + \ldots + b_5 v_{c0}^5\right)}$$

This calibration is equivalent to the calibration using the power meter. The procedure follows the steps of the calibration using the power meter.
Another way to calibrate the diodes "in situ" is to connect the power meter to the DUT port and follow the steps of the first or second procedure. This eliminates the need for the additional directional coupler or for the calibrated attenuator.

Another diode calibration method proceeds as follows. The power equations characterizing the six-port network analyzer are modified to include the unknowns from the diode calibration:

$$\frac{k_i v_i^{(1+b_{i1}v_i+b_{i2}v_i^2+\cdots)}}{k_3 v_3^{(1+b_{31}v_3+b_{32}v_3^2+\cdots)}} = A_i \frac{|1-q_i\Gamma|^2}{|1-q_3\Gamma|^2} \qquad (4.5-6)$$

where i = 4, 5, 6. The steepest descent method is then used to find not only the six-port calibration constants but also the diode calibration constants. The only requirement is knowledge of a good initial guess for the diode calibration constants. This is made possible by calibrating only one diode outside the six-port, at the design frequency and then using the data thus obtained as an initial guess for all diodes at all frequencies. This assumption is made valid by the fact that the diode calibration constants do not vary too much with frequency or from one detector to another (provided the detectors are of the same model). This method was also implemented and a good calibration from 4 to 12 GHz was obtained.

4.6 RESULTS

4.6.1 CW AND PULSED MEASUREMENTS RESULTS

The operation of the six-port reflectometer was investigated under both CW and pulsed signal operation conditions.

The CW operation of the reflectometer was investigated over a frequency range from 2 GHz to 12 GHz. The step size was chosen to be 0.1 GHz, thus offering a set of 101 intermediate frequencies.

The six-port reflectometer was calibrated using a matched load, an open, a short and an offset short with an offset of 50.48 degrees at 8 GHz.

Prior to this calibration, the diode detectors were calibrated at the frequency of 8 GHz (the design frequency and the mid band frequency as well) for input power levels ranging from -11 dBm to 9 dBm. The diode calibration followed the one using the voltage correction technique described in section 4.5. The diode detectors could have been calibrated at each frequency of interest, in order to get better accuracy in results, but it turned out that the improvement in measurements of the reflection coefficient was not significant. Therefore, the saving in time due to the calibration

only at one frequency (calibration of the diodes and not of the six-port itself) proved to be significant.

The six-port was calibrated using the procedure outlined in section 4.3. In order to achieve such a wide bandwidth the calibration was first performed from 4 GHz to 12 GHz using as loads a matched load, an open, a short, and an offset short with an offset of 50.48 degrees. The six-port was then calibrated from 2 GHz to 4 GHz using as loads a matched load, an open, a short, and an offset short with offset of 70.52 degrees. The reason for changing the fourth load is because to 50.48 degree offset looked almost as a short for frequencies around 2 GHz, and the calibration procedure converged to wrong values. The two calibrations were saved in different files and later merged into a single file. After the six-port was calibrated at all the frequencies of interest, the measurement of different loads was performed.

The performance of the six-port was investigated with the following loads: the four standards used in the calibration of the six-port, offset shorts with offsets of 70.52 degrees, 118.81 degrees and 239.81 degrees at 8 GHz, and a 3 dB attenuator with a short connected at one end. The values of the offsets in degrees were calculated from the physical lengths provided by the

manufacturer (Maury Microwave Corporation). The results obtained with these loads are given in Fig.4.6-1 through 4.6-8. The offset shorts with offsets of 50.48, 70.52, 118.81, and 239.81 are labeled as offset3, offset4, offset5, and offset6, respectively. The (a) plots show the magnitude of the reflection coefficient and the (b) plots show the phase of the same reflection coefficient.

Fig. 4.6-1 shows the magnitude of a matched load. The reflection coefficient has zero magnitude.

Fig. 4.6-2 shows the results for a short, which was used as a standard in the calibration procedure. For frequencies between 7.1 GHz and 12.2 GHz the errors in magnitude are less than 0.8 per cent. The errors in magnitude do not exceed 4.86 per cent over the entire frequency band, and the largest error occurs at 2.7 GHz. The phase errors do not exceed ±4.25 degrees, and the maximum error is reached at 3.8 GHz. The phase errors between 7.1 GHz and 12.2 GHz are less than ±0.5 degrees.

Fig. 4.6-3 shows the magnitude and phase of an offset short with a 50.48 degree offset at 8 GHz, which was used as a standard in the calibration procedure. The magnitude errors are less than ±5.18 per cent, with the largest error occuring at 5.1 GHz. The phase errors do not exceed ±4.93 degrees. The largest error in phase

occurs at 3.3 GHz.

The measurement results for an offset short with an offset at 8 GHz of 70.52 degrees are shown in Fig. 4.6-4. The magnitude errors do not exceed 5.33 per cent for frequencies below 12.4 GHz, and 9 per cent for frequencies between 12.5 GHz and 13.2 GHz. The magnitude errors become larger for frequencies above 13.3 GHz. The phase errors are less than ±4 degrees for frequencies below 13.2 GHz. The largest error in phase is 7 degrees and occurs at 14 GHz. These phase errors are considered with respect to the calculated value.

Fig. 4.6-5 shows the results for a 118.81 degree offset short (at 8 GHz). These results show a magnitude per cent error less than ±6.6 per cent, with the largest error of -11.9 per cent at 14 GHz. The phase errors do not exceed ±6.2 degrees. The largest phase error occurs at 3.5 GHz.

The results for the 239.81 degree offset short, at 8 GHz, are shown in Fig. 4.6-6. The magnitude errors are less than ±9.9 per cent. The largest error occurs at 2.6 GHz. The errors at 6.2 GHz and 6.7 GHz are +8.17 per cent and -7.35 per cent, respectively. Larger errors are also noticed at 14 GHz, where an error of -13.71 per cent occurs. The phase do not exceed ±7.5 degrees with an exception at 6.8 GHz, where an error of

-11.52 degrees occurs. The largest error occurs at 14 GHz and measures 18.72 degrees.

Fig. 4.6-7 shows the results for an open, which was used as a standard in the calibration procedure. The magnitude per cent errors do not exceed ±3 per cent. The phase errors are less than ±2.5 degrees.

The results obtained for the 3 dB attenuator with a short are compared to the results obtained from an HP-8409 ANA. The errors in magnitude are less than ±0.7 dB with an exception at 6.1 GHz where the error is of -1.7 dB. The phase errors are less than ±7.1 degrees except for the results at 7.2 GHz where the phase error is -15 degrees.

The errors at the low frequencies end are due to the fact that the centers of the circles representing the power ratios approach one another as the frequency approaches 2 GHz, thus, making the accuracy of the six-port measurements suffer.

The errors noticed around 14 GHz in Fig. 4.6-4 through 4.6-6 are due to the fact that the offset short that was used in the calibration procedure starts looking like an open around 14 GHz. In Fig. 4.6-3, the phase of offset3 is shown to be 5 degrees.

The performance of the six-port reflectometer operated with pulsed signals was investigated over a band of frequencies ranging from 4 GHz to 12 GHz.

The peak detector circuit was the one given in Fig.4.2-2. The diode detectors, together with the peak detector circuits, were calibrated again over a range of the input power from -11 dBm to 9 dBm. The power levels at each diode varied considerably for different loads. Variations in voltage levels at individual diodes of 15 dB were noticed. The need for recalibration stemmed from the presence of an additional non-linear device, the diode based peak detector, and the dc offset voltages that the operational amplifier exhibited. Fast quad operational amplifiers with no external dc offset adjustment were used. Each chip incorporated four operational amplifiers which were connected as shown in Fig. 4.2-2. The only difference between the circuits is the absence of the dc offset control potentiometer.

The pulse generator was adjusted such that the pulse width was 250 microseconds and the spacing betweem pulses was chosen such that different duty cycles were obtained. The choice of pulse duration of 250 microseconds was dictated by the limitations in slew rate and driving capabilities of the operational amplifier. The pulse duration also allowed for periods

of the pulse trains ranging from 2.5 milliseconds to 500 microseconds for duty cycles ranging from 10 to 50 per cent respectively. These period values were small enough for the RC circuit of the peak detector to be able to follow the peaks with the least drop in voltage value.

Results were obtained for pulsed signals with 50, 25, and 10 per cent duty cycles. The detected pulse trains were also displayed on an oscilloscope in order to examine the quality of the pulses. The peaks of the pulses could be measured using the oscilloscope, but this method is not suitable for an automated six-port reflectometer.

The voltage detection circuits were calibrated at 8 GHz for an input power level range from -11 dBm to 9 dBm, for each duty cycle. The same technique in calibrating the diodes that was used for the CW operation was employed for the pulsed signal operation. Then, the six-port reflectometer was calibrated over the frequency range from 4 GHz to 12 GHz, using an input power level of -1 dBm.

The magnitudes of the reflection coefficient for a matched load, short, an open, offset shorts with offsets of 50.48, 70.52, 118.81, and 239.81 degrees, and a 3 dB attenuator with a short are plotted on Fig.4.6-9 through 4.6-17. The phases of the reflection coefficient for

the same loads are plotted on Fig.4.6-9 through 4.6-17. The (a) plots show the magnitude of the reflection coefficient, and the (b) plots show the phase of the same reflection coefficient with the exception of the matched load for which the phase does not mean anything.

The matched load magnitude plot is given in Fig. 4.6-9 and shows errors less than 0.005 in magnitude for the different duty cycles. The results obtained from an HP-8409 Automatic Network Analyzer are also shown for comparison.

Fig. 4.6-10 shows the magnitude measurements for a short for pulsed signals with different duty cycles are compared to the results from an HP-8409 ANA. The largest error in magnitude is of 8.9 per cent and it occurs at 5.8 GHz for a duty cycle of 50 per cent. With the exception of this case, the errors in magnitude are less than ±4 per cent. The phases plots are shown on Fig. 4.6-11. The (a) plot shows the results obtained from an HP-8409 ANA, and the (b) plots show the results obtained from the six-port operated with pulsed signals of different duty cycles. The errors in phase in the six-port measurements are less than ±2.7 degrees with the exception of the results at 2 GHz where errors of ± 5.9 degrees occur for all duty cycles. The results from the HP-8409 show errors in phase of less that ±5.8

degrees.

Fig. 4.6-12 shows measurements of an offset short with offset of 50.48 degrees at 8 GHz. The magnitude plot shows errors less than ±10.5 per cent for 50 per cent duty cycle, less than ±2.1 per cent for 25 per cent duty cycle, and less than ±4 per cent for 10 per cent duty cycle. The HP-8409 ANA results show errors less than ±6.9 per cent. The phase plot shows a displacement from the HP-8409 ANA result, and the phase was therefore compared to the calculated value. At the center frequency of 8 GHz the calculated phase of the reflection coefficient is 79.04 degrees. The phases obtained from the six-port reflectometer are within ± 0.02 degrees from the calculated value, while the HP-8409 results are 2.26 degrees larger. Comparing the calculated value of the offset at 4.6 GHz, where the largest deviation from the linear phase is noticed, the following results are obtained. The phase of the reflection coefficient at 4.6 GHz is calculated to be 121.95 degrees. The results obtained with the six-port show errors of 3.37 degrees for 10 per cent duty cycle, 0.52 degrees for 25 per cent duty cycle, and 0.31 degrees for 50 per cent duty cycle. The PLANA resuls (PLANA is the program that controls the operation of the HP-8409 Automatic Network Analyzer) show an error of

3.75 degrees in the phase of the reflection coefficient. The differences in phase measurements between PLANA and the six-port reflectometer are less than 3.5 degrees.

The plots on Fig. 4.6-13 show measurement results for an offset short with offset of 70.52 degrees at 8 GHz. The magnitudes obtained from six-port reflectometer measurements indicate errors of less than ±3.8 per cent for 10 per cent duty cycle, less than ±5 per cent for the 25 per cent duty cycle, and less than ±6.6 per cent for 50 per cent duty cycle, with the exception of the results at 4.9 GHz, for 50 per cent duty cycle, where an error of 14 per cent is recorded. The PLANA measurements show errors of less than ±5.6 per cent in magnitude. The phase results obtained from the HP-8409 ANA and the six-port reflectometer differ from the calculated values by less than ±4 degrees. The only exception occurs for the six-port measurements for 25 per cent duty cycle at 7.2 GHz, where an error in phase of 8.52 degrees is recorded. This error is taken with respect to the calculated value of the offset at 7.2 GHz.

Fig. 4.6-14 shows reflection coefficient measurements of an offset short with offset of 118.81 degrees at 8 GHz. The magnitude plot shows errors less than

11.8 per cent for 10 per cent duty cycle, 13 per cent for 25 per cent duty cycle, and 8.8 per cent for 50 per cent duty cycle. The largest errors are obtained at 9.8 GHz for 10 per cent duty cycle, 9.7 GHz for 25 per cent duty cycle, and 10.1 GHz for 50 per cent duty cycle. The phase errors are less than 7.6 degrees for all duty cycles. The largest error of 7.6 degrees is obtained at 7.2 GHz for 25 per cent duty cycle.

Fig. 4.6-15 shows the results obtained for an offset short with an offset of 239.81 degrees at 8 GHz. The plot of the magnitude of the reflection coefficient shows errors less than 10 per cent throughout the frequency band with exceptions of errors of 17 per cent at 10.3 GHz for 10 per cent duty cycle, 16 per cent at 6.9 GHz for 25 per cent duty cycle, and 16.77 per cent at 10.6 GHz for 50 per cent duty cycle. The plot of the phase of the reflection coefficient shows errors in phase of less than ±6 degrees for all duty cycles and all frequencies except 6.9 GHz for 25 per cent duty cycle. The largest error in phase is 11.9 degrees and it occurs at 6.9 GHz for 25 per cent duty cycle. The PLANA measurements give accuracies of ±5.6 per cent in magnitude and ±5 degrees.

Fig. 4.6-16 shows results obtained from measurements of an open circuit. The magnitude plots show errors less than ±3.4 per cent for 10 per cent duty cycle, ±2 per cent for 25 per cent duty cycle, and ±8 per cent for 50 per cent duty cycle. The largest errors occur at 6.8 GHz (8 per cent) and 6.7 GHz (5.8 per cent). The magnitude measurement exhibits an accuracy of less than ±2 per cent for the remainder of the frequencies for 50 per cent duty cycle. The phase plots show accuracies in phase measurements of ±3 degrees with the exception of the results at 6.7 GHz and 6.8 GHz for 50 per cent duty cycle. There, the phase errors are 4.21 degrees and 6.19 degrees respectively.

All the phases of the offset shorts were referenced to values that were calculated from the manufacturer specifications. The measurements of the load made up of a 3 dB attenuator and a short are compared directly to the measurements obtained from an HP-8409 ANA. Fig. 4.6-17(a) shows the magnitude of the reflection coefficient in dB. The six-port results are different from -6 dB by at most 1.4 dB. This large difference occurs at 9.4 GHz for 10 per cent duty cycle. Fig. 4.6-17(b) shows the phase of the same load. The phase differences between the six-port results and the PLANA

results are less than ±9 degrees, with the largest difference of 12 degrees occuring at 7.1 GHz for 25 per cent duty cycle.

The larger errors are caused by errors in calibration at the frequencies at which they occur. These errors are caused by noise corrupted measurements which affected the diode calibration, the six-port calibration and the measurements of the loads. The operational amplifiers did not have dc offset adjustment, and for low amplitude pulses, these dc offsets caused errors in output voltages. Another source of errors may come from the ideal characterization of the calibration standards, affecting both the CW and the pulsed measurements results. The offset short was calibrated for frequencies from 12GHz to 18GHz. Measurements of this offset short on the HP-8510 Automatic Network Analyzer show that the behaviour of the standard deviates from ideal by about 3 percent in magnitude outside the calibration range.

The overall performance of the six-port reflectometer operated with pulsed signals is comparable with the performance of the reflectometer operated with CW signals.

The performance of the six-port reflectometer with

narrower pulses was also investigated. The pulse train was set to exhibit a pulse duration of 3 microseconds and a duty cycle of 10 per cent. The reflectometer was calibrated at 4.5 GHz, 8 GHz and 14 GHz. The performance was investigated for the same loads that were previously used.

Table 4.6-1 shows the results obtained at 4.5 GHz for all the loads. The errors in the magnitudes of the offset shorts are less than ±8.6 per cent. The errors in phase did not exceed ±9.5 degrees. The 3 dB attenuator with the short shows differences from the HP-8409 ANA results of the order of 0.6 dB in magnitude and 3.82 degrees in phase.

Table 4.6-2 shows the results at 8 GHz. The errors in magnitude are less than ±3.85 per cent and the phase errors do not exceed ±5.58 degrees. The largest errors occur in the measurement of the offset short with 118.81 degree offset at 8 GHz. The 3 dB attenuator with the short exhibits erors of 0.05 dB in magnitude and 3.29 degrees in phase with respect to the HP-8409 ANA measurements.

Table 4.6-3 shows the results at 14 GHz. The results show errors in magnitude less than ±7.68 per cent, and phase errors that do not exceed ±3.33 degrees.

The 3 dB attenuator with a short differs from the HP-8409 ANA measurements by 0.44 dB in magnitude and 10 degrees in phase.

4.6.2 DYNAMIC RANGE

The dynamic range of the six-port reflectometer is determined by the range of input power levels for which it operates. The dynamic range of the six-port network analyzer is mainly limited by the power detection circuit. The dynamic range of the detectors can be extended using a subcarrier modulation approach. This method gives improved results due to the fact that with the DC detection method, the detector noise is primarily 1/f noise, while at 10 KHz, the subcarrier frequency, the noise is primarily shot and thermal noise [39].

The dynamic range of the six-port reflectometer was investigated with CW signals, and plots of measurements of a short circuit for input power levels from -11 dBm to -1 dBm are shown in Fig. 4.6.2-1.

Fig. 4.6.2-1 shows the magnitude and the phase measurements versus frequency for input power levels of -11 dBm, -6 dBm, and -1 dBm. The largest errors occur at frequencies around 6.5 GHz. The magnitude errors are less than 14.37 per cent, and the largest error occurs at 6.3 GHz for an input power level of -11 dBm. The phase errors are less than 10 degrees with the exception of the results at 7.3 GHz for -11 dBm input power, where

the phase error measures 12.63 degrees. The results obtained for -1 dBm input power show magnitude errors less than 5.1 per cent, and phase errors less than 5.4 degrees, with a maximum in both magnitude and phase occuring at 6.6 GHz.

The main source of errors is the diode calibration. The calibration of the diode which samples the input power shows errors in estimating the low levels of voltages, where the diode is in the square law region. This effect occurs due to the shape of the curve used to calibrated the diodes, which fits the data for larger voltages and gives errors as high as 15 per cent in estimating low voltages. The calibrations of the other diodes give lower errors when calculating the corrected value for low voltages. These errors are less than 1 per cent. Therefore, the large errors at lower frequencies come from the calibration of the diode that samples the input power.

A larger dynamic range is predicted if the diodes are calibrated over a larger voltage range, which can be achieved by calibrating the diode outside the six-port circuit.

4.7 CONCLUSIONS

The performance of the six-port reflectometer operated with pulsed signals was investigated and it was found to be quite good.

The errors in measurements were of the same order of magnitude with the errors obtained when the six-port reflectometer was operated with CW signals. The errors in magnitude were around 10 per cent, and the errors in phase were less than 10 degrees throughout the frequency band.

The six-port configuration that was used exhibited quite a wide bandwidth ranging from 4 GHz to 12 GHz. This bandwidth can be extended to go from 2 GHz to 14 GHz and possibly more with the proper choice of calibration standards. The offset short that was employed in the calibration of the six-port would look like an open circuit around the frequency of 14 GHz, thus making the calibration of the six-port impossible around that frequency. The calibration standards have to be reasonably apart in order to be able to calibrate the six-port successfully. In order to use the minimum number of standards (four standards), the frequency range was limited to go from 4 GHz to 12 GHz.

The choice of diode detectors to get a measure of the power at the four power measuring ports provided the six-port reflectometer with speed in measurements and lower input power requirements. The diode detectors require a calibration prior to their use in the six-port reflectometer. Two new methods for the calibration of the diode detectors were introduced. These methods use only the measured voltages to calibrate the detectors and one of the new methods eliminates the use of any additional devices.

The detection of the peak voltages of the pulsed signals is acomplished with the aid of a peak detection circuit. The limitations on the pulse duration and duty cycle of the pulse train used to pulse modulate the RF signal are mainly due to the limitations of the peak detecting circuit. The detection of the peak voltages associated with the pulsed signals requires low levels of input power. The detection of RMS values requires considerably larger values of input power especially for low duty cycle pulse trains, thus making this method quite unsuitable for the operation of the six-port with pulsed signals.

The six-port was fabricated in microstrip because of the simplicity of the fabrication procedure and the low costs involved.

The six-port reflectometer operated with pulsed signals proved to be as accurate as when it is operated with CW signals, thus making the use of the six-port measurement concept useful in systems that employ pulsed signals only.

4.8 FUTURE RESEARCH SUGGESTIONS

The six-port reflectometer proved to be a device that can be used with pulsed signals as well as with CW signals. This fact makes it useful for applications in which systems are operated with pulsed signals.

An immediate possible application of the six-port reflectometer operated with pulsed signals is its use in phased array antennas. The six-port reflectometer can be incorporated in front of each element of the array in order to measure and possibly control the phase of that radiating element. This application requires the investigation of the capabilities of integration of the six-port reflectometer in larger systems, in which the size of the six-port is of importance. The diode detectors will have to be integrated in the six-port itself and methods of calibration of the detectors and of the six-port itself have to be developed. Methods of tranfer of the calibration constants from a circuit outside the system to a six-port incorporated in the system may prove to be quite useful in solving the calibration problem of the integrated reflectometer. The diode detectors, since they may have to be integrated in the six-port will have to be calibrated "in situ", which

requires the connection of calibration standards at the measurement port. This may be a problem if the six-port is integrated. A possible solution to this dilema could be the calibration of the diodes while calibrating the six-port itself, or the calibration of the detection circuit outside of the reflectometer. This implies that the detection circuit will not behave differently when incorporated in the six-port, and that the construction of the six-port is repeatable.

The solution to the peak detector problem which uses additional AM modulation of the pulses detected at the four diode detectors needs to be investigated. This solution involves the modulation of a carrier of 10 KHz by the detected pulse train. The choice of carrier frequency is based on the ease of amplification of the signal. It turns out that it is easier to amplify signals in the KHz and MHz range rather than DC signals or signals at microwave frequencies. The signals obtained after the AM modulation process will be amplified to levels at which a regular diode detector operates properly. The amplified signal can be peak detected with the aid of of only a diode based peak detector. This method may also be used to improve the dynamic range of operation of the six-port reflectometer.

```
    Network: Branch Coupler
    Frequencies:
       7 9 0.1 GHz
    Ports:
       #1 1 0
       #2 2 0
       #3 3 0
       #4 4 0
    Components:
       T1 = TRL(Zo = 50 ohms, EL = 90.01 deg, CF = 8 GHz)
       T2 = TRL(Zo = 35.35 ohms. EL = 90.01 deg, CF = 8
GHz)
    Connections:
       T2 1 2 0
       T1 2 3 0
       T2 3 4 0
       T1 4 1 0
    Outputs:
       o21 = dB(s21)
       o31 = dB(s31)
       o41 = dB(s41)
    End
```

Table 2.2-1: Listing of MIDAS simulation program for a quadrature hybrid.

```
Network: Six-port
Frequencies:
  7 9 0.1 GHz
Ports:
  #1 1 0
  #3 5 0
  #4 17 0
  #5 16 0
  #6 14 0
Components:
  branchsub = branch / 1 2 3 4 0 /
  T1 = TRL(Zo=50 ohms,EL = 0.01 deg, CF = 8 GHz)
  T2 = TRL(Zo=50 ohms,EL = 0.01 deg, CF = 8 GHz)
  T3 = TRL(Zo=50 ohms,EL = 45 deg, CF = 8 GHz)
  T4 = TRL(Zo=50 ohms,EL = 0.01 deg,CF = 8 GHz)
  T5 = TRL(Zo=50 ohms,El = 90.01 deg,CF = 8 GHz)
  T6 = TRL(Zo=50 ohms,EL = 0.01 deg, CF = 8 GHz)
  T7 = TRL(Zo=50 ohms,EL = 0.01 deg, CF = 8 GHz)
  T10 = TRL(Zo=70.71 ohms,EL = 90.01 deg, CF = 8 GHz)
  Rbal = 100 ohms
  Rload = 50 ohms
Connections:
  T1 1 2 0
  T2 3 6 0
  T3 7 10 0
  T4 9 20 0
  T5 8 11 0
  T6 18 23 0
  T7 15 21 0
  T10 11 13 0
  T10 11 12 0
  branchsub 2 3 5 4 0
  branchsub 6 7 9 8 0
  branchsub 17 13 18 19 0
  branchsub 12 14 16 15 0
  branchsub 20 21 23 22 0
  DUT = realload Ohms
  realload = 40
  Rbal 12 13
  Rload 4 0
  Rload 19 0
  Rload 22 0
  DUT 10 0
Outputs:
  o31 = dB(s31)
  o41 = dB(s41)
  o51 = dB(s51)
  o61 = dB(s61)
End
```

Table 2.2-2: Listing of the MIDAS simulation program for the six-port network.

Program AVNA/1 Cal: sixport Meas: Short

Freq.(GHz)	S11-mag Mag.	Phase	Diff-mag.	Diff-pha.
7.000	1.0000	180.000	0.0	0.0
7.100	1.0000	180.000	0.0	0.0
7.200	1.0000	180.000	0.0	0.0
7.300	1.0000	180.000	0.0	0.0
7.400	1.0000	180.000	0.0	0.0
7.500	1.0000	180.000	0.0	0.0
7.600	1.0000	180.000	0.0	0.0
7.700	1.0000	180.000	0.0	0.0
7.800	1.0000	180.000	0.0	0.0
7.900	1.0000	180.000	0.0	0.0
8.000	1.0000	180.000	0.0	0.0
8.100	1.0000	180.000	0.0	0.0
8.200	1.0000	180.000	0.0	0.0
8.300	1.0000	180.000	0.0	0.0
8.400	1.0000	180.000	0.0	0.0
8.500	1.0000	180.000	0.0	0.0
8.600	1.0000	180.000	0.0	0.0
8.700	1.0000	180.000	0.0	0.0
8.800	1.0000	180.000	0.0	0.0
8.900	1.0000	180.000	0.0	0.0
9.000	1.0000	180.000	0.0	0.0

Table 2.2-3: Simulation results of measured reflection coefficient, per cent magnitude error and phase error (degrees) versus frequency for a short.

Program: AVNA/1 Cal: Sixport Meas: Offset1

Freq.(GHz)	S11-mag Mag.	Phase	Diff-mag.	Diff-pha.
7.000	1.0000	140.625	0.0	0.0
7.100	1.0000	140.062	0.0	0.0
7.200	1.0000	139.500	0.0	0.0
7.300	1.0000	138.937	0.0	0.0
7.400	1.0000	138.375	0.0	0.0
7.500	1.0000	137.812	0.0	0.0
7.600	1.0000	137.250	0.0	0.0
7.700	1.0000	136.687	0.0	0.0
7.800	1.0000	136.125	0.0	0.0
7.900	1.0000	135.562	0.0	0.0
8.000	1.0000	135.000	0.0	0.0
8.100	1.0000	134.437	0.0	0.0
8.200	1.0000	133.875	0.0	0.0
8.300	1.0000	133.312	0.0	0.0
8.400	1.0000	132.750	0.0	0.0
8.500	1.0000	132.187	0.0	0.0
8.600	1.0000	131.625	0.0	0.0
8.700	1.0000	131.062	0.0	0.0
8.800	1.0000	130.500	0.0	0.0
8.900	1.0000	129.938	0.0	0.0
9.000	1.0000	129.375	0.0	0.0

Table 2.2-4: Simulation results of measured reflection coefficient, per cent magnitude error and phase error (degrees) versus frequency for a 22.5 degree offset short (at 8 GHz).

Program: AVNA/1 Cal: Sixport Meas: Offset2

Freq.(GHz)	S11-mag Mag.	Phase	Diff-mag.	Diff-pha.
7.000	0.9958	127.329	0.42%	0.1709
7.100	0.9978	126.817	0.22%	-0.0675
7.200	1.0008	125.977	-0.08%	0.0225
7.300	0.9983	125.216	0.17%	0.0337
7.400	0.9998	124.524	0.02%	-0.0237
7.500	1.0007	123.765	-0.07%	-0.0152
7.600	0.9988	122.945	0.12%	0.0546
7.700	1.0008	122.218	-0.08%	0.0324
7.800	1.0010	121.464	-0.10%	0.0364
7.900	1.0004	120.735	-0.04%	0.0147
8.000	1.0001	120.001	-0.01%	0.0015
8.100	0.9991	119.238	0.09%	0.0119
8.200	0.9996	118.527	0.04%	-0.0270
8.300	1.0003	117.759	-0.03%	-0.0087
8.400	1.0006	117.013	-0.06%	-0.0131
8.500	0.9996	116.232	0.04%	0.0180
8.600	1.0006	115.469	-0.06%	0.0310
8.700	1.0001	114.780	-0.01%	-0.0296
8.800	0.9990	114.002	0.10%	-0.0017
8.900	1.0002	112.521	-0.02%	-0.0219
9.000	1.0004	112.521	-0.04%	-0.0215

Table 2.2-5: Simulation results for measured reflection coefficient, per cent magnitude error and phase error (degrees) versus frequency for a 30 degree offset short (at 8 GHz).

Program: AVNA/1 Cal: Sixport Meas: Offset3

Freq.(GHz)	S11-mag Mag.	Phase	Diff-mag.	Diff-pha.
7.000	0.9981	101.178	0.19%	0.1221
7.100	1.0005	100.167	-0.05%	-0.0421
7.200	0.9997	98.956	0.03%	0.0439
7.300	0.9999	97.849	0.01%	0.0253
7.400	1.0000	96.765	0.00%	-0.0146
7.500	1.0000	95.618	0.00%	0.0070
7.600	1.0006	94.385	-0.06%	0.1148
7.700	1.0001	93.360	-0.01%	0.0148
7.800	1.0008	92.180	-0.08%	0.0698
7.900	0.9988	91.209	0.12%	-0.0835
8.000	0.9997	90.015	0.03%	-0.0149
8.100	1.0003	88.859	-0.03%	0.0155
8.200	0.9996	87.768	0.04%	-0.0177
8.300	0.9999	86.628	0.01%	-0.0029
8.400	0.9991	85.532	0.09%	-0.0318
8.500	1.0007	84.351	-0.07%	0.0236
8.600	1.0010	83.219	-0.10%	0.0309
8.700	1.0004	82.135	-0.04%	0.0105
8.800	0.9994	81.014	0.06%	-0.0141
8.900	0.9994	79.886	0.06%	-0.0109
9.000	0.9991	78.762	0.09%	-0.0116

Table 2.2-6: Simulation results of measured reflection coefficient, per cent magnitude error and phase error (degrees) versus frequency for a 45 degree offset short (at 8 GHz).

Program: AVNA/1 Cal: Sixport Meas: Offset4

Freq.(GHz)	S11-mag Mag.	Phase	Diff-mag.	Diff-pha.
7.100	0.9986	61.6840	0.14%	0.1910
7.100	1.0000	60.2593	0.00%	-0.0718
7.200	1.0005	58.3839	-0.05%	0.1161
7.300	1.0003	56.5775	-0.03%	0.2350
7.400	1.0008	55.2693	-0.08%	-0.1443
7.500	0.9984	53.4707	0.16%	-0.0332
7.600	1.0023	51.5782	-0.23%	0.1718
7.700	0.9989	50.0032	0.11%	0.0593
7.800	1.0014	48.3038	-0.14%	0.0712
7.900	0.9967	46.7694	0.33%	-0.0819
8.000	0.9996	45.0041	0.04%	-0.0041
8.100	0.9991	43.4133	0.09%	-0.1006
8.200	1.0020	41.7786	-0.20%	-0.1536
8.300	0.9998	40.0976	0.02%	-0.1600
8.400	0.9991	38.1384	0.09%	0.1116
8.500	1.0000	36.6992	0.00%	-0.1367
8.600	0.9998	34.8444	0.02%	0.0306
8.700	1.0002	33.0887	-0.02%	0.0988
8.800	1.0003	31.9254	-0.03%	-0.4254
8.900	1.0001	29.4239	-0.01%	0.3886
9.000	1.0010	27.9682	-0.10%	0.1568

Table 2.2-7: Simulation results of measured reflection coefficient, per cent magnitude error and phase error (degrees) versus frequency for a 67.5 degree offset short (at 8 GHz).

Program: AVNA/1 Cal: Sixport Meas: Match

Freq.(GHz)	S11-mag Mag.	Phase	Diff-mag.	Diff-pha.
7.000	0.0000	-35.803	0.00%	35.803
7.100	0.0000	96.465	0.00%	-96.465
7.200	0.0000	218.268	0.00%	-218.270
7.300	0.0000	32.822	0.00%	-32.822
7.400	0.0000	238.455	0.00%	-238.455
7.500	0.0000	52.706	0.00%	-52.706
7.600	0.0000	82.950	0.00%	-82.950
7.700	0.0000	174.600	0.00%	-174.600
7.800	0.0000	94.174	0.00%	-94.174
7.900	0.0000	268.390	0.00%	-269.390
8.000	0.0000	45.026	0.00%	-45.026
8.100	0.0000	264.982	0.00%	-264.982
8.200	0.0000	183.439	0.00%	-183.439
8.300	0.0000	142.385	0.00%	-142.385
8.400	0.0000	103.338	0.00%	-103.338
8.500	0.0000	-61.031	0.00%	61.031
8.600	0.0000	0.000	0.00%	0.000
8.700	0.0000	-84.056	0.00%	84.056
8.800	0.0000	-83.373	0.00%	83.373
8.900	0.0000	267.143	0.00%	-267.143
9.000	0.0000	-63.696	0.00%	63.696

Table 2.2-8: Simulation results of measured reflection coefficient, per cent magnitude error and phase error (degrees) versus frequency for a matched load. (The phase and phase error columns should be ignored since the magnitude is zero).

Program: AVNA/1 Cal: Sixport Meas: Load1

Freq.(GHz)	S11-mag Mag.	Phase	Diff-mag.	Diff-pha.
7.000	0.1111	179.702	-0.09%	0.2976
7.100	0.1104	179.590	0.54%	0.4098
7.200	0.1117	180.263	-0.63%	-0.2633
7.300	0.1110	180.036	0.00%	-0.0365
7.400	0.1112	180.411	-0.18%	-0.4106
7.500	0.1115	180.418	-0.45%	-0.4175
7.600	0.1113	179.589	-0.27%	0.4110
7.700	0.1099	180.268	0.99%	-0.2677
7.800	0.1115	180.216	-0.45%	-0.2157
7.900	0.1112	180.265	-0.18%	-0.2652
8.000	0.1113	179.289	-0.27%	0.7113
8.100	0.1100	179.706	0.90%	0.2937
8.200	0.1108	179.559	0.18%	0.4406
8.300	0.1111	179.652	-0.09%	0.3479
8.400	0.1118	180.008	-0.72%	-0.0078
8.500	0.1105	179.707	0.45%	0.2934
8.600	0.1110	178.580	0.00%	1.4200
8.700	0.1104	179.988	0.54%	0.0119
8.800	0.1116	180.447	-0.54%	-0.4475
8.900	0.1107	180.870	0.27%	-0.8696
9.000	0.1105	178.818	0.45%	1.1818

Table 2.2-9: Simulation results of measured reflection coefficient, per cent magnitude error and phase error (degrees) versus frequency for a load with $\Gamma = -0.111$.

Program: AVNA/1 Cal: Sixport Meas: Load2

Freq.(GHz)	S11-mag Mag.	Phase	Diff-mag.	Diff-pha.
7.000	0.1119	101.868	-0.81%	-0.6182
7.100	0.1103	99.638	0.63%	0.4874
7.200	0.1109	99.411	0.09%	-0.4114
7.300	0.1107	97.755	0.27%	0.1196
7.400	0.1111	97.096	-0.09%	-0.3460
7.500	0.1107	96.312	0.27%	-0.6874
7.600	0.1107	94.443	0.27%	0.0572
7.700	0.1108	92.806	0.18%	0.5688
7.800	0.1107	92.232	0.27%	0.0177
7.900	0.1123	91.671	-1.17%	-0.5459
8.000	0.1116	90.034	-0.54%	-0.0339
8.100	0.1117	88.727	-0.63%	0.1483
8.200	0.1130	87.768	-1.80%	-0.0179
8.300	0.1133	87.309	-2.07%	-0.6840
8.400	0.1113	85.612	-0.27%	-0.1121
8.500	0.1109	84.466	0.09%	-0.0910
8.600	0.1117	83.216	-0.63%	0.0336
8.700	0.1087	81.889	2.07%	0.2359
8.800	0.1148	81.840	-3.42%	-0.8397
8.900	0.1115	80.130	-0.45%	-0.2547
9.000	0.1120	79.208	-0.90%	-0.4579

Table 2.2-10: Simulation results of measured reflection coefficient, per cent magnitude error and phase error (degrees) versus frequency for a load with $|\Gamma| = 0.111$ and 45 degree offset from the short.

Program: AVNA/1 Cal: Sixport Meas: Open

Freq.(GHz)	S11-mag Mag.	Phase	Diff-mag.	Diff-pha.
7.000	1.0184	1.1658	-1.84%	-1.1658
7.100	0.9988	-0.0768	0.12%	0.0768
7.200	0.9992	-0.0083	0.08%	0.0083
7.300	1.0012	-0.0475	-0.12%	0.0475
7.400	1.0005	0.1886	-0.05%	-0.1886
7.500	1.0009	0.1530	-0.09%	-0.1530
7.600	1.0017	-0.3451	-0.17%	0.3451
7.700	1.0000	0.2836	0.00%	-0.2836
7.800	1.0014	0.1621	-0.14%	-0.1621
7.900	0.9993	0.0201	0.07%	-0.0201
8.000	0.9984	-0.0308	0.16%	0.0308
8.100	1.0013	-0.0088	-0.13%	0.0088
8.200	1.0014	-0.1499	-0.14%	0.1499
8.300	1.0048	-0.0163	-0.48%	0.0163
8.400	1.0022	0.0066	-0.22%	-0.0066
8.500	1.0013	-0.0538	-0.13%	0.0538
8.600	0.9988	0.0480	0.12%	-0.0480
8.700	0.9994	-0.1847	0.06%	0.1847
8.800	0.9979	0.0291	0.21%	-0.0291
8.900	1.0006	0.0022	-0.06%	-0.0022
9.000	0.9969	0.0160	0.31%	-0.0160

Table 2.2-11: Simulation results of measured reflection coefficient, per cent magnitude error and phase (degrees) versus frequency for an open.

Program: AVNA/1 Cal: Sixport Meas: Short

Freq.(GHz)	S11-mag Mag.	Phase	Diff-mag.	Diff-pha.
7.000	1.0000	180.000	0.00%	0.0
7.100	1.0000	180.000	0.00%	0.0
7.200	1.0000	180.000	0.00%	0.0
7.300	1.0000	180.000	0.00%	0.0
7.400	1.0000	180.000	0.00%	0.0
7.500	1.0000	180.000	0.00%	0.0
7.600	1.0000	180.000	0.00%	0.0
7.700	1.0000	180.000	0.00%	0.0
7.800	1.0000	180.000	0.00%	0.0
7.900	1.0000	180.000	0.00%	0.0
8.000	1.0000	180.000	0.00%	0.0
8.100	1.0000	180.000	0.00%	0.0
8.200	1.0000	180.000	0.00%	0.0
8.300	1.0000	180.000	0.00%	0.0
8.400	1.0000	180.000	0.00%	0.0
8.500	1.0000	180.000	0.00%	0.0
8.600	1.0000	180.000	0.00%	0.0
8.700	1.0000	180.000	0.00%	0.0
8.800	1.0000	180.000	0.00%	0.0
8.900	1.0000	180.000	0.00%	0.0
9.000	1.0000	180.000	0.00%	0.0

Table 2.2-12: Simulation results, using S-parameters to model the six-port operation, for reflection coefficient, per cent magnitude error and phase error (degrees) versus frequency for a short.

Program: AVNA/1 Cal: Sixport Meas: Offset1

Freq.(GHz)	S11-mag Mag.	Phase	Diff-mag.	Diff-pha.
7.000	1.0000	140.625	0.00%	0.0
7.100	1.0000	140.062	0.00%	0.0
7.200	1.0000	139.500	0.00%	0.0
7.300	1.0000	138.937	0.00%	0.0
7.400	1.0000	138.375	0.00%	0.0
7.500	1.0000	137.812	0.00%	0.0
7.600	1.0000	137.250	0.00%	0.0
7.700	1.0000	136.687	0.00%	0.0
7.800	1.0000	136.125	0.00%	0.0
7.900	1.0000	135.562	0.00%	0.0
8.000	1.0000	135.000	0.00%	0.0
8.100	1.0000	134.437	0.00%	0.0
8.200	1.0000	133.875	0.00%	0.0
8.300	1.0000	133.312	0.00%	0.0
8.400	1.0000	132.750	0.00%	0.0
8.500	1.0000	132.187	0.00%	0.0
8.600	1.0000	131.625	0.00%	0.0
8.700	1.0000	131.062	0.00%	0.0
8.800	1.0000	130.500	0.00%	0.0
8.900	1.0000	129.937	0.00%	0.0
9.000	1.0000	129.375	0.00%	0.0

Table 2.2-13: Simulation results, using S-parameters to model the six-port operation, for reflection coefficient, per cent magnitude error and phase error (degrees) versus frequency, for a 22.5 degree offset short (at 8 GHz).

Program: AVNA/1 Cal: Sixport Meas: Offset2

Freq.(GHz)	S11-mag Mag.	Phase	Diff-mag.	Diff-pha.
7.000	1.0000	127.500	0.00%	0.0
7.100	1.0000	126.750	0.00%	0.0
7.200	1.0000	126.000	0.00%	0.0
7.300	1.0000	125.250	0.00%	0.0
7.400	1.0000	124.500	0.00%	0.0
7.500	1.0000	123.750	0.00%	0.0
7.600	1.0000	123.000	0.00%	0.0
7.700	1.0000	122.250	0.00%	0.0
7.800	1.0000	121.500	0.00%	0.0
7.900	1.0000	120.750	0.00%	0.0
8.000	1.0000	120.000	0.00%	0.0
8.100	1.0000	119.250	0.00%	0.0
8.200	1.0000	118.500	0.00%	0.0
8.300	1.0000	117.750	0.00%	0.0
8.400	1.0000	117.000	0.00%	0.0
8.500	1.0000	116.250	0.00%	0.0
8.600	1.0000	115.500	0.00%	0.0
8.700	1.0000	114.750	0.00%	0.0
8.800	1.0000	114.000	0.00%	0.0
8.900	1.0000	113.250	0.00%	0.0
9.000	1.0000	112.500	0.00%	0.0

Table 2.2-14: Simulation results, using S-parameters to model the six-port operation, for reflection coefficient, per cent magnitude error and phase error (degrees) versus frequency, for a 30 degrees offset short (at 8 GHz).

Program: AVNA/1 Cal: Sixport Meas: Offset3

Freq.(GHz)	S11-mag Mag.	Phase	Diff-mag.	Diff-pha.
7.000	1.0000	101.250	0.00%	0.0
7.100	1.0000	100.125	0.00%	0.0
7.200	1.0000	99.000	0.00%	0.0
7.300	1.0000	97.875	0.00%	0.0
7.400	1.0000	96.750	0.00%	0.0
7.500	1.0000	95.625	0.00%	0.0
7.600	1.0000	94.500	0.00%	0.0
7.700	1.0000	93.375	0.00%	0.0
7.800	1.0000	92.250	0.00%	0.0
7.900	1.0000	91.125	0.00%	0.0
8.000	1.0000	90.000	0.00%	0.0
8.100	1.0000	88.875	0.00%	0.0
8.200	1.0000	87.750	0.00%	0.0
8.300	1.0000	86.625	0.00%	0.0
8.400	1.0000	85.500	0.00%	0.0
8.500	1.0000	84.375	0.00%	0.0
8.600	1.0000	83.250	0.00%	0.0
8.700	1.0000	82.125	0.00%	0.0
8.800	1.0000	81.000	0.00%	0.0
8.900	1.0000	79.875	0.00%	0.0
9.000	1.0000	78.750	0.00%	0.0

Table 2.2-15: Simulation results, using S-parameters to model the six-port operation, for reflection magnitude, per cent magnitude error and phase error (degrees) versus frequency for a 45 degree offset short (at 8 GHz).

Program: AVNA/1 Cal: Sixport Meas: Offset4

Freq.(GHz)	S11-mag Mag.	Phase	Diff-mag.	Diff-pha.
7.000	1.0000	61.875	0.00%	0.0
7.100	1.0000	60.187	0.00%	0.0
7.200	1.0000	58.500	0.00%	0.0
7.300	1.0000	56.812	0.00%	0.0
7.400	1.0000	55.125	0.00%	0.0
7.500	1.0000	53.438	0.00%	0.0
7.600	1.0000	51.750	0.00%	0.0
7.700	1.0000	50.063	0.00%	0.0
7.800	1.0000	48.375	0.00%	0.0
7.900	1.0000	46.688	0.00%	0.0
8.000	1.0000	45.000	0.00%	0.0
8.100	1.0000	43.313	0.00%	0.0
8.200	1.0000	41.625	0.00%	0.0
8.300	1.0000	39.938	0.00%	0.0
8.400	1.0000	38.250	0.00%	0.0
8.500	1.0000	36.563	0.00%	0.0
8.600	1.0000	34.875	0.00%	0.0
8.700	1.0000	33.188	0.00%	0.0
8.800	1.0000	31.500	0.00%	0.0
8.900	1.0000	29.813	0.00%	0.0
9.000	1.0000	28.125	0.00%	0.0

Table 2.2-16: Simulation results, using S-parameters to model the six-port operation, for reflection coefficient, per cent magnitude error and phase error (degrees) versus frequency, for a 67.5 degree offset short (at 8 GHz).

Program: AVNA/1 Cal: Sixport Meas: Match

Freq.(GHz)	S11-mag Mag.	Phase	Diff-mag.	Diff-pha.
7.000	0.0000	-53.700	0.00%	53.700
7.100	0.0000	0.000	0.00%	0.000
7.200	0.0000	-3.882	0.00%	3.882
7.300	0.0000	-76.610	0.00%	76.610
7.400	0.0000	58.300	0.00%	-58.300
7.500	0.0000	137.269	0.00%	-137.269
7.600	0.0000	61.259	0.00%	-61.259
7.700	0.0000	87.186	0.00%	-87.186
7.800	0.0000	84.823	0.00%	-84.823
7.900	0.0000	40.602	0.00%	-40.602
8.000	0.0000	45.022	0.00%	-45.022
8.100	0.0000	228.972	0.00%	-228.972
8.200	0.0000	-87.068	0.00%	87.068
8.300	0.0000	91.106	0.00%	-91.106
8.400	0.0000	128.934	0.00%	-128.934
8.500	0.0000	237.722	0.00%	-237.722
8.600	0.0000	88.634	0.00%	-88.634
8.700	0.0000	86.548	0.00%	-86.548
8.800	0.0000	75.227	0.00%	-75.227
8.900	0.0000	93.316	0.00%	-93.316
9.000	0.0000	71.104	0.00%	-71.104

Table 2.2-17: Simulation results, using S-parameters to model the six-port operation, for reflection coefficient, per cent magnitude error and phase error (degrees) versus frequency for a matched load. The phase and phase error columns should be ignored since the magnitude is zero.

Program: AVNA/1 Cal: Sixport Meas: Load1

Freq.(GHz)	S11-mag Mag.	Phase	Diff-mag.	Diff-pha.
7.000	0.1110	180.000	0.00%	0.0
7.100	0.1110	180.000	0.00%	0.0
7.200	0.1110	180.000	0.00%	0.0
7.300	0.1110	180.000	0.00%	0.0
7.400	0.1110	180.000	0.00%	0.0
7.500	0.1110	180.000	0.00%	0.0
7.600	0.1110	180.000	0.00%	0.0
7.700	0.1110	180.000	0.00%	0.0
7.800	0.1110	180.000	0.00%	0.0
7.900	0.1110	180.000	0.00%	0.0
8.000	0.1110	180.000	0.00%	0.0
8.100	0.1110	180.000	0.00%	0.0
8.200	0.1110	180.000	0.00%	0.0
8.300	0.1110	180.000	0.00%	0.0
8.400	0.1110	180.000	0.00%	0.0
8.500	0.1110	180.000	0.00%	0.0
8.600	0.1110	180.000	0.00%	0.0
8.700	0.1110	180.000	0.00%	0.0
8.800	0.1110	180.000	0.00%	0.0
8.900	0.1110	180.000	0.00%	0.0
9.000	0.1110	180.000	0.00%	0.0

Table 2.2-18: Simulation results, using S-parameters to model the six-port operation, for reflection coefficient, per cent magnitude error and phase error (degrees) versus frequency for a load with $\Gamma = -0.111$.

Program: AVNA/1 Cal: Sixport Meas: Load3

Freq.(GHz)	S11-mag			
	Mag.	Phase	Diff-mag.	Diff-pha.
7.000	0.1110	90.000	0.00%	0.0
7.100	0.1110	90.000	0.00%	0.0
7.200	0.1110	90.000	0.00%	0.0
7.300	0.1110	90.000	0.00%	0.0
7.400	0.1110	90.000	0.00%	0.0
7.500	0.1110	90.000	0.00%	0.0
7.600	0.1110	90.000	0.00%	0.0
7.700	0.1110	90.000	0.00%	0.0
7.800	0.1110	90.000	0.00%	0.0
7.900	0.1110	90.000	0.00%	0.0
8.000	0.1110	90.000	0.00%	0.0
8.100	0.1110	90.000	0.00%	0.0
8.200	0.1110	90.000	0.00%	0.0
8.300	0.1110	90.000	0.00%	0.0
8.400	0.1110	90.000	0.00%	0.0
8.500	0.1110	90.000	0.00%	0.0
8.600	0.1110	90.000	0.00%	0.0
8.700	0.1110	90.000	0.00%	0.0
8.800	0.1110	90.000	0.00%	0.0
8.900	0.1110	90.000	0.00%	0.0
9.000	0.1110	90.000	0.00%	0.0

Table 2.2-19: Simulation results, using S-parameters to model the six-port operation, for reflection coefficient, per cent magnitude error and phase error (degrees) versus frequency for a load with $\Gamma = j0.111$.

Program: AVNA/1 Cal: Sixport Meas: Open

Freq.(GHz)	S11-mag Mag.	Phase	Diff-mag.	Diff-pha.
7.000	1.0000	-0.0001	0.00%	0.0001
7.100	1.0000	-0.0001	0.00%	0.0001
7.200	1.0000	0.0000	0.00%	0.0000
7.300	1.0000	-0.0001	0.00%	0.0001
7.400	1.0000	0.0001	0.00%	-0.0001
7.500	1.0000	0.0000	0.00%	0.0000
7.600	1.0000	0.0000	0.00%	0.0000
7.700	1.0000	0.0000	0.00%	0.0000
7.800	1.0000	0.0000	0.00%	0.0000
7.900	1.0000	0.0000	0.00%	0.0000
8.000	1.0000	0.0000	0.00%	0.0000
8.100	1.0000	0.0000	0.00%	0.0000
8.200	1.0000	0.0000	0.00%	0.0000
8.300	1.0000	0.0000	0.00%	0.0000
8.400	1.0000	0.0000	0.00%	0.0000
8.500	1.0000	0.0000	0.00%	0.0000
8.600	1.0000	0.0001	0.00%	-0.0001
8.700	1.0000	0.0000	0.00%	0.0000
8.800	1.0000	0.0000	0.00%	0.0000
8.900	1.0000	0.0001	0.00%	-0.0001
9.000	1.0000	-0.0001	0.00%	0.0001

Table 2.2-20: Simulation results, using S-parameters to model the six-port operation, for reflection coefficient, per cent magnitude error and phase error (degrees) versus frequency for an open.

Characteristic impedance (ohms)	Width of line (mils)
44.64	65.40
50.00	54.72
70.71	29.18
100.00	13.56

Table 3.2-1: Widths of microstrip transmission lines for different characteristic impedances for 5880 Duroid copper cladding with 20 mil height

Standard	Mag.	Phase	Mag. diff.	Pha. diff.
Short	0.9230	180.465	-7.70%	+0.465
Offset Short 3 (50.48 deg. @ 8 GHz)	1.0517	113.628	+5.17%	-9.582
Offset Short 4 (70.52 deg. @ 8 GHz)	1.0002	100.538	+0.02%	-0.127
Offset Short 5 (118.81 deg. @ 8 GHz)	1.0866	47.988	+8.66%	+1.649
Offset Short 6 (239.81 deg. @ 8 GHz)	0.9980	-89.874	-0.20%	-0.878
Open	1.0021	0.097	-0.21%	+0.097
3 dB Atten. with Short	-7.066 dB	80.137	-0.824 dB	-2.463

Table 4.6-1: Pulsed measurements at 4.5 GHz (pulse duration = 3 microseconds, pulse period = 30 microseconds).

Standard	Mag.	Phase	Mag. diff.	Pha. diff.
Short	1.0268	180.297	+2.68%	+0.297
Offset Short 3 (50.48 deg. @ 8 GHz)	1.0184	78.406	+1.84%	-0.641
Offset Short 4 (70.52 deg. @ 8 GHz)	0.9707	41.704	-2.93%	+2.747
Offset Short 5 (118.81 deg. @ 8 GHz)	0.9615	-52.036	-3.85%	+5.580
Offset Short 6 (239.81 deg. @ 8 GHz)	0.9951	62.5248	-0.49%	+2.141
Open	0.9897	0.074	-1.03%	+0.074
3 dB Atten. with Short	-6.518 dB	91.790	-0.05 dB	+3.290

Table 4.6-2: Pulsed measurements at 8 GHz (pulse duration = 3 microseconds, pulse period = 30 microseconds).

Standard	Mag.	Phase	Mag. diff.	Pha. diff.
Short	0.9998	178.356	-0.02%	-1.654
Offset Short 3 (50.48 deg. @ 8 GHz)	0.9552	6.399	-4.48%	+3.078
Offset Short 4 (70.52 deg. @ 8 GHz)	0.9706	-66.994	-2.94%	-0.174
Offset Short 5 (118.81 deg. @ 8 GHz)	0.9990	121.032	-0.10%	-3.133
Offset Short 6 (239.81 deg. @ 8 GHz)	0.9232	59.284	-7.68%	-1.381
Open	0.9939	0.679	-0.61%	+0.679
3 dB Atten. with Short	-6.8 dB	200.55	-0.44 dB	+10.050

Table 4.6-3: Pulsed measurements at 14 GHz (pulse duration = 3 microseconds, pulse period = 30 microseconds).

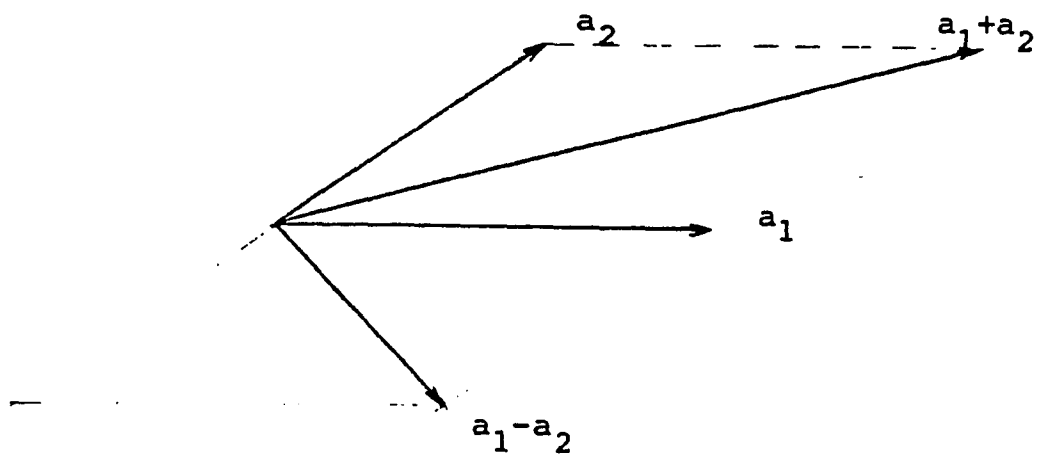

Fig.1.1-1: Unknown phasor a_2 relative to known phasor a_1, and the sum and difference of a_1 and a_2

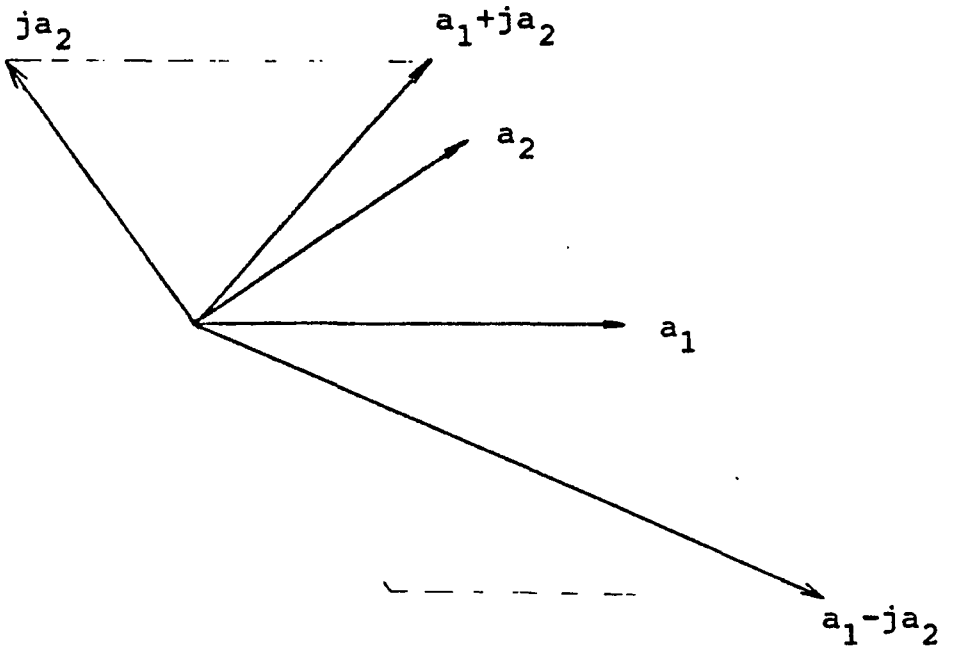

Fig.1.1-2: Unknown phasor a_2, the rotated unknown phasor ja_2 and the sum and difference of a_1 and ja_2

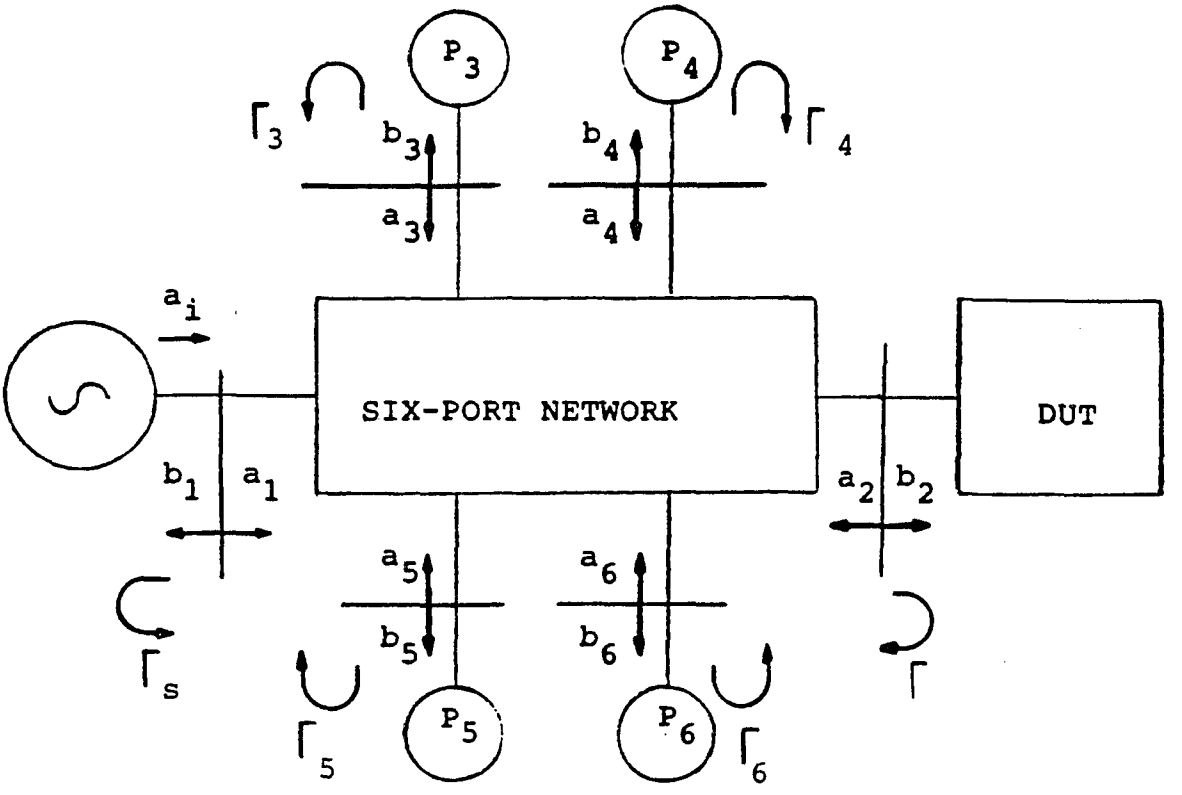

Fig.1.1-3: Six-port network with unmatched power meters and device under test

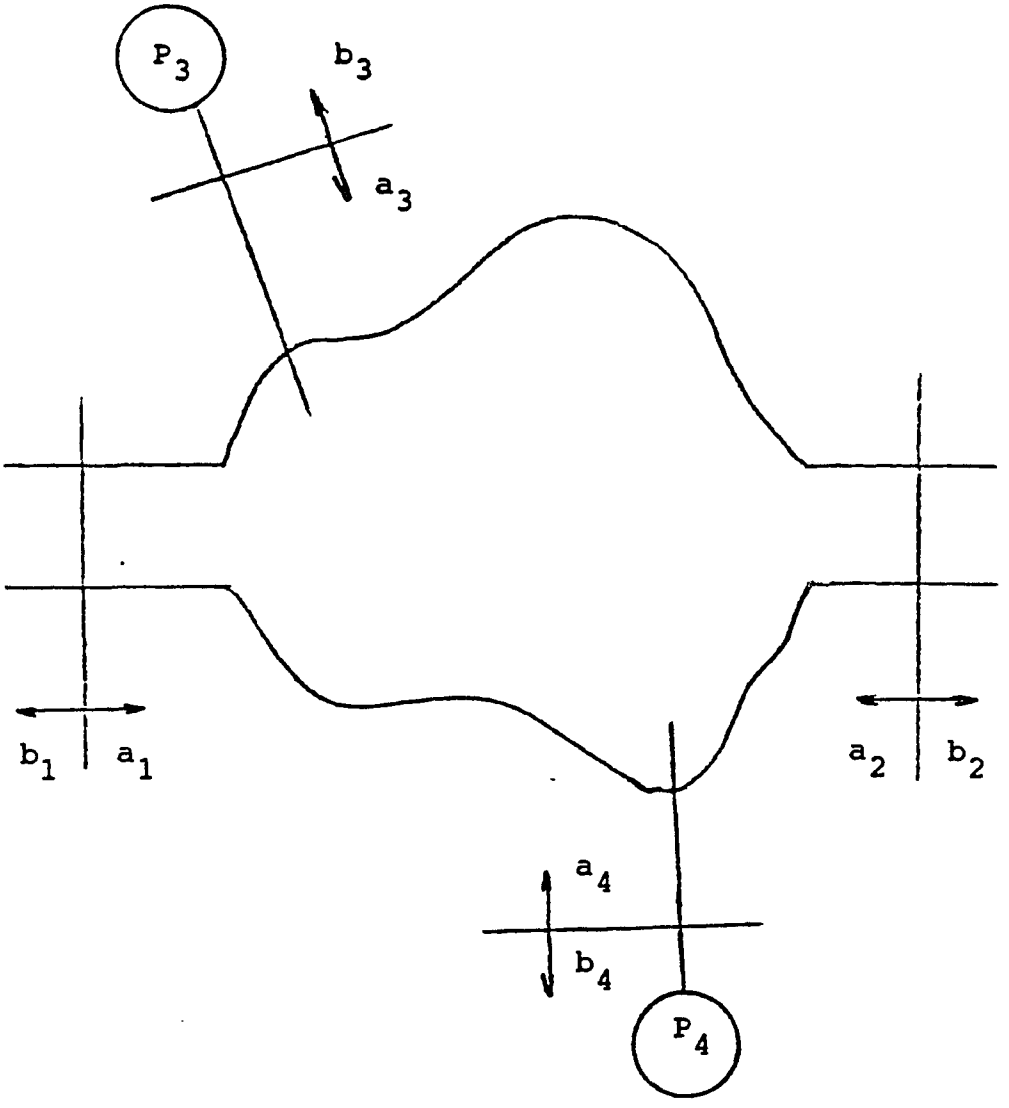

Fig.1.1-4: Four-port microwave junction with input, output, and two power measuring ports

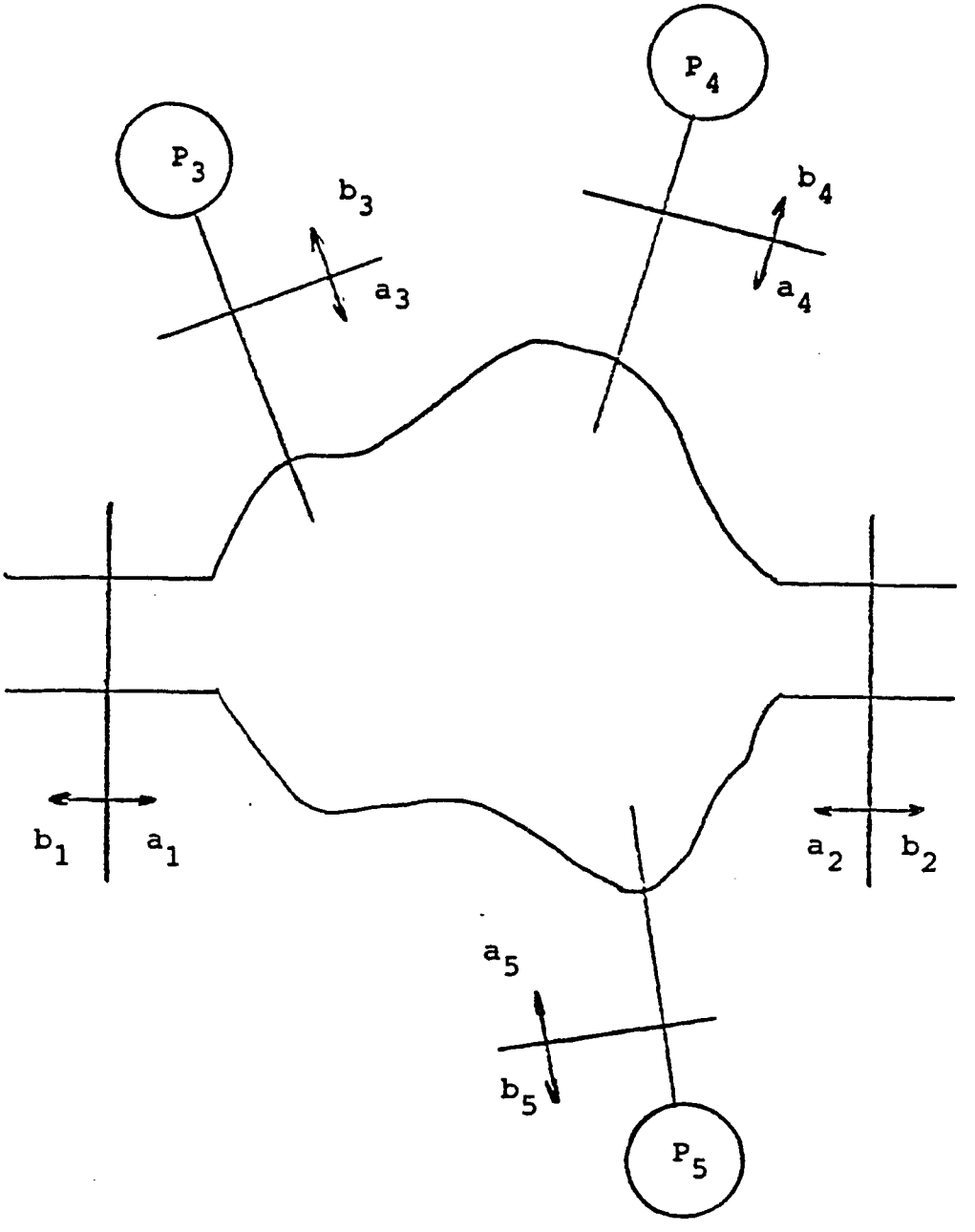

Fig.1.1-5: Five-port microwave junction with input, output and three power measuring ports

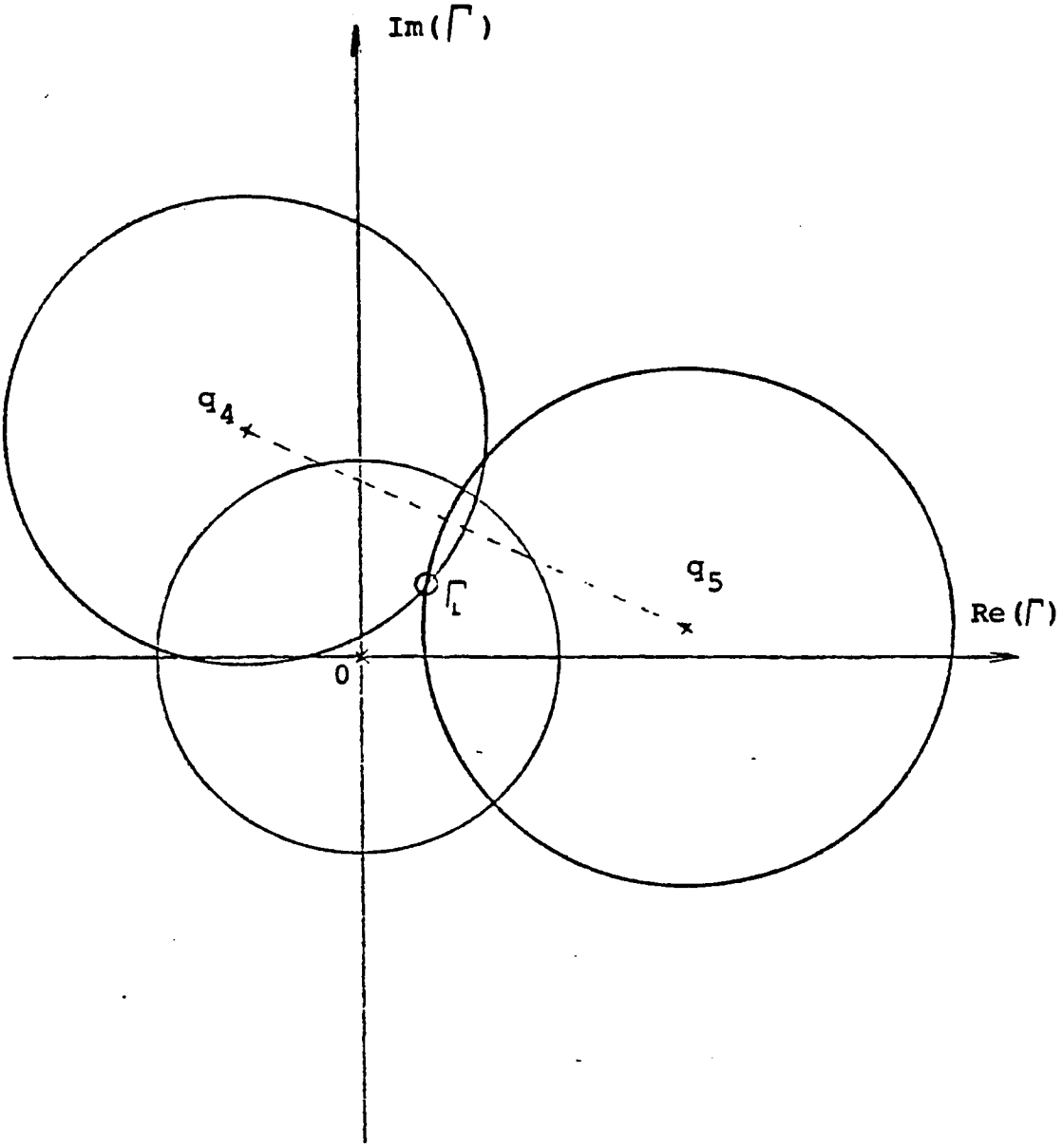

Fig.1.1-6: The two intesections of the circles representing the power ratio equations associated with a five-port

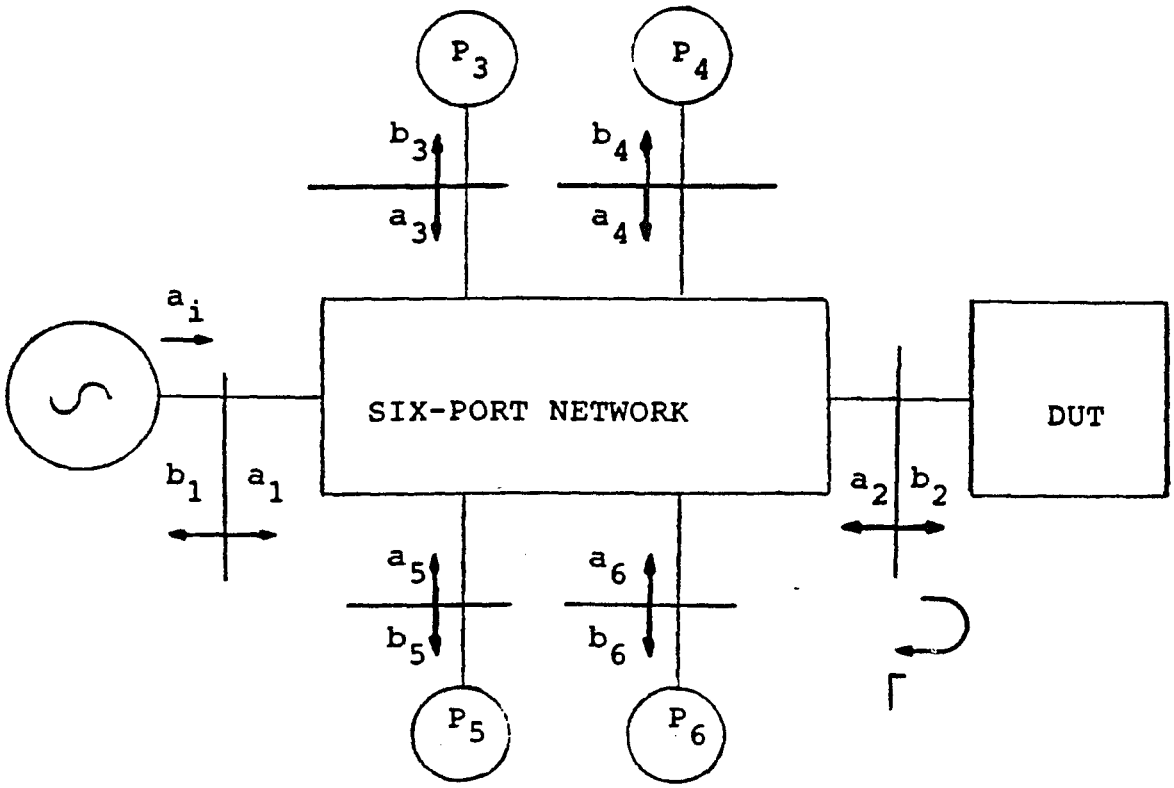

Fig.1.1-7: Six-port network with input, output and four power measuring ports

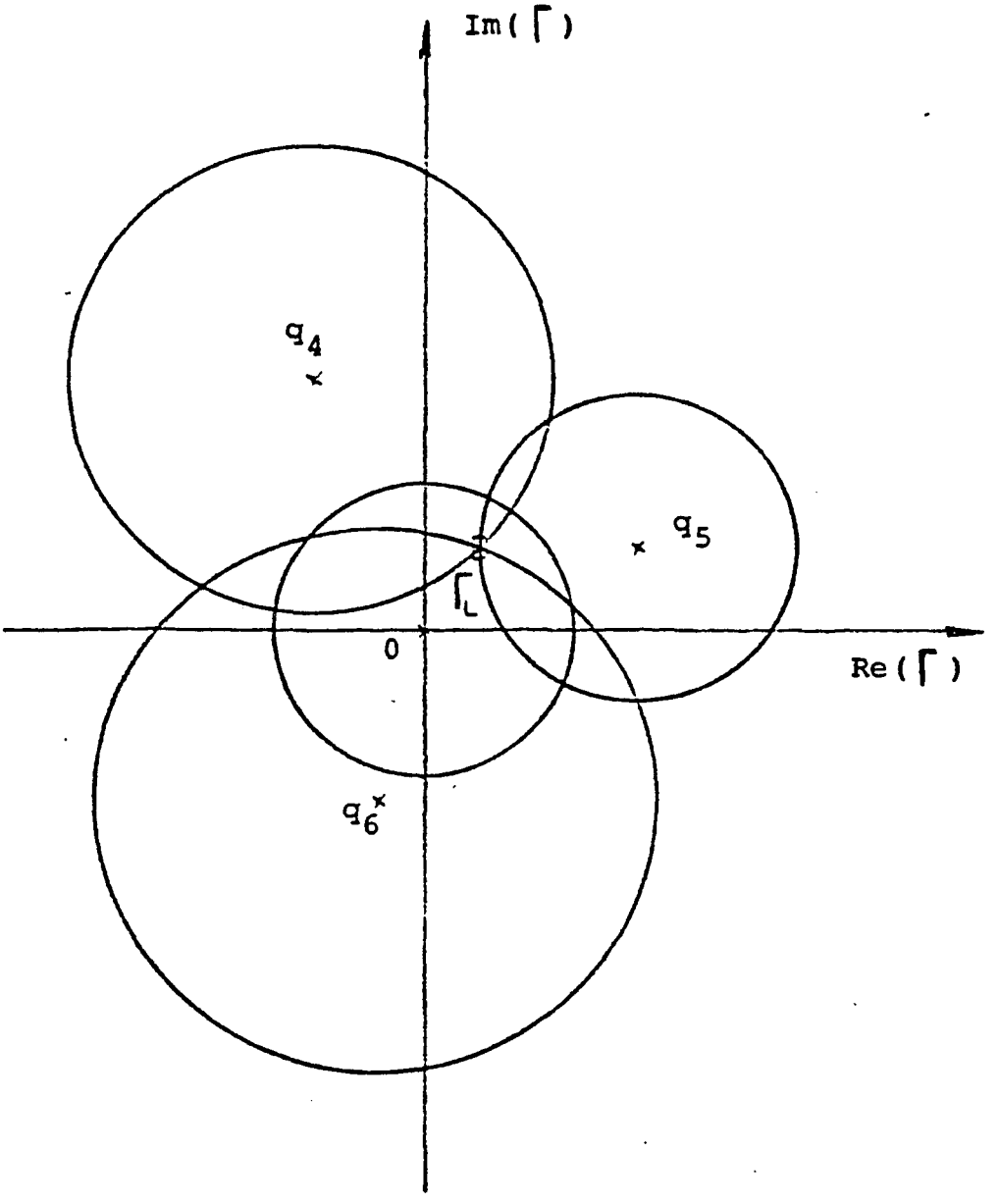

Fig.1.1-8: The intersection of three circles representing the power ratio equations associated with a six-port

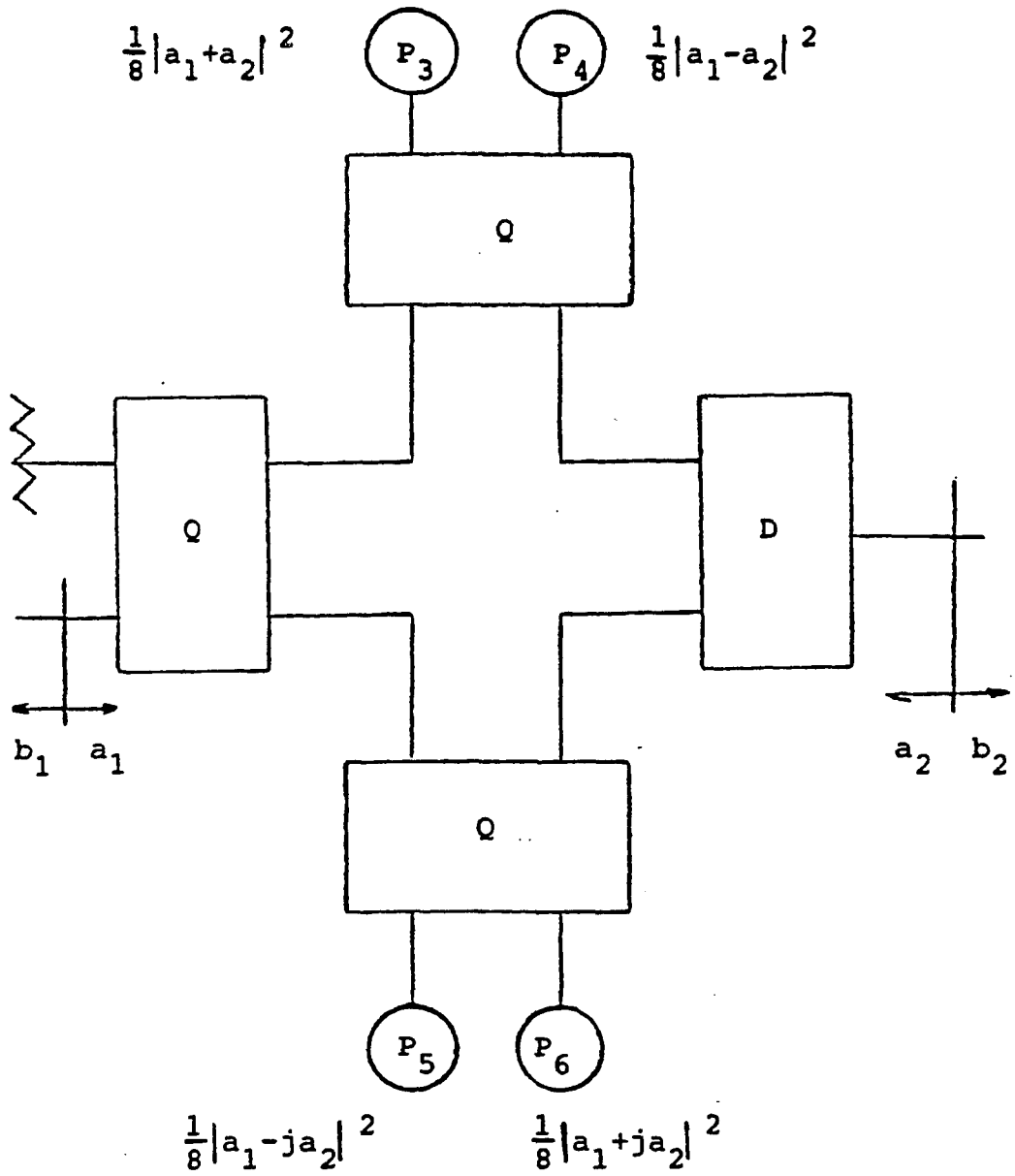

Fig.1.2-1: Six-port correlator. Power outputs are given assuming matched power meters.

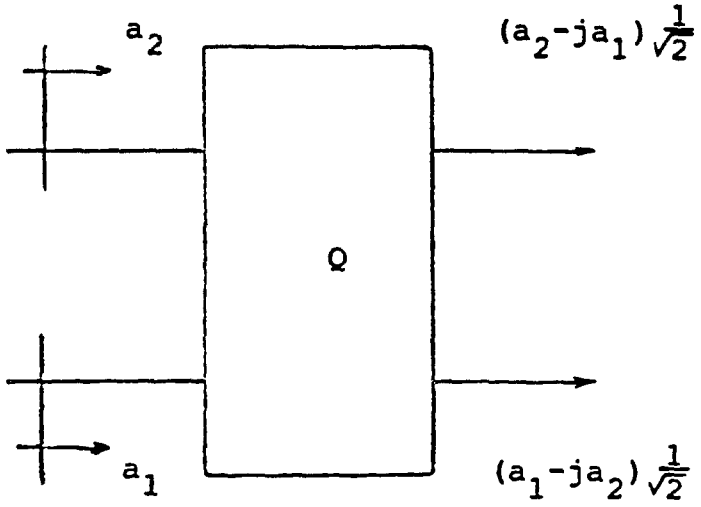

(a) Quadrature Hybrid

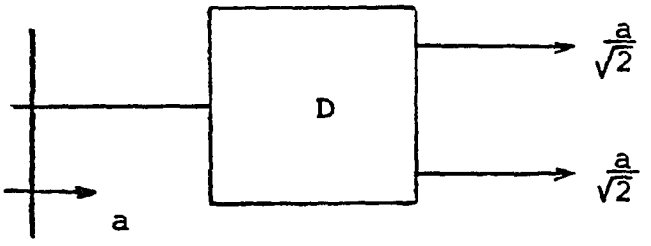

(b) Power Divider

Fig.1.2-2: (a) Quadrature hybrid, and (b) in-phase power divider

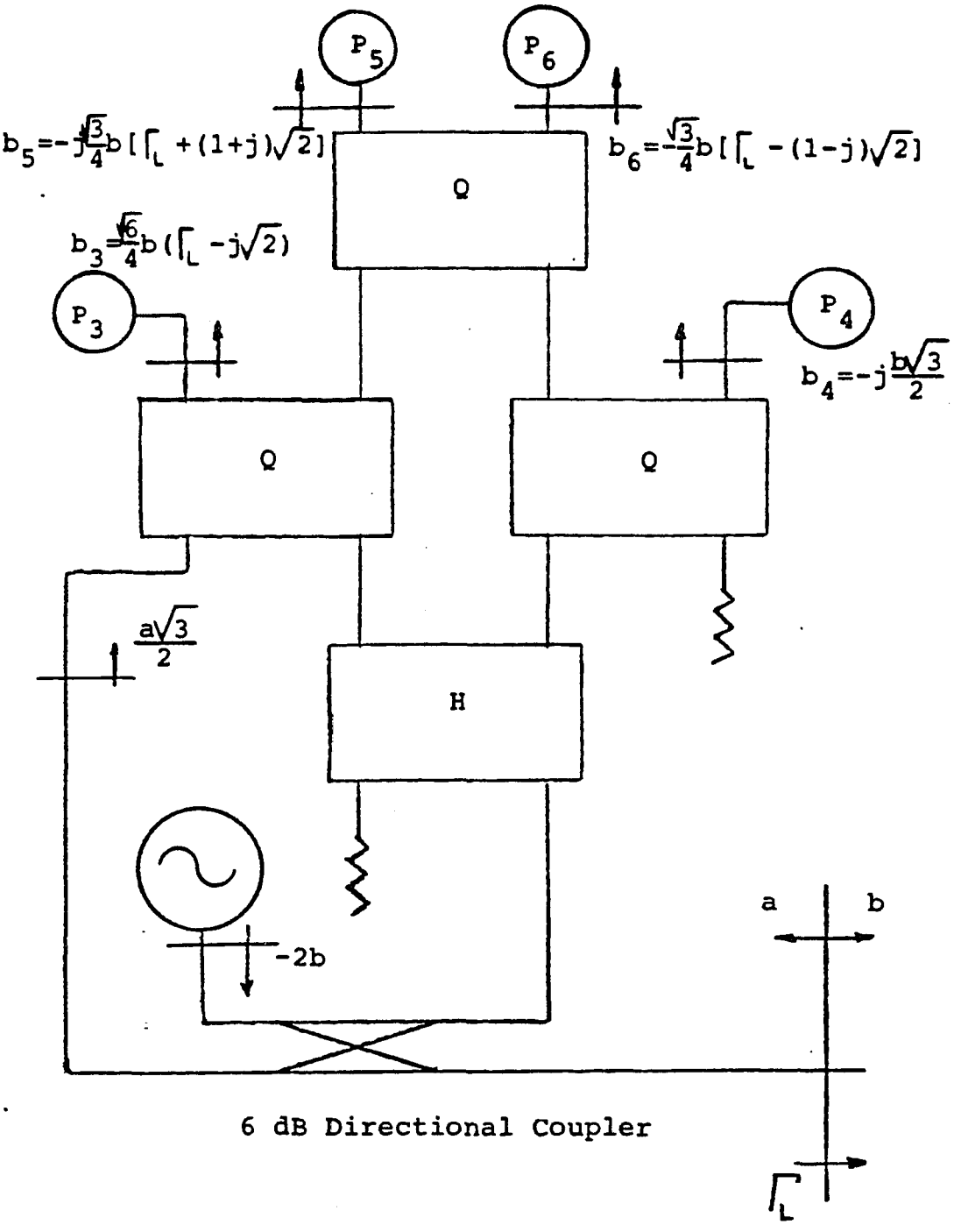

6 dB Directional Coupler

Fig.1.2-3: Six-port reflectometer configuration designed by Engen [10]

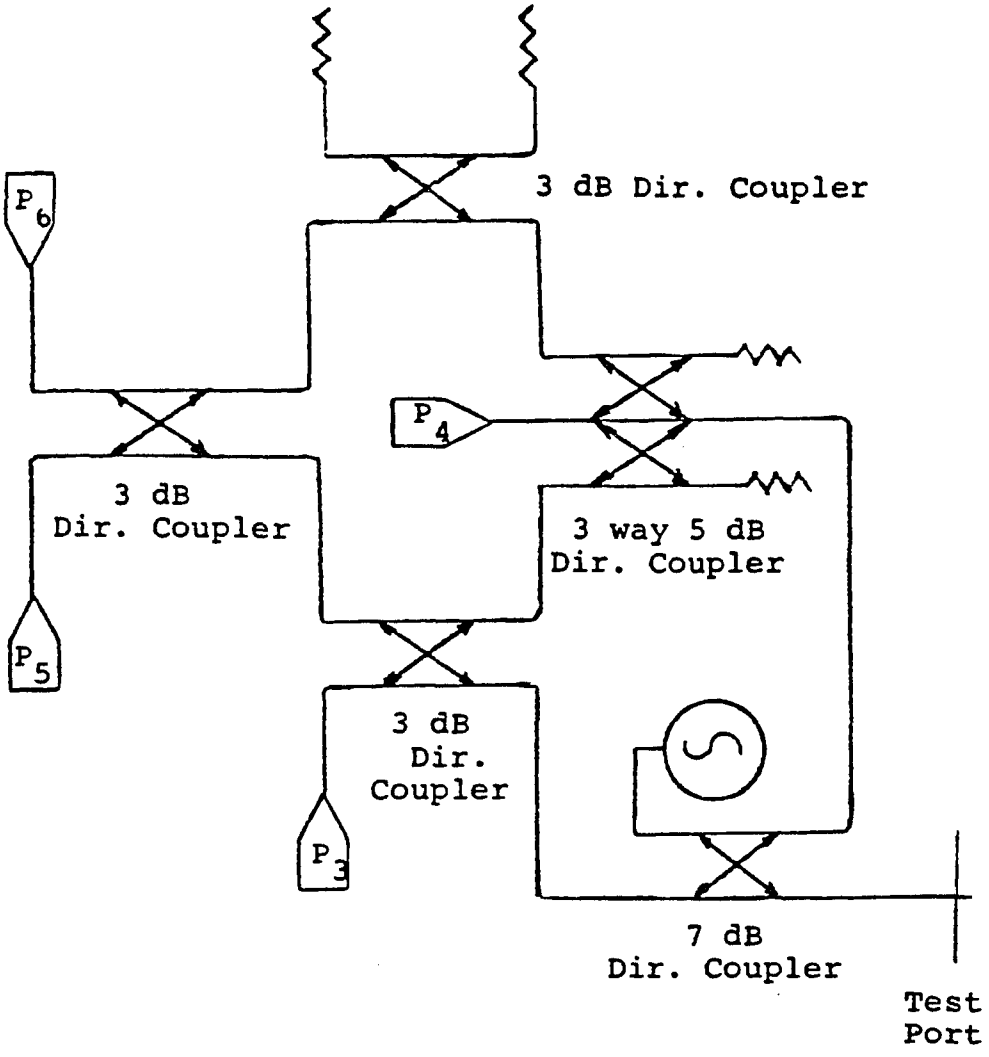

Fig.1.2-4: Six-port reflectometer designed by Wiedman [13]

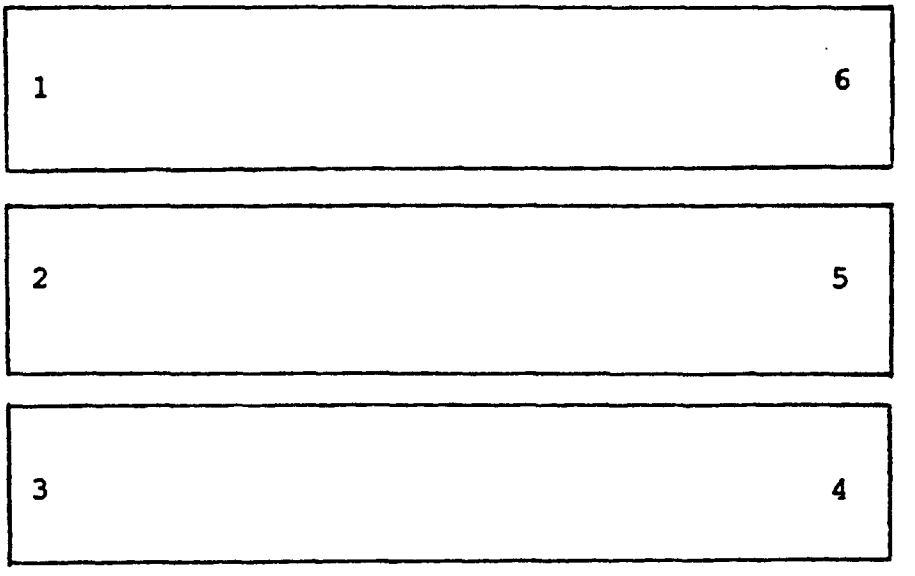

Fig.1.2-5: Three-line coupler to be considered for six-port reflectometry

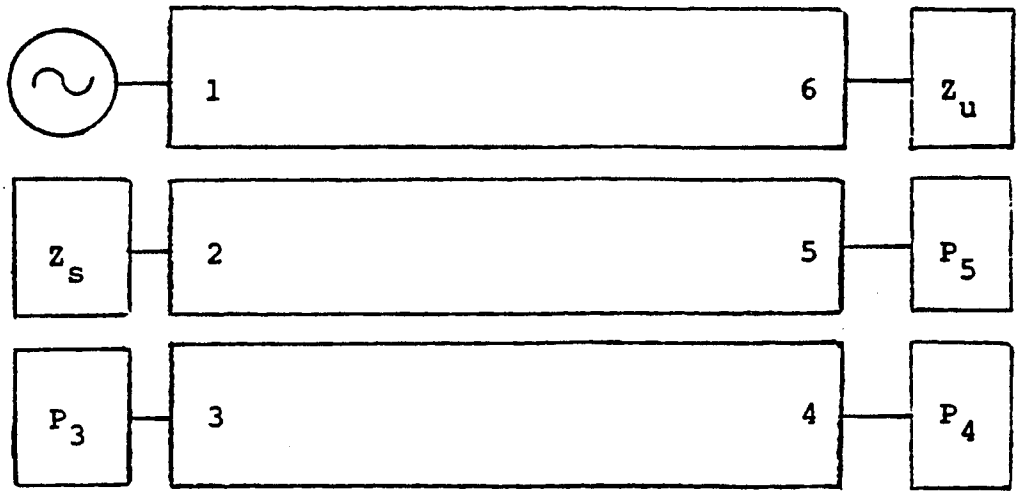

Fig.1.2-6: Six-port reflectometer using three coupled lines designed by Collier and El-Deeb [17]

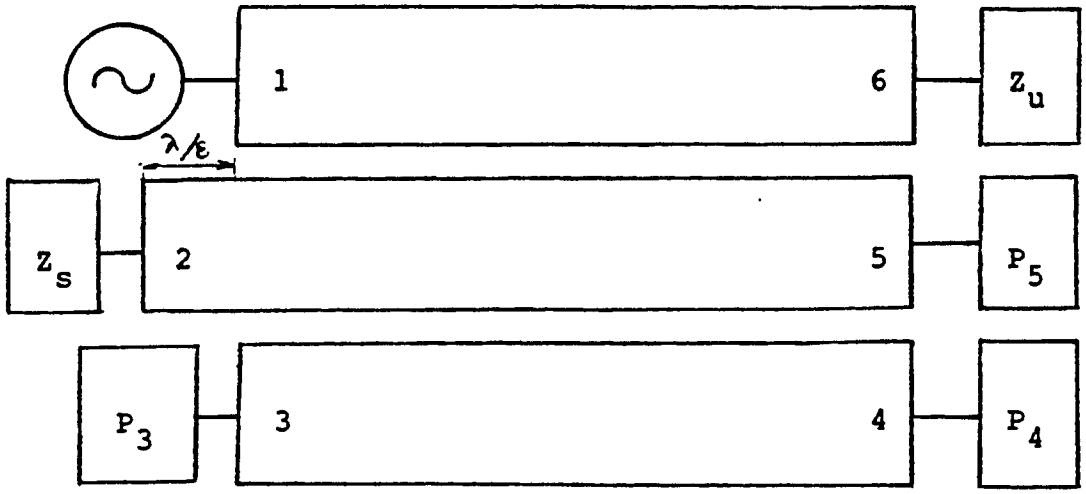

Fig.1.2-7: Six-port reflectometer using a three-line coupler designed by El-Deeb [25].

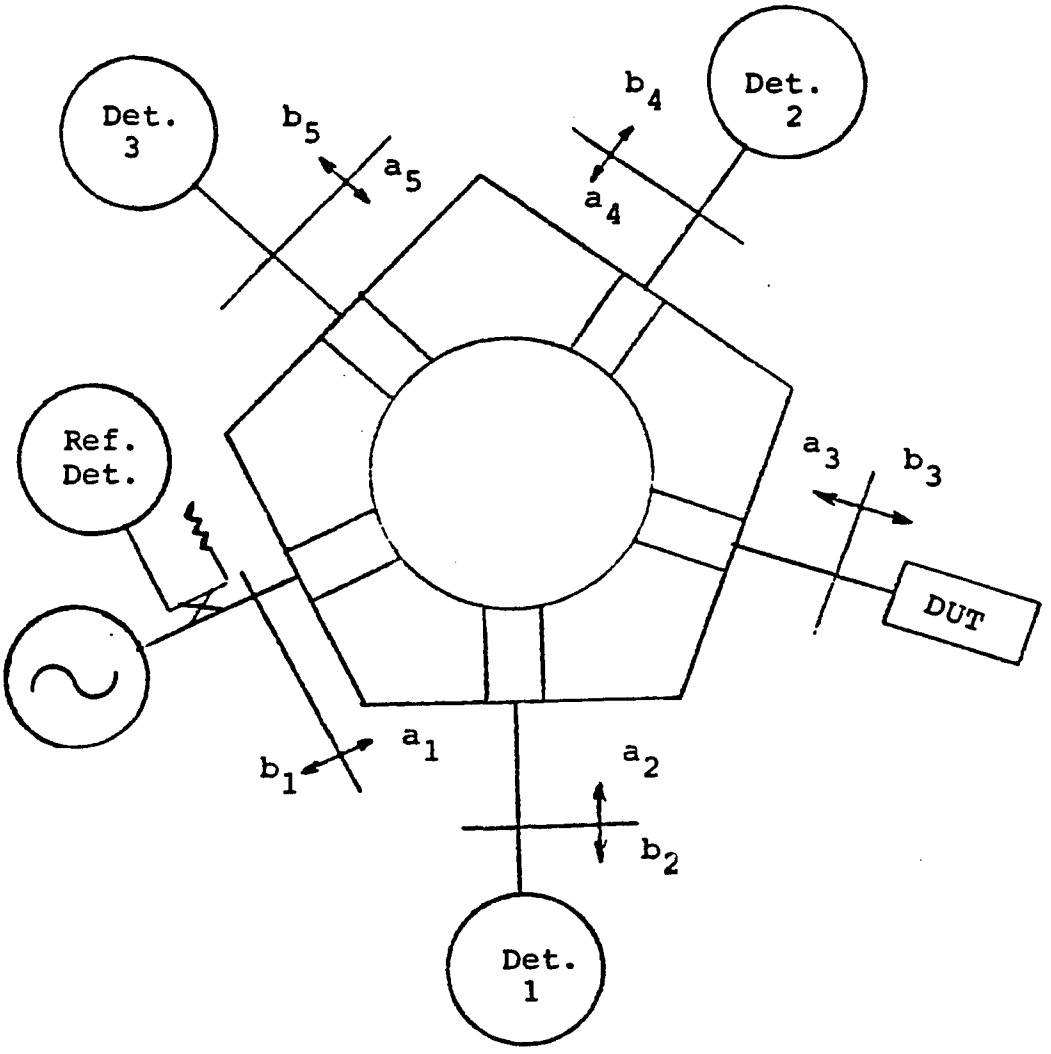

Fig.1.2-8: Six-port reflectometer using a symmetrical five-port and a directional coupler, designed by Hansson and Riblet [24]

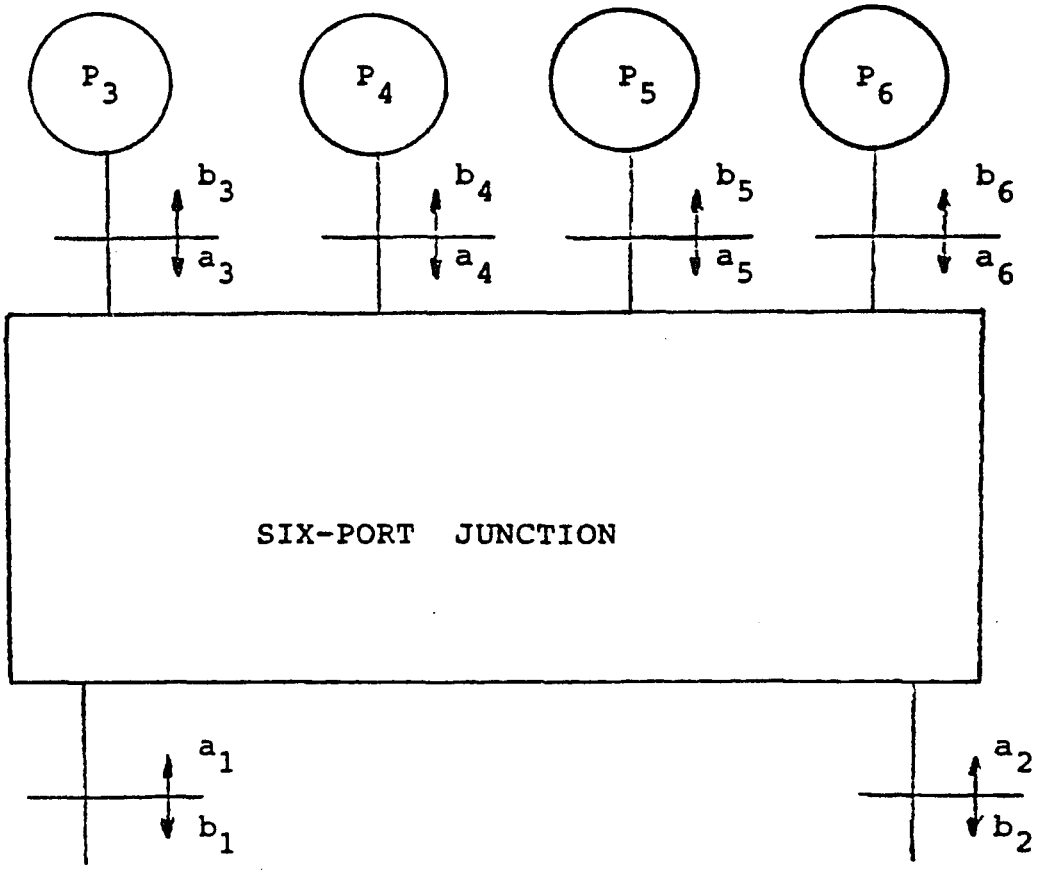

Fig.1.2-9: General six-port network with input, output and four power measuring ports used to investigate the properties of a symmetrical six-port for six-port reflectometry

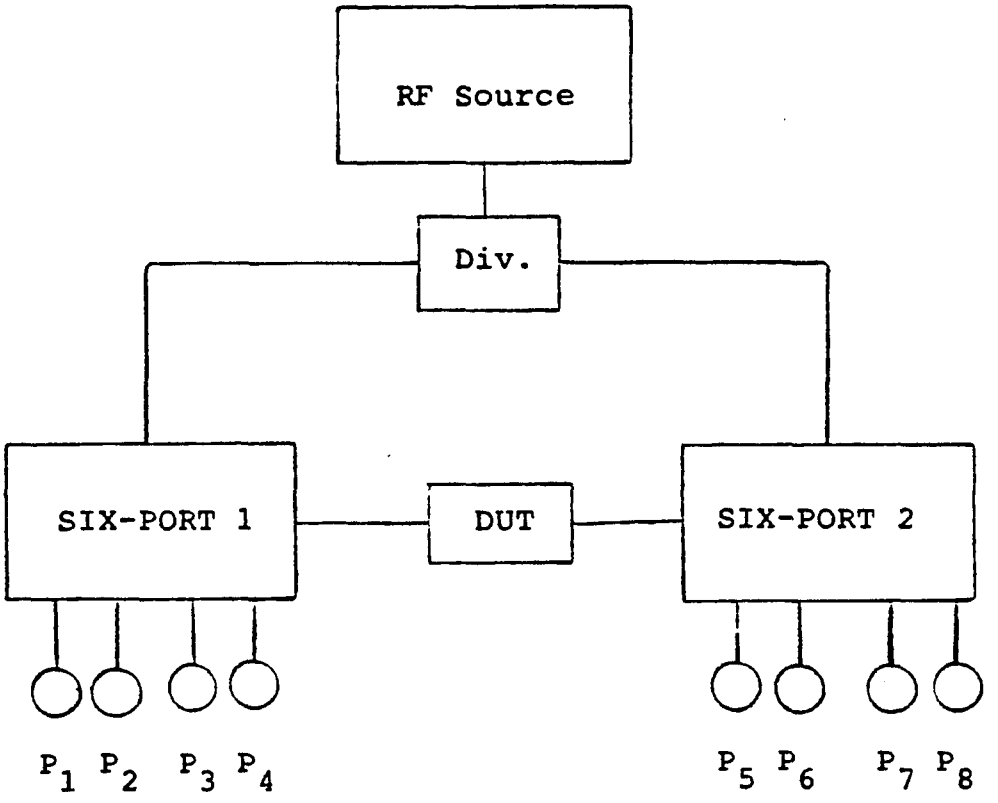

Fig.1.2-10: Dual six-port network analyzer

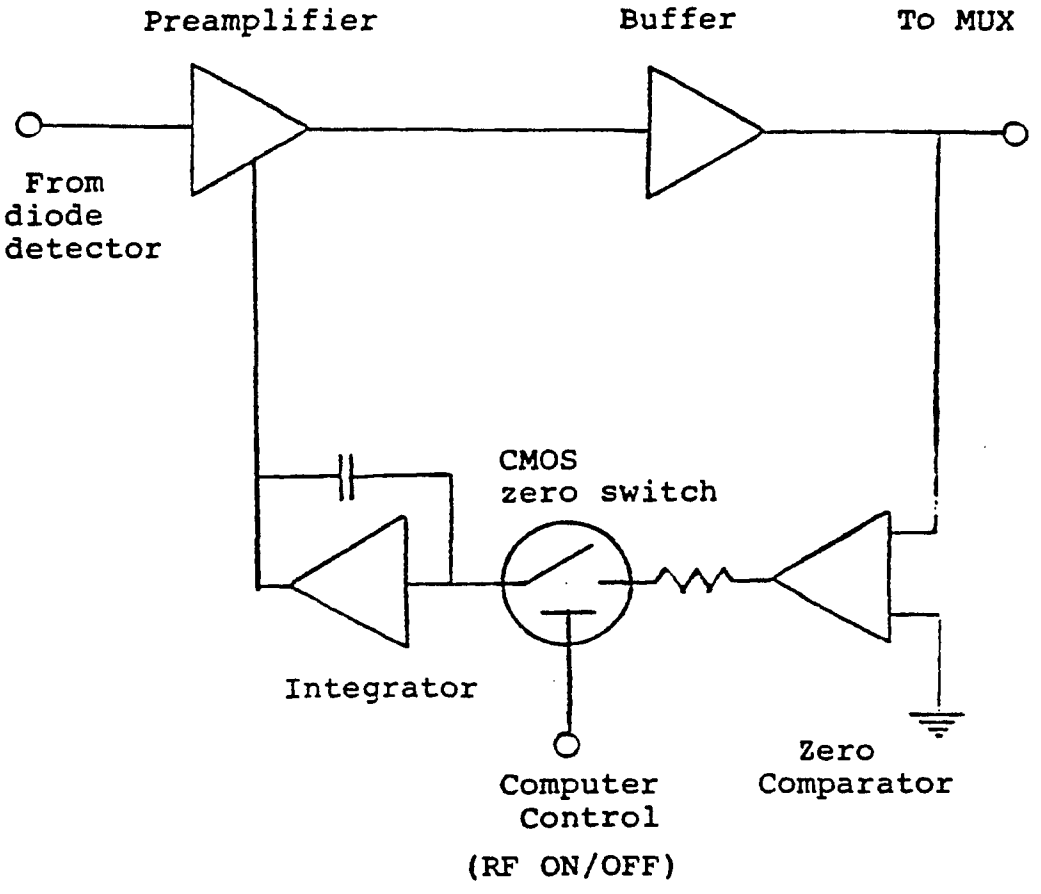

Fig.1.2-11: Auto leveling circuit used by Somlo and Hunter [20] to level the voltage at diode detectors, for six-port operation with uncalibrated diodes

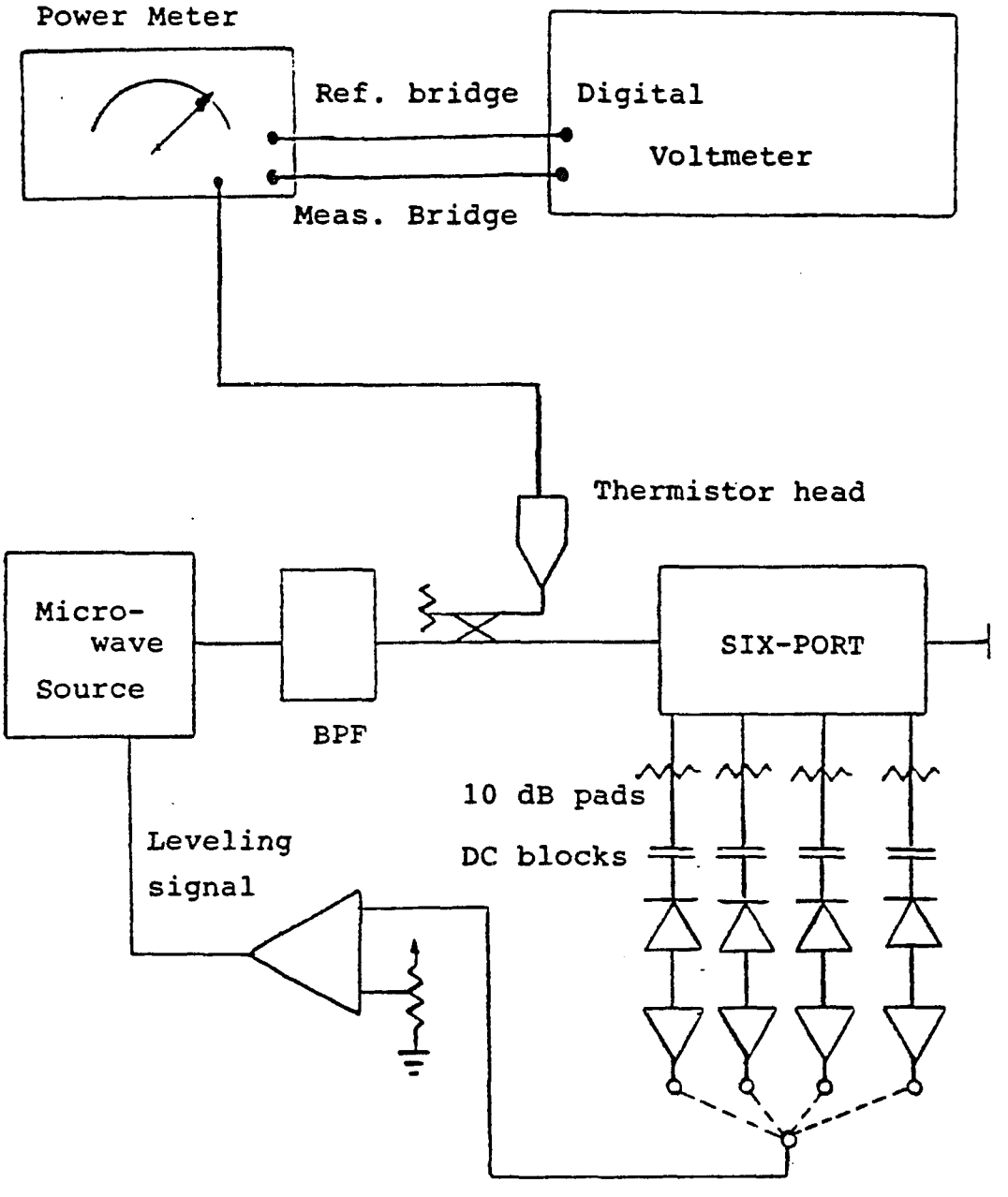

Fig.1.2-12: Six-port reflectometer operated with uncalibrated diode detectors [20]. System block diagram

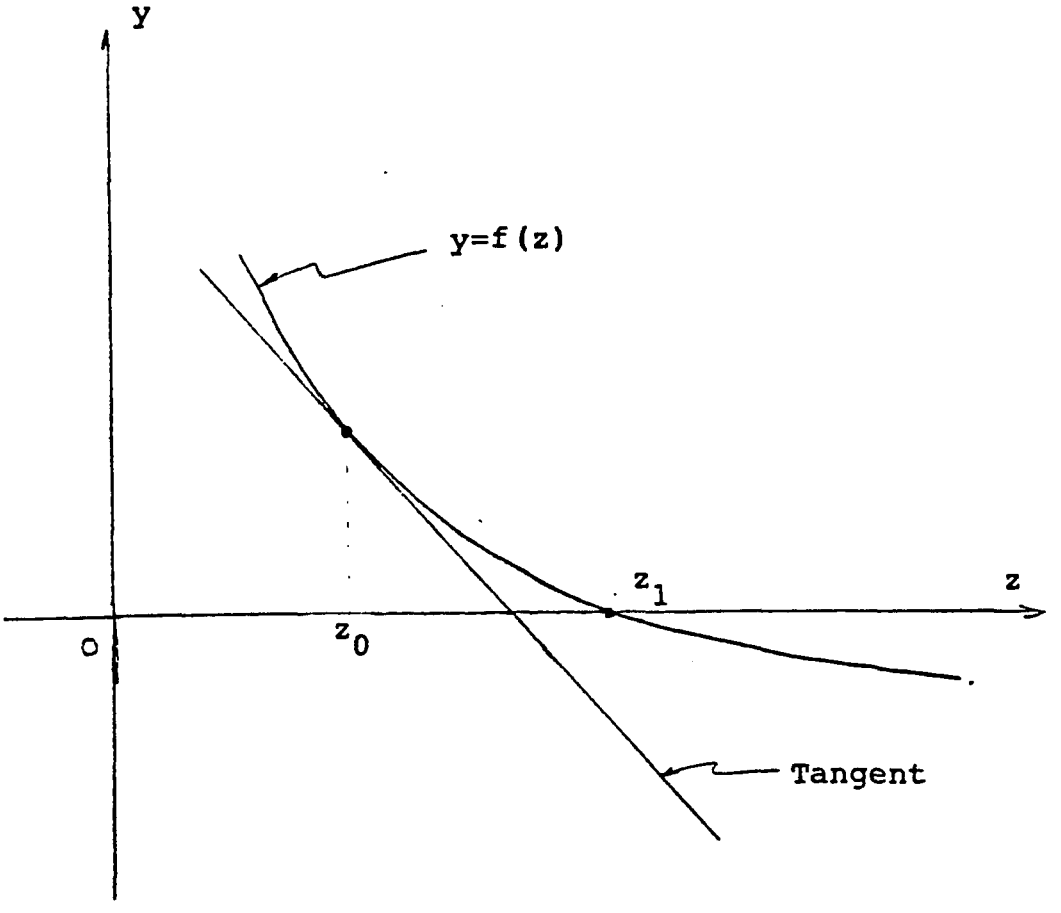

Fig. 1.3-1: Newton's method for a one dimensional problem

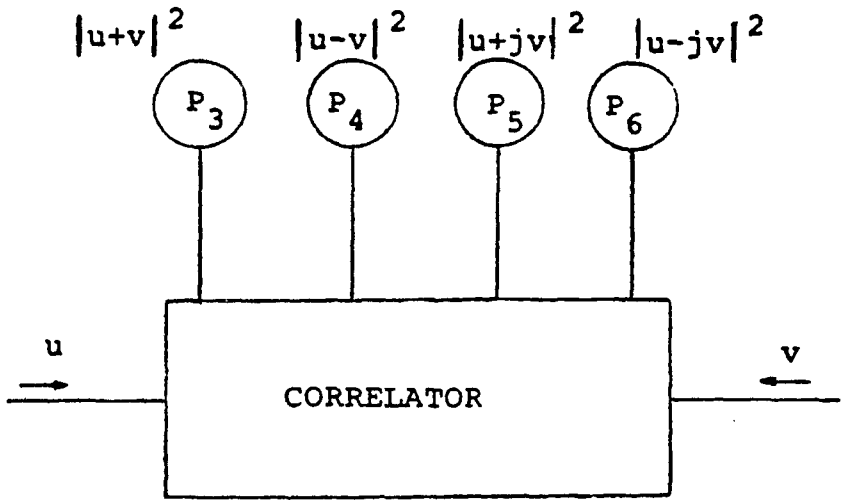

Fig.2.2-1: Six-port correlator which implements equations (1.1-5) through (1.1-8)

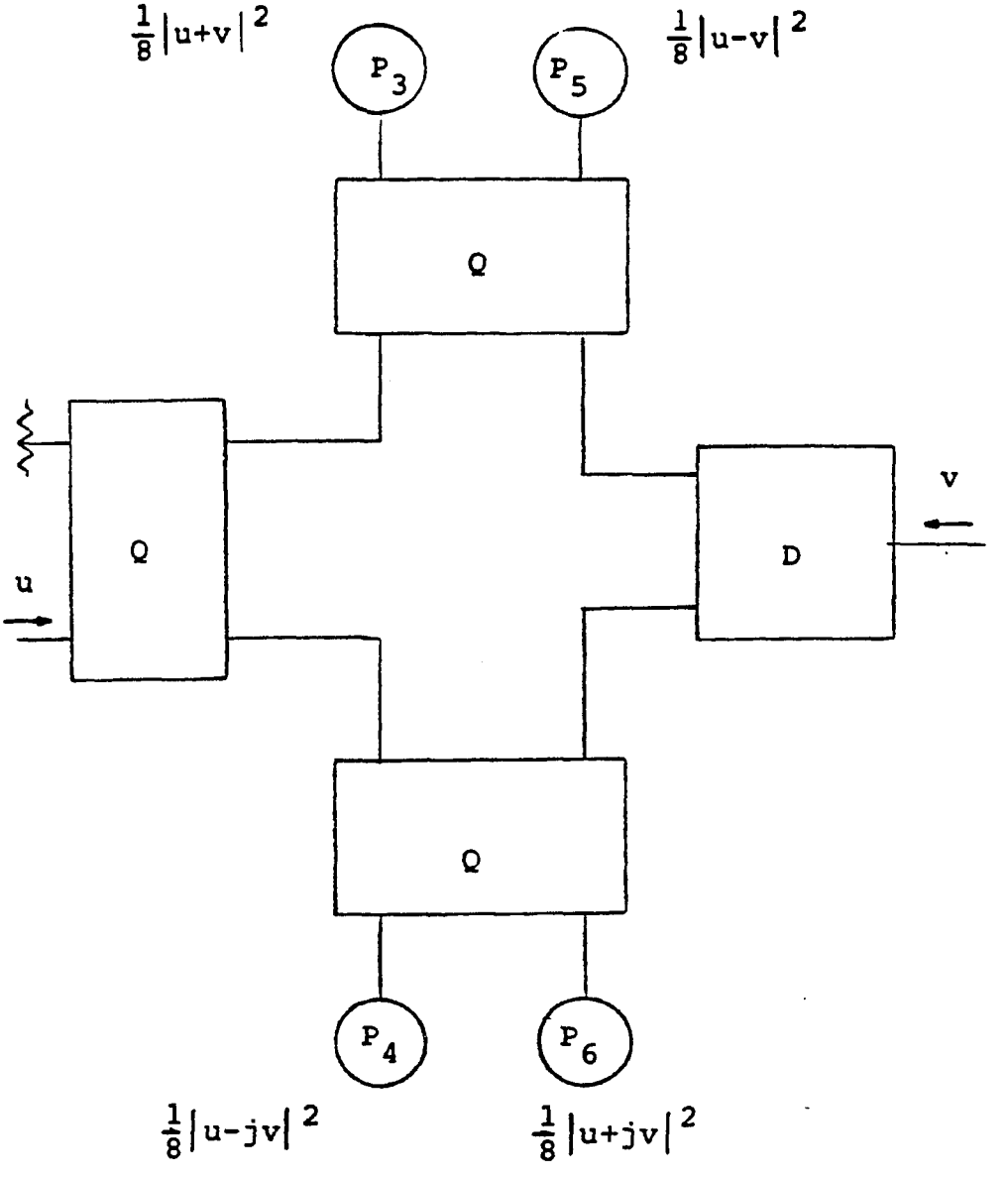

Fig.2.2-2: Six-port correlator implemented using three quadrature hybrids and an in-phase power divider

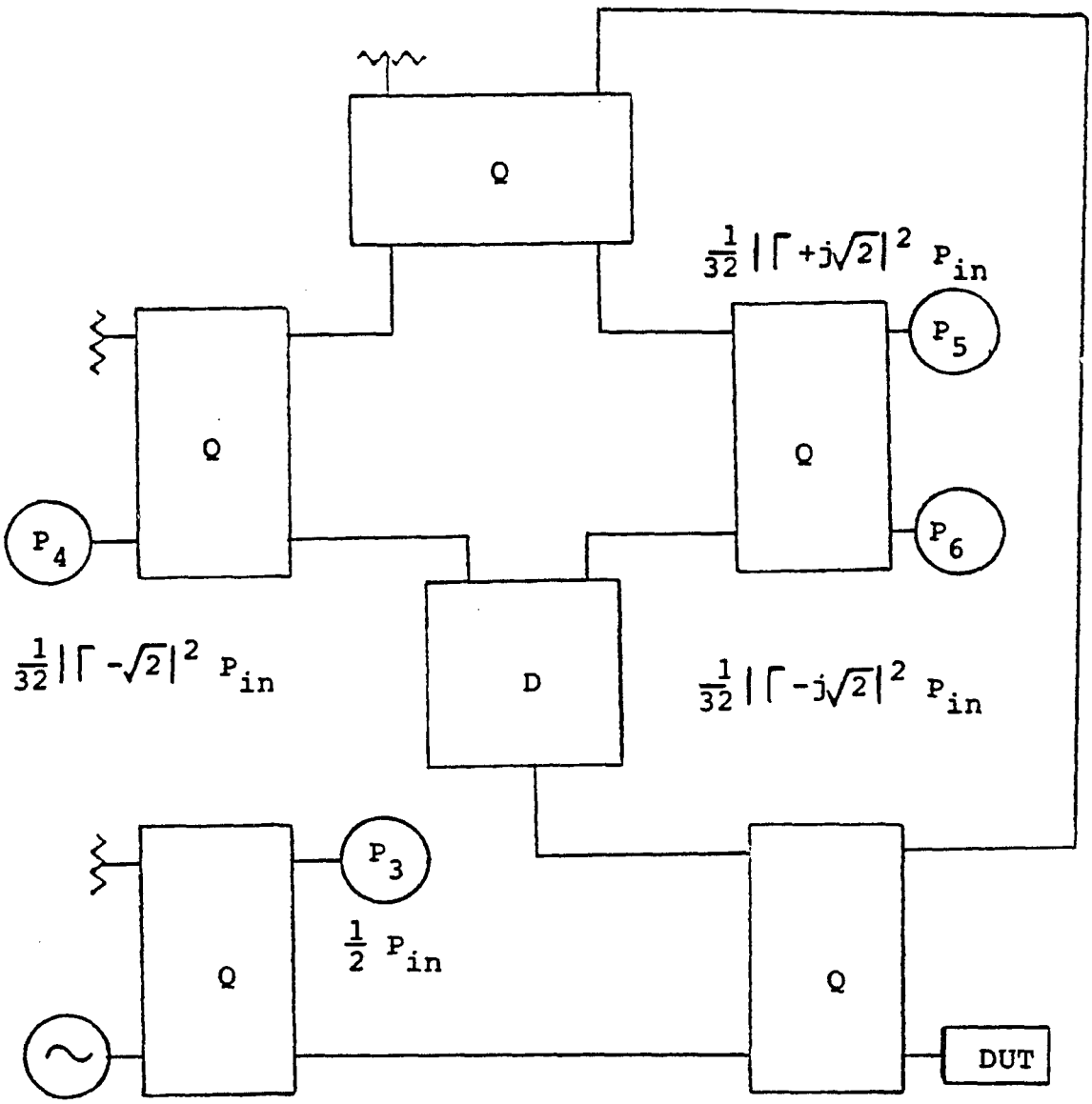

Fig.2.2-3: Six-port reflectometer with correlator as central element. An additional quadrature hybrid is used to sample the input power.

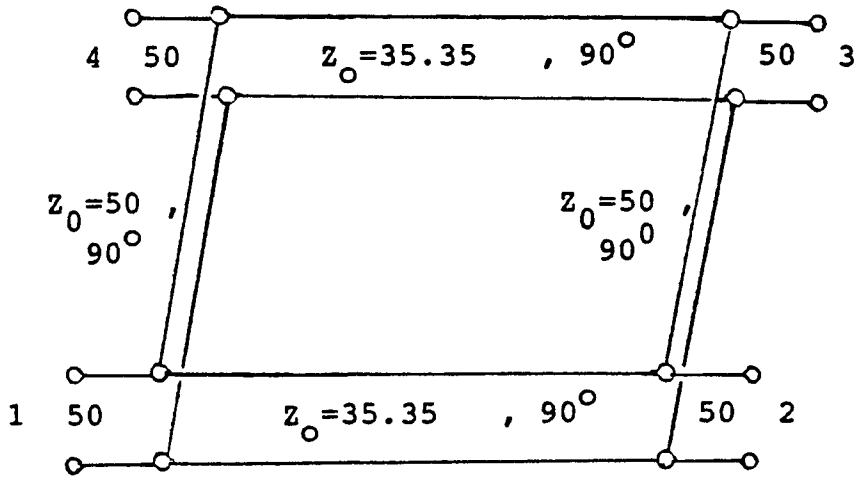

Fig.2.2-4: Transmission line model of a quadrature hybrid used in the MIDAS simulation program

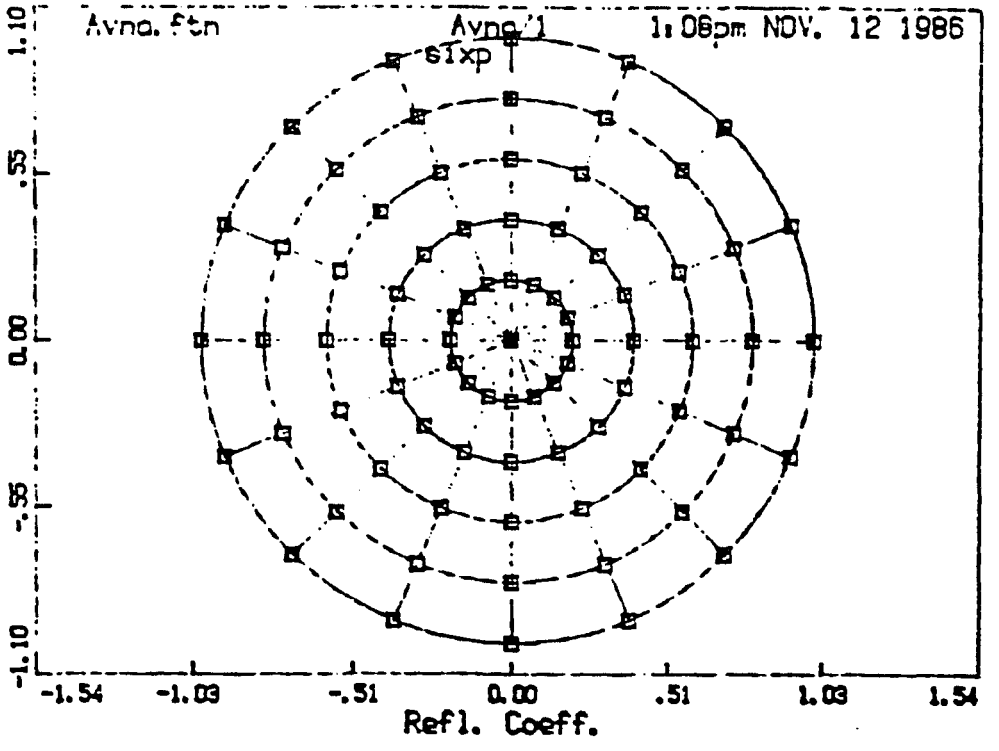

Fig.2.2-5: Simulation results for "measured" loads with magnitudes of 0.0, 0.2, 0.4, 0.6, 0.8, and 1.0 and phases22.5 degrees apart

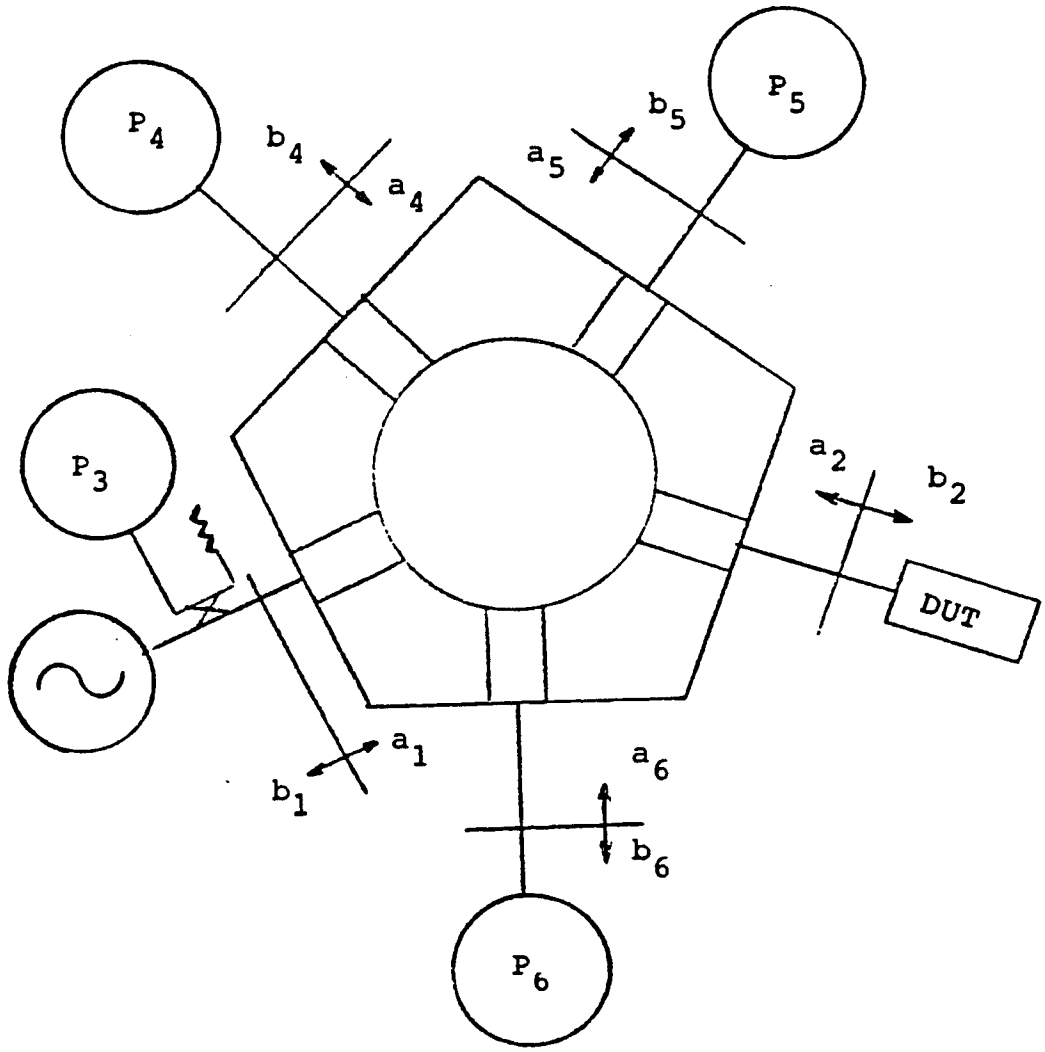

Fig.3.1-1: Six-port configuration used for CW and pulsed measurements

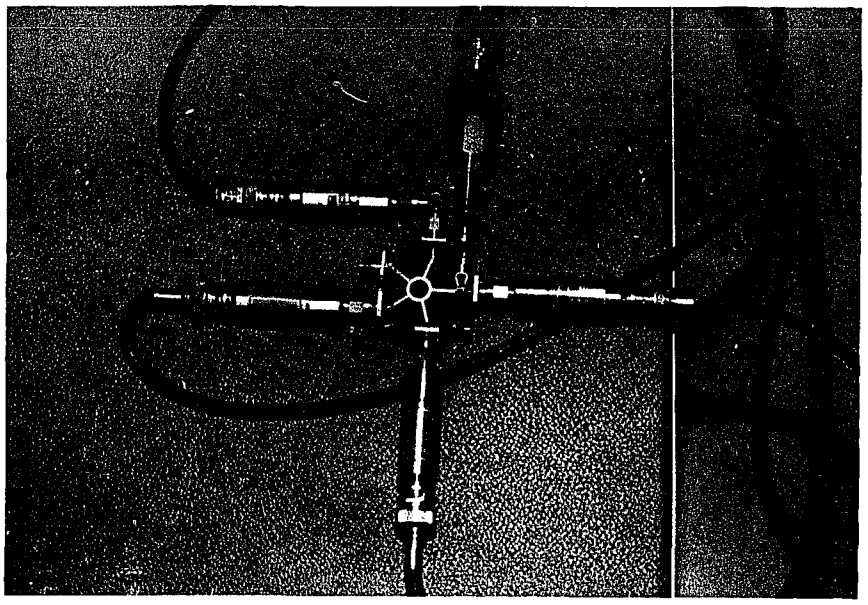

Fig.3.2-1: Photograph of the six-port network used for physical measurements

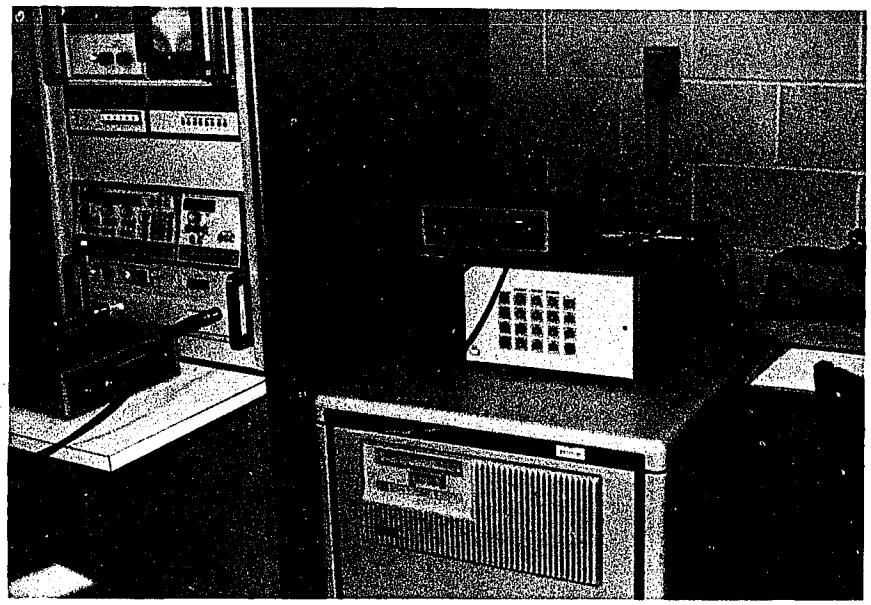

Fig.3.2-2: Photograph of six-port reflectometer system including six-port network, signal generator, Data Aquisition and Control unit, pulse generator, and HP-1000 computer

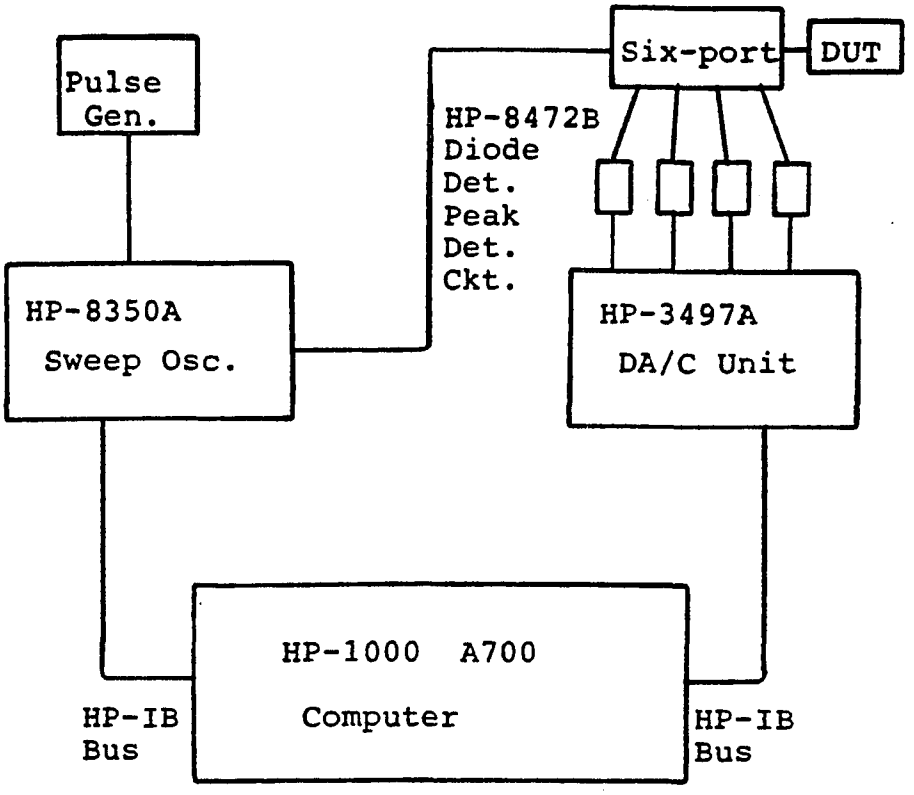

Fig.3.3-1: Block diagram of six-port reflectometer system configuration

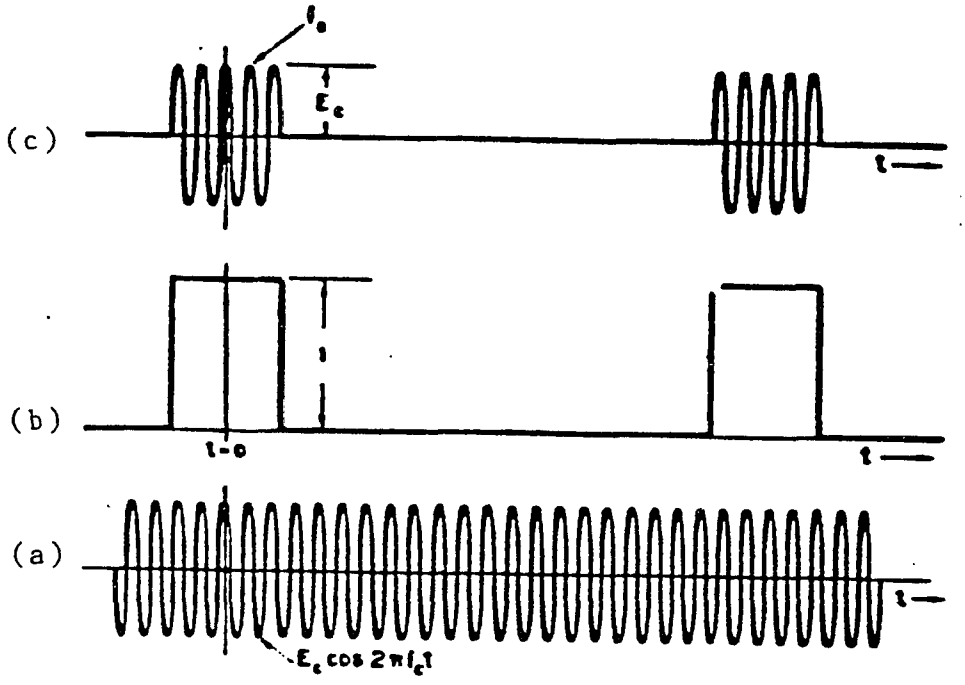

Fig.4.1-1: PAM signal (c) which is obtained as an RF signal (a) is amplitude modulated by a train of pulses (b)

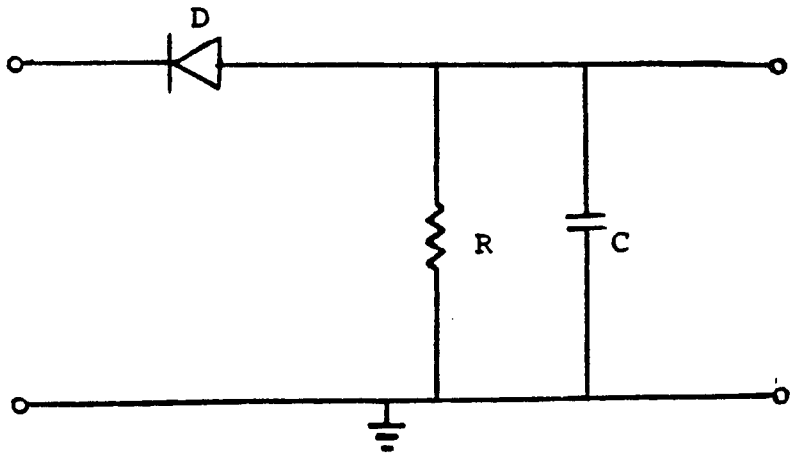

D: 1N4003
R= 10 kohms
C= 10 mmF

Fig.4.2-1: Typical peak detector

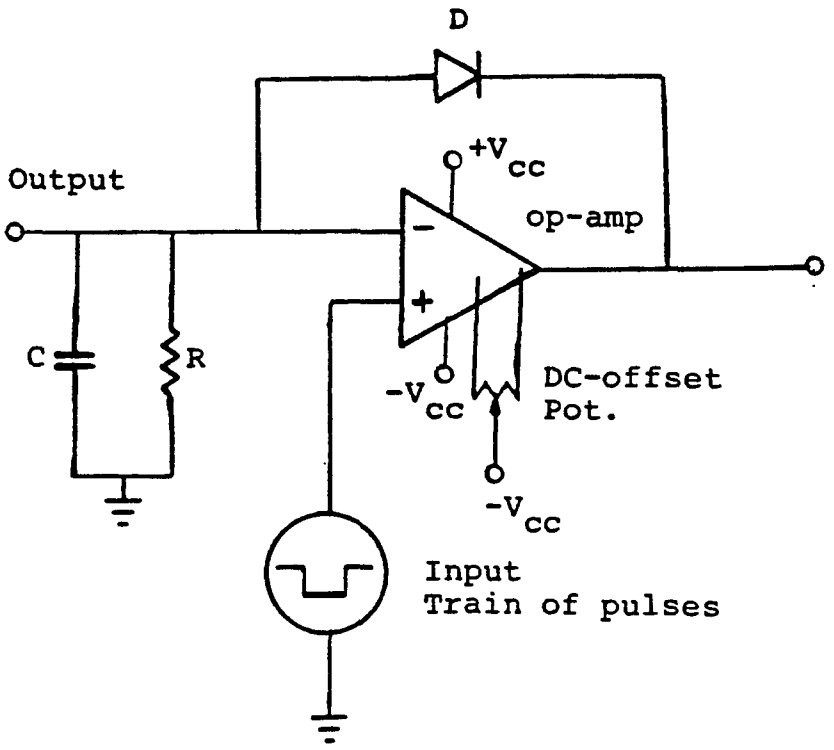

D: 1N4003

op-amp: MC 34084P

C= 10 mmF

R= 10 Kohms

Fig.4.2-2: Peak detector circuit with "zero" turn on voltage for the diode

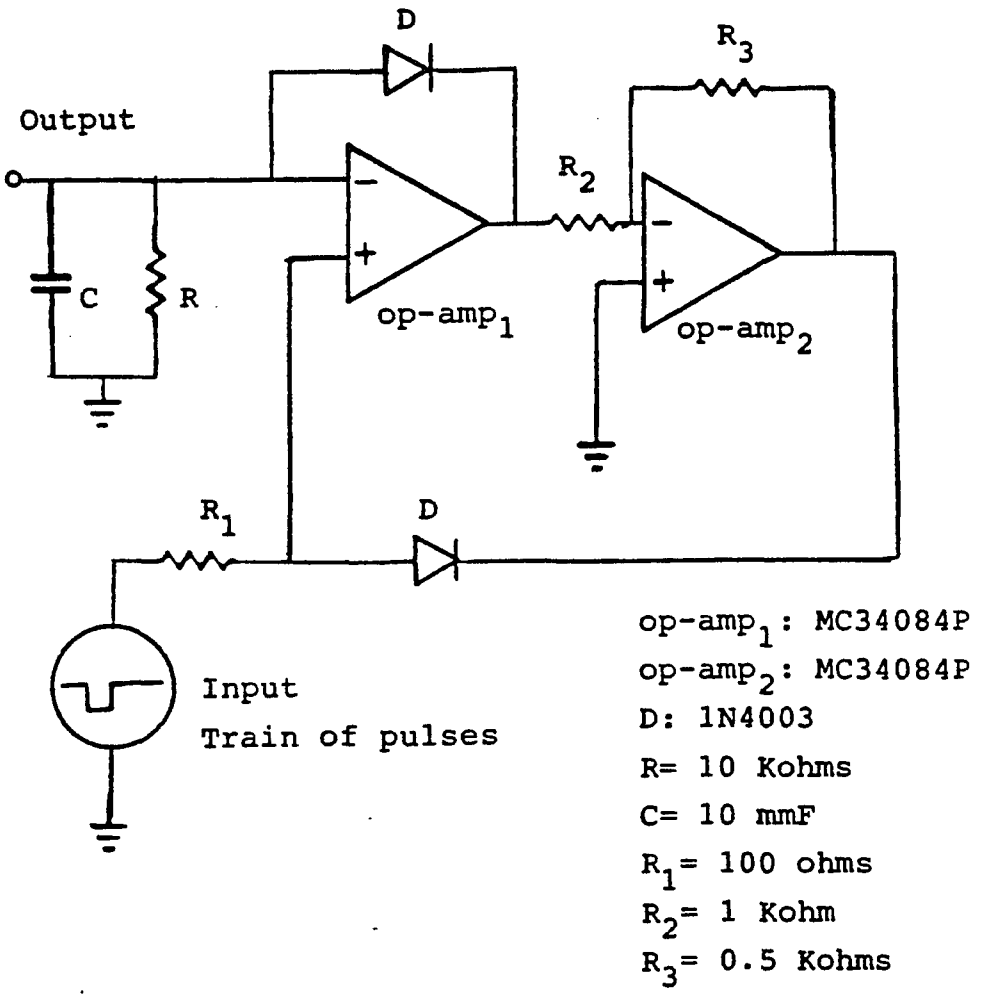

Fig.4.2-3: Peak detector circuit with feedback loop for control of the output voltage at the first operational amplifier

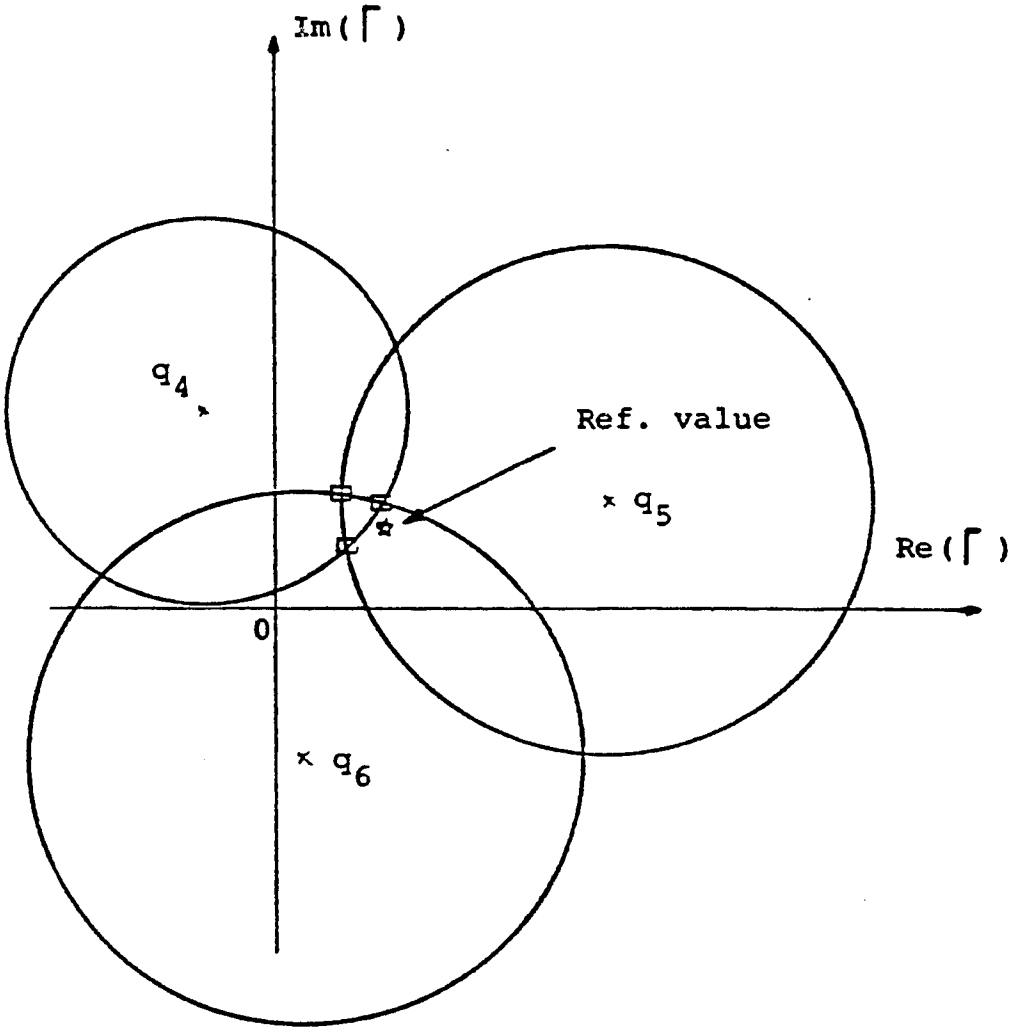

Fig.4.4-1: Intersections of the three circles representing the power ratio equations for the six-port

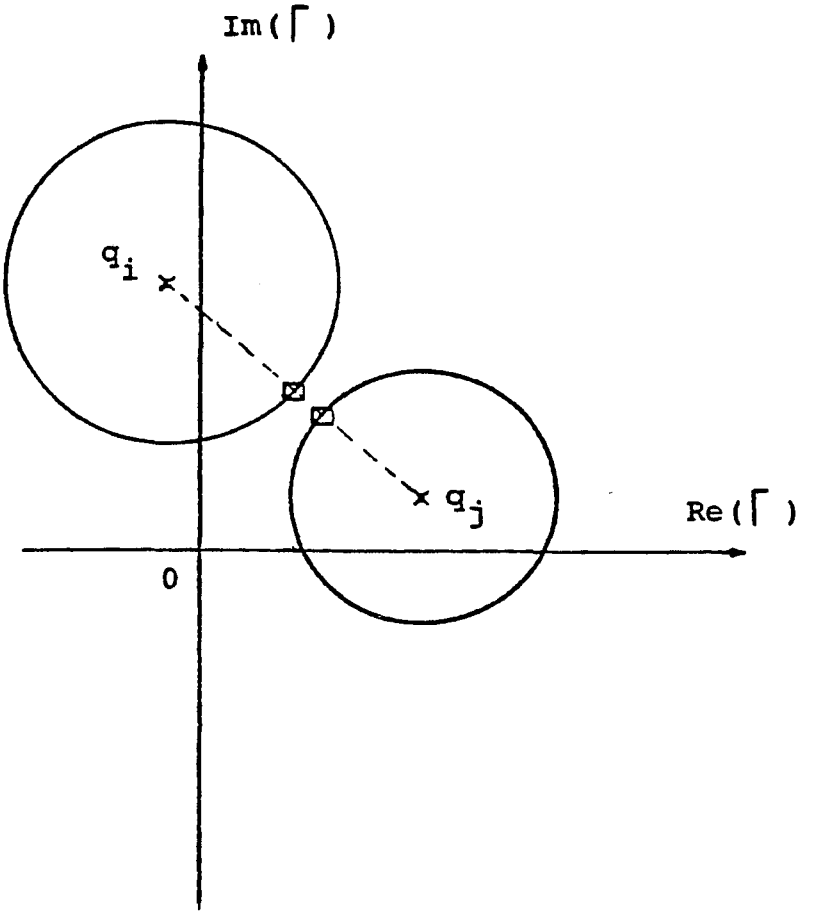

Fig.4.4-2: Approximation of the "intersection" of two circles which do not physically intersect.

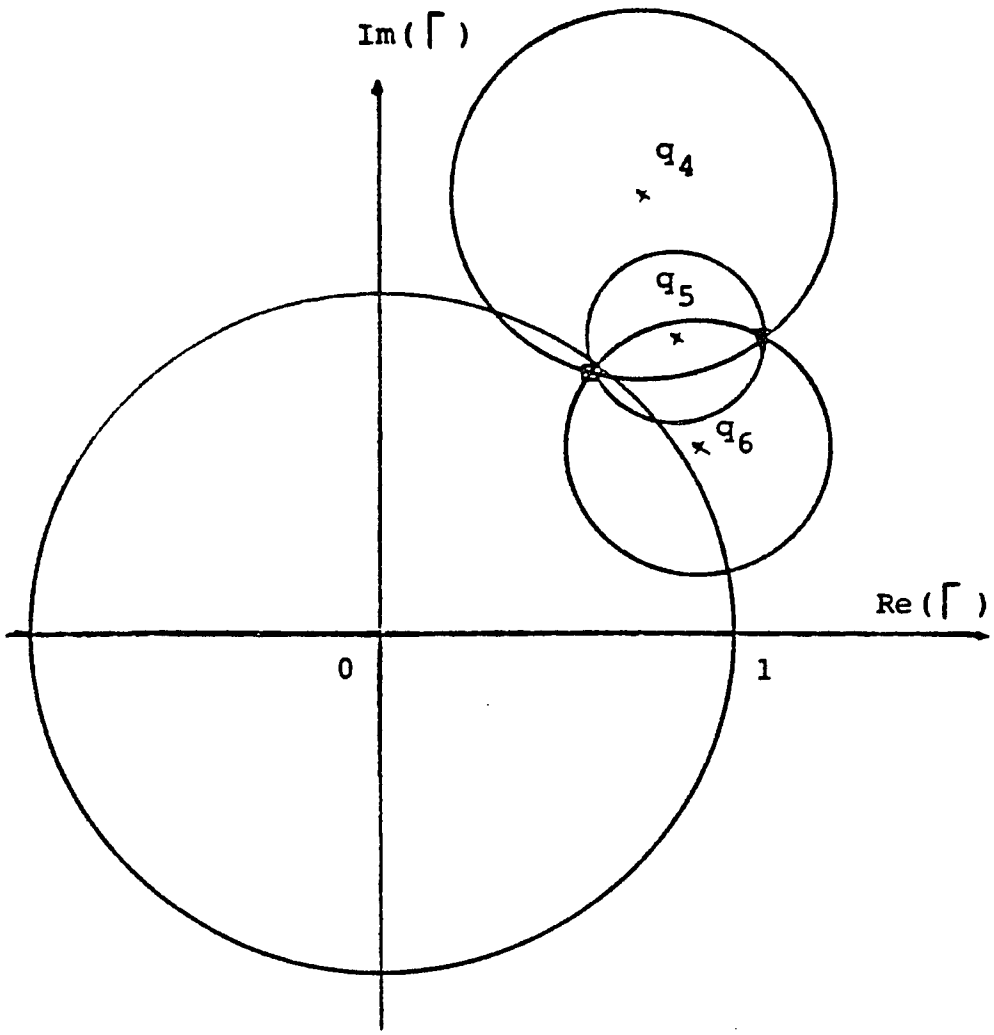

Fig.4.4-3: Possible intersections of three circles with centers on a straight line

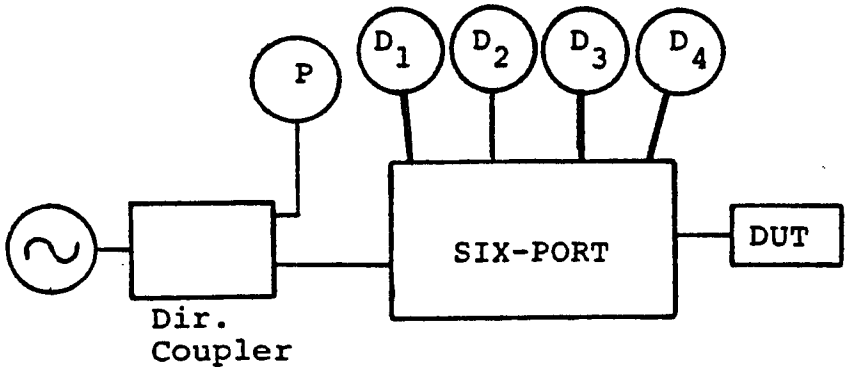

Fig.4.5-1: Circuit diagram for "in situ" calibration of diode detectors used in six-port reflectometry. An additional power meter and a directional coupler are used.

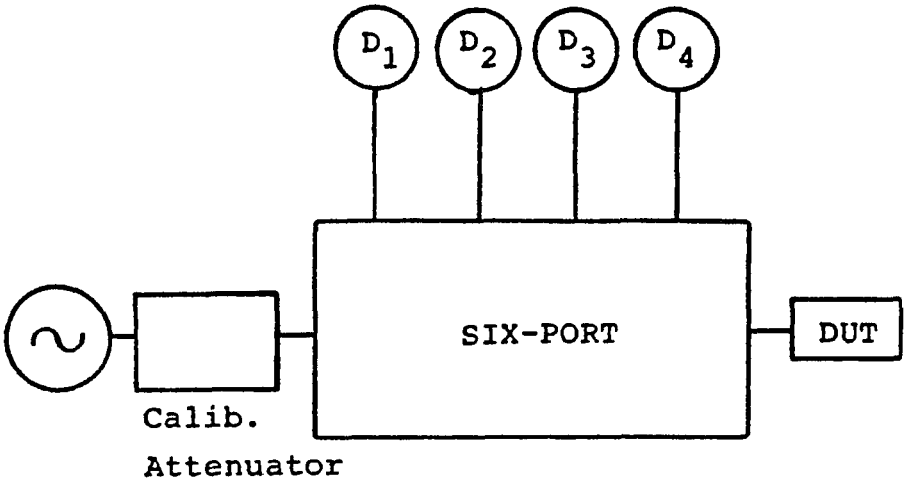

Fig.4.5-2: Circuit diagram for "in situ" calibration of diode detectors used in six-port reflectometry. Circuit used in the "voltage correction method"

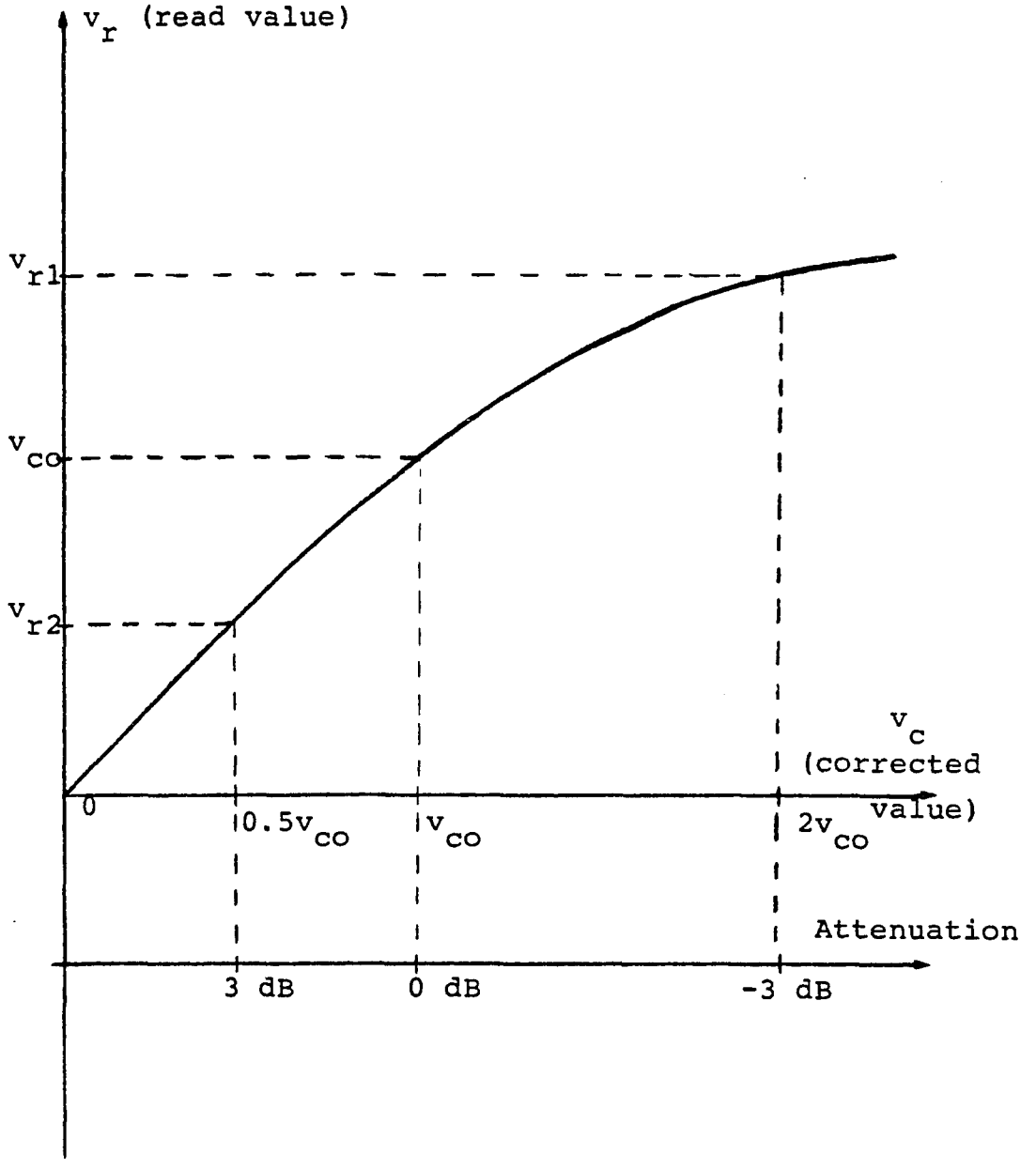

Fig.4.5-3: Diode calibration curve for read voltage versus corrected voltage and attenuation relative to the initial setting

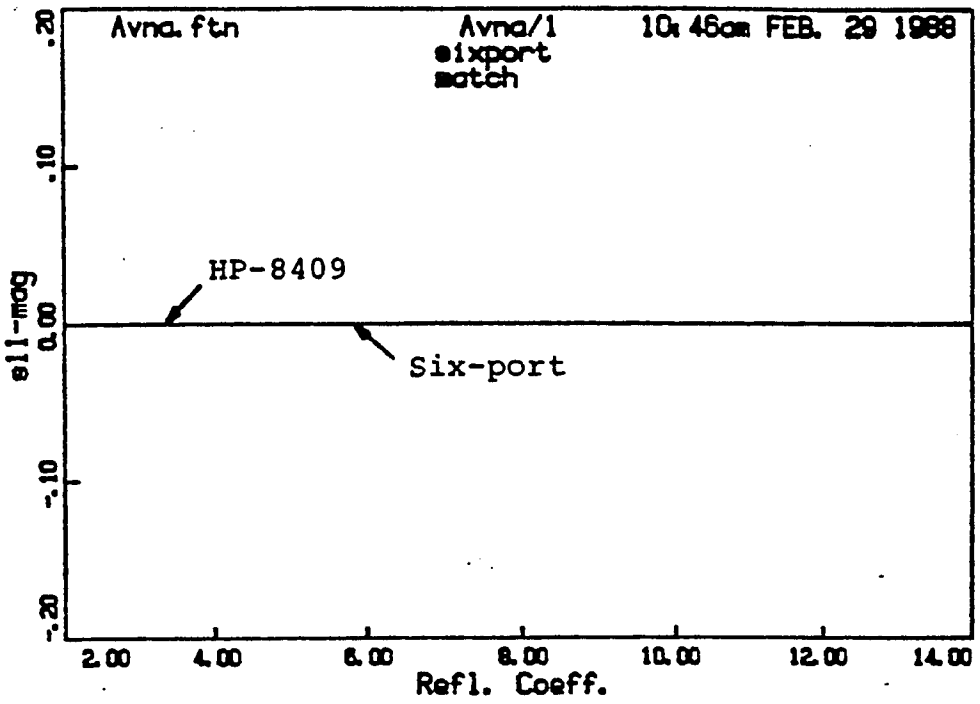

Fig.4.6-1: CW measurement results for a matched load (standard in the six-port calibration). Magnitude versus frequency for HP-8409 ANA and six-port reflectometer

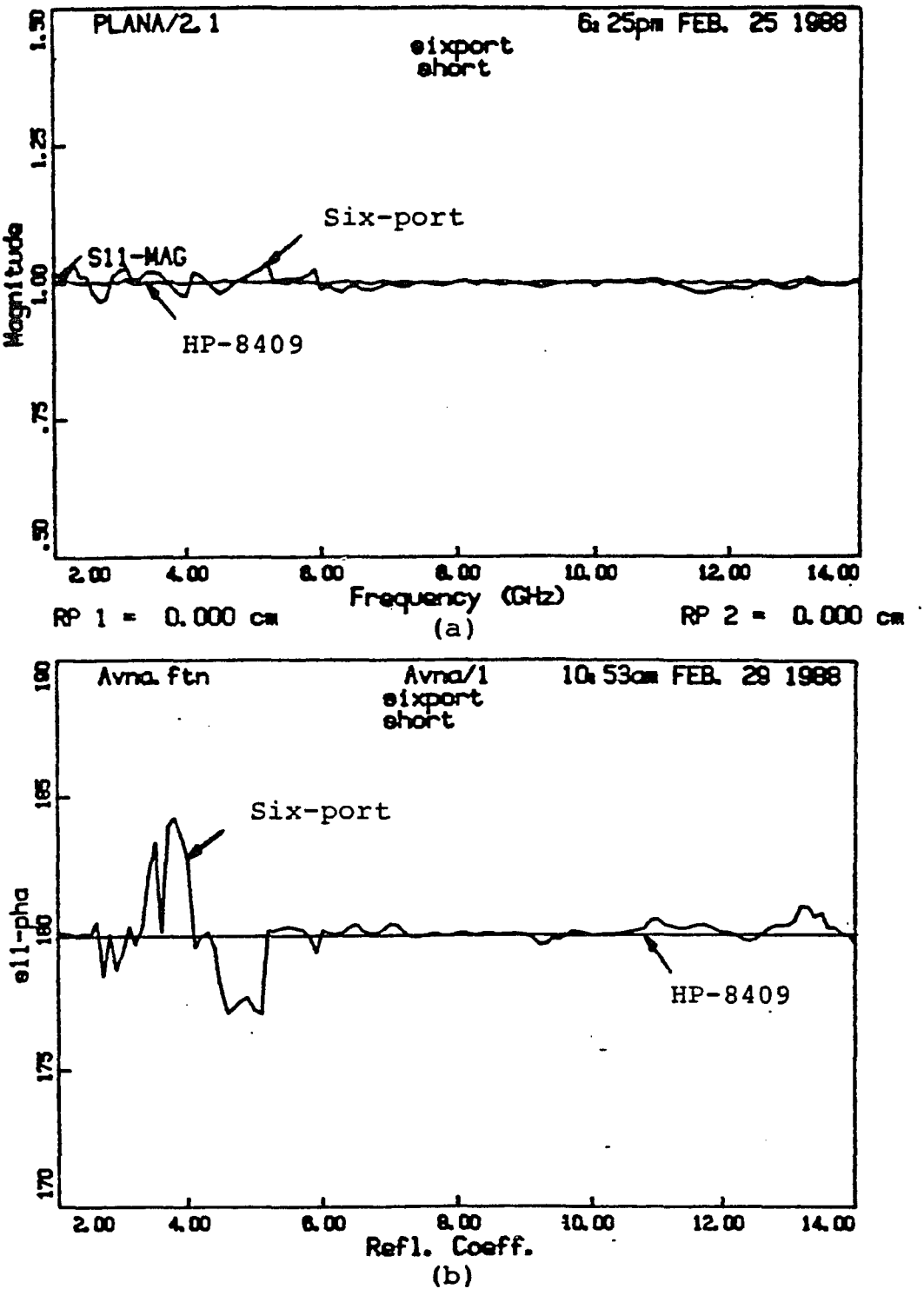

Fig.4.6-2: CW measurement results for a short (standard in the six-port calibration). Magnitude (a) and phase (b) versus frequency for HP-8409 and six-port reflectometer

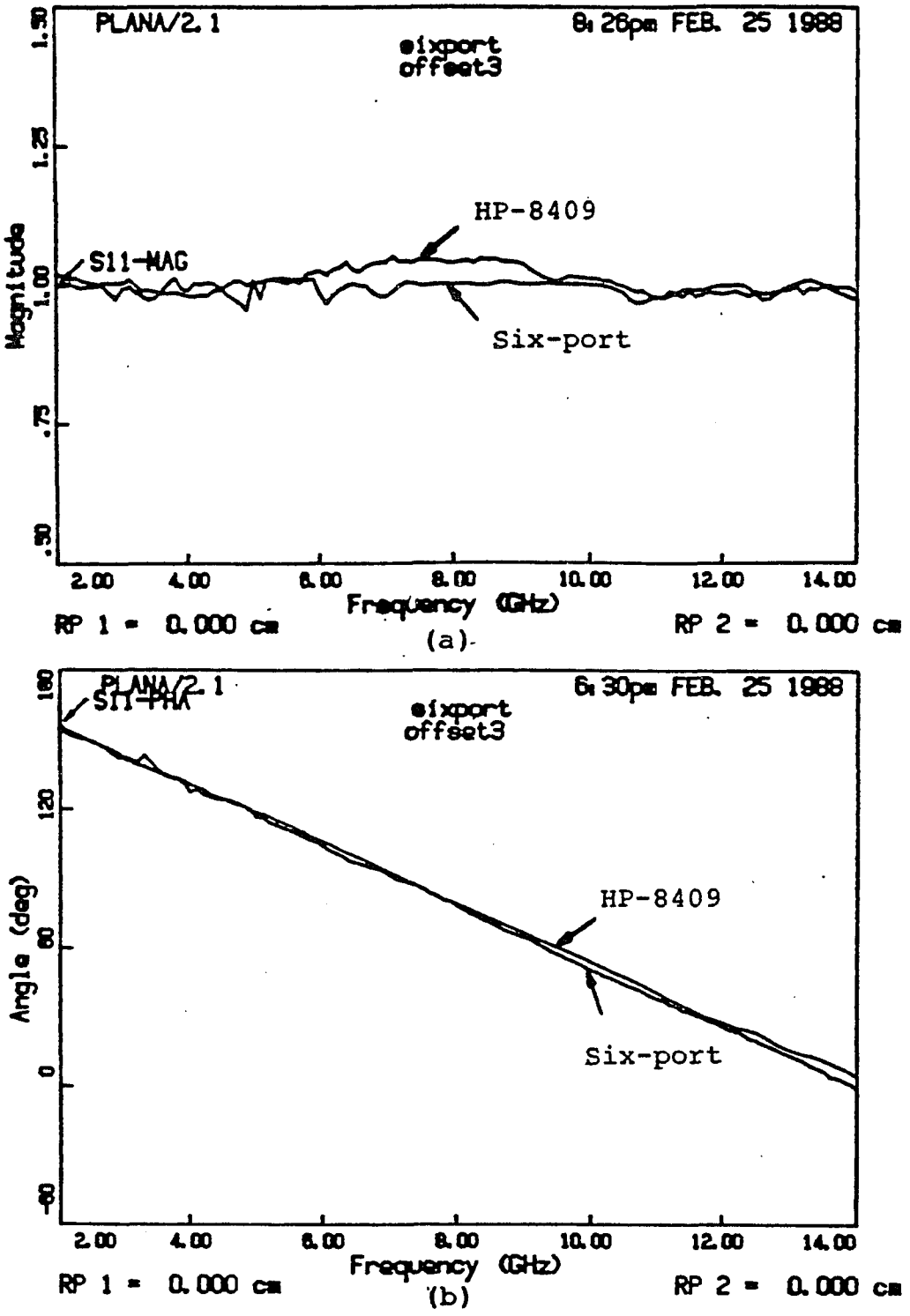

Fig.4.6-3: CW measurement results for an offset short with an offset of 50.48 degrees at 8 GHz (standard in the six-port calibration). Magnitude (a) and phase (b) versus frequency for HP-8409 and six-port reflectometer

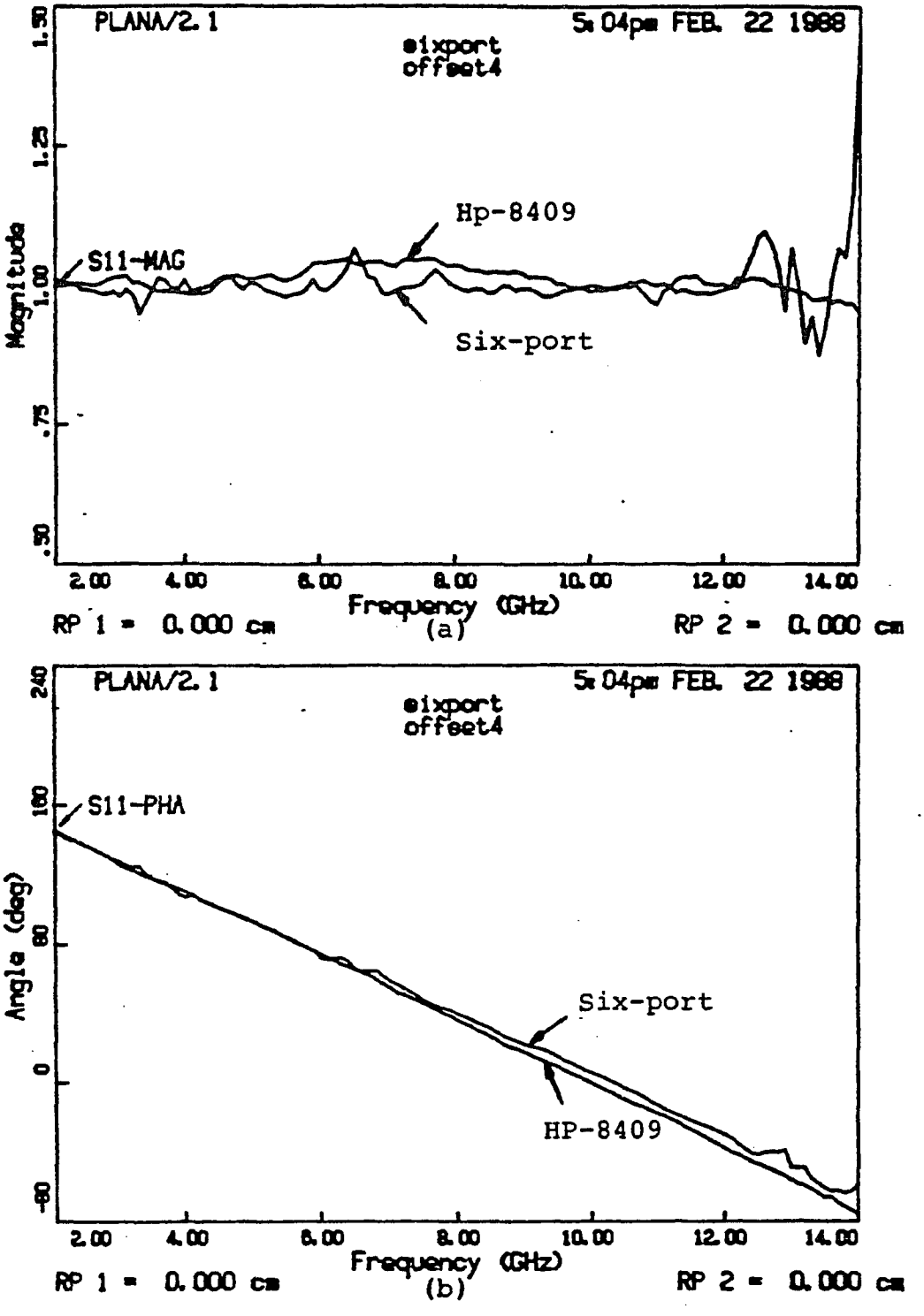

Fig.4.6-4: CW measurement results for an offset short with an offset of 70.52 degrees at 8 GHz. Magnitude (a) and phase (b) versus frequency for HP-8409 and six-port reflectometer

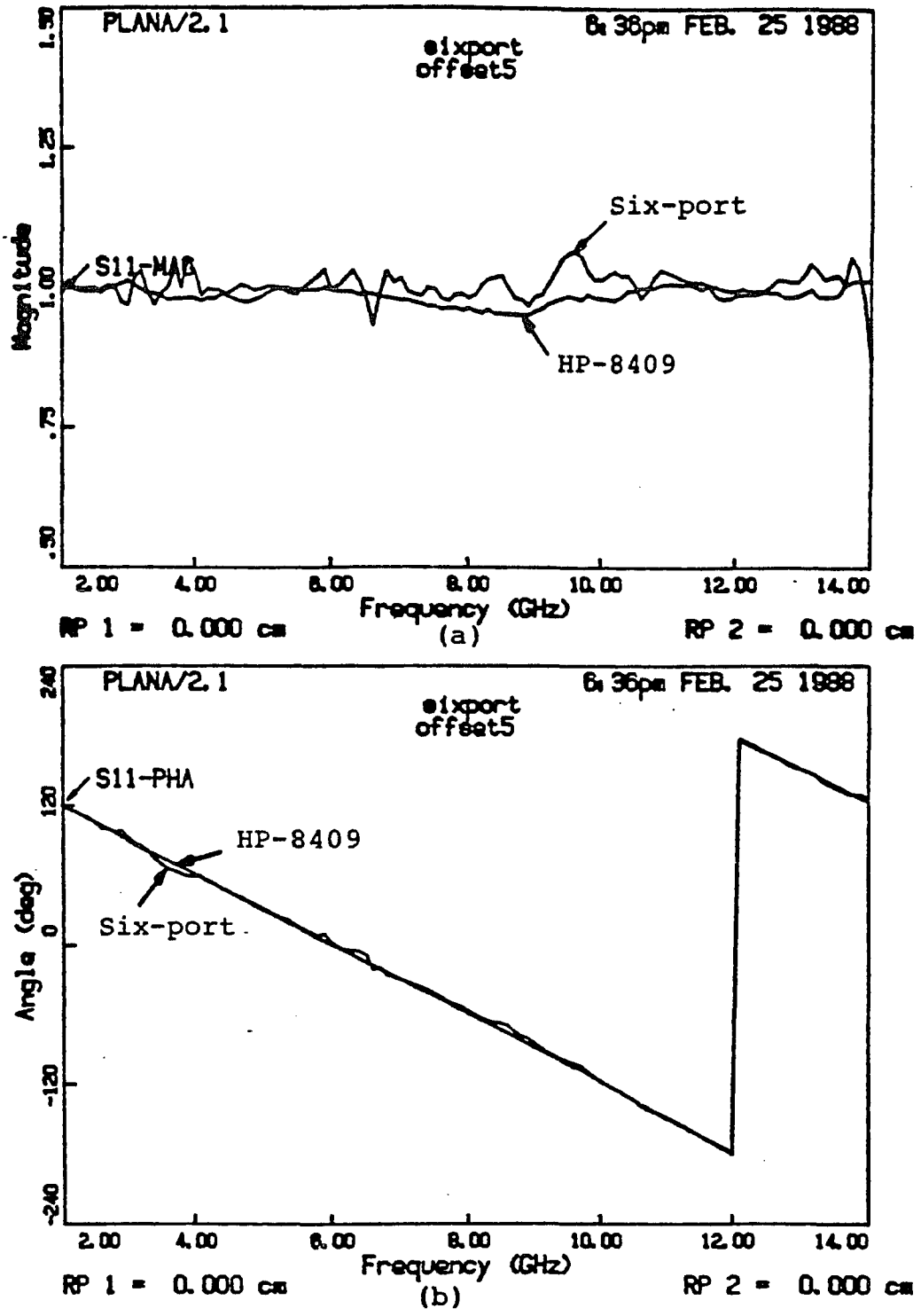

Fig.4.6-5: CW measurement results for an offset short with an offset of 118.81 degrees at 8 GHz. Magnitude (a) and phase (b) versus frequency for HP-8409 and six-port reflectometer

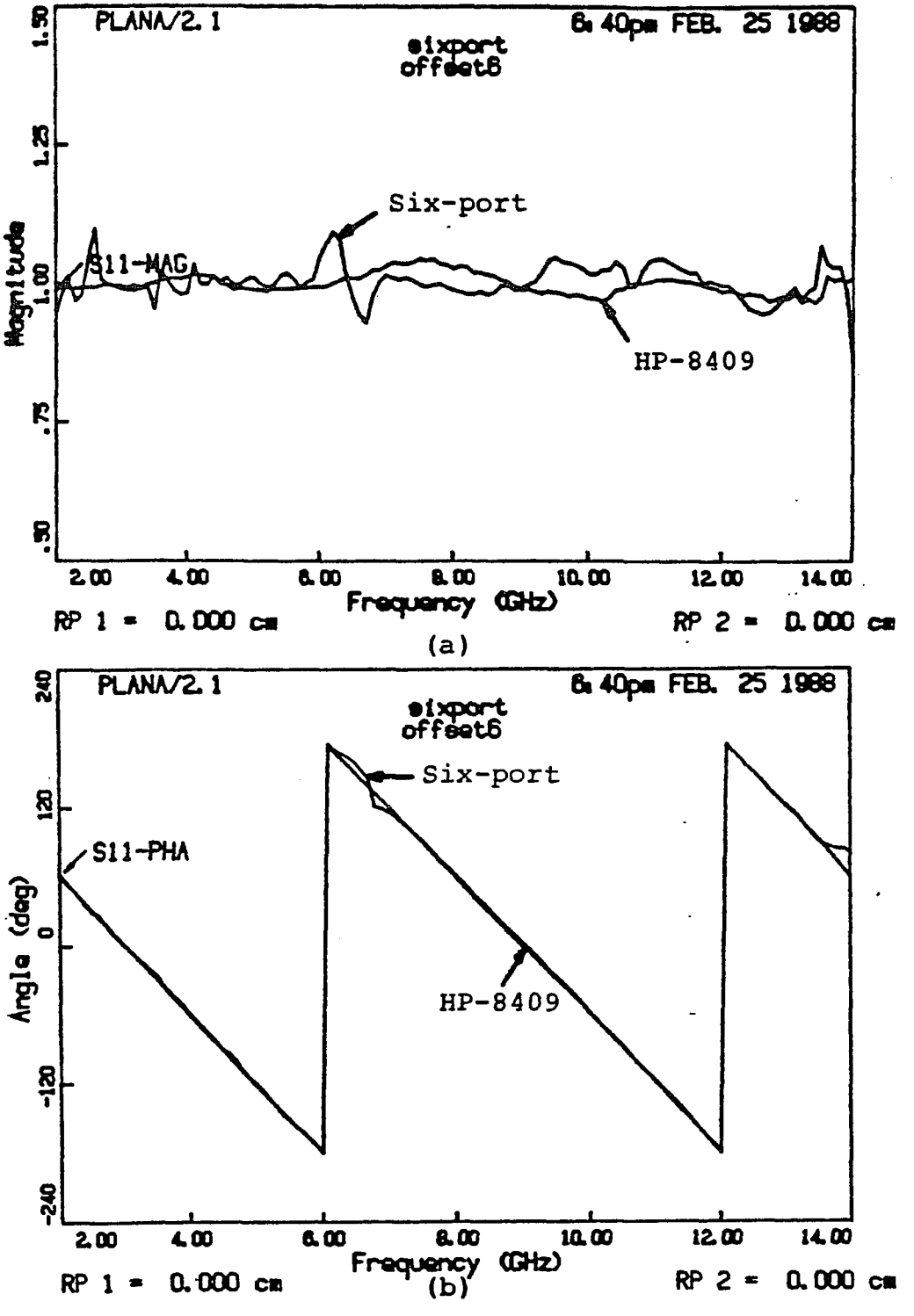

Fig.4.6-6: CW measurement results for an offset short with an offset of 239.81 degrees at 8 GHz. Magnitude (a) and phase (b) versus frequency for HP-8409 and six-port reflectometer

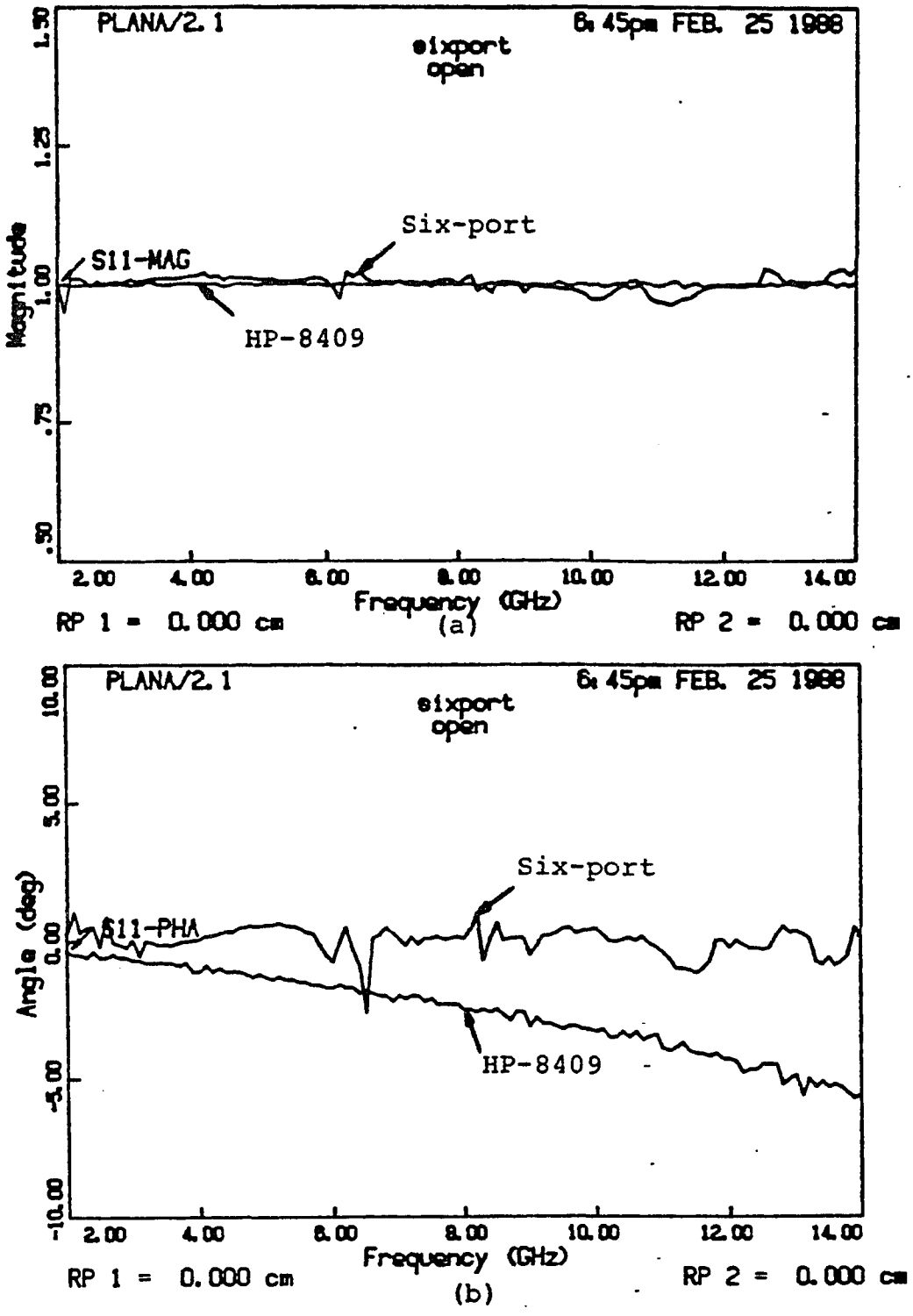

Fig.4.6-7: CW measurement results for an open (standard in the six-port calibration). Magnitude (a) and phase (b) versus frequency for HP-8409 and six-port reflectometer

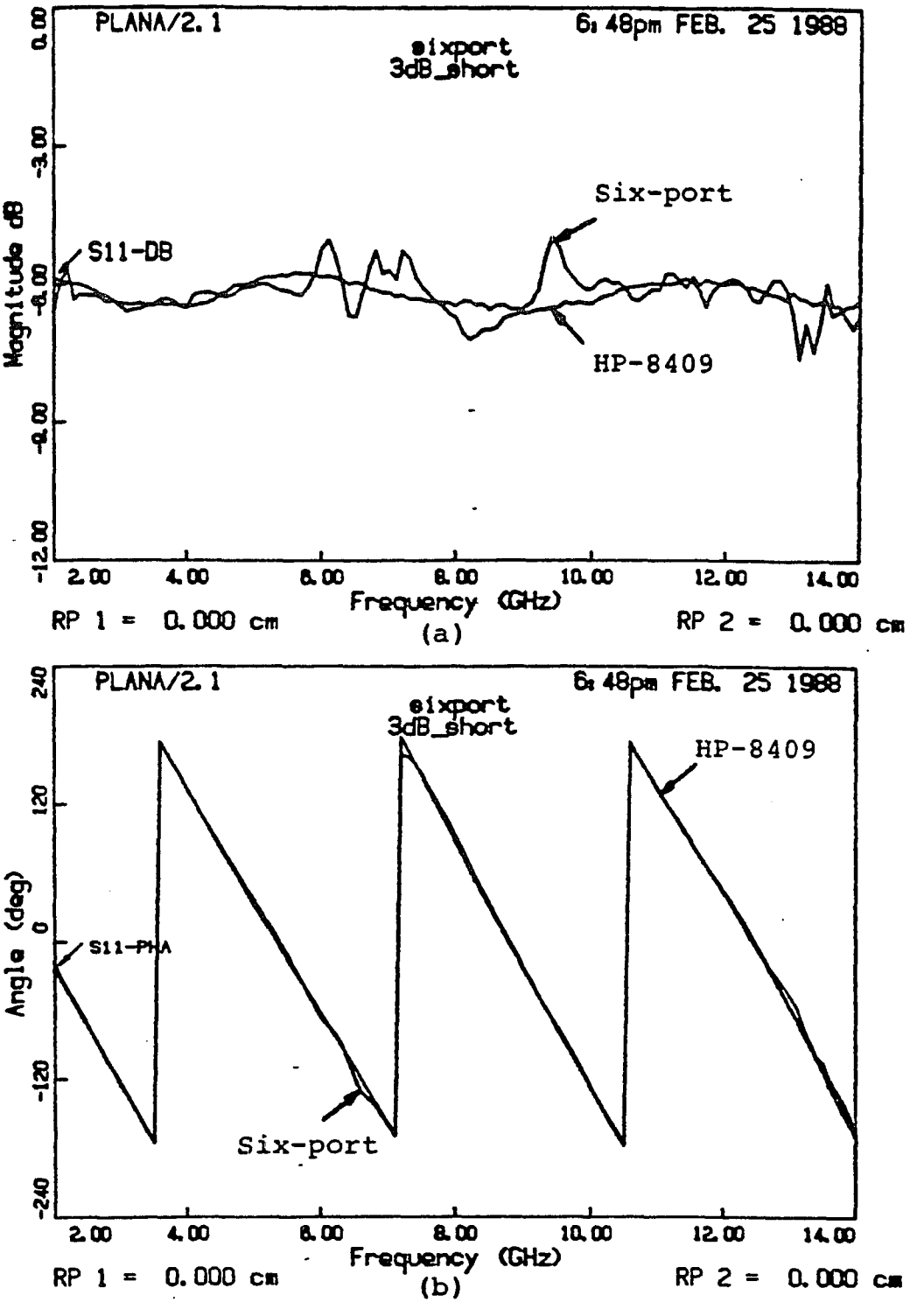

Fig.4.6-8: CW measurement results for a load made up of a 3 dB attenuator and a short. Magnitude (a) and phase (b) versus frequency for HP-8409 and six-port reflectometer

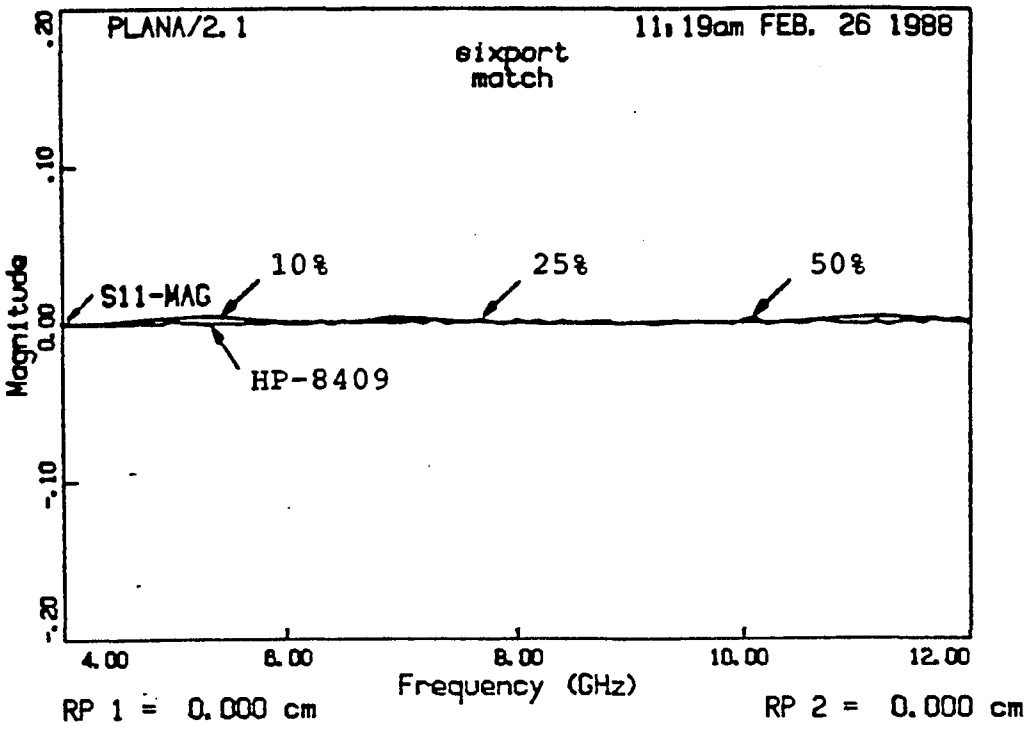

Fig.4.6-9: Pulsed signals measurement results for a matched load (standard in the six-port calibration) for 10, 25 and 50 per cent duty cycle and 250 microseconds pulse duration. Magnitude versus frequency for CW results from HP-8409 and pulsed results from six-port

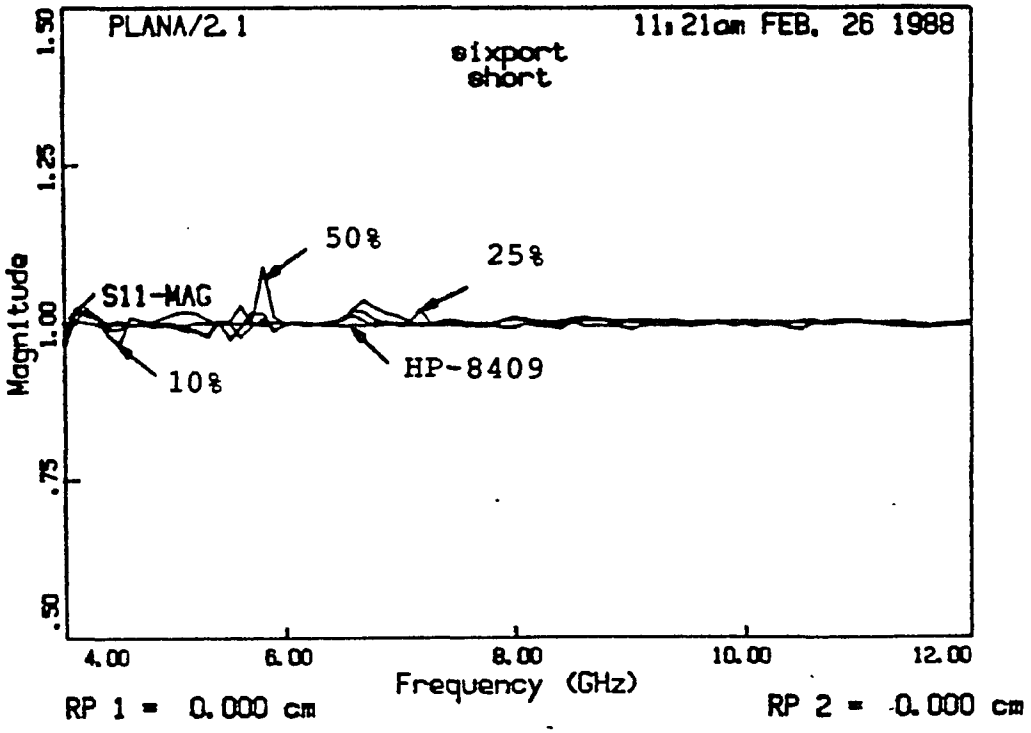

Fig.4.6-10: Pulsed signals measurement results for a short (standard in the six-port calibration). Magnitude versus frequency for CW results from HP-8409 and pulsed signals results for 10, 25, 50 per cent duty cycles and 250 microsecond pulse duration obtained with six-port reflectometer.

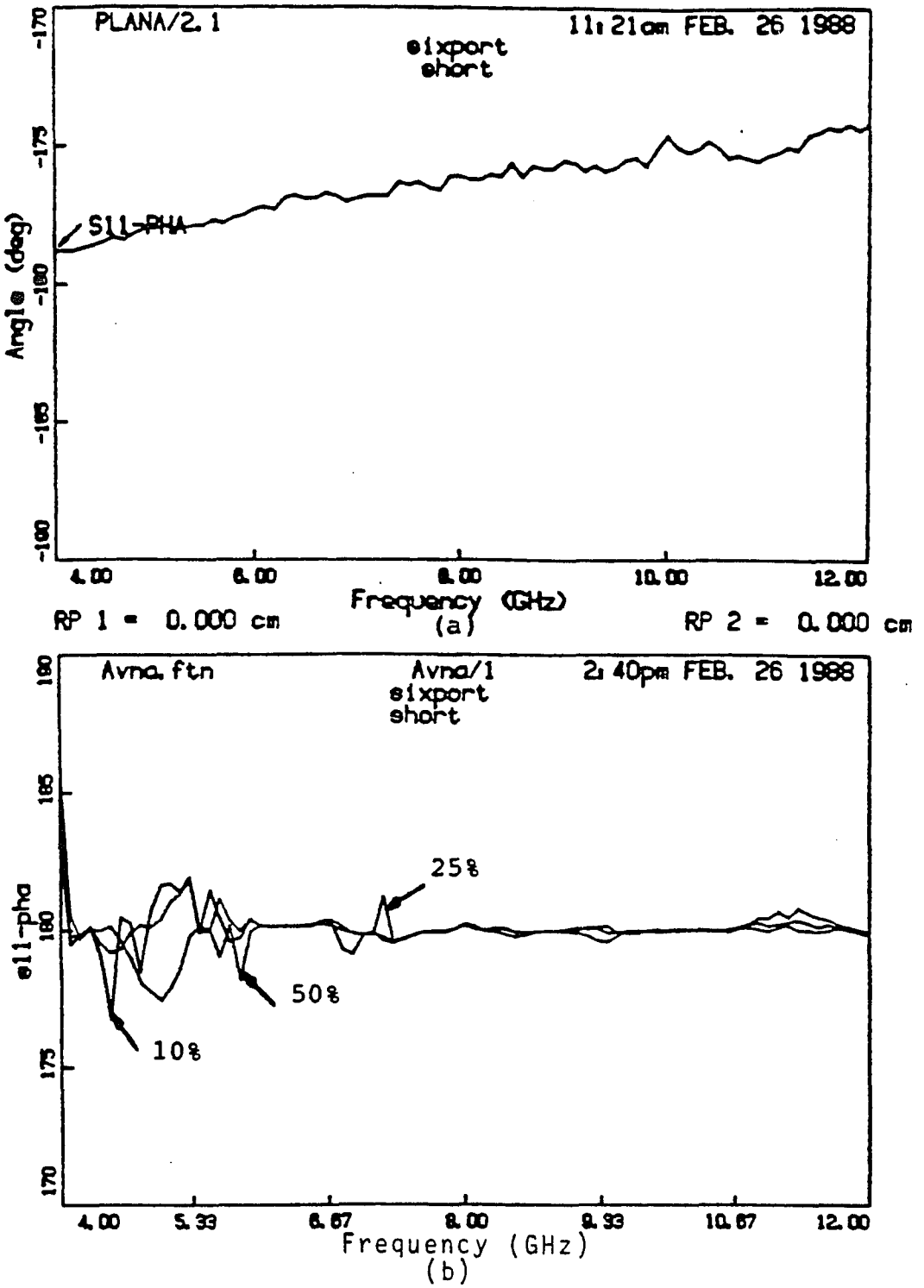

Fig.4.6-11: Pulsed signals measurement results for a short (standard in the six-port calibration). Phase versus frequency for HP-8409 (a) and six-port reflectometer (b) for 10, 25, 50 per cent duty cycle pulsed signals, with 250 microsecond pulse duration

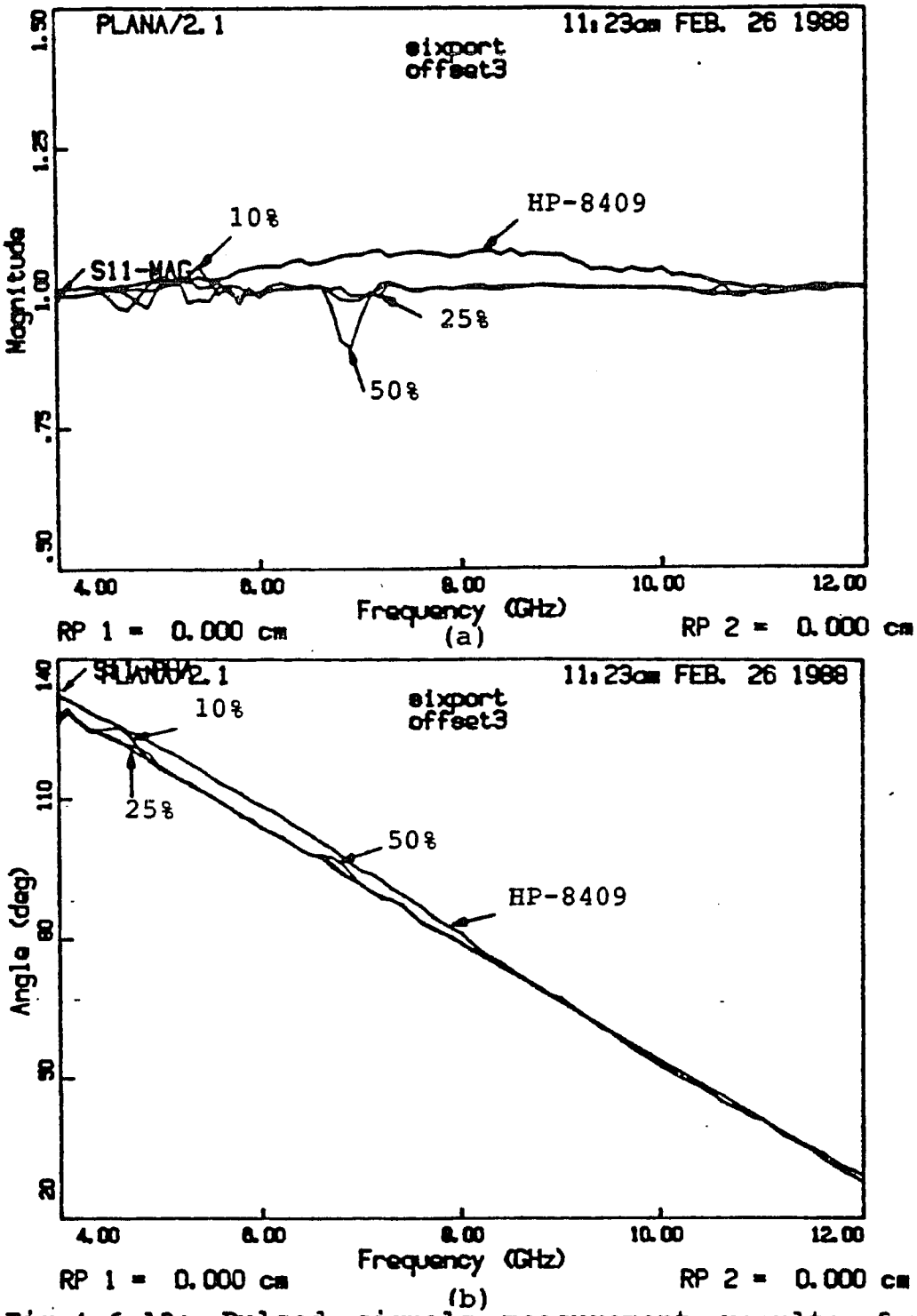

Fig.4.6-12: Pulsed signals measurement results for an offset short with an offset of 50.48 degrees at 8 GHz (standard in the six-port calibration). Mgnitude (a) and phase (b) versus frequency for HP-8409 and six-port reflectometer with 10, 25, 50 per cent duty cycle pulsed signals (250 microseconds pulse duration)

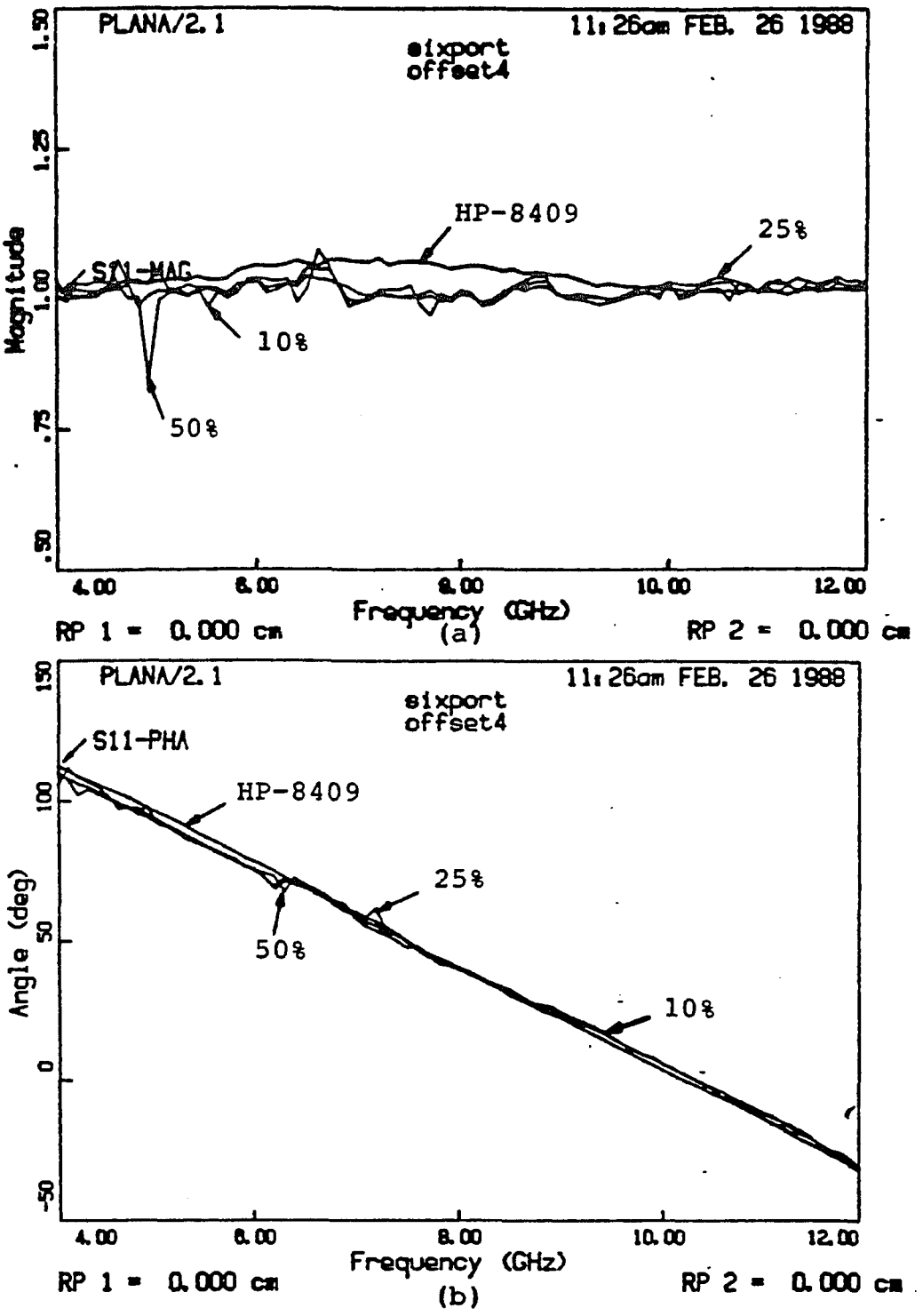

Fig.4.6-13: Pulsed signals measurement results for an offset short with an offset of 70.52 degrees at 8 GHz. Magnitude (a) and phase (b) versus frequency for HP-8409 and six-port reflectometer with 10, 25, 50 per cent pulsed signals (250 microsecond pulse duration)

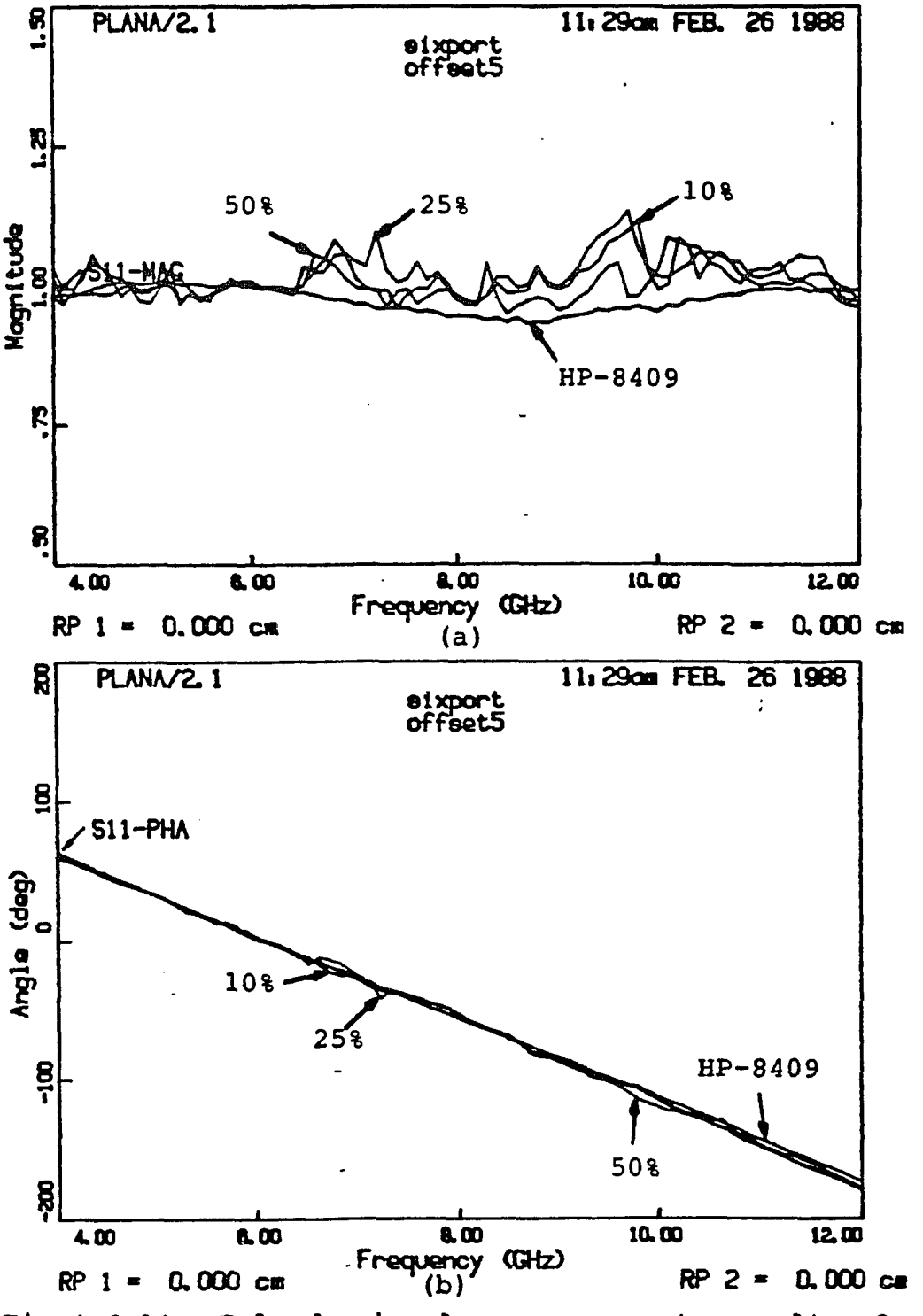

Fig.4.6-14: Pulsed signals measurement results for an offset short with offset of 118.81 degrees at 8 GHz. Magnitude (a) and phase (b) versus frequency for HP-8409 and six-port reflectometer with 10, 25, 50 per cent pulsed signals (250 microsecond pulse duration)

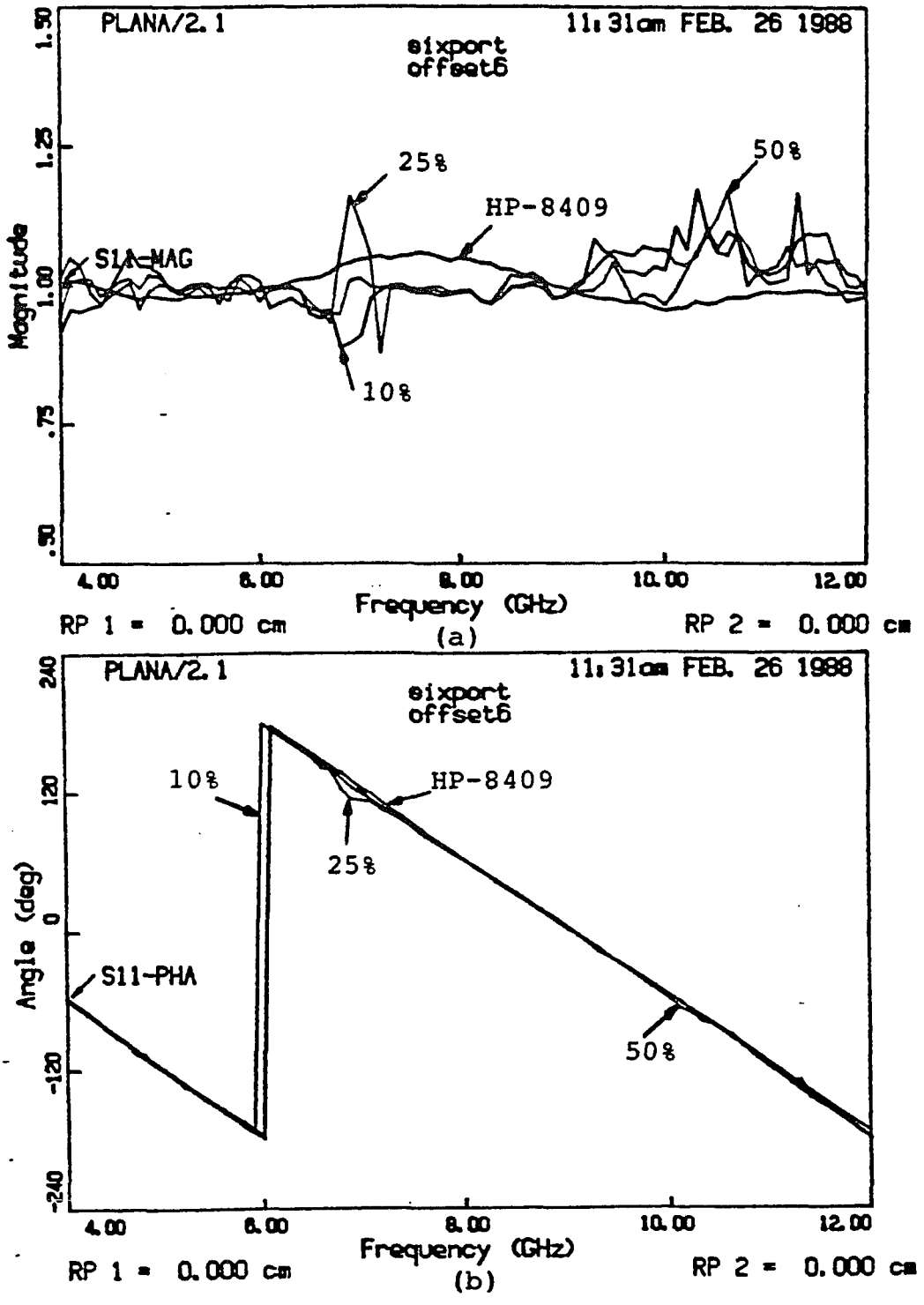

Fig.4.6-15: Pulsed signals measurement results for an offset short with an offset of 239.81 degrees at 8 GHz. Magnitude (a) and phase(b) versus frequency for HP-8409 and six-port reflectometer with 10, 15, 20 per cent pulsed signals (250 microsecond pulse duration)

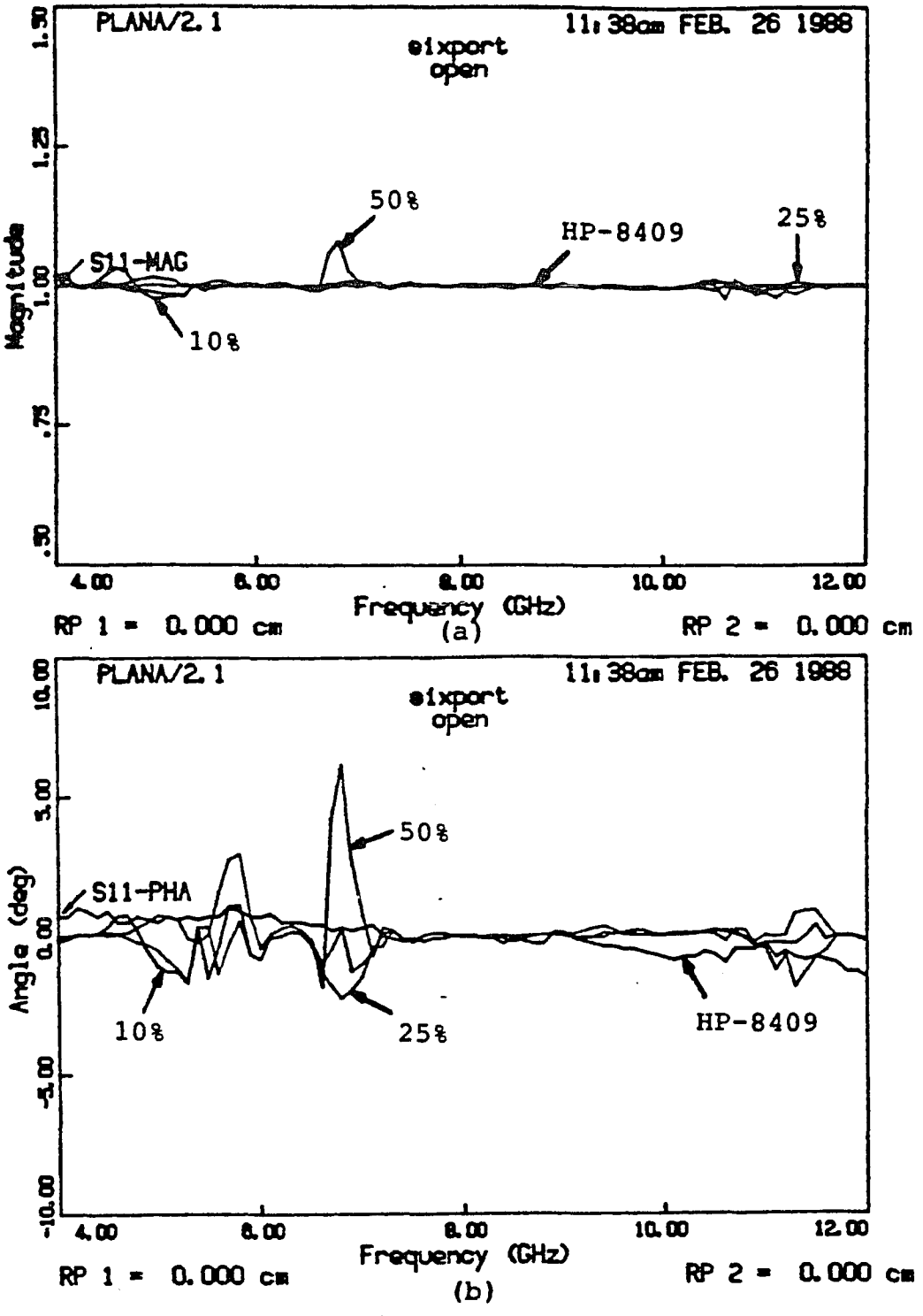

Fig.4.6-16: Pulsed signals measurement results for an open (standard in the six-port calibration). Magnitude (a) and phase (b) versus frequency for HP-8409 and six-port reflectometer with 10, 25, 50 per cent pulsed signals (250 microsecond pulse duration)

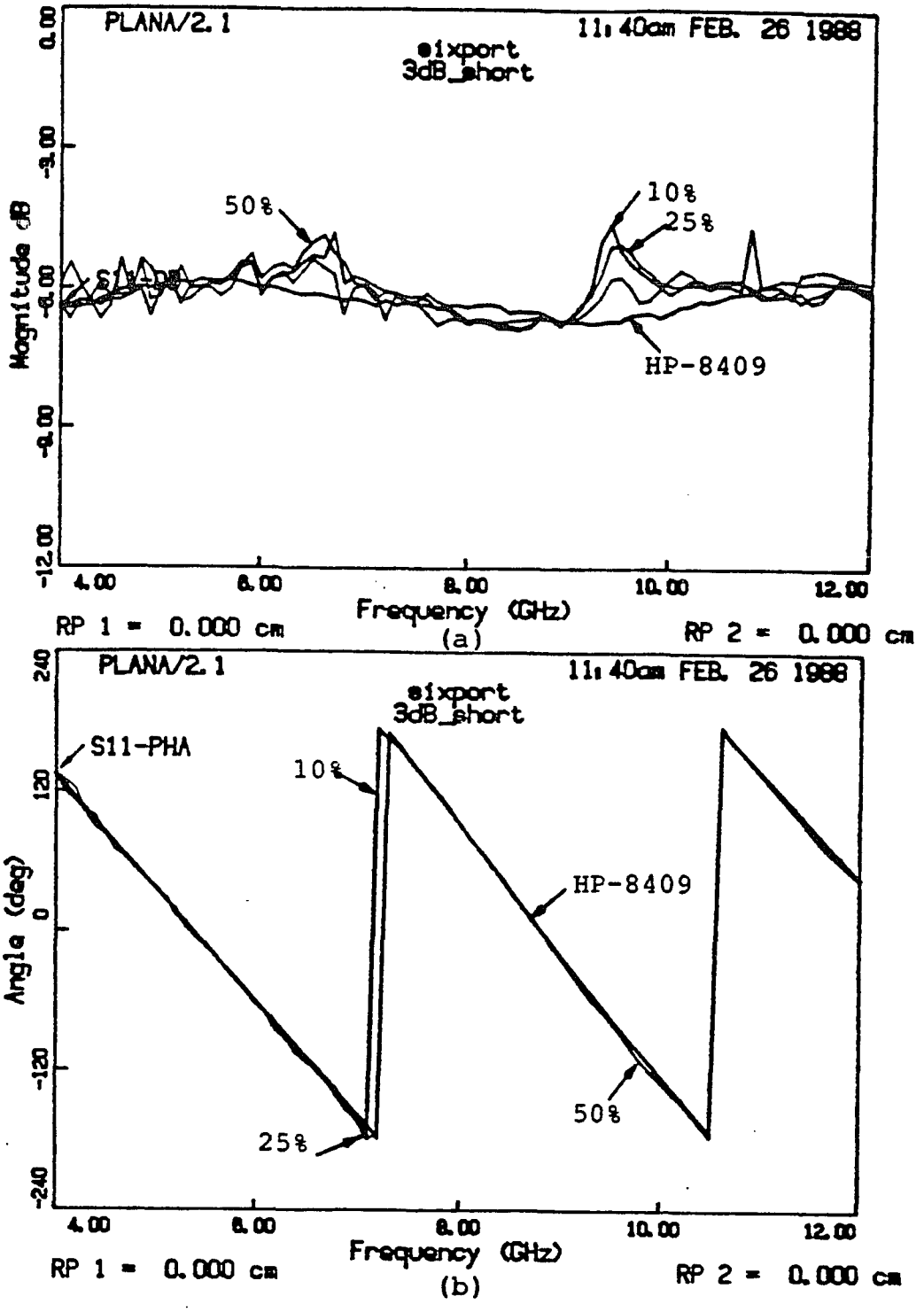

Fig.4.6-17: Pulsed signals measurement results for a 3 dB attenuator with a short. Magnitude (a) and phase (b) versus frequency for HP-8409 and six0port reflectometer with 10, 25, 50 per cent pulsed signals (250 microsecond pulse duration)

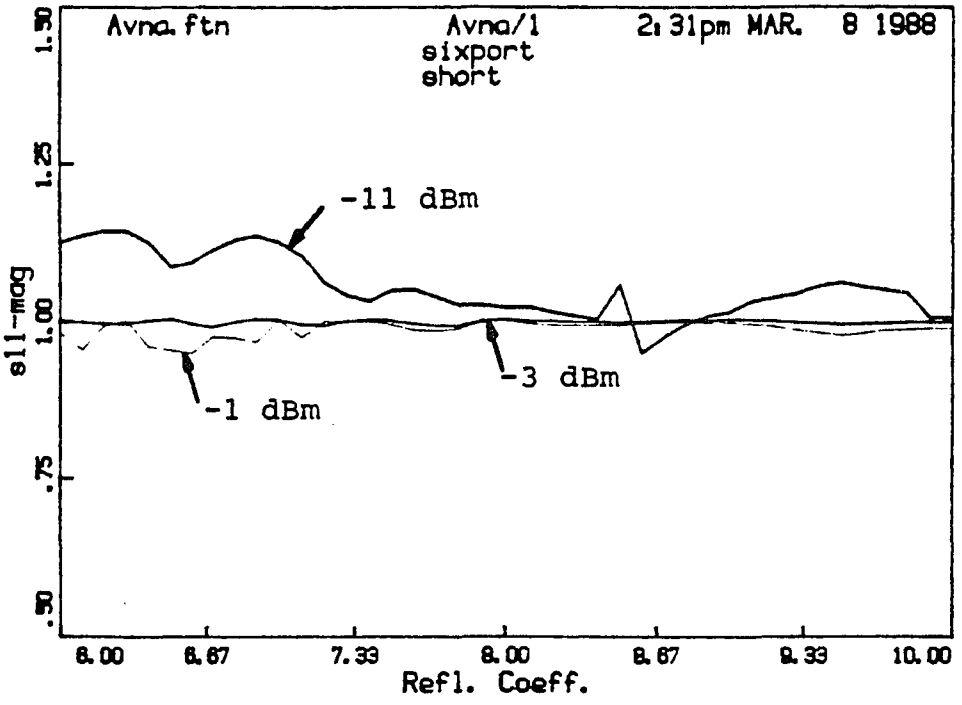

(a)

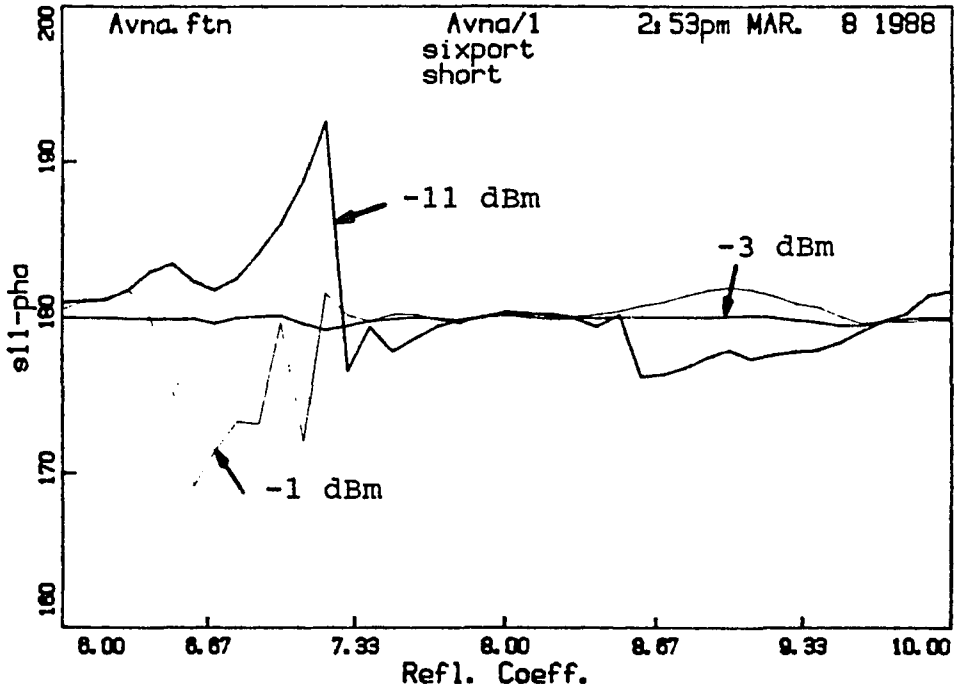

(b)

Fig.4.6.2-1: CW measurements of a short for different levels of input power from -11 dBm to -1 dBm. Magnitude (a) and phase (b) versus frequency.

5. APPENDIX

APPENDIX A

DERIVATION OF EXPRESSIONS OF THE b_j WAVES

Equations (1.1-15) expressed the relationship between the b_j waves, and the S-parameters and the reflection coefficients of each power meter, as follows:

$$b_j = a_1 S_{j1} + S_{j2}\Gamma b_2 + \sum_{k=3}^{6} S_{jk}\Gamma_k b_k \qquad (A-1)$$

Rearranging these equations into a more convenient form, we get:

$$-b_1 + S_{12}\Gamma b_2 + S_{13}\Gamma_3 b_3 + S_{14}\Gamma_4 b_4 + S_{15}\Gamma_5 b_5 + S_{16}\Gamma_6 b_6 = -S_{11} a_1$$

$$0 + (S_{22}\Gamma - 1) b_2 + S_{23}\Gamma_3 b_3 + S_{24}\Gamma_4 b_4 + S_{25}\Gamma_5 b_5 + S_{26}\Gamma_6 b_6 = -S_{21} a_1$$

$$0 + S_{32}\Gamma b_2 + (S_{33}\Gamma_3 - 1) b_3 + S_{34}\Gamma_4 b_4 + S_{35}\Gamma_5 b_5 + S_{36}\Gamma_6 b_6 = -S_{31} a_1$$

$$0 + S_{42}\Gamma b_2 + S_{43}\Gamma_3 b_3 + (S_{44}\Gamma_4 - 1) b_4 + S_{45}\Gamma_5 b_5 + S_{46}\Gamma_6 b_6 = -S_{41} a_1$$

$$0 + S_{52}\Gamma b_2 + S_{53}\Gamma_3 b_3 + S_{54}\Gamma_4 b_4 + (S_{55}\Gamma_5 - 1) b_5 + S_{56}\Gamma_6 b_6 = -S_{51} a_1$$

$$0 + S_{62}\Gamma b_2 + S_{63}\Gamma_3 b_3 + S_{64}\Gamma_4 b_4 + S_{65}\Gamma_5 b_5 + (S_{66}\Gamma_6 - 1)b_6 = -S_{61}a_1 \qquad (A-2)$$

In order to solve the above linear system of equations, we make use of Kramer's rule, which requires the evaluation of the determinant of the system's matrix shown below:

$$\Delta = det \begin{pmatrix} -1 & S_{12}\Gamma & S_{13}\Gamma_3 & S_{14}\Gamma_4 & S_{15}\Gamma_5 & S_{16}\Gamma_6 \\ 0 & S_{22}\Gamma - 1 & S_{23}\Gamma_3 & S_{24}\Gamma_4 & S_{25}\Gamma_5 & S_{26}\Gamma_6 \\ 0 & S_{32}\Gamma & S_{33}\Gamma_3 - 1 & S_{34}\Gamma_4 & S_{35}\Gamma_5 & S_{36}\Gamma_6 \\ 0 & S_{42}\Gamma & S_{43}\Gamma_3 & S_{44}\Gamma_4 - 1 & S_{45}\Gamma_5 & S_{46}\Gamma_6 \\ 0 & S_{52}\Gamma & S_{53}\Gamma_3 & S_{54}\Gamma_4 & S_{55}\Gamma_5 - 1 & S_{56}\Gamma_6 \\ 0 & S_{62}\Gamma & S_{63}\Gamma_3 & S_{64}\Gamma_4 & S_{65}\Gamma_5 & S_{66}\Gamma_6 - 1 \end{pmatrix}$$

Using Kramer's rule to obtain the solution of the above system, we have to evaluate the determinant of the above matrix, and also a series of determinants obtained by replacing the appropriate column with the column made out of the elements of the right hand side of the equations.

Only the second column of the determinant of the of the system's matrix contains Γ, therefore it contains only first order terms in Γ. It may be put in a general form :

$$\Delta = A\Gamma + B \qquad (A-3)$$

where A and B are complex constants that depend on the S-parameters and the reflection coefficients Γ_3, Γ_4, Γ_5, Γ_6.

Since we are interested in the expressions for b_3, b_4, b_5, b_6 only, we need to look at the matrices whose determinants are involved in the numerator of their Kramer solution.

Without loss of generality, we shall choose to look at b_3 only. The conclusions that we draw will be valid for b_4, b_5, and b_6. The numerator of the solution for b_3 involves the following determinant:

$$\Delta_3 = det\begin{pmatrix} -1 & S_{12}\Gamma & -S_{11}a_1 & S_{14}\Gamma_4 & S_{15}\Gamma_5 & S_{16}\Gamma_6 \\ 0 & S_{22}\Gamma - 1 & -S_{21}a_1 & S_{24}\Gamma_4 & S_{25}\Gamma_5 & S_{26}\Gamma_6 \\ 0 & S_{32}\Gamma & -S_{31}a_1 & S_{34}\Gamma_4 & S_{35}\Gamma_5 & S_{36}\Gamma_6 \\ 0 & S_{42}\Gamma & -S_{41}a_1 & S_{44}\Gamma_4 - 1 & S_{45}\Gamma_5 & S_{46}\Gamma_6 \\ 0 & S_{52}\Gamma & -S_{51}a_1 & S_{54}\Gamma_4 & S_{55}\Gamma_5 - 1 & S_{56}\Gamma_6 \\ 0 & S_{62}\Gamma & -S_{61}a_1 & S_{64}\Gamma_4 & S_{65}\Gamma_5 & S_{66}\Gamma_6 - 1 \end{pmatrix}$$

Since a_1 appears as a multiplicative constant in column 3, and linear combinations of Γ appear in column 2, the expression for Δ_3 takes the following form:

$$\Delta_3 = a_1(C\Gamma + D) \qquad (A-4)$$

where C and D are complex constants that depend on the S-parameters of the six-port junction and the reflection coefficients Γ_i, $i = 3,4,5,6$. Similarly:

$$\Delta_4 = a_1(E\Gamma + F) \qquad (A-5)$$

$$\Delta_5 = a_1(G\Gamma + H) \qquad (A-6)$$

$$\Delta_6 = a_1(K\Gamma + L) \qquad (A-7)$$

Therefore, the solutions for b_3, b_4, b_5, and b_6 become:

$$b_3 = \frac{\Delta_3}{\Delta} = \frac{C\Gamma + D}{A\Gamma + B} a_1 \qquad (A-8)$$

$$b_4 = \frac{\Delta_4}{\Delta} = \frac{E\Gamma + F}{A\Gamma + B} a_1 \qquad (A-9)$$

$$b_5 = \frac{\Delta_5}{\Delta} = \frac{G\Gamma + H}{A\Gamma + B} a_1 \qquad (A-10)$$

$$b_6 = \frac{\Delta_6}{\Delta} = \frac{K\Gamma + L}{A\Gamma + B} a_1 \qquad (A-11)$$

The powers at ports 3, 4, 5, and 6 are given by:

$$P_j = \frac{1}{2}|b_j|^2 - \frac{1}{2}|a_j|^2 = \frac{1}{2}\left(1 - |\Gamma_j|^2\right)|b_j|^2 \qquad (A-12)$$

where j=3, 4, 5, 6. Therefore:

$$P_3 = \frac{1}{2}\left(1 - |\Gamma_3|^2\right)\frac{|C\Gamma + D|^2}{|A\Gamma + B|^2}|a_1|^2 \qquad (A-13)$$

$$P_4 = \frac{1}{2}\left(1 - |\Gamma_4|^2\right)\frac{|E\Gamma + F|^2}{|A\Gamma + B|^2}|a_1|^2 \qquad (A-14)$$

$$P_5 = \frac{1}{2}\left(1 - |\Gamma_5|^2\right)\frac{|G\Gamma + H|^2}{|A\Gamma + B|^2}|a_1|^2 \qquad (A-15)$$

$$P_6 = \frac{1}{2}\left(1 - |\Gamma_6|^2\right)\frac{|K\Gamma + L|^2}{|A\Gamma + B|^2}|a_1|^2 \qquad (A-16)$$

Denoting $|a_1|^2/2 = P_{in}$ and :

$$A'_3 = \frac{1}{2}\left(1 - |\Gamma_3|^2\right)\frac{|D|^2}{|B|^2} \qquad (A-17)$$

$$A'_4 = \frac{1}{2}\left(1 - |\Gamma_4|^2\right)\frac{|E|^2}{|B|^2} \qquad (A-18)$$

$$A'_5 = \frac{1}{2}\left(1 - |\Gamma_5|^2\right)\frac{|G|^2}{|B|^2} \qquad (A-19)$$

$$A'_6 = \frac{1}{2}\left(1 - |\Gamma_6|^2\right)\frac{|K|^2}{|B|^2} \qquad (A-20)$$

and

$$q_3 = -\frac{C}{D}$$

$$q_4 = -\frac{F}{E}$$

$$q_5 = -\frac{H}{G} \qquad (A-21)$$

$$q_6 = -\frac{L}{K}$$

$$q = -\frac{A}{B}$$

we have:

$$P_3 = A'_3 \frac{|1 - q_3\Gamma|^2}{|1 - q\Gamma|^2} P_{in} \qquad (A-22)$$

$$P_4 = A'_4 \frac{|\Gamma - q_4|^2}{|1 - q\Gamma|^2} P_{in} \qquad (A-23)$$

$$P_5 = A'_5 \frac{|\Gamma - q_5|^2}{|1 - q\Gamma|^2} P_{in} \qquad (A-24)$$

$$P_6 = A'_6 \frac{|\Gamma - q_6|^2}{|1 - q\Gamma|^2} P_{in} \qquad (A-25)$$

APPENDIX B

CALCULATION OF THE CENTER AND RADIUS OF THE CIRCLES

The power equations at the four measurement ports of the six-port reflectometer are given by:

$$p_i = A_i \frac{|\Gamma - q_i|^2}{|1 - q_3\Gamma|^2} \qquad (B-1)$$

Replacing the complex quantities q_i, $i = 3,4,5,6$ and Γ, by their rectangular form (real and imaginary parts), we get:

$$p_i\left[1 + (r_3^2 + s_3^2)(x^2 + y^2) - 2xr_3 + 2ys_3\right] =$$
$$A_i(x^2 + y^2 - 2xr_i - 2ys_i + r_i^2 + s_i^2) \qquad (B-2)$$

Collecting terms which contain x^2, y^2, x, and y together, we get:

$$\left[A_i - p_i(r_3^2 + s_3^2)\right](x^2 + y^2) + 2(p_i r_3 - A_i r_i)x + 2(-p_i s_3 - A_i s_i)y =$$
$$p_i - A_i(r_i^2 + s_i^2) \qquad (B-3)$$

Let us make the following substitution:

$$a_i = A_i - p_i\left(r_3^2 + s_3^2\right) \qquad (B-4)$$

$$b_i = -\left(p_i r_3 - A_i r_i\right) \qquad (B-5)$$

$$c_i = p_i s_3 + A_i s_i \qquad (B-6)$$

$$d_i = p_i - A_i\left(r_i^2 + s_i^2\right) \qquad (B-7)$$

The equation becomes:

$$a_i x^2 + a_i y^2 - 2b_i x - 2c_i y = d_i \qquad (B-8)$$

Dividing by a_i, we get:

$$x^2 + y^2 - 2\frac{b_i}{a_i}x - 2\frac{c_i}{a_i}y = \frac{d_i}{a_i} \qquad (B-9)$$

Completing squares in the above equation, we get:

$$x^2 - 2\frac{b_i}{a_i}x + \frac{b_i^2}{a_i^2} + y^2 - 2\frac{c_i}{a_i}y + \frac{c_i^2}{a_i^2} = \frac{d_i}{a_i} + \frac{b_i^2 + c_i^2}{a_i^2} \qquad (B-10)$$

Thus:

$$\left(x-\frac{b_i}{a_i}\right)^2+\left(y-\frac{c_i}{a_i}\right)^2=\frac{d_i}{a_i}+\frac{b_i^2+c_i^2}{a_i^2} \qquad (B-11)$$

Therefore, (B-1) represents the equation of a circle with the center and radius specified by:

Center : $C\left(\frac{b_i}{a_i},\frac{c_i}{a_i}\right)$

Radius : $R=\sqrt{\frac{d_i}{a_i}+\frac{b_i^2+c_i^2}{a_i^2}}$

APPENDIX C

CONDITIONS FOR A=D=0 IN SECTION 1.1.4.

As shown in section 1.1.4, we have the following equations:

$$a_1 = \frac{1}{S_{21}}\left(b_2 - S_{22}a_2 - S_{23}\Gamma_3 b_3 - S_{24}\Gamma_4 b_4\right) \qquad (C-1)$$

$$b_3 = S_{31}a_1 + S_{32}a_2 + S_{33}\Gamma_3 b_3 + S_{34}\Gamma_4 b_4 \qquad (C-2)$$

$$b_4 = S_{41}a_1 + S_{42}a_2 + S_{43}\Gamma_3 b_3 + S_{44}\Gamma_4 b_4 \qquad (C-3)$$

Substitute (C-1) into (C-2) and (C-3), and get:

$$b_3 = \frac{S_{31}}{S_{21}}\left(b_2 - S_{22}a_2 - S_{23}\Gamma_3 b_3 - S_{24}\Gamma_4 b_4\right) + S_{32}a_2 +$$

$$+ S_{33}\Gamma_3 b_3 + S_{34}\Gamma_4 b_4 \qquad (C-4)$$

$$b_4 = \frac{S_{41}}{S_{21}}\left(b_2 - S_{22}a_2 - S_{23}\Gamma_3 b_3 - S_{24}\Gamma_4 b_4\right) + S_{42}a_2 +$$

$$+ S_{43}\Gamma_3 b_3 + S_{44}\Gamma_4 b_4 \qquad (C-5)$$

Collecting terms that contain the same factor b_n, $n = 2,3,4$, and a_2, we get:

$$\left(1 + \frac{S_{31}S_{23}\Gamma_3}{S_{21}} - S_{33}\Gamma_3\right)b_3 + \left(\frac{S_{31}S_{24}\Gamma_4}{S_{21}} - S_{34}\Gamma_4\right)b_4 =$$

$$= \left(S_{32} - \frac{S_{31}S_{22}}{S_{21}}\right)a_2 + \frac{S_{31}}{S_{21}}b_2 \qquad (C-6)$$

$$\left(\frac{S_{41}S_{23}\Gamma_3}{S_{21}} - S_{43}\Gamma_3\right)b_3 + \left(1 + \frac{S_{41}S_{24}\Gamma_4}{S_{21}} - S_{44}\Gamma_4\right)b_4 =$$

$$= \left(S_{42} - \frac{S_{41}S_{22}}{S_{21}}\right)a_2 + \frac{S_{41}}{S_{21}}b_2 \qquad (C-7)$$

Making the following simplifying substitutions:

$$u_{11} = 1 + \frac{S_{31}S_{23}\Gamma_3}{S_{21}} - S_{33}\Gamma_3$$

$$u_{12} = \frac{S_{31}S_{24}\Gamma_4}{S_{21}} - S_{34}\Gamma_4$$

$$u_{21} = \frac{S_{41}S_{23}\Gamma_3}{S_{21}} - S_{43}\Gamma_3$$

$$u_{22} = 1 + \frac{S_{41} S_{24} \Gamma_4}{S_{21}} - S_{44} \Gamma_4$$

Also:

$$v_{11} = S_{23} - \frac{S_{31} S_{22}}{S_{21}}$$

$$v_{12} = \frac{S_{31}}{S_{21}}$$

$$v_{21} = S_{42} - \frac{S_{41} S_{22}}{S_{21}}$$

$$v_{22} = \frac{S_{41}}{S_{21}}$$

The system of equations becomes:

$$u_{11} b_3 + u_{12} b_4 = v_{11} a_2 + v_{12} b_2 \qquad (C-8)$$

$$u_{21} b_3 + u_{22} b_4 = v_{21} a_2 + v_{22} b_2 \qquad (C-9)$$

Solving the above system by Kramer's method, we get:

$$b_3 = \frac{(v_{11}a_2 + v_{12}b_2)u_{22} - (v_{21}a_2 + v_{22}b_2)u_{12}}{u_{11}u_{22} - u_{12}u_{21}} \qquad (C-10)$$

$$b_4 = \frac{(v_{21}a_2 + v_{22}b_2)u_{11} - (v_{11}a_2 + v_{12}b_2)u_{21}}{u_{11}u_{22} - u_{12}u_{21}} \qquad (C-11)$$

Therefore:

$$b_3 = A'a_2 + B'b_2 \qquad (C-12)$$

$$b_4 = C'a_2 + D'b_2 \qquad (C-13)$$

where

$$A' = \frac{v_{11}u_{22} - v_{21}u_{12}}{u_{11}u_{22} - u_{12}u_{21}} \qquad (C-14)$$

$$B' = \frac{v_{12}u_{22} - v_{22}u_{12}}{u_{11}u_{22} - u_{12}u_{21}} \qquad (C-15)$$

$$C' = \frac{v_{21}u_{11} - v_{11}u_{21}}{u_{11}u_{22} - u_{12}u_{21}} \qquad (C-16)$$

$$D' = \frac{v_{22}u_{11} - v_{12}u_{21}}{u_{11}u_{22} - u_{12}u_{21}} \qquad (C-17)$$

The conditions that A' and D' be zero are the following:

$$v_{11}u_{22} - v_{21}u_{12} = 0 \qquad (C-18)$$

$$v_{22}u_{11} - v_{12}u_{21} = 0 \qquad (C-19)$$

Substituting the values of the v's and u's in terms of the S-parameters, condition (C-18) becomes:

$$\left(S_{32} - \frac{S_{31}S_{22}}{S_{21}}\right)\left(1 + \frac{S_{41}S_{24}\Gamma_4}{S_{21}} - S_{44}\Gamma_4\right) -$$

$$\left(\frac{S_{31}S_{24}\Gamma_4}{S_{21}} - S_{34}\Gamma_4\right)\left(S_{42} - \frac{S_{41}S_{22}}{S_{21}}\right) = 0$$

In order to simplify these conditions, assume that $\Gamma_3 = \Gamma_4 = 0$ (matched power detectors). The above equation becomes:

$$S_{32} - \frac{S_{31} S_{22}}{S_{21}} = 0$$

Thus:

$$S_{32} S_{21} - S_{31} S_{22} = 0 \qquad (C-20)$$

The condition that D' be zero, for $\Gamma_3 = \Gamma_4 = 0$ becomes:

$$\frac{S_{41}}{S_{21}} - 0 = 0 \qquad (C-21)$$

Thus:

$$S_{41} = 0 \qquad (C-22)$$

Similarly we get the conditions for $B' = C' = 0$ to be:

$$\frac{S_{31}}{S_{21}} = 0 \qquad (C-23)$$

and

$$S_{42} - \frac{S_{41} S_{22}}{S_{21}} = 0$$

Thus:

$$\frac{S_{42} S_{21} - S_{41} S_{22}}{S_{21}} = 0 \qquad (C-24)$$

$$S_{31} = 0 \qquad (C-25)$$

$$S_{42} S_{21} - S_{41} S_{22} = 0 \qquad (C-26)$$

APPENDIX D

CALCULATION OF POWER OUTPUTS IN FIG.1.2-1

Consider the correlator from Fig.1.2-1 redrawn in Fig.D-1, where all the incoming and outgoing waves are shown. The S-matrices of a quadrature hybrid and power divider, in a general form, are:

$$S_Q = \begin{pmatrix} 0 & A & 0 & B \\ A & 0 & B & 0 \\ 0 & B & 0 & A \\ B & 0 & A & 0 \end{pmatrix} \qquad , \qquad S_D = \begin{pmatrix} 0 & \gamma & \gamma \\ \gamma & -\gamma^2 & \gamma^2 \\ \gamma & \gamma^2 & -\gamma^2 \end{pmatrix}$$

where:

$$|A| = |B| = \gamma = \frac{1}{\sqrt{2}}$$

Assuming that the four power meters are matched, we have:

$$a_2^2 = a_4^2 = a_2^3 = a_4^3 = 0$$

Also:

$$a_3^1 = 0$$

The b-waves associated with each device are given by:

$$b_1^1 = A a_2^1 + B a_4^1 \qquad b_1^2 = A a_2^2 + B a_4^2$$

$$b_2^1 = A a_1^1 + B a_3^1 \qquad b_2^2 = A a_1^2 + B a_3^2$$

$$b_3^1 = B a_2^1 + A a_4^1 \qquad b_3^2 = B a_2^2 + A a_4^2$$

$$b_4^1 = B a_1^1 + A a_3^1 \qquad b_4^2 = B a_1^2 + A a_3^2$$

$$b_1^3 = A a_2^3 + B a_4^3 \qquad b_1^4 = \gamma a_2^4 + \Gamma a_3^4$$

$$b_2^3 = A a_1^3 + B a_3^3 \qquad b_2^4 = \gamma a_1^4 - \gamma^2 a_2^4 + \gamma^2 a_3^4$$

$$b_3^3 = B a_2^3 + B a_4^3 \qquad b_3^4 = \gamma a_1^4 + \gamma^2 a_2^4 - \gamma^2 a_3^4$$

Thus, because of the matched power meters:

$$b_1^2 = 0, \quad b_3^2 = 0, \quad b_1^3 = 0, \quad b_3^3 = 0$$

$$b_2^1 = A a_1^1, \quad b_4^1 = B a_1^1$$

Because of the interconnections between devices, we may write that:

$$a_2^1 = b_1^2 = 0, \qquad a_4^1 = b_1^3 = 0, \qquad a_2^4 = b_3^2 = 0, \qquad a_3^4 = b_3^3 = 0$$

$$b_1^4 = \gamma a_2^4 + \gamma a_3^4 = 0, \qquad b_2^4 = \gamma a_1^4, \qquad b_3^4 = \gamma a_1^4$$

$$a_1^3 = b_4^1 = B a_1^1, \qquad a_3^3 = b_2^4 = \gamma a_1^4$$

$$a_1^2 = b_2^1 = A a_1^1, \qquad a_3^2 = b_2^4 = \gamma a_1^4$$

The powers at ports 3,4,5,and 6 are given by:

$$P_3 = \frac{1}{2}|b_2^3|^2 - \frac{1}{2}|a_2^3|^2 = \frac{1}{2}|b_2^3|^2 = \frac{1}{2}|A a_1^3 + B a_3^3|^2$$

$$P_4 = \frac{1}{2}|b_4^3|^2 - \frac{1}{2}|a_4^3|^2 = \frac{1}{2}|b_4^3|^2 = \frac{1}{2}|B a_1^3 + A a_3^3|^2$$

$$P_5 = \frac{1}{2}|b_2^2|^2 - \frac{1}{2}|a_2^2|^2 = \frac{1}{2}|b_2^2|^2 = \frac{1}{2}|A a_1^2 + B a_3^2|^2$$

$$P_6 = \frac{1}{2}|b_4^2|^2 - \frac{1}{2}|a_4^2|^2 = \frac{1}{2}|b_4^2|^2 = \frac{1}{2}|B a_1^2 + A a_3^2|^2$$

Denoting a_1^1 by u and a_1^4 by v and noticing that :

$$a_1^2 = A a_1^1 = A u \quad , \qquad a_3^2 = \gamma a_1^4 = \gamma v$$

$$a_1^3 = B a_1^1 = B u \quad , \qquad a_3^3 = \gamma a_1^4 = \gamma v$$

the power equations become:

$$P_3 = \frac{1}{2}|ABu + B\gamma v|^2 = \frac{1}{2}\gamma^4 \left| u + \frac{\gamma}{A} v \right|^2$$

$$P_4 = \frac{1}{2}|BBu + A\gamma v|^2 = \frac{1}{2}\gamma^4 \left| u + \frac{A\gamma}{B^2} v \right|^2$$

$$P_5 = \frac{1}{2}|AAu + B\gamma v|^2 = \frac{1}{2}\gamma^4 \left| u + \frac{B\gamma}{A^2} v \right|^2$$

$$P_6 = \frac{1}{2}|BA + A\gamma v|^2 = \frac{1}{2}\gamma^4 \left| u + \frac{\gamma}{B} v \right|^2$$

Depending on where the reference planes at the four ports of each quadrature hybrid are situated, the relationship between A and B differs, and therefore, the power equations will take different expressions. The

displacement of the reference planes by some fraction of the wavelength causes a displacement in the phase angles of the waves.

If the reference planes are not displaced at all, we get:

$$A = -j\gamma \quad , \qquad B = -\gamma$$

Thus, the power equations become:

$$P_3 = \frac{1}{2}\gamma^4 |u + jv|^2$$

$$P_4 = \frac{1}{2}\gamma^4 |u - jv|^2$$

$$P_5 = \frac{1}{2}\gamma^4 |u + v|^2$$

$$P_6 = \frac{1}{2}\gamma^4 |u - v|^2$$

If we have a displacement of $\lambda/4$ of the reference planes of the quadrature hybrids, then:

$$A = -\gamma \quad , \qquad B = j\gamma$$

Thus, the power terms become:

$$P_3 = \frac{1}{2}\gamma^4 |u - v|^2$$

$$P_4 = \frac{1}{2}\gamma^4 |u + v|^2$$

$$P_5 = \frac{1}{2}\gamma^4 |u + jv|^2$$

$$P_6 = \frac{1}{2}\gamma^4 |u - jv|^2$$

If we have a displacement of $3\lambda/4$ of the reference planes of the quadrature hybrids, then:

$$A = \gamma \quad , \qquad B = -j\gamma$$

Thus, the power terms become:

$$P_3 = \frac{1}{2}\gamma^4 |u+v|^2$$

$$P_4 = \frac{1}{2}\gamma^4 |u-v|^2$$

$$P_5 = \frac{1}{2}\gamma^4 |u-jv|^2$$

$$P_6 = \frac{1}{2}\gamma^4 |u+jv|^2$$

where:

$$u = a_1^1 \quad , \qquad v = a_1^4$$

Comparing Fig. D-1 with Fig. 1.2-1, we notice that:

$$a_1 = a_1^1 \quad , \qquad a_2 = a_1^4$$

Therefore:

$$u = a_1 \quad , \qquad v = a_2$$

Also: $\frac{1}{2}\gamma^4 = \frac{1}{8}$

The power outputs in Fig.1.2-1 are given for a displacement of $3\lambda/4$ displacement of the reference planes.

APPENDIX E

CALCULATION OF POWER OUTPUTS IN FIG.2.2-3

Consider the six-port circuit from Fig.2.2-3 redrawn in Fig.E-1, in which the correlator is depicted as a single device, and the incoming and outgoing waves associated with the two additional quadrature hybrids are shown. Since the four power outputs of the correlator are not independent, as shown in section 1.1.1, port 3 was matched, and port 7 associated with the quadrature hybrid from the input was selected to be the fourth power measuring port of the six-port. The b-waves associated with the two additional quadrature hybrids are related to the a-waves through the S-parameters as follows:

$$a_1 = a_{in} \qquad b_1 = A a_2 = A b_1^0$$

$$a_2 = b_1^0 \qquad b_2 = A a_1 = A a_{in}$$

$$a_3 = 0 \qquad b_3 = B a_2 = B b_1^0$$

$$a_4 = 0 \qquad b_4 = B a_1 = B a_{in}$$

and:

$$a_1^0 = b_2 \qquad b_1^0 = A a_2^0$$

$$a_2^0 = \Gamma b_2^0 \qquad b_2^0 = A a_1^0$$

$$a_3^0 = b_1^4 = 0 \qquad b_3^0 = B a_2^0$$

$$a_4^0 = b_1^1 = 0 \qquad b_4^0 = B a_1^0$$

(from Appendix D)

The powers at ports 4,5,6, and 7 are calculated as follows:

$$u = b_4^0 = B a_1^0 = B b_2 = B A a_{in}$$

$$v = b_3^0 = B a_2^0 = B \Gamma b_2^0 = B \Gamma A a_1^0 = B \Gamma A^2 a_{in}$$

$$b_4 = B a_{in}$$

$$P_4 = \frac{1}{2} \left| B^2 u + A \gamma v \right|^2 = \frac{1}{2} \left| B^2 B A + A \gamma B \Gamma A^2 \right|^2 \left| a_{in} \right|^2$$

$$P_5 = \frac{1}{2}\left|A^2 u + B\gamma v\right|^2 = \frac{1}{2}\left|A^2 BA + B\gamma B\Gamma A^2\right|^2 \left|a_{in}\right|^2$$

$$P_6 = \frac{1}{2}\left|BAu + A\gamma v\right|^2 = \frac{1}{2}\left|BABA + A\gamma B\Gamma A^2\right|^2 \left|a_{in}\right|^2$$

$$P_7 = \frac{1}{2}\left|b_4\right|^2 - \frac{1}{2}\left|a_4\right|^2 = \frac{1}{2}\left|b_4\right|^2 = \frac{1}{2}\left|B\right|^2 \left|a_{in}\right|^2$$

Thus:

$$P_4 = \left|A^3 B\gamma\right|^2 \left|\Gamma + \frac{B^2}{\gamma A^2}\right|^2 P_{in}$$

$$P_5 = \left|A^2 B^2 \gamma\right|^2 \left|\Gamma + \frac{A}{B\gamma}\right|^2 P_{in}$$

$$P_6 = \left|A^3 B\gamma\right|^2 \left|\Gamma + \frac{B}{A\gamma}\right|^2 P_{in}$$

$$P_7 = \left|B\right|^2 P_{in}$$

$$\left|A\right| = \left|B\right| = \gamma = \frac{1}{\sqrt{2}} \quad , \qquad A = -j\gamma, \quad B = -\gamma$$

Thus, the power outputs of the six-port in Fig.2.2-3 are given by:

$$P_4 = \gamma^{10}\left|\Gamma - \frac{1}{\gamma}\right|^2 P_{in} = \frac{1}{32}\left|\Gamma - \sqrt{2}\right|^2 P_{in}$$

$$P_5 = \gamma^{10}\left|\Gamma + j\frac{1}{\gamma}\right|^2 P_{in} = \frac{1}{32}\left|\Gamma + j\sqrt{2}\right|^2 P_{in}$$

$$P_6 = \gamma^{10}\left|\Gamma - j\frac{1}{\gamma}\right|^2 P_{in} = \frac{1}{32}\left|\Gamma - j\sqrt{2}\right|^2 P_{in}$$

$$P_7 = \gamma^2 P_{in} = \frac{1}{2} P_{in}$$

APPENDIX F

```
ftn7x,s
$files(0,1)
      program sixportest2
ccccccccccccccccccccccccccccccccccccccccccccccccccccccccccccccccccccccc
c     This program performs the calibration of the six-port            c
c     reflectometer, restoring files of measured data from the memory.c
c     It stores the calibration constants in a file named by the user.c
c ccccccccccccccccccccccccccccccccccccccccccccccccccccccccccccccccccccc
      common /c1/lusig,ludac,fstart,fstop,fstep,power
      common /c2/nsize,me,ca
      common /c3/titlec,titlem
      real*4 refl1(181),refl2(181),freq(181)
      real*4 r4(181),r5(181),r6(181),s4(181),s5(181),s6(181)
      real*4 a4(181),a5(181),a6(181),r3(181),s3(181)
      real*4 al4(4),a24(4),a34(4),a44(4),a54(4),a64(4)
      complex*8 b4,b5,b6,b1,b2,b3
      integer lusig,ludac,nsize
      real power,fstart,fstop,fstep
      character*10 titlec,titlem
      data the/'help'/,tcal/'cal'/,tame/'meas'/,tali/'list'/,tpl/'plot'/
      data tq/'quit'/
      call start_prompt
c     write(1,'(/" Welcome to AVNA/1 "/)')
c     write(1,'(/" Version : January 1985"/)')
      lusig=12
      ludac=47
      me=0
      ca=0
49    call command(task)
      if(task.eq.tcal)go to 60
      go to 999
60    call calibrate(a4,a5,a6,r3,r4,r5,r6,s3,s4,s5,s6,al4,a24,a34,a44,a5
     &4,a64)
      go to 49
999   write(1,'(/" This concludes the program."/)')
      write(1,'(/" Bye bye ! "/)')
      end
c
c
c     ********************** SUBROUTINE CALIBRATE *****************
c
ccccccccccccccccccccccccccccccccccccccccccccccccccccccccccccccccccccccc
c     The calibration routine uses four standards                      c
ccccccccccccccccccccccccccccccccccccccccccccccccccccccccccccccccccccccc
      subroutine calibrate(a4,a5,a6,r3,r4,r5,r6,s3,s4,s5,s6,al4,a24,a34,
     &a44,a54,a64)
      common /c1/lusig,ludac,fstart,fstop,fstep,power
      common /c2/nsize,me,ca
      common /c3/titlec,titlem
      real*4 pl4(181),pl5(181),pl6(181),p24(181)
      real*4 a4(181),a5(181),a6(181),r4(181),r5(181),r6(181),r3(181)
      real*4 al4(4),a24(4),a34(4),a44(4),a54(4),a64(4)
      real*4 x1,x2,x3,x4,y1,y2,y3,y4,x,y,f,fc,pi
      real*4 s3(181),s4(181),s5(181),s6(181)
      real*4 p25(181),p26(181),p34(181),p35(181),p36(181),p44(181)
      real*4 p13(181),p23(181),p33(181),p43(181)
      real*4 calvec1(8),vector1(8),calvect(8)
      real*4 p45(181),p46(181),sys(8,8),vector(9)
      real*4 c(4,4),d4(4),d5(4),d6(4),ft(4)
      complex*8 b4,b5,b6,b1,b2,b3,gam
```

```
      complex*8 gam1,gam2,gam3,gam4,gamm4,gamm5,gamm6,gamm3,ggaamm
      character*10 titlec,titlem
      character*10 tfname,tfnam3
      data tcyy/'y'/
      pi=3.141592
      if(ca.eq.0)go to 650
      write(1,'(/" The system is already calibrated. Do you want a new c
     &alibration ? (y/n) :_"/)')
      read(1,'(a1)')tans
      if(tans.eq.tcn)go to 660
      write(1,'(" Enter title :_")')
      read(1,'(a10)')titlec
ccccccccccccccccccccccccccccccccccccccccccccc
c     Frequency specification starts here.     c
ccccccccccccccccccccccccccccccccccccccccccccc
650   call fandp_set
      nsize=(fstop-fstart)/fstep+1
      write(1,'("The number of steps is :",i3)')nsize
c
      pi=3.141592
ccccccccccccccccccccccccccccccccccccccccccccccccccccccccccccccccccccc
c     Frequency specification ends.                                    c
c     Restore of standards' measurement data files starts here.  c
ccccccccccccccccccccccccccccccccccccccccccccccccccccccccccccccccccccc
      write(1,'(/" Prepare connection for calibration as follows:"/)')
      write(1,'(/" Connect load 1. Does it have offset?(1/0):_"/)')
      read(1,*)nans3
      if(nans3.eq.1)go to 852
      write(1,'(" Enter the value of gamma:_")')
      read(1,*)x
      read(1,*)y
      gam1=cmplx(x*cos(y*pi/180),x*sin(y*pi/180))
      write(1,*)gam1
      go to 853
852   write(1,'(" Enter the offset at 8 GHz in degrees:_")')
      read(1,*)adeg1
      write(1,'(" Enter the magnitude:_")')
      read(1,*)samag1
      fc=8.0
853   write(1,'(" Enter the file name:_")')
      read(1,'(a)')tfname
      call infile(nsize,p13,p14,p15,p16,tfname)
c
      write(1,'(/" Connect load 2. Does it have offset?(1/0):_"/)')
      read(1,*)nans4
      if(nans4.eq.1)go to 862
      write(1,'(" Enter the value of gamma:_")')
      read(1,*)x
      read(1,*)y
      gam2=cmplx(x*cos(y*pi/180),x*sin(y*pi/180))
      write(1,*)gam2
      go to 863
862   write(1,'(" Enter the offset at 8 GHz in degrees:_")')
      read(1,*)adeg2
      write(1,'(" Enter the magnitude:_")')
      read(1,*)samag2
      fc=8.0
863   write(1,'(" Enter the file name:_")')
      read(1,'(a)')tfname
      call infile(nsize,p23,p24,p25,p26,tfname)
```

```
c
      write(1,'(/" Connect offset short1. Enter offset in deg.:_"/)')
      read(1,*)adeg3
      write(1,'(/" Enter the magnitude      :_"/)')
      read(1,*)samag3
      write(1,'(/" Enter the center freq. fc:_"/)')
      read(1,*)fc
      write(1,'(" Enter the file name:_")')
      read(1,'(a)')tfname
      call infile(nsize,p33,p34,p35,p36,tfname)
c
c
      write(1,'(/" Connect offset short2. Enter offset in deg.:_"/)')
      read(1,*)adeg4
      write(1,'(/" Enter the magnitude      :_"/)')
      read(1,*)samag4
      write(1,'(/" Enter the center freq. fc:_"/)')
      read(1,*)fc
      write(1,'(" Enter the file name:_")')
      read(1,'(a)')tfname
      call infile(nsize,p43,p44,p45,p46,tfname)
ccccccccccccccccccccccccccccccccccccccccccccccccccccccccccccccccc
c     Restore of measurement files for the standards stops here. c
c     The diode calibration data file is restored next           c
ccccccccccccccccccccccccccccccccccccccccccccccccccccccccccccccccc
      write(1,'(" Enter the name of diode calibration file:_")')
      read(1,'(a10)')tfname
      write(1,'(" Restoring the diode calibration....")')
      call diode(nsize,a14,a24,a34,a44,a54,a64,tfname)
      write(1,'(" Calibrating the diode voltages....")')
ccccccccccccccccccccccccccccccccccccccccccccccccccccccccccccccccc
c     The measurement data files are corrected using the diode   c
c     calibration.                                               c
ccccccccccccccccccccccccccccccccccccccccccccccccccccccccccccccccc
      call caldiode(nsize,a14,a24,a34,a44,a54,a64,p13,p14,p15,p16)
      call caldiode(nsize,a14,a24,a34,a44,a54,a64,p23,p24,p25,p26)
      call caldiode(nsize,a14,a24,a34,a44,a54,a64,p33,p34,p35,p36)
      call caldiode(nsize,a14,a24,a34,a44,a54,a64,p43,p44,p45,p46)
633   write(1,'(" Enter the error approximation fraction(0 - 1):_")')
      read(1,*)ec1
      write(1,'(" Enter the level of approximation:_")')
      read(1,*)tol
cccc
ccccccccccccccccccccccccccccccccccccccccccccccccccccccccccccccccc
c     The calculation of the initial guess in the steepest descentc
c     method is dane at the center frequency fc.                 c
ccccccccccccccccccccccccccccccccccccccccccccccccccccccccccccccccc
      f=fc
      if(nans3.eq.1)go to 3728
      x1=real(gam1)
      y1=imag(gam1)
      go to 3729
3728  x1=samag1*cos(3.141592-(f/fc)*(adeg1*3.141592/180)*2)
      y1=samag1*sin(3.141592-(f/fc)*(adeg1*3.141592/180)*2)
3729  if(nans4.eq.1)go to 3725
      x2=real(gam2)
      y2=imag(gam2)
      go to 3724
3725  x2=samag2*cos(3.141592-(f/fc)*(adeg2*3.141592/180)*2)
      y2=samag2*sin(3.141592-(f/fc)*(adeg2*3.141592/180)*2)
```

```
3724  x3=samag3*cos(3.141592-(f/fc)*(adeg3*3.141592/180)*2)
      y3=samag3*sin(3.141592-(f/fc)*(adeg3*3.141592/180)*2)
      x4=samag4*cos(3.141592-(f/fc)*(adeg4*3.141592/180)*2)
      y4=samag4*sin(3.141592-(f/fc)*(adeg4*3.141592/180)*2)
      kk=int((f-fstart)/fstep+1)
      write(1,*)f
      write(1,*)kk
      c(1,1)=1.0
      c(2,1)=1.0
      c(3,1)=1.0
      c(4,1)=1.0
c
      c(1,2)=x1**2+y1**2
      c(2,2)=x2**2+y2**2
      c(3,2)=x3**2+y3**2
      c(4,2)=x4**2+y4**2
c
      c(1,3)=-2*x1
      c(2,3)=-2*x2
      c(3,3)=-2*x3
      c(4,3)=-2*x4
c
      c(1,4)=2*y1
      c(2,4)=2*y2
      c(3,4)=2*y3
      c(4,4)=2*y4
c
      d4(1)=p14(kk)
      d4(2)=p24(kk)
      d4(3)=p34(kk)
      d4(4)=p44(kk)
c
      d5(1)=p15(kk)
      d5(2)=p25(kk)
      d5(3)=p35(kk)
      d5(4)=p45(kk)
c
      d6(1)=p16(kk)
      d6(2)=p26(kk)
      d6(3)=p36(kk)
      d6(4)=p46(kk)
      nnk=4
      call linsys(c,d4,ft,nnk,ier)
      aa4=ft(1)
      ar4=ft(3)/ft(1)
      as4=ft(4)/ft(1)
      diff4=ft(2)-(ft(3)**2+ft(4)**2)/ft(1)
      write(1,'(" diff4 = ",e12.9)')diff4
      nnk=4
      call linsys(c,d5,ft,nnk,ier)
      aa5=ft(1)
      ar5=ft(3)/ft(1)
      as5=ft(4)/ft(1)
      diff5=ft(2)-(ft(3)**2+ft(4)**2)/ft(1)
      write(1,'(" diff5 = ",e12.9)')diff5
      nnk=4
      call linsys(c,d6,ft,nnk,ier)
      aa6=ft(1)
      ar6=ft(3)/ft(1)
      as6=ft(4)/ft(1)
```

```
      diff6=ft(2)-(ft(3)**2+ft(4)**2)/ft(1)
      write(1,'(" diff6 = ",e12.9)')diff6
      write(1,*)aa4,ar4,as4,aa5,ar5,as5,aa6,ar6,as6
cccccccccccccccccccccccccccccccccccccccccccccccccccccccccccccccccc
c     The steepest descent starts at the center frequency and  c
c     continues up and down in frequency over the whole range. c
cccccccccccccccccccccccccccccccccccccccccccccccccccccccccccccccccc
cccc
      nindic=0
      nindex=0
8812  zo1=ar4
      zo2=as4
      zo3=ar5
      zo4=as5
      zo5=ar6
      zo6=as6
      zo7=0.0
      zo8=0.0
631   k=int((fc-fstart)/fstep)+1
630   f=fstart+(k-1)*fstep
      write(1,*)f
      tol=1e-10
      frac=1.02
      decrf=0.5
      ec1=1.0
      if(nans3.eq.1)go to 728
      x1=real(gam1)
      y1=imag(gam1)
      go to 729
728   x1=samag1*cos(3.141592-(f/fc)*(adeg1*3.141592/180)*2)
      y1=samag1*sin(3.141592-(f/fc)*(adeg1*3.141592/180)*2)
729   if(nans4.eq.1)go to 725
      x2=real(gam2)
      y2=imag(gam2)
      go to 724
725   x2=samag2*cos(3.141592-(f/fc)*(adeg2*3.141592/180)*2)
      y2=samag2*sin(3.141592-(f/fc)*(adeg2*3.141592/180)*2)
724   x3=samag3*cos(3.141592-(f/fc)*(adeg3*3.141592/180)*2)
      y3=samag3*sin(3.141592-(f/fc)*(adeg3*3.141592/180)*2)
      x4=samag4*cos(3.141592-(f/fc)*(adeg4*3.141592/180)*2)
      y4=samag4*sin(3.141592-(f/fc)*(adeg4*3.141592/180)*2)
cccc
      z1=zo1
      z2=zo2
      z3=zo3
      z4=zo4
      z5=zo5
      z6=zo6
      z7=zo7
      z8=zo8
      alph=1.0
      nitter=20000
ccccccccccccccccccccccccccccccccccccccccccccccccccccccccccccccccccc
c     The method goes through at most 20000 iterations for each f.c
ccccccccccccccccccccccccccccccccccccccccccccccccccccccccccccccccccc
      do 4070,kk=1,nitter
c
      vector(1)=-p24(k)*(1+(x2**2+y2**2)*(z7**2+z8**2)-2*x2*z7+2*y2*z8)+
     &p14(k)*(1+(x2**2+y2**2)*(z1**2+z2**2)-2*x2*z1+2*y2*z2)
      vector(2)=-p34(k)*(1+(x3**2+y3**2)*(z7**2+z8**2)-2*x3*z7+2*y3*z8)+
```

```
     &p14(k)*(1+(x3**2+y3**2)*(z1**2+z2**2)-2*x3*z1-2*y3*z2)
      vector(3)=-p44(k)*(1+(x4**2+y4**2)*(z7**2+z8**2)-2*x4*z7+2*y4*z8)+
     &p14(k)*(1+(x4**2+y4**2)*(z1**2+z2**2)-2*x4*z1+2*y4*z2)
      vector(4)=-p25(k)*(1+(x2**2+y2**2)*(z7**2+z8**2)-2*x2*z7+2*y2*z8)+
     &p15(k)*(1+(x2**2+y2**2)*(z3**2+z4**2)-2*x2*z3+2*y2*z4)
      vector(5)=-p35(k)*(1+(x3**2+y3**2)*(z7**2+z8**2)-2*x3*z7+2*y3*z8)+
     &p15(k)*(1+(x3**2+y3**2)*(z3**2+z4**2)-2*x3*z3+2*y3*z4)
      vector(6)=-p45(k)*(1+(x4**2+y4**2)*(z7**2+z8**2)-2*x4*z7+2*y4*z8)+
     &p15(k)*(1+(x4**2+y4**2)*(z3**2+z4**2)-2*x4*z3+2*y4*z4)
      vector(7)=-p26(k)*(1+(x2**2+y2**2)*(z7**2+z8**2)-2*x2*z7+2*y2*z8)+
     &p16(k)*(1+(x2**2+y2**2)*(z5**2+z6**2)-2*x2*z5+2*y2*z6)
      vector(8)=-p36(k)*(1+(x3**2+y3**2)*(z7**2+z8**2)-2*x3*z7+2*y3*z8)+
     &p16(k)*(1+(x3**2+y3**2)*(z5**2+z6**2)-2*x3*z5+2*y3*z6)
      vector(9)=-p46(k)*(1+(x4**2+y4**2)*(z7**2+z8**2)-2*x4*z7+2*y4*z8)+
     &p16(k)*(1+(x4**2+y4**2)*(z5**2+z6**2)-2*x4*z5+2*y4*z6)
      ag1=0.0
      do 3649,kjkq=1,9
      ag1=ag1+vector(kjkq)**2
3649  continue
ccccccccccccccccccccccccccccccccccccccccccccccccccccc
c     The calculation of the gradient starts here.  c
ccccccccccccccccccccccccccccccccccccccccccccccccccccc
      aw1=2*vector(1)*p14(k)*(2*z1*(x2**2+y2**2)-2*x2)+2*vector(2)*p14(k
     &)*(2*z1*(x3**2+y3**2)-2*x3)+2*vector(3)*p14(k)*(2*z1*(x4**2+y4**2)
     &-2*x4)
      aw2=2*vector(1)*p14(k)*(2*z2*(x2**2+y2**2)+2*y2)+2*vector(2)*p14(k
     &)*(2*z2*(x3**2+y3**2)+2*y3)+2*vector(3)*p14(k)*(2*z2*(x4**2+y4**2)
     &+2*y4)
      aw3=2*vector(4)*p15(k)*(2*z3*(x2**2+y2**2)-2*x2)+2*vector(5)*p15(k
     &)*(2*z3*(x3**2-y3**2)-2*x3)+2*vector(6)*p15(k)*(2*z3*(x4**2+y4**2)
     &-2*x4)
      aw4=2*vector(4)*p15(k)*(2*z4*(x2**2+y2**2)+2*y2)+2*vector(5)*p15(k
     &)*(2*z4*(x3**2+y3**2)+2*y3)+2*vector(6)*p15(k)*(2*z4*(x4**2+y4**2)
     &+2*y4)
      aw5=2*vector(7)*p16(k)*(2*z5*(x2**2+y2**2)-2*x2)+2*vector(8)*p16(k
     &)*(2*z5*(x3**2+y3**2)-2*x3)+2*vector(9)*p16(k)*(2*z5*(x4**2+y4**2)
     &-2*x4)
      aw6=2*vector(7)*p16(k)*(2*z6*(x2**2+y2**2)+2*y2)+2*vector(8)*p16(k
     &)*(2*z6*(x3**2+y3**2)+2*y3)+2*vector(9)*p16(k)*(2*z6*(x4**2+y4**2)
     &-2*y4)
      aw7=-2*(p24(k)*vector(1)+p25(k)*vector(4)+p26(k)*vector(7))*(2*z7*
     &(x2**2+y2**2)-2*x2)-2*(p34(k)*vector(2)+p35(k)*vector(5)+p36(k)*ve
     &ctor(8))*(2*z7*(x3**2+y3**2)-2*x3)-2*(p44(k)*vector(3)+p45(k)*vect
     &or(6)+p46(k)*vector(9))*(2*z7*(x4**2+y4**2)-2*x4)
      aw8=-2*(p24(k)*vector(1)+p25(k)*vector(4)+p26(k)*vector(7))*(2*z8*
     &(x2**2+y2**2)+2*y2)-2*(p34(k)*vector(2)+p35(k)*vector(5)+p36(k)*ve
     &ctor(8))*(2*z8*(x3**2+y3**2)+2*y3)-2*(p44(k)*vector(3)+p45(k)*vect
     &or(6)+p46(k)*vector(9))*(2*z8*(x4**2+y4**2)+2*y4)
      awwo=(aw1**2+aw2**2+aw3**2+aw4**2+aw5**2+aw6**2+aw7**2+aw8**2)**0.
     &5
c      write(1,'(" awwo=",e12.9)')awwo
      if(awwo.eq.0.0)go to 4090
      aw1=aw1/awwo
      aw2=aw2/awwo
      aw3=aw3/awwo
      aw4=aw4/awwo
      aw5=aw5/awwo
      aw6=aw6/awwo
      aw7=aw7/awwo
      aw8=aw8/awwo
```

```
c
3333  aaph=-alph
      q1=z1+aaph*aw1
      q2=z2+aaph*aw2
      q3=z3+aaph*aw3
      q4=z4+aaph*aw4
      q5=z5+aaph*aw5
      q6=z6+aaph*aw6
      q7=z7+aaph*aw7
      q8=z8+aaph*aw8
ccccccccccccccccccccccccccccccccccccccccccccccccccccccccccccc
c     The new values of the equations are evaluated.    c
ccccccccccccccccccccccccccccccccccccccccccccccccccccccccccccc
      vector(1)=-p24(k)*(1+(x2**2+y2**2)*(q7**2+q8**2)-2*x2*q7+2*y2*q8)+
     &p14(k)*(1+(x2**2+y2**2)*(q1**2+q2**2)-2*x2*q1+2*y2*q2)
      vector(2)=-p34(k)*(1+(x3**2+y3**2)*(q7**2+q8**2)-2*x3*q7+2*y3*q8)+
     &p14(k)*(1+(x3**2+y3**2)*(q1**2+q2**2)-2*x3*q1+2*y3*q2)
      vector(3)=-p44(k)*(1+(x4**2+y4**2)*(q7**2+q8**2)-2*x4*q7+2*y4*q8)+
     &p14(k)*(1+(x4**2+y4**2)*(q1**2+q2**2)-2*x4*q1+2*y4*q2)
      vector(4)=-p25(k)*(1+(x2**2+y2**2)*(q7**2+q8**2)-2*x2*q7+2*y2*q8)+
     &p15(k)*(1+(x2**2+y2**2)*(q3**2+q4**2)-2*x2*q3+2*y2*q4)
      vector(5)=-p35(k)*(1+(x3**2+y3**2)*(q7**2+q8**2)-2*x3*q7+2*y3*q8)+
     &p15(k)*(1+(x3**2+y3**2)*(q3**2+q4**2)-2*x3*q3+2*y3*q4)
      vector(6)=-p45(k)*(1+(x4**2+y4**2)*(q7**2+q8**2)-2*x4*q7+2*y4*q8)+
     &p15(k)*(1+(x4**2+y4**2)*(q3**2+q4**2)-2*x4*q3+2*y4*q4)
      vector(7)=-p26(k)*(1+(x2**2+y2**2)*(q7**2+q8**2)-2*x2*q7+2*y2*q8)+
     &p16(k)*(1+(x2**2+y2**2)*(q5**2+q6**2)-2*x2*q5+2*y2*q6)
      vector(8)=-p36(k)*(1+(x3**2+y3**2)*(q7**2+q8**2)-2*x3*q7+2*y3*q8)+
     &p16(k)*(1+(x3**2+y3**2)*(q5**2+q6**2)-2*x3*q5+2*y3*q6)
      vector(9)=-p46(k)*(1+(x4**2+y4**2)*(q7**2+q8**2)-2*x4*q7+2*y4*q8)+
     &p16(k)*(1+(x4**2+y4**2)*(q5**2+q6**2)-2*x4*q5+2*y4*q6)
      ag3=0.0
      do 3659,kjkq=1,9
      ag3=ag3+vector(kjkq)**2
3659  continue
      if(ag3.lt.tol)go to 4090
      if((ag1-ag3).lt.0.0)go to 4027
ccccccccccccccccccccccccccccccccccccccccccccccccccccccccccccc
c     Only if the new equations values are smaller than the old ones, c
c     the variables are updated. This way, the new set of variables   c
c     moves in the direction of the minimum with variable step size.  c
ccccccccccccccccccccccccccccccccccccccccccccccccccccccccccccc
      z1=q1
      z2=q2
      z3=q3
      z4=q4
      z5=q5
      z6=q6
      z7=q7
      z8=q8
      alph=1.0
      go to 4070
4027  alph=alph*decrf
      if(alph.lt.0.0000001)go to 4090
      go to 3333
4070  continue
4090  write(1,'(" ag3=",2x,e12.9,2x,"nitter=",i6)')ag3,kk
      write(1,'(" z1-8:",(8f12.8))')z1,z2,z3,z4,z5,z6,z7,z8
      do 4050,kik=1,9
      write(1,'(2x,e12.9,"_")')vector(kik)
```

```
4050  continue
ccccccccccccccccccccccccccccccccccccccccccccccccccccccccccccccccccccccc
c     After the method converges, the constants are stored in arrays c
c     and used as initial guess for the next frequency.              c
ccccccccccccccccccccccccccccccccccccccccccccccccccccccccccccccccccccccc
2223  a4(k)=pl4(k)
      r4(k)=z1
      s4(k)=z2
      r3(k)=z7
      s3(k)=z8
      a5(k)=pl5(k)
      r5(k)=z3
      s5(k)=z4
      a6(k)=pl6(k)
      r6(k)=z5
      s6(k)=z6
c
      zo1=z1
      zo2=z2
      zo3=z3
      zo4=z4
      zo5=z5
      zo6=z6
      zo7=z7
      zo8=z8
      if(nindic.eq.0)go to 8800
      k=k-1
      if(k.ge.1)go to 630
      go to 8811
8800  k=k+1
      if(k.le.nsize)go to 630
      nindic=1
      go to 8812
8811  ca=1
      write(1,'(/" The calibration procedure is completed. "/)')
      write(1,'(" Automatic calibration backup: ")')
      write(1,'(" Enter the name of the destination file:_")')
      read(1,'(a10)')tfnam3
ccccccccccccccccccccccccccccccccccccccccccccccccccccccccccccccccccccccc
c     The calibration data is saved in a file via the save routine   c
ccccccccccccccccccccccccccccccccccccccccccccccccccccccccccccccccccccccc
      call save(nsize,a3,r3,s3,a4,r4,s4,a5,r5,s5,a6,r6,s6,tfnam3,a14,a24
     &,a34,a44,a54,a64)
660   return
      end
c
c
c     ************************ SUBROUTINE COMMAND ********************
c
      subroutine command(task)
      write(1,'(" Command ? : _")')
      read(1,'(a4)')task
      return
      end
c
c
c     ******************* SUBROUTINE START_PROMPT ********************
c
      subroutine start_prompt
      write(1,'("Welcome to SIXPORT !")')
```

```
      write(1,'(/"Version date: May 4, 1987"/)')
      return
      end
c
c
c     ******************** SUBROUTINE FandP_SET ************************
c
      subroutine fandp_set
      common /c1/lusig,ludac,fstart,fstop,fstep,power
2000  write(1,'(/"Enter frequency range as start,stop,step(GHz):_"/)')
      read(1,*)fstart,fstop,fstep
      if((fstop-fstart)/fstep.le.181)go to 2010
      write(1,'(/"There are more than 181 steps. Try again !"/)')
      go to 2000
2010  write(1,'(/"Enter the power level in dBm :_"/)')
      read(1,*)power
      return
      end
c
c
c     ******************** SUBROUTINE END_PROMPT *********************
c
      subroutine end_prompt
      write(1,'(/"This concludes the program. Bye bye !"/)')
      return
      end
c
c
c     ********************** SUBROUTINE INFILE ***************************
c
      subroutine infile(nsize,p13,p14,p15,p16,tfname)
      real*4 p13(181),p14(181),p15(181),p16(181)
      character*10 tfname
      open(10,file=tfname)
      k=1
901   read(10,'(4e12.9)',end=902,err=960)p3,p4,p5,p6
902   p13(k)=abs(p3)
      p14(k)=abs(p4)
      p15(k)=abs(p5)
      p16(k)=abs(p6)
      k=k+1
      if(k.le.nsize)go to 901
      close(10)
960   return
      end
c
c
c     ******************** SUBROUTINE MULTIPLY ***************************
c
      subroutine multiply(sys,vector,calvect,nnn)
      real*4 sys(11,11),vector(11),calvect(11)
      do 8999,k=1,nnn
      sum=0
      do 8989,l=1,nnn
      sum=sum+sys(k,l)*vector(l)
8989  continue
      calvect(k)=sum
c      write(6,'(" vector1(",i2,") = ",e12.9)')k,calvect(k)
8999  continue
      return
```

```
      end
c
c
c     ********************* SUBROUTINE LINSYS ***************************
c
      subroutine linsys(c,d4,ft,nnk,ier)
      real*4 c(4,4),d4(4),ft(4),ci(4,5)
      do 101,k=1,nnk
      do 102,l=1,nnk
      ci(k,l)=c(k,l)
      write(1,'(3x,e12.9,"_")')ci(k,l)
102   continue
      ci(k,nnk+1)=d4(k)
      write(1,'(3x,e12.9)')ci(k,l)
101   continue
      do 108,k=1,nnk
      l=1
109   if(ci(k,l).eq.0.0)go to 103
      atemp=ci(k,l)
      go to 104
103   l=l+1
      if(l.le.nnk)go to 109
104   do 105,i=1,nnk+1
      ci(k,i)=ci(k,i)/atemp
105   continue
      j=1
110   if(j.eq.k)go to 106
      atempl=ci(j,l)
      do 107,m=1,nnk+1
      ci(j,m)=ci(j,m)-ci(k,m)*atempl
107   continue
106   j=j+1
      if(j.le.nnk)go to 110
108   continue
      do 111,k=1,nnk
      do 112,i=1,nnk
      if(ci(i,k).eq.0.0)go to 112
      ft(k)=ci(i,nnk+1)
112   continue
111   continue
      return
      end
c
c
c     ********************** SUBROUTINE SAVE ************************
c
      subroutine save(nsize,a3,r3,s3,a4,r4,s4,a5,r5,s5,a6,r6,s6,tfname,a
     &l4,a24,a34,a44,a54,a64)
      common /c1/lusig,ludac,fstart,fstop,fstep,power
      real*4 a3,r3(*),s3(*),a4(*),r4(*),s4(*),a5(*),r5(*),s5(*)
      real*4 al4(*),a24(*),a34(*),a44(*),a54(*),a64(*)
      real*4 a6(*),r6(*),s6(*)
      character*10 tfname
      open(10,file=tfname)
      write(10,'(4f8.4)')fstart,fstop,fstep,power
      k=1
4191  write(10,'(4e12.9)')al4(1),al4(2),al4(3),al4(4)
      write(10,'(4e12.9)')a24(1),a24(2),a24(3),a24(4)
      write(10,'(4e12.9)')a34(1),a34(2),a34(3),a34(4)
      write(10,'(4e12.9)')a44(1),a44(2),a44(3),a44(4)
```

```
      write(10,'(4e12.9)')a54(1),a54(2),a54(3),a54(4)
      write(10,'(4e12.9)')a64(1),a64(2),a64(3),a64(4)
      write(10,'(3e12.9)')r3(k),s3(k),a4(k)
      write(10,'(5e12.9)')r4(k),s4(k),a5(k),r5(k),s5(k)
      write(10,'(3e12.9)')a6(k),r6(k),s6(k)
4902  k=k+1
      if(k.le.nsize)go to 4191
4196  close(10)
4960  return
      end
c
c
c  ************************* SUBROUTINE DIODE *************************
c
      subroutine diode(nsize,a14,a24,a34,a44,a54,a64,tfname)
      real*4 a14(4),a24(4),a34(4),a44(4),a54(4),a64(4)
      character*10 tfname
      open(10,file=tfname)
      read(10,'(6e12.9)',end=5604,err=5609)aa1,aa2,aa3,aa4,aa5,aa6
5604  a14(1)=aa1
      a24(1)=aa2
      a34(1)=aa3
      a44(1)=aa4
      a54(1)=aa5
      a64(1)=aa6
      read(10,'(6e12.9)',end=5605,err=5609)aa1,aa2,aa3,aa4,aa5,aa6
5605  a14(2)=aa1
      a24(2)=aa2
      a34(2)=aa3
      a44(2)=aa4
      a54(2)=aa5
      a64(2)=aa6
      read(10,'(6e12.9)',end=5606,err=5609)aa1,aa2,aa3,aa4,aa5,aa6
5606  a14(3)=aa1
      a24(3)=aa2
      a34(3)=aa3
      a44(3)=aa4
      a54(3)=aa5
      a64(3)=aa6
      read(10,'(6e12.9)',end=5607,err=5609)aa1,aa2,aa3,aa4,aa5,aa6
5607  a14(4)=aa1
      a24(4)=aa2
      a34(4)=aa3
      a44(4)=aa4
      a54(4)=aa5
      a64(4)=aa6
      close(10)
      write(1,'(4e12.9)')a14(1),a14(2),a14(3),a14(4)
      write(1,'(4e12.9)')a24(1),a24(2),a24(3),a24(4)
      write(1,'(4e12.9)')a34(1),a34(2),a34(3),a34(4)
      write(1,'(4e12.9)')a44(1),a44(2),a44(3),a44(4)
      write(1,'(4e12.9)')a54(1),a54(2),a54(3),a54(4)
      write(1,'(4e12.9)')a64(1),a64(2),a64(3),a64(4)
5609  return
      end
c
c
c   ************************* SUBROUTINE CALDIODE ********************
c
      subroutine caldiode(nsize,a14,a24,a34,a44,a54,a64,p13,p14,p15,p16)
```

```
      real*4 p13(181),p14(181),p15(181),p16(181)
      real*4 a14(4),a24(4),a34(4),a44(4),a54(4),a64(4)
      character*10 tfname
      dc 6650,kid=1,nsize
      p1333333=a14(1)*p13(kid)**(1+a24(1)*p13(kid)+a34(1)*p13(kid)**2+a4
     &4(1)*p13(kid)**3+a54(1)*p13(kid)**4+a64(1)*p13(kid)**5)
      p1444444=a14(2)*p14(kid)**(1+a24(2)*p14(kid)+a34(2)*p14(kid)**2+a4
     &4(2)*p14(kid)**3+a54(2)*p14(kid)**4+a64(2)*p14(kid)**5)
      p1555555=a14(3)*p15(kid)**(1+a24(3)*p15(kid)+a34(3)*p15(kid)**2+a4
     &4(3)*p15(kid)**3+a54(3)*p15(kid)**4+a64(3)*p15(kid)**5)
      p1666666=a14(4)*p16(kid)**(1+a24(4)*p16(kid)+a34(4)*p16(kid)**2+a4
     &4(4)*p16(kid)**3+a54(4)*p16(kid)**4+a64(4)*p16(kid)**5)
      p14(kid)=p1444444/p1333333
      p15(kid)=p1555555/p1333333
      p16(kid)=p1666666/p1333333
      write(1,'(4e12.9)')p1333333,p1444444,p1555555,p1666666
      write(1,'(3e12.9)')p14(kid),p15(kid),p16(kid)
      write(1,'(" ")')
6650  continue
      write(1,'("************")')
      return
      end
```

```
ftn7x
$files(0,1)
      program pintl
      common /c1/lusig,ludac,fstart,fstop,fstep,power
      character*12 tfname
      real*4 p13,p14,p15,p16
      lusig=12
      ludac=47
      call fandp_set
      nsize=int((fstop-fstart)/fstep)+1
      write(1,*)nsize
      write(1,'(" Enter the name of the file to be created:_")')
      read(1,'(a12)')tfname
      write(1,'("Do you want to account for residual voltages?:(1/0)")')
      read(1,*)nres
      k=1
      pow=power
      f=fstart
6458  do 6454,kik=1,15
6455  call sweep(f,pow,kritter)
      call dacvolt(p1,p2,p3,p4)
6454  continue
      kritter=0
      if(nres.eq.0)go to 6751
      f123=8
      call sweep(f123,pow,kritter)
      write(12,'("rf0")')
      yy=1.0
6752  yy=yy+1.0
      if(yy.le.600000)go to 6752
      call dacvolt(p10,p20,p30,p40)
      write(12,'("rf1")')
6751  open(10,file=tfname)
645   pow=power
6457  call sweep(f,pow,kritter)
c      if(nres.eq.0)go to 6729
c      write(12,'("rf0")')
c      call dacvolt(p10,p20,p30,p40)
c      write(12,'("rf1")')
6729  call dacvolt(p1,p2,p3,p4)
6456  p13=p4-nres*p40
      p14=p1-nres*p10
      p15=p2-nres*p20
      p16=p3-nres*p30
c6456  p13=p4-p40
c      p14=p1-p10
c      p15=p2-p20
c      p16=p3-p30
      write(10,'(4e12.9)')p13,p14,p15,p16
      write(1,'(4e12.9)')p13,p14,p15,p16
671   f=f+fstep
      k=k+1
      if(k.le.nsize)go to 645
      close(10)
      call sweep(f,pow)
      end
c
c
c     ******************** SUBROUTINE FandP_SET ************************
```

```
c
      subroutine fandp_set
      common /c1/lusig,ludac,fstart,fstop,fstep,power
2000  write(1,'(/"Enter frequency range as start,stop,step(GHz):_"/)')
      read(1,*)fstart,fstop,fstep
      if(int((fstop-fstart)/fstep+1).le.181)go to 2010
      write(1,'(/"There are more than 181 steps. Try again !"/)')
      go to 2000
2010  write(1,'(/"Enter the power level in dBm :_"/)')
      read(1,*)power
      return
      end
c
c
c     ******************** SUBROUTINE END_PROMPT ********************
c
      subroutine end_prompt
      write(1,'(/"This concludes the program. Bye bye !"/)')
      return
      end
c
c
c
c     ******************** SUBROUTINE DACVOLT ************************
c
      subroutine dacvolt(p1,p2,p3,p4)
      common /c1/lusig,ludac,fstart,fstop,fstep,power
c      ntp=10
      ntp=20
      nchan=0
c      do 4545,kase=1,3
c      call dacunit(ntp,p1,nchan)
c      call wait
c4545  continue
      call dacunit(ntp,p1,nchan)
      call wait
      call dacunit(ntp,p1,nchan)
      call wait
      nchan=10
c      do 4546,kase=1,3
c      call dacunit(ntp,p2,nchan)
c      call wait
c4546  continue
      call dacunit(ntp,p2,nchan)
      call wait
      nchan=1
c      do 4547,kase=1,3
c      call dacunit(ntp,p3,nchan)
c      call wait
c4547  continue
      call dacunit(ntp,p3,nchan)
      call wait
      nchan=11
c      do 4548,kase=1,3
c      call dacunit(ntp,p4,nchan)
c      call wait
c4548  continue
      call dacunit(ntp,p4,nchan)
      call wait
      rofp4=p1/p4
```

```
      rofp5=p2/p4
      rofp6=p3/p4
      write(1,'(" p 4,5,6,3:",2x,e12.9,2x,e12.9,2x,e12.9,2x,e12.9)')p1,p
     &2,p3,p4
      write(1,'("rofpees 4,5,6",2x,e12.9,2x,e12.9,2x,e12.9)')rofp4,rofp5
     &,rofp6
      return
      end
c
c
c     ********************* SUBROUTINE SWEEP ************************
c
      subroutine sweep(f,pow,kritter)
      common /c1/lusig,ludac,fstart,fstop,fstep,power
c      write(1,'(" Change the frequency to",f5.2," GHz")')f
c      write(1,'(" When ready, press return_")')
c      read(1,'(a1)')tans
      kritter=kritter+1
      if(f.gt.fstop)go to 3020
      if(f.gt.fstart)go to 3000
      if(kritter.gt.1)go to 3000
      write(lusig,'("p1",f5.2,"dmfa",f5.3,"gz")')pow,fstart
      write(lusig,'("fb",f5.3,"gzst50ms")')fstop
3000  write(lusig,'("cw",f5.3,"gzp1",f5.2,"dm")')f,pow
      go to 3040
3020  write(lusig,'("fa",f5.3,"gzfb",f5.3,"gzst50ms")')fstart,fstop
3040  return
      end
c
c
c     ******************** SUBROUTINE DACUNIT ************************
c
      subroutine dacunit(ntp,voltav,nchan)
      dimension ameas(20)
c      dimension ameas(20)
c      character*240 array
cc      character*120 array1
c      write(47,'("VT2AI",i3,"VW60")')nchan
      write(47,'("AI",i3,"VW60")')nchan
c      write(47,'("AC",i3,"VT4VF1VS1VN",i3,"VT3VW100VS")')nchan,ntp
c     write(47,'("AC",i3,"VT4VF1VS1VN",i3,"VT3VW60VS")')nchan,ntp
cc      write(47,'("AC",i3,"VT4VF1VS1VN",i3,"VT3VW60VS")')nchan,ntp
c      read(47,'(a240)')array
cc      write(47,'("AC",i3,"VT4VF1VS1VN",i3,"VT3VW60VS")')nchan,ntp
      read(47,*)voltav
      sum=0.0
      do 7010,kiki=1,5
      write(47,'("AI",i3,"VW60")')nchan
      read(47,*)ameas(kiki)
      sum=sum+ameas(kiki)
7010  continue
      voltav=sum/5.0
c      read(47,'(a120)')array1
c      ipos=0
c      j=1
c7010  call convert(array,value,ipos)
cc      call convert(array1,value1,ipos)
c      ameas(j)=value
cc      ameas(j+10)=value1
c      j=j+1
```

```
c      ipos=ipos+12
c      if(j.eq.21)go to 7099
c      go to 7010
c7099  call avvalue(ameas,voltav,ntp)
      return
      end
c
c
c     ********************** SUBROUTINE CONVERT *********************
c
      subroutine convert(array,value,ipos)
      real value
      dimension mag(7)
      character*240 array
      k=ipos+1
      msign=ichar(array(k:k))
      mag(6)=ichar(array(k+1:k+1))-48
      do i=1,5
      m=k+2+i
      mag(6-i)=ichar(array(m:m))-48
      end do
      amagn=0
      l=6
6005  amagn=10*amagn+mag(l)
      l=l-1
      if(l.eq.0)go to 6010
      go to 6005
6010  expsgn=ichar(array(k+9:k+9))
      expon=ichar(array(k+10:k+10))-48
      if(expsgn.eq.45)go to 6000
      if(msign.eq.45)value=-amagn*10**(expon-5)
      value=amagn*10**(expon-5)
      go to 6020
6000  if(msign.eq.45)value=-amagn*10**(-expon-5)
      value=amagn*10**(-expon-5)
6020  return
      end
c
c
c     ********************** SUBROUTINE AVVALUE *********************
c
      subroutine avvalue(ameas,voltav,ntp)
c      dimension ameas(10)
      dimension ameas(20)
      voltav=0.
      kkl=0
      do i=11,ntp
      voltav=voltav+ameas(i)
      kkl=kkl+1
      end do
      voltav=voltav/kkl
      return
      end
c
c
c     ********************** SUBROUTINE WAIT ************************
c
      subroutine wait
      y=1.0
8999  y=y+1.0
```

```
      if(y.gt.1000.0)go to 8000
      go to 8999
8000  return
      end
```

```
ftn7x,s
$files(0,1)
      program sixportest2m
      common /c1/lusig,ludac,fstart,fstop,fstep,power
      common /c2/nsize,me,ca
      common /c3/titlec,titlem
      real*4 refl1(141),refl2(141)
      real*4 r4(141),r5(141),r6(141),s4(141),s5(141),s6(141)
      real*4 a4(141),a5(141),a6(141),r3(141),s3(141)
      real*4 a14(4),a24(4),a34(4),a44(4),a54(4),a64(4)
      complex*8 b4,b5,b6,b1,b2,b3
      integer lusig,ludac,nsize
      real power,fstart,fstop,fstep
      character*10 titlec,titlem
      data the/'help'/,tcal/'cal'/,tame/'meas'/,tali/'list'/,tpl/'plot'/
      data tq/'quit'/
      call start_prompt
      lusig=12
      ludac=47
      me=0
      ca=0
49    call command(task)
      if(task.eq.the)go to 50
      if(task.eq.tcal)go to 60
      if(task.eq.tame)go to 70
      if(task.eq.tali)go to 80
      if(task.eq.tpl)go to 90
      if(task.eq.tq)go to 999
      go to 49
50    call help
      go to 49
60    call calibrate(a14,a24,a34,a44,a54,a64,a4,a5,a6,r3,r4,r5,r6,s3,s4,
     &s5,s6)
      go to 49
70    call measure(refl1,refl2,a14,a24,a34,a44,a54,a64,a4,a5,a6,r3,r4,r5
     &,r6,s3,s4,s5,s6)
      go to 49
80    call list(refl1,refl2)
      go to 49
90    call plot(refl1,refl2,r3,r4,r5,r6,s3,s4,s5,s6)
      go to 49
999   write(1,'(/" This concludes the program."/)')
      write(1,'(/" Bye bye ! "/)')
      end
c
c
c     ************************ SUBROUTINE HELP ************************
c
      subroutine help
      return
      end
c
c
c     ************************ SUBROUTINE CALIBRATE *******************
c
      subroutine calibrate(a14,a24,a34,a44,a54,a64,a4,a5,a6,r3,r4,r5,r6,
     &s3,s4,s5,s6)
      common /c1/lusig,ludac,fstart,fstop,fstep,power
      common /c2/nsize,me,ca
      common /c3/titlec,titlem
```

```
      real*4 a4(141),a5(141),a6(141),r4(141),r5(141),r6(141),r3(141)
      real*4 a14(4),a24(4),a34(4),a44(4),a54(4),a64(4)
      real*4 x1,x2,x3,x4,y1,y2,y3,y4,x,y,f,fc,pi
      real*4 s3(141),s4(141),s5(141),s6(141)
      character*10 titlec,titlem
      character*10 tfnam3
      character*10 tfname,tfname1,tfname2,tfname3,tfname4
      pi=3.141592
      write(1,'(" Enter title :_")')
      read(1,'(a10)')titlec
      ca=1
      write(1,'(" Restoring the calibration constants.....")')
c      write(1,'(" Enter the name of the diode calibration file:_")')
c      read(1,'(a10)')tfname1
      write(1,'(" Enter the name of the file for restore:_")')
      read(1,'(a10)')tfnam3
      call restore(nsize,a14,a24,a34,a44,a54,a64,r3,s3,a4,r4,s4,a5,r5,s5
     &,a6,r6,s6,tfnam3)
      write(1,'(" Do you want to update the calibration ?(1/0):_")')
      read(1,*)nnas
      if(nnas.eq.0)go to 9495
      write(1,'(" Enter the name of the good load file:_")')
      read(1,'(a10)')tfname
      call infile(nsize,a4,a5,a6,tfname)
9495  write(1,'(/" The calibration procedure is completed. "/)')
      return
      end
c
c
c     ************************ SUBROUTINE MEASURE ********************
c
      subroutine measure(refl1,refl2,a14,a24,a34,a44,a54,a64,a4,a5,a6,r3
     &,r4,r5,r6,s3,s4,s5,s6)
      common /c1/lusig,ludac,fstart,fstop,fstep,power
      common /c2/nsize,me,ca
      common /c3/titlec,titlem
      real*4 a4(141),a5(141),a6(141),r3(141),r4(141),r5(141),r6(141)
      real*4 a14(4),a24(4),a34(4),a44(4),a54(4),a64(4)
      real*4 delta4,delta5,delta6,eta4,eta5,eta6,tau4,tau5,tau6,eps4
      real*4 alpha11,alpha12,alpha21,alpha22,beta1,beta2,x,y,eps5,eps6
      real*4 f,fc,pi
      real*4 refl1(141),refl2(141),p4(141),p5(141),p6(141)
      real*4 s3(141),s4(141),s5(141),s6(141),p3(141)
      real*4 aitx(2),aity(2)
      complex*8 b1,b2,b3,b4,b5,b6,gam,gamm
      character*10 tfname,titlem,titlec
      data tcyy/'y'/
      if(ca.eq.0)go to 777
      write(1,'(" Enter title:_")')
      read(1,'(a10)')titlem
c     write(1,'(" Specify distance from reference plane of DUT:_")')
c     read(1,*)dist
c      nrep=0
c703   k=1
c
706   write(1,'("Do you want to restore a file ? (y/n):_")')
      read(1,'(a1)')tans
      if(tans.ne.tcyy)go to 701
      write(1,'(" Enter the file name:_")')
      read(1,'(a)')tfname
```

```
      call infile(nsize,p3,p4,p5,p6,tfname)
      go to 703
701   if(me.eq.0)go to 750
      write(1,'(/" Measurement already performed .  Do you want a new me
     &asurement ? (y/n):_"/)')
      read(1,'(a1)')tans
      if(tans.eq.tcyy)go to 750
      go to 778
750   write(1,'(" Connect device under test. When ready, press return._"
     &)')
      read(1,'(a1)')tans
c      f=fstart
c      k=1
c700   call sweep(f)
c      call dacvolt(pp1,pp2,pp3,pp4)
c      p4(k)=pp1/pp4
c      p5(k)=pp2/pp4
c      p6(k)=pp3/pp4
c      f=f+fstep
c      write(6,'(/" p 4,5,6:",2x,e12.9,2x,e12.9,2x,e12.9)')p4(k),p5(k),p6
c     &(k)
c      k=k+1
c      if(k.le.nsize)go to 700
c      call sweep(f)
703   nindicm=0
      write(1,'(" Enter the center frequency:_")')
      read(1,*)fc
c      fc=8.0
c703   k=1
      k=int((fc-fstart)/fstep+1)
      write(1,'(" Enter the threshold for steepest descend:_")')
      read(1,*)atol
      write(1,'(" Enter the threshold of error:_")')
      read(1,*)cra
c      write(1,'(" Enter the number of iterations:_")')
c      read(1,*)nitter
c720   write(6,'(" a4,a5,a6:",2x,e12.9,2x,e12.9,2x,e12.9)')a4(k),a5(k),a6
c     &(k)
c      write(6,'(" r4,r5,r6:",2x,e12.9,2x,e12.9,2x,e12.9)')r4(k),r5(k),r6
c     &(k)
c      write(6,'(" s4,s5,s6:",2x,e12.9,2x,e12.9,2x,e12.9)')s4(k),s5(k),s6
c     &(k)
c      write(6,'(" r3,s3:",2x,e12.9,2x,e12.9)')r3(k),s3(k)
c720   delta4=p4(k)*(r3(k)**2+s3(k)**2)-a4(k)*(r4(k)**2+s4(k)**2)
720   f=fstart+(k-1)*fstep
      write(1,*)f
c
      p133kid3=p3(k)
      p144kid4=p4(k)
      p155kid5=p5(k)
      p166kid6=p6(k)
      p1333333=a14(1)*p133kid3**(1+a24(1)*p133kid3+a34(1)*p133kid3**2+a4
     &4(1)*p133kid3**3+a54(1)*p133kid3**4+a64(1)*p133kid3**5)
      p1444444=a14(2)*p144kid4**(1+a24(2)*p144kid4+a34(2)*p144kid4**2+a4
     &4(2)*p144kid4**3+a54(2)*p144kid4**4+a64(2)*p144kid4**5)
      p1555555=a14(3)*p155kid5**(1+a24(3)*p155kid5+a34(3)*p155kid5**2+a4
     &4(3)*p155kid5**3+a54(3)*p155kid5**4+a64(3)*p155kid5**5)
      p1666666=a14(4)*p166kid6**(1+a24(4)*p166kid6+a34(4)*p166kid6**2+a4
     &4(4)*p166kid6**3+a54(4)*p166kid6**4+a64(4)*p166kid6**5)
      p14=p1444444/p1333333
```

```
      p15=p1555555/p1333333
      p16=p1666666/p1333333
      p4(k)=p14
      p5(k)=p15
      p6(k)=p16
      delta4=p4(k)*(r3(k)**2+s3(k)**2)-a4(k)*(r4(k)**2+s4(k)**2)
      delta5=p5(k)*(r3(k)**2+s3(k)**2)-a5(k)*(r5(k)**2+s5(k)**2)
      delta6=p6(k)*(r3(k)**2+s3(k)**2)-a6(k)*(r6(k)**2+s6(k)**2)
c      write(6,'(" delta 4,5,6:",2x,e12.9,2x,e12.9,2x,e12.9)')delta4,delt
c     &a5,delta6
      eta4=2*(r4(k)*a4(k)-r3(k)*p4(k))
      eta5=2*(r5(k)*a5(k)-r3(k)*p5(k))
      eta6=2*(r6(k)*a6(k)-r3(k)*p6(k))
c      write(6,'(" eta 4,5,6:",2x,e12.9,2x,e12.9,2x,e12.9)')eta4,eta5,eta
c     &6
      eps4=2*(s3(k)*p4(k)-s4(k)*a4(k))
      eps5=2*(s3(k)*p5(k)-s5(k)*a5(k))
      eps6=2*(s3(k)*p6(k)-s6(k)*a6(k))
c      write(6,'(" eps 4,5,6:",2x,e12.9,2x,e12.9,2x,e12.9)')eps4,eps5,eps
c     &6
      tau4=a4(k)-p4(k)
      tau5=a5(k)-p5(k)
      tau6=a6(k)-p6(k)
c      write(6,'(" tau 4,5,6:",2x,e12.9,2x,e12.9,2x,e12.9)')tau4,tau5,tau
c     &6
      alpha11=eta4*delta5-eta5*delta4
      alpha12=eps4*delta5-eps5*delta4
      alpha21=eta4*delta6-eta6*delta4
      alpha22=eps4*delta6-eps6*delta4
c      write(6,'(" alpha 11,12,21,22:",2x,e12.9,2x,e12.9,2x,e12.9,2x,e12.
c     &9)')alpha11,alpha12,alpha21,alpha22
      beta1=tau4*delta5-tau5*delta4
      beta2=tau4*delta6-tau6*delta4
c      write(6,'(" beta 1,2:",2x,e12.9,2x,e12.9)')beta1,beta2
      ref11(k)=(beta1*alpha22-beta2*alpha12)/(alpha11*alpha22-alpha12*al
     &pha21)
      ref12(k)=(beta2*alpha11-beta1*alpha21)/(alpha11*alpha22-alpha12*al
     &pha21)
      x=ref11(k)
      y=ref12(k)
      asmag4=(tau4-x*eta4-y*eps4)/delta4
      asmag5=(tau5-x*eta5-y*eps5)/delta5
      asmag6=(tau6-x*eta6-y*eps6)/delta6
      write(1,*)x,y
      write(1,*)asmag4,asmag5,asmag6
      x2=x
      y2=y
      con24=a4(k)*(1+(r4(k)**2+s4(k)**2)*(x2**2+y2**2)-2*r4(k)*x2+2*s4(k
     &)*y2)-p4(k)*(1+(r3(k)**2+s3(k)**2)*(x2**2+y2**2)-2*r3(k)*x2+2*s3(k
     &)*y2)
      con25=a5(k)*(1+(r5(k)**2+s5(k)**2)*(x2**2+y2**2)-2*r5(k)*x2+2*s5(k
     &)*y2)-p5(k)*(1+(r3(k)**2+s3(k)**2)*(x2**2+y2**2)-2*r3(k)*x2+2*s3(k
     &)*y2)
      con26=a6(k)*(1+(r6(k)**2+s6(k)**2)*(x2**2+y2**2)-2*r6(k)*x2+2*s6(k
     &)*y2)-p6(k)*(1+(r3(k)**2+s3(k)**2)*(x2**2+y2**2)-2*r3(k)*x2+2*s3(k
     &)*y2)
      write(1,'(" con4,5,6:",2x,e12.9,2x,e12.9,2x,e12.9)')con24,con25,co
     &n26
      f=fstart+(k-1)*fstep
      if(f.eq.fc)go to 6667
```

```
      acon456=con24**2+con25**2+con26**2
      amagnit=(x**2+y**2)**0.5
      if(acon456.gt.atol)go to 6664
      if(amagnit.gt.1.1)go to 6664
      go to 6667
6664  v4=p4(k)*(r3(k)**2+s3(k)**2)-a4(k)*(r4(k)**2+s4(k)**2)
      v5=p5(k)*(r3(k)**2+s3(k)**2)-a5(k)*(r5(k)**2+s5(k)**2)
      v6=p6(k)*(r3(k)**2+s3(k)**2)-a6(k)*(r6(k)**2+s6(k)**2)
      vv4=r4(k)*a4(k)-r3(k)*p4(k)
      vv5=r5(k)*a5(k)-r3(k)*p5(k)
      vv6=r6(k)*a6(k)-r3(k)*p6(k)
      x4=-vv4/v4
      x5=-vv5/v5
      x6=-vv6/v6
      vw4=s3(k)*p4(k)-s4(k)*a4(k)
      vw5=s3(k)*p5(k)-s5(k)*a5(k)
      vw6=s3(k)*p6(k)-s6(k)*a6(k)
      y4=-vw4/v4
      y5=-vw5/v5
      y6=-vw6/v6
      didi4=a4(k)-p4(k)
      didi5=a5(k)-p5(k)
      didi6=a6(k)-p6(k)
      rad4=(didi4/v4+vv4**2/v4**2+vw4**2/v4**2)**0.5
      rad5=(didi5/v5+vv5**2/v5**2+vw5**2/v5**2)**0.5
      rad6=(didi6/v6+vv6**2/v6**2+vw6**2/v6**2)**0.5
      write(1,*)x4,y4,rad4
      write(1,*)x5,y5,rad5
      write(1,*)x6,y6,rad6
      cona=1.5
8827  if(nindicm.eq.1)go to 8821
      kref=k-1
      go to 8823
8821  kref=k+1
8823  xref=refl1(kref)*cos(refl2(kref)*3.141592/180)
      yref=refl1(kref)*sin(refl2(kref)*3.141592/180)
      write(1,'("  xref,yref:  ",2x,e12.9,2x,e12.9)')xref,yref
      refmag=(xref**2+yref**2)**0.5
      nspec1=0
      nspec2=0
      nspec3=0
8829  call circle(x4,y4,rad4,x5,y5,rad5,aitx,aity,ninter)
      x451=aitx(1)
      y451=aity(1)
      x452=aitx(2)
      y452=aity(2)
c      if(ninter.eq.1)go to 8482
c      aitmag1=(aitx(1)**2+aity(1)**2)**0.5
c      aitmag2=(aitx(2)**2+aity(2)**2)**0.5
c      if(aitmag1.le.1.20 .and. aitmag2.le.1.20)go to 8483
c      if(aitmag1.gt.1.20 .and. aitmag2.le.1.20)go to 8484
c      if(aitmag1.le.1.20 .and. aitmag2.gt.1.20)go to 8482
c8483  diss1=abs(((aitx(1)-x6)**2+(aity(1)-y6)**2)**0.5-rad6)
c      diss2=abs(((aitx(2)-x6)**2+(aity(2)-y6)**2)**0.5-rad6)
c      if(diss1.lt.diss2)go to 8482
c      if(diss2.lt.diss1)go to 8484
ccc      if(aitmag1.lt.1.10)go to 8483
ccc      if(aitmag2.lt.1.10)go to 8484
ccc8483  if(aitmag2.le.aitmag1)go to 8484
ccc      if(ninter.eq.1)go to 8482
```

```
      dist1=((xref-aitx(1))**2+(yref-aity(1))**2)**0.5
      dist2=((xref-aitx(2))**2+(yref-aity(2))**2)**0.5
      if(abs(dist1-dist2).gt.(cra*refmag))go to 8481
      nspec1=1
      go to 8486
8481  write(1,*)dist1,dist2
      if(dist1.gt.dist2)go to 8484
8482  sx1=aitx(1)
      sy1=aity(1)
      go to 8486
8484  sx1=aitx(2)
      sy1=aity(2)
8486  call circle(x5,y5,rad5,x6,y6,rad6,aitx,aity,ninter)
      x561=aitx(1)
      y561=aity(1)
      x562=aitx(2)
      y562=aity(2)
c      if(ninter.eq.1)go to 8582
c      aitmag1=(aitx(1)**2+aity(1)**2)**0.5
c      aitmag2=(aitx(2)**2+aity(2)**2)**0.5
c      if(aitmag1.le.1.20 .and. aitmag2.le.1.20)go to 8583
c      if(aitmag1.gt.1.20 .and. aitmag2.le.1.20)go to 8584
c      if(aitmag1.le.1.20 .and. aitmag2.gt.1.20)go to 8582
c8583  diss1=abs(((aitx(1)-x4)**2+(aity(1)-y4)**2)**0.5-rad4)
c      diss2=abs(((aitx(2)-x4)**2+(aity(2)-y4)**2)**0.5-rad4)
c      if(diss1.lt.diss2)go to 8582
c      if(diss2.lt.diss1)go to 8584
ccc      if(aitmag1.lt.1.17)go to 8583
ccc      if(aitmag2.lt.1.17)go to 8584
ccc8583  if(aitmag2.le.aitmag1)go to 8584
ccc      if(ninter.eq.1)go to 8482
      dist1=((xref-aitx(1))**2+(yref-aity(1))**2)**0.5
      dist2=((xref-aitx(2))**2+(yref-aity(2))**2)**0.5
      if(abs(dist1-dist2).gt.(cra*refmag))go to 8581
      nspec2=1
      go to 8586
8581  write(1,*)dist1,dist2
      if(dist1.gt.dist2)go to 8584
8582  sx2=aitx(1)
      sy2=aity(1)
      go to 8586
8584  sx2=aitx(2)
      sy2=aity(2)
8586  call circle(x6,y6,rad6,x4,y4,rad4,aitx,aity,ninter)
      x641=aitx(1)
      y641=aity(1)
      x642=aitx(2)
      y642=aity(2)
      dist1=((xref-aitx(1))**2+(yref-aity(1))**2)**0.5
      dist2=((xref-aitx(2))**2+(yref-aity(2))**2)**0.5
      if(abs(dist1-dist2).gt.(cra*refmag))go to 8681
      nspec3=1
      go to 8686
8681  write(1,*)dist1,dist2
      if(dist1.gt.dist2)go to 8684
8682  sx3=aitx(1)
      sy3=aity(1)
      go to 8686
8684  sx3=aitx(2)
      sy3=aity(2)
```

```
8686  if(nspec1.eq.0 .and. nspec2.eq.0 .and. nspec3.eq.0)go to 7998
      if(nspec1.eq.1 .and. nspec2.eq.0 .and. nspec3.eq.0)go to 7401
      if(nspec1.eq.1 .and. nspec2.eq.0 .and. nspec3.eq.1)go to 7413
      if(nspec1.eq.1 .and. nspec2.eq.1 .and. nspec3.eq.0)go to 7412
      if(nspec1.eq.1 .and. nspec2.eq.1 .and. nspec3.eq.1)go to 7430
      if(nspec1.eq.0 .and. nspec2.eq.1 .and. nspec3.eq.0)go to 7402
      if(nspec1.eq.0 .and. nspec2.eq.1 .and. nspec3.eq.1)go to 7423
      if(nspec1.eq.0 .and. nspec2.eq.0 .and. nspec3.eq.1)go to 7403
7401  dist1=((x451-sx2)**2+(y451-sy2)**2)**0.5
      dist2=((x451-sx3)**2+(y451-sy3)**2)**0.5
      dist3=((x452-sx2)**2+(y452-sy2)**2)**0.5
      dist4=((x452-sx3)**2+(y452-sy3)**2)**0.5
      dist5=((sx2-sx3)**2+(sy2-sy3)**2)**0.5
c7401  xxx1=(x451+sx2+sx3)/3
      xxx1=(x451+sx2+sx3)/3
      yyy1=(y451+sy2+sy3)/3
      xxx2=(x452+sx2+sx3)/3
      yyy2=(y452+sy2+sy3)/3
      go to 7441
7402  dist1=((x561-sx1)**2+(y561-sy1)**2)**0.5
      dist2=((x561-sx3)**2+(y561-sy3)**2)**0.5
      dist3=((x562-sx1)**2+(y562-sy1)**2)**0.5
      dist4=((x562-sx3)**2+(y562-sy3)**2)**0.5
      dist5=((sx1-sx3)**2+(sy1-sy3)**2)**0.5
c7402  xxx1=(x561+sx1+sx3)/3
      xxx1=(x561+sx1+sx3)/3
      yyy1=(y561+sy1+sy3)/3
      xxx2=(x562+sx1+sx3)/3
      yyy2=(y562+sy1+sy3)/3
      go to 7441
7403  dist1=((x641-sx1)**2+(y641-sy1)**2)**0.5
      dist2=((x641-sx2)**2+(y641-sy2)**2)**0.5
      dist3=((x642-sx1)**2+(y642-sy1)**2)**0.5
      dist4=((x642-sx2)**2+(y642-sy2)**2)**0.5
      dist5=((sx1-sx2)**2+(sy1-sy2)**2)**0.5
c7403  xxx1=(x641+sx2+sx1)/3
      xxx1=(x641+sx2+sx1)/3
      yyy1=(y641+sy2+sy1)/3
      xxx2=(x642+sx2+sx1)/3
      yyy2=(y642+sy2+sy1)/3
7441  write(1,*)xxx1,yyy1
      write(1,*)xxx2,yyy2
      diss1=dist1+dist2+dist5
      diss2=dist3+dist4+dist5
      write(1,*)diss1,diss2
c7441  diss1=((xxx1-xref)**2+(yyy1-yref)**2)**0.5
c      diss2=((xxx2-xref)**2+(yyy2-yref)**2)**0.5
      if(diss1.gt.diss2)go to 7102
      x=xxx1
      y=yyy1
      go to 7999
7102  x=xxx2
      y=yyy2
      go to 7999
7412  dist1=((x451-x561)**2+(y451-y561)**2)**0.5
      dist2=((x451-x562)**2+(y451-y562)**2)**0.5
      dist3=((x452-x561)**2+(y452-y561)**2)**0.5
      dist4=((x452-x562)**2+(y452-y562)**2)**0.5
      dist5=((x561-sx3)**2+(y561-sy3)**2)**0.5
      dist6=((x562-sx3)**2+(y562-sy3)**2)**0.5
```

```
      dist7=((sx3-x451)**2+(sy3-y451)**2)**0.5
      dist8=((sx3-x452)**2+(sy3-y452)**2)**0.5
c7412  xxx1=(x451+x561+sx3)/3
      xxx1=(x451+x561+sx3)/3
      yyy1=(y451+y561+sy3)/3
      xxx2=(x451+x562+sx3)/3
      yyy2=(y451+y562+sy3)/3
      xxx3=(x452+x561+sx3)/3
      yyy3=(y452+y561+sy3)/3
      xxx4=(x452+x562+sx3)/3
      yyy4=(y452+y562+sy3)/3
      go to 7452
7423  dist1=((x641-x561)**2+(y641-y561)**2)**0.5
      dist2=((x641-x562)**2+(y641-y562)**2)**0.5
      dist3=((x642-x561)**2+(y642-y561)**2)**0.5
      dist4=((x642-x562)**2+(y642-y562)**2)**0.5
      dist5=((x561-sx1)**2+(y561-sy1)**2)**0.5
      dist6=((x562-sx1)**2+(y562-sy1)**2)**0.5
      dist7=((sx1-x641)**2+(sy1-y641)**2)**0.5
      dist8=((sx1-x642)**2+(sy1-y642)**2)**0.5
c7423  xxx1=(x641+x561+sx1)/3
      xxx1=(x641+x561+sx1)/3
      yyy1=(y641+y561+sy1)/3
      xxx2=(x641+x562+sx1)/3
      yyy2=(y641+y562+sy1)/3
      xxx3=(x642+x561+sx1)/3
      yyy3=(y642+y561+sy1)/3
      xxx4=(x642+x562+sx1)/3
      yyy4=(y642+y562+sy1)/3
      go to 7452
7413  dist1=((x451-x641)**2+(y451-y641)**2)**0.5
      dist2=((x451-x642)**2+(y451-y642)**2)**0.5
      dist3=((x452-x641)**2+(y452-y641)**2)**0.5
      dist4=((x452-x642)**2+(y452-y642)**2)**0.5
      dist5=((x641-sx2)**2+(y641-sy2)**2)**0.5
      dist6=((x642-sx2)**2+(y642-sy2)**2)**0.5
      dist7=((sx2-x451)**2+(sy2-y451)**2)**0.5
      dist8=((sx2-x452)**2+(sy2-y452)**2)**0.5
c7413  xxx1=(x451+x641+sx2)/3
      xxx1=(x451+x641+sx2)/3
      yyy1=(y451+y641+sy2)/3
      xxx2=(x451+x642+sx2)/3
      yyy2=(y451+y642+sy2)/3
      xxx3=(x452+x641+sx2)/3
      yyy3=(y452+y641+sy2)/3
      xxx4=(x452+x642+sx2)/3
      yyy4=(y452+y642+sy2)/3
7452  write(1,*)xxx1,yyy1
      write(1,*)xxx2,yyy2
      write(1,*)xxx3,yyy3
      write(1,*)xxx4,yyy4
      diss1=dist1+dist5+dist7
      diss2=dist2+dist6+dist7
      diss3=dist3+dist5+dist8
      diss4=dist4+dist6+dist8
c7452  diss1=((xxx1-xref)**2+(yyy1-yref)**2)**0.5
c      diss2=((xxx2-xref)**2+(yyy2-yref)**2)**0.5
c      diss3=((xxx3-xref)**2+(yyy3-yref)**2)**0.5
c      diss4=((xxx4-xref)**2+(yyy4-yref)**2)**0.5
      if(diss1.gt.diss2)go to 7122
```

```
      if(diss1.gt.diss3)go to 7123
      if(diss1.gt.diss4)go to 7124
      x=xxx1
      y=yyy1
      go to 7999
7122  if(diss2.gt.diss3)go to 7123
      if(diss2.gt.diss4)go to 7124
      x=xxx2
      y=yyy2
      go to 7999
7123  if(diss3.gt.diss4)go to 7124
      x=xxx3
      y=yyy3
      go to 7999
7124  x=xxx4
      y=yyy4
      go to 7999
7430  diss1=((x451-x561)**2+(y451-y561)**2)**0.5
      diss2=((x451-x562)**2+(y451-y562)**2)**0.5
      diss3=((x452-x561)**2+(y452-y561)**2)**0.5
      diss4=((x452-x562)**2+(y452-y562)**2)**0.5
      diss5=((x561-x641)**2+(y561-y641)**2)**0.5
      diss6=((x561-x642)**2+(y561-y642)**2)**0.5
      diss7=((x562-x641)**2+(y562-y641)**2)**0.5
      diss8=((x562-x642)**2+(y562-y642)**2)**0.5
      diss9=((x641-x451)**2+(y641-y451)**2)**0.5
      diss10=((x641-x452)**2+(y641-y452)**2)**0.5
      diss11=((x642-x451)**2+(y642-y451)**2)**0.5
      diss12=((x642-x452)**2+(y642-y452)**2)**0.5
      dist1=diss1+diss5+diss9
      dist2=diss1+diss6+diss11
      dist3=diss2+diss7+diss9
      dist4=diss2+diss8+diss11
      dist5=diss3+diss5+diss10
      dist6=diss3+diss6+diss12
      dist7=diss4+diss7+diss10
      dist8=diss4+diss8+diss12
c7430  xxx1=(x451+x561+x641)/3
      xxx1=(x451+x561+x641)/3
      yyy1=(y451+y561+y641)/3
      xxx2=(x451+x561+x642)/3
      yyy2=(y451+y561+y642)/3
      xxx3=(x451+x562+x641)/3
      yyy3=(y451+y562+y641)/3
      xxx4=(x451+x562+x642)/3
      yyy4=(y451+y562+y642)/3
      xxx5=(x452+x561+x641)/3
      yyy5=(y452+y561+y641)/3
      xxx6=(x452+x561+x642)/3
      yyy6=(y452+y561+y642)/3
      xxx7=(x452+x562+x641)/3
      yyy7=(y452+y562+y641)/3
      xxx8=(x452+x562+x642)/3
      yyy8=(y452+y562+y642)/3
c      dist1=((xxx1-xref)**2+(yyy1-yref)**2)**0.5
c      dist2=((xxx2-xref)**2+(yyy2-yref)**2)**0.5
c      dist3=((xxx3-xref)**2+(yyy3-yref)**2)**0.5
c      dist4=((xxx4-xref)**2+(yyy4-yref)**2)**0.5
c      dist5=((xxx5-xref)**2+(yyy5-yref)**2)**0.5
c      dist6=((xxx6-xref)**2+(yyy6-yref)**2)**0.5
```

```
c      dist7=((xxx7-xref)**2+(yyy7-yref)**2)**0.5
c      dist8=((xxx8-xref)**2+(yyy8-yref)**2)**0.5
      if(dist1.gt.dist2)go to 7602
      if(dist1.gt.dist3)go to 7603
      if(dist1.gt.dist4)go to 7604
      if(dist1.gt.dist5)go to 7605
      if(dist1.gt.dist6)go to 7606
      if(dist1.gt.dist7)go to 7607
      if(dist1.gt.dist8)go to 7608
      x=(x451+x561+x641)/3
      y=(y451+y561+y641)/3
      go to 7999
7608  x=(x452+x562+x642)/3
      y=(y452+y562+y642)/3
      go to 7999
7602  if(dist2.gt.dist3)go to 7603
      if(dist2.gt.dist4)go to 7604
      if(dist2.gt.dist5)go to 7605
      if(dist2.gt.dist6)go to 7606
      if(dist2.gt.dist7)go to 7607
      if(dist2.gt.dist8)go to 7608
      x=(x451+x561+x642)/3
      y=(y451+y561+y642)/3
      go to 7999
7603  if(dist3.gt.dist4)go to 7604
      if(dist3.gt.dist5)go to 7605
      if(dist3.gt.dist6)go to 7606
      if(dist3.gt.dist7)go to 7607
      if(dist3.gt.dist8)go to 7608
      x=(x451+x562+x641)/3
      y=(y451+y562+y641)/3
      go to 7999
7604  if(dist4.gt.dist5)go to 7605
      if(dist4.gt.dist6)go to 7606
      if(dist4.gt.dist7)go to 7607
      if(dist4.gt.dist8)go to 7608
      x=(x451+x562+x642)/3
      y=(y451+y562+y642)/3
      go to 7999
7605  if(dist5.gt.dist6)go to 7606
      if(dist5.gt.dist7)go to 7607
      if(dist5.gt.dist8)go to 7608
      x=(x452+x561+x641)/3
      y=(y452+y561+y641)/3
      go to 7999
7606  if(dist6.gt.dist7)go to 7607
      if(dist6.gt.dist8)go to 7608
      x=(x452+x561+x642)/3
      y=(y452+y561+y642)/3
      go to 7999
7607  if(dist7.gt.dist8)go to 7608
      x=(x452+x562+x641)/3
      y=(y452+y562+y641)/3
      go to 7999
c8686  x=(sx1+sx2+sx3)/3
7998  x=(sx1+sx2+sx3)/3
      y=(sy1+sy2+sy3)/3
7999  x2=x
      y2=y
cc
```

```
      con24=a4(k)*(1+(r4(k)**2+s4(k)**2)*(x2**2+y2**2)-2*r4(k)*x2+2*s4(k
     &)*y2)-p4(k)*(1+(r3(k)**2+s3(k)**2)*(x2**2+y2**2)-2*r3(k)*x2+2*s3(K
     &)*y2)
      con25=a5(k)*(1+(r5(k)**2+s5(k)**2)*(x2**2+y2**2)-2*r5(k)*x2+2*s5(k
     &)*y2)-p5(k)*(1+(r3(k)**2+s3(k)**2)*(x2**2+y2**2)-2*r3(k)*x2+2*s3(K
     &)*y2)
      con26=a6(k)*(1+(r6(k)**2+s6(k)**2)*(x2**2+y2**2)-2*r6(k)*x2+2*s6(k
     &)*y2)-p6(k)*(1+(r3(k)**2+s3(k)**2)*(x2**2+y2**2)-2*r3(k)*x2+2*s3(k
     &)*y2)
      write(1,'(" con4,5,6:",2x,e12.9,2x,e12.9,2x,e12.9)')con24,con25,co
     &n26
ccccccccccccccccccccccccccccccccc
6667  write(1,'(" x,y = :",e12.9,2x,e12.9)')x,y
      amagnit=(x**2+y**2)**0.5
      if(x.gt.0)go to 721
      if(x.eq.0)go to 722
      phase=atan(y/x)*180/3.141592+180
      go to 723
721   phase=atan(y/x)*180/3.141592
      go to 723
722   if(y.gt.0)go to 726
      if(y.lt.0)go to 727
      phase=0
      go to 723
726   phase=90
      go to 723
727   phase=-90
723   refl1(k)=amagnit
      refl2(k)=phase
ccc      if(phase.lt.-180.0)go to 792
ccc      if(phase.gt.180.0)go to 795
ccc      go to 797
ccc792   refl2(k)=phase+360.0
ccc      go to 797
ccc795   refl2(k)=phase-360.0
797   freq9=fstart+(k-1)*fstep
c      write(6,'(6x,"S11(",f6.4,") = ",f6.4," < ",f6.3," deg ")')freq9,r
c     &efl1(k),refl2(k)
      if(nindicm.eq.0)go to 714
      k=k-1
      if(k.gt.0)go to 720
      go to 774
714   k=k+1
c      if(k.le.nsize)go to 720
      if(k.le.nsize)go to 720
      k=int((fc-fstart)/fstep+1)-1
      if(k.le.0)go to 774
      nindicm=1
      go to 720
774   me=1
      write(1,'(/" The measurement procedure is completed. "/)')
c      call plotgs(r3,r4,r5,r6,s3,s4,s5,s6,a4,a5,a6,p4,p5,p6,refl1,refl2)
      go to 778
777   write(1,'(/" Warning ! The system is not calibrated !"/)')
778   return
      end
c
c
c     ********************** SUBROUTINE LIST **********************
c
```

```
      subroutine list(refl1,refl2)
      common /c1/lusig,ludac,fstart,fstop,fstep,power
      common /c2/nsize,me,ca
      common /c3/titlec,titlem
      character*10 titlec,titlem
      real*4 refl1(141),refl2(141)
      if(me.eq.0)go to 888
c     go to 889
810   write(1,'(/" What would you like to list from the given table ?")'
     &)

      write(1,'(/"   1. s11-mag  ")')
      write(1,'("   2. s11-db   (1/2)_")')
      read(1,'(i1)')mquest
      write(1,'(/" Enter LU of listing device (TERM=1, PRINTER=6):")')
      read(1,'(i1)')nlu
      if(mquest.eq.1)go to 820
      if(mquest.eq.2)go to 830
      write(1,'(/" Unrecognized parameter. Try again.")')
      go to 810
820   write(nlu,'(/3x,"Program AVNA/1",2x,"Cal:",a10,2x,"Meas:",a10)')ti
     &tlec,titlem
      write(nlu,'(/3x,"Freq(GHz)",4x,"S11-mag")')
      write(nlu,'(16x,"Mag.",9x,"Phase")')
      do k=1,nsize
      frequen=fstart+(k-1)*fstep
      write(nlu,'(3x,f6.3,7x,f7.4,7x,f7.4)')frequen,refl1(k),refl2(k)
      end do
      go to 889
830   write(nlu,'(/3x,"Program AVNA/1",2x,"Cal:",a10,2x,"Meas:",a10)')ti
     &tlec,titlem
      write(nlu,'(/3x,"Freq(GHz)",4x,"S11-dB")')
      write(nlu,'(16x,"Mag.(dB)",5x,"Phase")')
      do k=1,nsize
      frequen=fstart+(k-1)*fstep
      dbmag=20*log10(refl1(k))
      write(nlu,'(3x,f6.4,7x,f7.4,7x,f7.4)')frequen,dbmag,refl2(k)
      end do
      go to 889
888   write(1,'(/" Warning ! No data available for listing !"/)')
889   return
      end
c
c
c     ********************** SUBROUTINE PLOT **********************
c
      subroutine plot(refl1,refl2,freq,r3,r4,r5,r6,s3,s4,s5,s6)
      common /c1/lusig,ludac,fstart,fstop,fstep,power
      common /c2/nsize,me,ca
      common /c3/titlec,titlem
      real*4 refl1(141),refl2(141),freq(141)
      real*4 r3(141),r4(141),r5(141),r6(141),s3(141),s4(141),s5(141)
      real*4 s6(141)
      character*7 tone,two,three,tans,tfour
      character*10 titlec,titlem
      data tone/'s11-mag'/,two/'s11-dB'/,three/'s11-pha'/,tfour/'q-point
     &s'/
      npts=nsize
      if(me.eq.0)go to 1111
      do 1331,lik=1,nsize
```

```
      freq(lik)=fstart+(lik-1)*fstep
1331  continue
1030  write(1,'(" What do you want to plot ?:   ")')
      write(1,'("       1. s11-mag  ")')
      write(1,'("       2. s11-dB   ")')
      write(1,'("       3. s11-pha  ")')
      write(1,'("       4. q-points   :_")')
      read(1,'(a7)')tans
      if(tans.eq.tone)go to 1000
      if(tans.eq.two)go to 1100
      if(tans.eq.three)go to 1200
      if(tans.eq.tfour)go to 1300
      write(1,'(" Unrecognized parameter. Try again. ")')
      go to 1112
1000  call graph(refl1,freq,npts,tans)
      go to 1112
1200  call graph(refl2,freq,npts,tans)
      go to 1112
1100  call graph(refl1,freq,npts,tans)
      go to 1112
1300  write(1,'(" Which q-point (3,4,5,6)?:_")')
      read(1,*)nnna
      if(nnna.eq.3)go to 1305
      if(nnna.eq.4)go to 1310
      if(nnna.eq.5)go to 1320
      if(nnna.eq.6)go to 1330
1305  call graph(s3,r3,npts,tans)
      go to 1112
1310  call graph(s4,r4,npts,tans)
      go to 1112
1320  call graph(s5,r5,npts,tans)
      go to 1112
1330  call graph(s6,r6,npts,tans)
      go to 1112
1111  write(1,'(/" Warning ! No data available for plotting !"/)')
1112  return
      end
c
c
c     ********************** SUBROUTINE COMMAND ********************
c
      subroutine command(task)
      write(1,'(" Command ? : _")')
      read(1,'(a4)')task
      return
      end
c
c
c     ****************** SUBROUTINE START_PROMPT *******************
c
      subroutine start_prompt
      write(1,'("Welcome to SIXPORT9M.")')
      write(1,'(/"Version date: May 4, 1987"/)')
      return
      end
c
c
c     ******************** SUBROUTINE FandP_SET ********************
c
      subroutine fandp_set
```

```
      common /c1/lusig,ludac,fstart,fstop,fstep,power
2000  write(1,'(/"Enter frequency range as start,stop,step(GHz):_"/)')
      read(1,*)fstart,fstop,fstep
      if((fstop-fstart)/fstep.le.200)go to 2010
      write(1,'(/"There are more than 61 steps. Try again !"/)')
      go to 2000
2010  write(1,'(/"Enter the power level in dBm :_"/)')
      read(1,*)power
      return
      end
c
c
c     ******************** SUBROUTINE END_PROMPT ********************
c
      subroutine end_prompt
      write(1,'(/"This concludes the program. Bye bye !"/)')
      return
      end
c
c
c     ********************** SUBROUTINE SWEEP ************************
c
      subroutine sweep(f)
      common /c1/lusig,ludac,fstart,fstop,fstep,power
c      write(1,'(" Change the frequency to",f5.2," GHz")')f
c      write(1,'(" When ready, press return_")')
c      read(1,*)nans
      if(f.gt.fstop)go to 3020
      if(f.gt.fstart)go to 3000
      write(lusig,'("pl",f5.2,"dmfa",f5.3,"gz")')power,fstart
      write(lusig,'("fb",f5.3,"gzst50ms")')fstop
3000  write(lusig,'("cw",f5.3,"gz")')f
      go to 3040
3020  write(lusig,'("fa",f5.3,"gzfb",f5.3,"gzst50ms")')fstart,fstop
3040  return
      end
c
c
c     ********************** SUBROUTINE GRAPH ************************
c
      subroutine graph(refl1,refl2,npts,tans)
c
      common /c1/lusig,ludac,fstart,fstop,fstep,power
      common /c3/titlec,titlem
      real*4 refl1(141),refl2(141)
      complex*8 ydat(141)
      character*10 titlec,titlem
      character*1 ans,yes,term
      character*7 two,tans,tfour
      character*20 fname
      include graphlib.inp
c
      data yes/'y'/,term/'t'/,two/'s11-dB'/,tfour/'q-points'/
c
      write(1,'("...plotting on terminal or plotter (t/p) ? _")')
      read(1,'(a)')ans
      if(ans.eq.term)then
      lutv=1
      lutvt=2
      else
```

```
      write(1,'("...plotter LU ? _")')
      read(1,*)lutv
      write(1,'("...plotter lutvt (7 or else)?_")')
      read(1,*)lutvt
      end if
c
      irep=1
  101 continue
      do 102,i=1,npts
      x=refl2(i)
      if(tans.ne.two)go to 123
      y=20*alog10(refl1(i))
      go to 124
123   y=refl1(i)
124   ydat(i)=cmplx(x,y)
c      write(6,*)ydat(i)
102   continue
      write(1,'(" Select scales (1), or self scaling (2) :_")')
      read(1,'(i1)')ians
      if(ians.eq.2)go to 103
      write(1,'(" Enter horizontal and vertical scales .")')
      write(1,'("       Horizontal : xmin,xmax :_")')
      read(1,*)xaxmin,xaxmax
      write(1,'("       Vertical   : ymin,ymax :_")')
      read(1,*)yaxmin,yaxmax
      go to 127
103   call findmax(refl2,npts,xaxmax,xaxmin,tans)
      call findmax(refl1,npts,yaxmax,yaxmin,tans)
127   idat=npts
      marker=0
      nmarker=0
      call lplot(lutvt,lutv,ydat,idat,irep,xaxmax,xaxmin,yaxmax,yaxmin,t
     &ans,marker,nmarker)
c
      irep=irep+1
      write(1,'("...plotted curve",i4)')irep
      irep=irep+1
      write(1,'("...another curve ? _")')
      read(1,'(a)')ans
      if(ans.eq.yes)go to 101
c
      write(1,'("...plotting done")')
      return
      end
c
c
c     ********************* SUBROUTINE FINDMAX **********************
c
      subroutine findmax(refl1,npts,voltmax,voltmin,tans)
      real*4 refl1(*)
      character*7 two,tans
      data two/'sll-dB'/
      if(tans.ne.two)go to 5126
      voltmax=20*log10(refl1(1))
      voltmin=20*log10(refl1(1))
      do 1=1,npts
      alrefl=20*log10(refl1(1))
      if(voltmax.ge.alrefl)go to 5211
      voltmax=alrefl
5211  if(voltmin.le.alrefl)go to 5212
```

```
      voltmin=alref1
5212  continue
      end do
      go to 5222
5126  voltmax=ref11(1)
      voltmin=ref11(1)
      do k=1,npts
      if(voltmax.ge.ref11(k))go to 5000
      voltmax=ref11(k)
5000  if(voltmin.le.ref11(k))go to 5010
      voltmin=ref11(k)
5010  continue
      end do
5222  write(1,*)voltmax,voltmin
      if((voltmax-voltmin).gt.0.1)go to 5020
      voltmax=voltmax+1.0
      voltmin=voltmin-1.0
5020  return
      end
c
c
c     ********************** SUBROUTINE INFILE *************************
c
      subroutine infile(nsize,p3,p4,p5,p6,tfname)
      real*4 p3(141),p4(141),p5(141),p6(141)
      character*10 tfname
      write(1,'(" Enter the duty cycle in percent :_")')
      read(1,*)duty
      open(10,file=tfname)
      k=1
901   read(10,'(4e12.9)',end=902,err=960)pp3,pp4,pp5,pp6
902   p3(k)=abs(pp3*100/duty)
      p4(k)=abs(pp4*100/duty)
      p5(k)=abs(pp5*100/duty)
      p6(k)=abs(pp6*100/duty)
      k=k+1
      if(k.le.nsize)go to 901
      close(10)
960   return
      end
c
c
c     ********************** SUBROUTINE RESTORE **********************
c
      subroutine restore(nsize,a14,a24,a34,a44,a54,a64,r3,s3,a4,r4,s4,a5
     &,r5,s5,a6,r6,s6,tfname)
      common /c1/lusig,ludac,fstart,fstop,fstep,power
      real*4 r3(*),s3(*),a4(*),r4(*),s4(*),a5(*),r5(*),s5(*)
      real*4 a6(*),r6(*),s6(*)
      real*4 a14(*),a24(*),a34(*),a44(*),a54(*),a64(*)
      character*10 tfname
      open(10,file=tfname)
      read(10,'(4f8.4)')fstart,fstop,fstep,power
      nsize=int((fstop-fstart)/fstep+1)
      k=1
6191  read(10,'(4e12.9)',err=6960)a14(1),a14(2),a14(3),a14(4)
      read(10,'(4e12.9)',err=6960)a24(1),a24(2),a24(3),a24(4)
      read(10,'(4e12.9)',err=6960)a34(1),a34(2),a34(3),a34(4)
      read(10,'(4e12.9)',err=6960)a44(1),a44(2),a44(3),a44(4)
      read(10,'(4e12.9)',err=6960)a54(1),a54(2),a54(3),a54(4)
```

```
      read(10,'(4e12.9)',err=6960)a64(1),a64(2),a64(3),a64(4)
      read(10,'(3e12.9)',err=6960)r3(k),s3(k),a4(k)
      read(10,'(5e12.9)',err=6960)r4(k),s4(k),a5(k),r5(k),s5(k)
      read(10,'(3e12.9)',err=6960)a6(k),r6(k),s6(k)
6902  k=k+1
      if(k.le.nsize)go to 6191
6196  close(10)
6960  return
      end
c
c
c     ************ SUBROUTINE CIRCLE *********************************
c
      subroutine circle(cx1,cy1,r1,cx2,cy2,r2,aitx,aity,ninter)
      real*4 x1,x2,y1,y2,r1,r2,x0,y0,ateta,alph,res
c      real*4 xr1(4),yr1(4),ress1(4),xr2(4),yr2(4),ress2(4)
      real*4 aitx(2),aity(2)
      write(1,'(" Received param1:",2x,e12.9,2x,e12.9,2x,e12.9)')cx1,cy1
     &,r1
      write(1,'(" Received param2:",2x,e12.9,2x,e12.9,2x,e12.9)')cx2,cy2
     &,r2
      x1=cx1
      x2=cx2
      y1=cy1
      y2=cy2
      dist=((x1-x2)**2+(y1-y2)**2)**0.5
      r=r1+r2
      rrr=abs(r1-r2)
      if(dist.le.r .and. dist.ge.rrr)go to 1001
      write(1,'(" The circles do not intersect. ")')
      write(1,'(" Trying to approximate intersection. ")')
      alph=0.25
c      write(1,'(" Enter the step size (alph):_")')
c      read(1,*)alph
      go to 8001
1001  alph=0.1
      ninter=2
      nroot=0
      ateta=0.0
      x0=x1+r1*cos(ateta*3.141592/180)
      y0=y1+r1*sin(ateta*3.141592/180)
      res0=(x0-x2)**2+(y0-y2)**2-r2**2
3001  ateta=ateta+alph
      xo=x1+r1*cos(ateta*3.141592/180)
      yo=y1+r1*sin(ateta*3.141592/180)
      reso=(xo-x2)**2+(yo-y2)**2-r2**2
      if(reso.eq.0.0)go to 280
      pres=res0*reso
      if(pres.gt.0.0)go to 180
      nroot=nroot+1
      xr=(x0+xo)/2
      yr=(y0+yo)/2
      aitx(nroot)=xr
      aity(nroot)=yr
      ninter=2
      write(1,'(" The root is (x,y) :",2x,e12.9,2x,e12.9)')xr,yr
      go to 180
280   write(1,'(" The root is (x,y) :",2x,e12.9,2x,e12.9)')xo,yo
      nroot=nroot+1
      aitx(nroot)=xo
```

```
      aity(nroot)=yo
180   res0=reso
      x0=xo
      y0=yo
      if(ateta.ge.360)go to 995
      go to 3001
995   go to 990
c995   if(nroot.ne.0.0)go to 990
8001  ateta=0.0
      xmin1=0.0
      xmin2=0.0
      ymin1=0.0
      ymin2=0.0
      res1min=1e38
      res2min=1e38
8003  x01=x1+r1*cos(ateta*3.141592/180)
      y01=y1+r1*sin(ateta*3.141592/180)
      x02=x2+r2*cos(ateta*3.141592/180)
      y02=y2+r2*sin(ateta*3.141592/180)
      res01=abs(((x01-x2)**2+(y01-y2)**2)**0.5-r2)
      res02=abs(((x02-x1)**2+(y02-y1)**2)**0.5-r1)
      if(res01.gt.res1min)go to 8007
      res1min=res01
      xmin1=x01
      ymin1=y01
8007  if(res02.gt.res2min)go to 8002
      res2min=res02
      xmin2=x02
      ymin2=y02
8002  ateta=ateta+alph
      if(ateta.lt.360)go to 8003
      xmmm=(xmin1+xmin2)/2
      ymmm=(ymin1+ymin2)/2
      err1=(xmmm-x1)**2+(ymmm-y1)**2-r1**2
      err2=(xmmm-x2)**2+(ymmm-y2)**2-r2**2
      write(1,'(" The closest root is: ",2x,e12.9,2x,e12.9)')xmmm,ymmm
      write(1,'(" The errors are     : ",2x,e12.9,2x,e12.9)')err1,err2
      aitx(1)=xmmm
      aity(1)=ymmm
      aitx(2)=1e38
      aity(2)=1e38
      ninter=1
990   return
      end
```

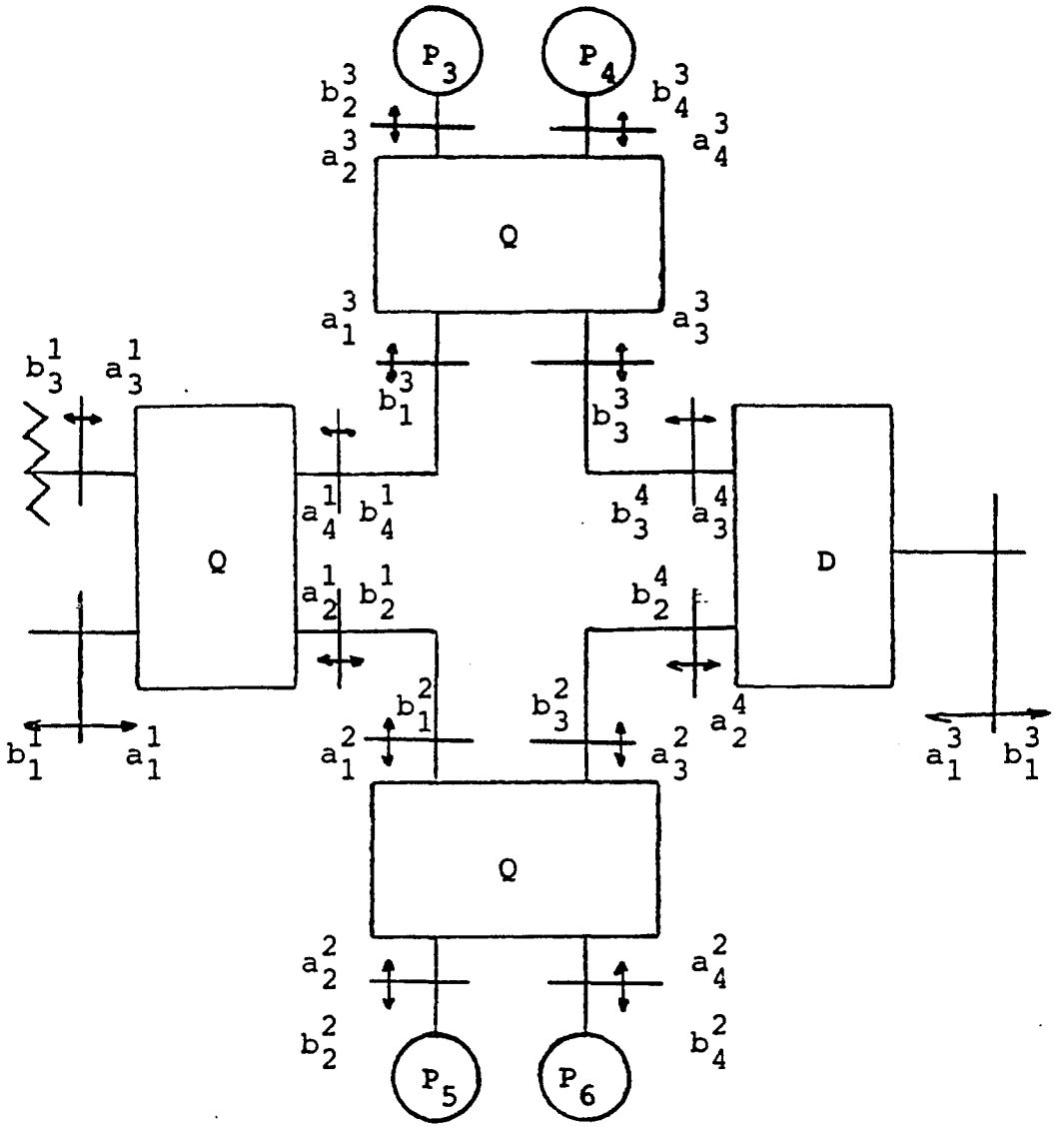

Fig.D-1: Six-port correlator circuit with a and b waves for all components

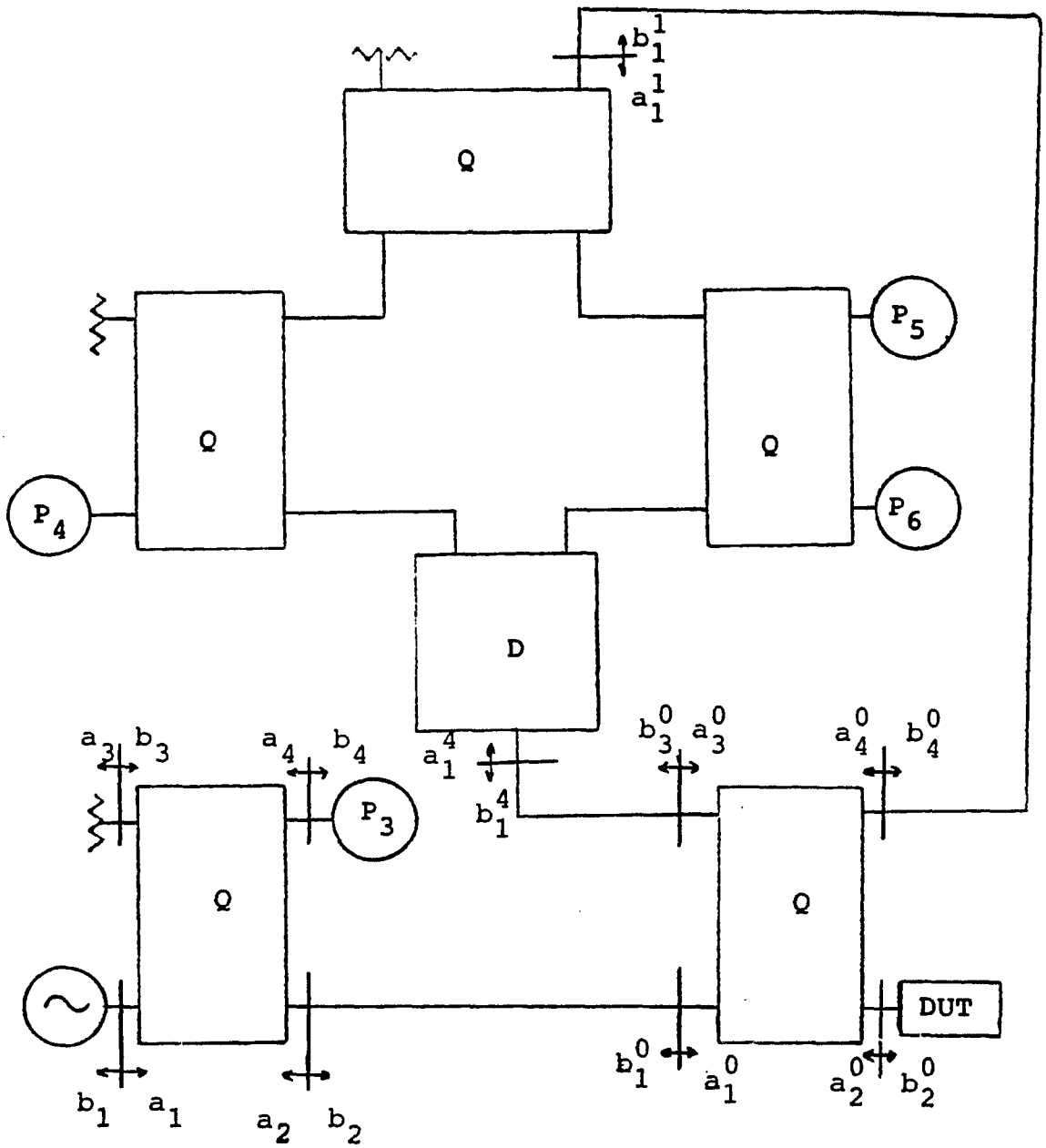

Fig.E-1: Six-port reflectometer circuit with a and b waves for all components

6 . REFERENCES

[1] Glenn F. Engen, "Power Equations: A New Concept in The Description and Evaluation of Microwave Systems", IEEE Trans. Instrum. Meas., vol. IM-20, No. 1, pp. 49-57, Febr. 1971.

[2] Cletus A. Hoer, "The Six-Port Coupler: A New Approach to Measuring Voltage, Current, Power, Impedance, and Phase", IEEE Trans. Instrum. Meas., vol. IM-21, No. 4, pp. 466-470, Nov. 1972.

[3] Glenn F. Engen and Cletus A. Hoer, "Application of an Arbitrary 6-Port Junction to power Measurement Problem", IEEE Trans. Instrum. Meas., vol. IM-21, No. 4, pp. 470-474, Nov. 1972.

[4] Algie L. Lance, Gunther U. Sorger, Wendell D. Seal and Paul M. Fujimoto, "Practical Analysis of Reflectometers and Power Equation Concept", IEEE Trans. Instrum. Meas., vol. IM-22, No. 3, pp. 261-267, Sept. 1973.

[5] Glenn F. Engen, "Calibration of An Arbitrary Six-Port Junction for Measurement of Active and Passive Circuit Parameters", IEEE Trans. Instrum. Meas., vol. IM-22, No. 4, pp. 295-299, Dec. 1973.

[6] Cletus A. Hoer, "Using Six-Port and Eight-Port Junctions to Measure Active and Passive Circuit Parameters", NBS Tech. Note 673, Sept. 1975.

[7] Cletus A. Hoer and Keith C. Roe, "Using an Arbitrary Six-Port Junction to Measure Complex Voltage Ratios", IEEE Trans. on MTT, vol. MTT-23, No. 12, pp. 978-984, Dec. 1975.

[8] Glenn F. Engen, "The Six-Port Measurement Technique. A Status Report", Microwave Journal, pp. 18, 1975.

[9] Glenn F. Engen, "The Six-Port Reflectometer: An Alternative Network Analyzer", IEEE Trans. on MTT, vol. MTT-25, No. 12, pp. 1075-1079, Dec. 1977.

[10] Glenn F. Engen, "An Improved Circuit for Implementing The Six-Port Technique of Microwave Measurements", IEEE Trans. on MTT, vol. MTT-25, No. 12, pp. 1080-1083, Dec. 1977.

[11] Harry M. Cronson and Leon Susman, "A Six-Port Automatic Network Analyzer", IEEE Trans. on MTT, vol. MTT-25, No. 12, pp. 1086-1091, Dec. 1977.

[12] Cletus A. Hoer, "A Network Analyzer Incorporating Two Six-Port Reflectometers", IEEE Trans. on MTT, vol. MTT-25, No.12, pp.1070-1074, Dec. 1977.

[13] Manly P. Weidman, "A Semiautomated Six-Port for Measuring Millimeter- Wave Power and Complex Reflection Coefficient", IEEE Trans. on MTT, vol. MTT-25, No.12, pp. 1083-1085, Dec. 1977.

[14] Glenn F. Engen, "Calibrating the Six-Port Reflectometer by Means of Sliding Terminations", IEEE Trans. on MTT, vol. MTT-26, No.12, pp. 951-957, Dec. 1978.

[15] Glenn F. Engen and Cletus A. Hoer, "Thru-Reflect-Line: An Improved Technique for Calibrating the Dual Six-Port Automatic Network Analyzer", IEEE Trans. on MTT, vol. MTT-27, No.12, pp. 987-993, Dec. 1979.

[16] Cletus A. Hoer, "Performance of a Dual Six-Port Automatic Network Analyzer", IEEE Trans. on MTT, vol. MTT-27, No.12, pp. 993-998, Dec. 1979.

[17] Richard J. Collier and Nabil A. El-Deeb, "On the Use of a Microstrip Three-Line System as a Six-Port Reflectometer", IEEE Trans. on MTT, vol. MTT-27, No. 10, pp.847-853, Oct. 1979.

[18] Harry M. Cronson and Leon Susman, "A Dual Six-Port Automatic Network Analyzer", IEEE Trans. on MTT, vol. MTT-29, No.4, pp. 372-378, April 1981.

[19] Jeffrey A. Paul and Percy C.H. Yen, "Millimeter-Wave Passive Components and Six-Port Network Analyzer in Dielectric Waveguide", IEEE Trans. on MTT, vol. MTT-29, No. 9, pp. 948-953, Sept. 1981.

[20] P.I. Somlo and John D. Hunter, "A Six-Port Reflectometer and its Complete Characterization by Convenient Calibration Procedures", IEEE Trans. on MTT, vol. MTT-30, No. 2, pp. 186-192, Febr. 1982.

[21] Harry M. Cronson and Robert A. Fong-Tom, "A 94-GHz Diode-Based Single Six-Port Reflectometer", IEEE Trans. on MTT, vol. MTT-30, No. 8, pp. 1260-1264, Aug. 1982.

[22] Gordon P. Riblet and E.R. Bertil Hansson, "Aspects of the Calibration of a Single Six-Port Using a Load and Offset Reflection Standards", IEEE Trans. on MTT, vol. MTT-30, No. 12, pp. 2120-2125, Dec. 1982.

[23] Cletus A. Hoer, "Choosing Line Lengths for Calibrating Network Analyzers", IEEE Trans. on MTT, vol. MTT-31, No. 1, pp. 76-78, Jan. 1983.

[24] E.R. Bertil Hansson and Gordon P. Riblet, "An Ideal Six-Port Network Consisting of a Matched Reciprocal Lossless Five-Port and a Perfect Directional Coupler", IEEE Trans. on MTT, vol. MTT-31, No. 3, pp. 284-288, March 1983.

[25] Nabil A. El-Deeb, "The Calibration and Performance of a Microstrip Six-Port Reflectometer", IEEE Trans. on MTT, vol. MTT-31, No. 7, pp. 509-514, July 1983.

[26] John R. Forrest, "High Precision Phase Shifting Techniques", RADC-TR-83-218, Final Technical Report, Nov. 1983.

[27] Dong Il Kim, Kiyomichi Araki and Yoshiyuki Naito, "Properties of Symmetrical Five-Port Circuit an Its Broad-Band Design", IEEE Trans. on MTT, vol. MTT-32, No. 1, pp. 51-57, Jan. 1984.

[28] John R. Juroshek and Cletus A. Hoer, "A Dual Six-Port Network Analyzer Using Diode Detectors", IEEE Trans. on MTT, vol. MTT-32, No. 1, pp. 78-82, Jan. 1984.

[29] Gordon P. Riblet and E.R. Bertil Hansson, "Some Properties of the Matched Symmetrical Six-Port Junction", IEEE Trans. on MTT, vol. MTT-32, No. 2, pp. 164-171, Febr. 1984.

[30] Robert A Fong-Tom, "Evaluation of a 94-GHz Diode Based Dual Six-Port Network Analyzer", 1984 IEEE MTT-S Digest, 26-2, pp. 567-568.

[31] J.A. Dobrowolski, E. Bridges and L. Shafai, "A Calibration Method for a Six-Port Reflectometer which Minimizes the Effect of Power Measurement Errors", 1984 IEEE MTT-S Digest, 26-4, pp. 572-574.

[32] E.J. Griffin and T.E. Hodgetts, "Theoretical Comparison of Six-Port Reflectometer Junction Designs", 1984 IEEE MTT-S Digest, 26-5, pp. 575-577.

[33] John R. Juroshek and Cletus A. Hoer, "A High-Power Automatic Network Analyzer for Measuring the RF Power Absorbed by Biological Samples in a TEM Cell", IEEE Trans. on MTT, vol. MTT-32, No. 8, pp. 818-824, Aug. 1984.

[34] Leopoldine Kaliouby and Renato G. Bosisio, "A New Method for Six-Port Swept Frequency Automatic Network Analyzer", IEEE Trans. on MTT, vol. MTT-32, No. 12, pp. 1678-1682, Dec. 1984.

[35] Nak Sam Chung, Jeong Hwan Kim and Joon Shin, "A Dual Six-Port Automatic Network Analyzer and Its Performance", IEEE Trans. on MTT, vol. MTT-32, No. 12, pp. 1683-1686, Dec. 1984.

[36] J.D. Hunter and P.I. Somlo, "An Explicit Six-Port Calibration Method using Five Standards", IEEE Trans. on MTT, vol. MTT-33, No. 1, pp. 69-72, Jan. 1985.

[37] L.D. Hill and E.J. Griffin, "Automatic Stepped-Frequency Six-Port Reflectometer for WG22", IEE Proceedings, vol. 132, Pt.H, No.2, pp. 77-81, April 1985.

[38] L.D. Hill, "Six-Port Reflectometer for the 75-105 GHz Band", IEE Proceedings, vol. 132, Pt.H, No.2, pp.141-143, April 1985.

[39] John R. Juroshek and Cletus A. Hoer, "A Technique for Extending the Dynamic Range of a Dual Six-Port Network Analyzer", IEEE Trans. on MTT, vol. MTT-33, No.6, pp. 453-459, June 1985.

[40] Ulrich Stumper, "A Six-Port Reflectometer Operating at Submillimeter Wavelengths", European Microwave Conference, Paris, Sept 1985.

[41] S.K. Judah, "Calibration of Multiport Reflectometers", IEE Proceedings, vol. 132, Pt.H, No.7, pp. 468-470, Dec. 1985.

[42] Cletus A. Hoer, "Summary of NBS Calibration Services and Systems", IEEE Proceedings, vol. 74, No.1, pp. 32-35, Jan. 1986.

[43] Mark Berman and P.I. Somlo, "Efficient Procedures for Fitting Circles and Ellipses with Application to Sliding Termination Measurement, IEEE Trans. Instrum. Meas., vol IM-35, No. 1, pp. 31-35, March 1986.

[44] Marc D. Rafal and William T. Joines, "Optimizing the Design of the Six-Port Junction", Paper, Duke University.

[45] A.L. Cullen, "The Six-Port and the Microprocessor in Microwave Measurements", Paper, University College London.

[46] Leopoldine Kaliouby and Renato G. Bosisio, "Applications of Network Analysis Using a New Real-Time Six-Port ANA", Ecole Polytechnique, Montreal, Quebec, Canada, Paper.

[47] R.L. Burden and J.D. Faires, "Numerical Analysis", Prindle, Weber & Schmidt Publishers, Third Edition, 1985.

[48] Harry M. Cronson and Leon Susman, "A New Calibration Technique for Automated Broadband Microwave Measurements", Proceedings of the 6th Anual European Microwave Conference, Rome, Italy, Sept. 1976.